Eva Morava
Matthias Baumgartner
Marc Patterson
Shamima Rahman
Johannes Zschocke
Verena Peters *Editors*

JIMD Reports

Volume 42

SSIEM

Springer

JIMD Reports
Volume 42

Eva Morava
Editor-in-Chief

Matthias Baumgartner · Marc Patterson · Shamima Rahman · Johannes Zschocke
Editors

Verena Peters
Managing Editor

JIMD Reports
Volume 42

Springer

SSIEM

ISSN 2192-8304 ISSN 2192-8312 (electronic)
JIMD Reports
ISBN 978-3-662-58364-7 ISBN 978-3-662-58365-4 (eBook)
https://doi.org/10.1007/978-3-662-58365-4

Contents

JIMD Reports
DOI 10.1007/8904_2017_64

RESEARCH REPORT

Acute Pancreatitis Secondary to Severe Hypertriglyceridaemia in a Patient with Type 1a Glycogen Storage Disease: Emergent Use of Plasmapheresis

E. Rivers • B. C. Reynolds • S. Bunn • N. J. Leech • J. Straker • H. J. Lambert

Received: 31 December 2016 / Revised: 21 September 2017 / Accepted: 29 September 2017 / Published online: 14 October 2017

Abstract Acute pancreatitis is a well-recognised complication of hypertriglyceridaemia. High serum triglycerides may develop in the autosomal recessive disorder glycogen storage disease (GSD). Plasmapheresis has been effective in reducing triglyceride levels in pancreatitis secondary to other conditions but not previously described in GSD. We describe a 16-year-old male with type 1a GSD who presented with severe abdominal pain, tachycardia and tachypnoea. Abdominal computed tomography (CT) demonstrated acute pancreatitis. Serum triglycerides were 91.8 mM. Despite intravenous fluids and morphine sulphate, he remained seriously ill, and plasmapheresis was therefore started. After daily plasma exchange for 6 days, triglyceride levels dropped to 5 mM. This was associated with a rapid resolution of pancreatitis. Plasmapheresis is effective in rapidly reducing hypertriglyceridaemia from numerous causes, including glycogen storage disease, and may facilitate recovery from acute pancreatitis.

Introduction

Type 1a glycogen storage disease (GSD) is an autosomal recessive disorder, characterised by fasting hypoglycaemia, hepatomegaly and growth retardation, presenting typically in the first 3–4 months of life (Froissart et al. 2011). Deficiency of glucose-6-phosphatase prevents conversion of glucose-6-phosphate to glucose. Intermediaries and alternate pathways lead to the deposition of glycogen and use of alternate fuels. This can lead to severe hypertriglyceridaemia (Wolfsdorf and Weinstein 2003).

We describe a 16-year-old boy with type 1a GSD who developed severe pancreatitis secondary to hypertriglyceridaemia, successfully treated in the acute phase with plasmapheresis. We discuss the possible role of plasmapheresis in the acute management of life-threatening sequelae of hypertriglyceridaemia. We believe this is the first reported use of plasmapheresis in GSD.

Patient Report

A 16-year-old Caucasian boy of non-consanguineous parents regularly attended our service for management of type 1a GSD. Initial presentation was at the age of 3 months, with notably lipaemic serum during an intercurrent vomiting illness. The diagnosis was suggested by an increase of triglycerides and cholesterol, and liver biopsy analysis showed absent glucose-6-phosphatase activity. Genotyping was not a standard practice in the era of diagnosis.

Long-term childhood management included regular 2–3 hourly feeds of uncooked cornstarch and carbohydrate-based food aiming to provide 1.5–2 g/kg carbohydrate and overnight gastrostomy feeds with Maxijul (latterly Vitajoule) delivering 0.2 g/kg/h for 12 h and allopurinol. Growth was adequate, but from the age of 3 years onwards, weight remained persistently on or above the 97th centile. Development was normal. Glycosade was trialled at the age of 12 years and was useful in lengthening the interval in daylight intake to 3.5 h but did not change

Communicated by: Jaak Jaeken, Em. Professor of Paediatrics

E. Rivers · S. Bunn · J. Straker · H. J. Lambert
Great North Children's Hospital, Newcastle upon Tyne, UK

N. J. Leech
Royal Victoria Infirmary, Newcastle upon Tyne, UK

B. C. Reynolds (✉)
Royal Hospital for Children, Glasgow, UK
e-mail: pinkdoc@Doctors.org.uk; ben.reynolds@ggc.scot.nhs.uk

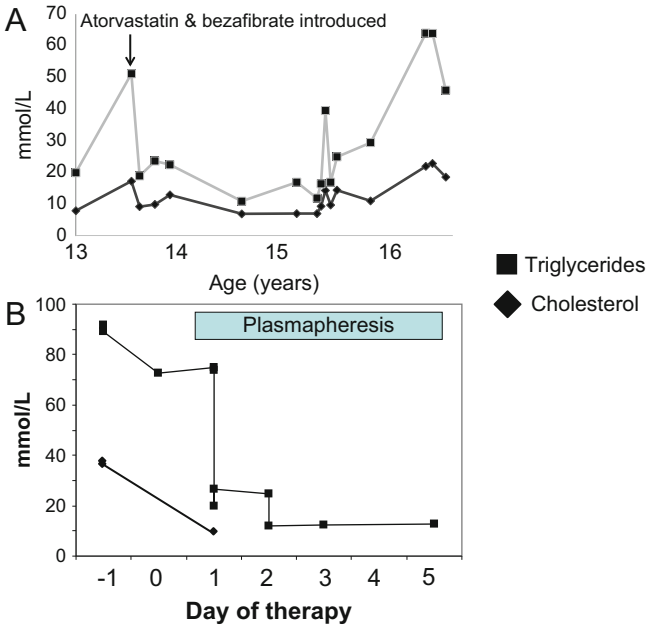

Fig. 1 (**a**) Cholesterol and triglyceride trends 3 years prior to admission. (**b**) Cholesterol and triglyceride trends with administration of plasmapheresis

the need for overnight glucose or improve serum triglycerides (Fig. 1a). Atorvastatin and bezafibrate were introduced at age 13 following an acute rise in cholesterol and triglycerides, with resolution to the previous (still elevated) baseline (Fig. 1a). Multiple short-term elective hospitalisations throughout childhood confirmed an absolute requirement for supplements, with the most recent occurring 2 months prior to his acute presentation. Triglyceride and cholesterol controls were suboptimal for much of the paediatric time course with uncertainty regarding dietary concordance by the family (Fig. 1a). Shortly prior to admission, lipid control deteriorated with persistent hypertriglyceridaemia (70 mM, normal <1.7 mM) and hypercholesterolaemia (21 mM, normal <5.2 mM).

He then presented acutely with severe abdominal pain. He was tachycardic (130/min) and tachypnoeic (40/min) and required 1 l of oxygen to maintain his saturations above 95%. Abdominal computed tomography (CT) demonstrated extensive inflammatory changes in the peritoneum and retroperitoneum, consistent with a radiological diagnosis of acute pancreatitis, though the pancreas itself appeared normal. Serum triglycerides and cholesterol were markedly elevated at 91.8 mM and 28.3 mM, respectively.

He was initially managed with intravenous fluids with 10% dextrose to reduce glycogenolysis and intravenous morphine sulphate for analgesia. He received 10% dextrose at 5 ml/kg/h for the first few hours of admission and then at a rate sufficient to correct for 5% dehydration over 48 h. In view of ongoing severe symptoms and mortality risk, plasmapheresis was performed on an Aquarius System (Baxter industries). Five percent human albumin solution was used to exchange 3 l with a final infusion of Octaplas 600 ml at the end of each session. Despite the marked viscosity of the patient's plasma, there were no issues with filtration, and the circuit did not require replacement during any session.

Within 48 h, after two sessions, the patient reported improvement in pain scores, and his tachypnoea and tachycardia settled. TG, cholesterol and CRP levels fell rapidly (Fig. 1b). The macroscopic appearance of his plasma within the machine also cleared. He received daily plasma exchange for 6 days, following which his triglyceride level dropped to 5.0 mM associated with rapid symptomatic resolution of the acute pancreatitis.

Unfortunately he then developed pyrexia. Culture from the central venous catheter identified *Staphylococcus aureus*, so this was removed.

He has not had any further episodes of acute pancreatitis. TGs remain controlled <10 mmol/l, but he has required very high doses of bezafibrate with a significant adverse effect profile. Genetic profiling was undertaken for other dyslipidaemias, but no mutations were identified in *LPL*, *LMF1*, *ApoC2*, *ApoA5* and *GPI-HPB1* and no duplications or deletions in *LPL* MLPA.

Discussion

We report a paediatric patient with markedly elevated triglycerides and cholesterol who developed acute potentially life-threatening pancreatitis. Plasmapheresis was instituted with success to achieve a short-term rapid reduction in hypertriglyceridaemia.

Acute pancreatitis is a recognised complication of hypertriglyceridaemia of any cause; indeed hypertriglyceridaemia is the aetiology in 1.3–3.8% of pancreatitis. Proposed mechanisms include hydrolysis of triglycerides by lipase to free fatty acids with a directly toxic effect on pancreatic acinar cells and elevated serum viscosity from increased chylomicrons predisposing to ischaemia (Kadikoylu et al. 2010; Tsuang et al. 2009; Chen et al. 2004). It is generally accepted that a triglyceride level greater than 11.2 mM (1,000 mg/dl) is needed to precipitate an episode of acute pancreatitis (Kadikoylu et al. 2010; Tsuang et al. 2009; Ewald and Kloer 2012). In our patient, the initial triglyceride level was 91.8 mM (8,123 mg/dl). The chronic management preceding the admission was suboptimal, despite frequent outpatient reviews and discussions.

Conventional management is to reduce triglycerides using lipid-lowering agents, fluids and dietary restriction (Wolfsdorf and Weinstein 2003). However, this is effective over days to weeks as opposed to plasma exchange where the triglyceride level can be significantly reduced in 2–3 h (Tsuang et al. 2009). This may be beneficial in the acute

phase of pancreatitis if the episode is clinically judged to be severe/life-threatening and potentially in acute recurrent pancreatitis, with reported cases of reduction in the frequency of episodes following treatment with plasma exchange (Yadav and Pitchumoni 2003; Stefanutti et al. 2013; Piolot et al. 1996; Kyriakidis et al. 2006).

Plasma exchange has been reported as an effective treatment for reducing serum triglycerides in acute pancreatitis secondary to other causes (e.g. chylomicronemia syndrome (Lennertz et al. 1999), extreme gestational hyperlipidaemia (Saravanan et al. 1996) and drug-induced hyperlipidaemia (Routy et al. 2001)), but we believe it has not previously been described in patients with type 1a GSD. The absence of any randomised controlled trial assessing the role of plasmapheresis in hypertriglyceridaemic pancreatitis has been highlighted (Valdivielso et al. 2014). Consensus guidelines on the use of apheresis suggest a possible role, with caution that a proven benefit on outcome is lacking and that treatment decisions must be individualised (Schwartz et al. 2013). A single controlled trial with historical controls failed to demonstrate superior outcomes, attributed by the authors to delay in initiation of apheresis (Yeh et al. 2003). Recommendations are that plasmapheresis be commenced as early as possible when felt necessary (Ewald and Kloer 2012). In our case, the severity and acuity of the pancreatitis prompted our decision to treat with apheresis within 48 h of admission.

Therapeutic plasma exchange is not without risk (Schwartz et al. 2013; Sanford and Balogun 2011). Central venous access is required, with the potential for catheter-related complications including infection. Apheresis is an extracorporeal procedure requiring suitably trained providers. If serial plasmapheresis sessions are required, consideration must be given to replacement of plasma components. Plasmapheresis may also remove medications, the timing of which may require adjustment in relation to delivery of apheresis. Though the reduction in triglycerides with plasmapheresis may be significant, it is typically transient, and other lipid-lowering strategies should be optimised. Standard of care remains dietary management and medications; plasmapheresis should only be considered when the patient is at a significant risk of imminent clinical harm.

Despite the potential for complications related to the viscosity of the plasma, our patient received a standard plasmapheresis prescription and did not suffer any technical or clinical complications. The only subsequent complication was central venous catheter infection, which was resolved by prompt removal of the infected catheter.

Conclusion

Plasmapheresis is an effective and rapid treatment for hypertriglyceridaemia of a variety of causes and may facilitate recovery in acute severe/life-threatening pancreatitis. This treatment modality appears similarly effective in our patient with a background of glycogen storage disease type 1. Clinicians should consider early short-term use of plasmapheresis in severe acute pancreatitis secondary to hypertriglyceridaemia.

Compliance with Ethics Guidelines

Emma Rivers, Ben Reynolds, Su Bunn, Jayne Straker, Nicola Leech and Heather Lambert declare they have no conflict of interest.

This study does not contain any studies with human or animal subjects performed by any of the authors.

This article has been planned and reported by Emma Rivers and Ben Reynolds, with comments from Su Bunn, Jayne Straker, Nicola Leech and Heather Lambert.

References

Chen J-H, Lai H-W, Liao C-S (2004) Therapeutic plasma exchange in patients with hyperlipidemic pancreatitis. World J Gastroenterol 10(15):2272–2274

Ewald N, Kloer H-U (2012) Treatment options for severe hypertriglyceridaemia: the role of apheresis. Clin Res Cardiol 7 (Suppl 1):31–35

Froissart R, Piraud M, Boudjemline AM et al (2011) Glucose-6-phosphatase deficiency. Orphanet J Rare Dis 6:27

Kadikoylu G, Yukselen V, Yavasoglu I et al (2010) Emergent therapy with therapeutic plasma exchange in acute recurrent pancreatitis due to severe hypertriglyceridemia. Transfus Apher Sci 43 (3):285–289

Kyriakidis AV, Raitsiou B, Sakagianni A et al (2006) Management of acute severe hyperlipidemic pancreatitis. Digestion 73:259–264

Lennertz A, Parhofer KG, Samtleben W et al (1999) Therapeutic plasma exchange in patients with chylomicronemia syndrome complicated by acute pancreatitis. Ther Apher 3(3):227–233

Piolot A, Nadler F, Cavallero E et al (1996) Prevention of recurrent acute pancreatitis in patients with severe hypertriglyceridaemia: value of regular plasmapheresis. Pancreas 13:96–99

Routy JP, Smith GH, Blank DW et al (2001) Plasmapheresis in the treatment of an acute pancreatitis due to protease inhibitor-induced hypertriglyceridemia. J Clin Apher 16(3):157–159

Sanford KW, Balogun RA (2011) Therapeutic apheresis in critically ill patients. J Clin Apher 26:249–251

Saravanan P, Blumenthal S, Anderson C et al (1996) Plasma exchange for dramatic gestational hyperlipaemic pancreatitis. J Clin Gastroenterol 22(4):295–298

Schwartz J, Winters JL, Padmanabhan A et al (2013) Guidelines on the use of therapeutic apheresis in clinical practice – evidence-based approach from the writing committee of the American Society for Apheresis: the sixth special issue. J Clin Apher 28:145–284

Stefanutti C, Labbadia G, Morozzi C (2013) Severe hypertriglyceridemia-related acute pancreatitis. Ther Apher Dial 17(2):130–137

Tsuang W, Navaneethan U, Ruiz L et al (2009) Hypertriglyceridemic pancreatitis: presentation and management. Am J Gastroenterol 104:984–991

Valdivielso P, Ramirez-Bueno A, Ewald N (2014) Current knowledge of hypertriglyceridemic pancreatitis. Eur J Intern Med 25:689–694

Wolfsdorf JI, Weinstein DA (2003) Glycogen storage diseases. Rev Endocr Metab Disord 1:95–102

Yadav D, Pitchumoni CS (2003) Issues in hyperlipidemic pancreatitis. J Clin Gastroenterol 36(1):54–62

Yeh J, Chen JH, Chiu HC (2003) Plasmapheresis for hyperlipidemic pancreatitis. J Clin Apher 18:181–185

JIMD Reports
DOI 10.1007/8904_2017_67

RESEARCH REPORT

A Third Case of Glycogen Storage Disease IB and Giant Cell Tumour of the Mandible: A Disease Association or Iatrogenic Complication of Therapy

Raajiv Prasad • Jane Estrella • John Christodoulou • Geoffrey McKellar • Michel C. Tchan

Received: 25 May 2017 / Revised: 16 October 2017 / Accepted: 18 October 2017 / Published online: 09 November 2017

Abstract We report the third case of Glycogen Storage Disease type 1b (GSD 1b) with Giant Cell Tumour (GCT) of the mandible, associated with Granulocyte Colony Stimulating Factor (G-CSF) use. G-CSF in GSD 1b is indicated for persistent neutropaenia, sepsis, inflammatory bowel disease and severe diarrhoea. Our patient was 12 years old at GCT diagnosis and had been treated with G-CSF from 5 years of age. He underwent therapy with interferon followed by local resection which was successful in initial control of the disease. Histology demonstrated spindle shaped stromal cells together with numerous interspersed multinuclear osteoclastic giant cells. G-CSF has been hypothesized to induce osteoclastic differentiation and thus may be involved in the pathogenesis of GCT formation. At age 19 years he required a repeat operation for local recurrence. He currently continues on G-CSF and was commenced on denosumab for control of the GCT with no recurrence to date. A cause and effect relationship between G-CSF therapy and the development of GCT in GSD type 1b remains to be established.

Communicated by: Avihu Boneh, MD, PhD, FRACP

R. Prasad
Hobart Clinical School, University of Tasmania, Hobart, TAS, Australia

J. Estrella
Western Sydney University Clinical School, Campbelltown Campus, Campbelltown, NSW, Australia

J. Estrella
Department of Endocrinology, Campbelltown Hospital, Campbelltown, NSW, Australia

J. Christodoulou
Neurodevelopmental Genomics Research Group, Murdoch Children's Research Institute, Parkville, VIC, Australia

J. Christodoulou
Department of Paediatrics, Melbourne Medical School, University of Melbourne, Melbourne, VIC, Australia

G. McKellar
Department of Oral and Maxillofacial Surgery, Westmead Hospital, Westmead, NSW, Australia

M. C. Tchan (✉)
Department of Genetic Medicine, Westmead Hospital, Westmead, NSW, Australia
e-mail: michel.tchan@health.nsw.gov.au

M. C. Tchan
Sydney Medical School, University of Sydney, Camperdown, NSW, Australia

Introduction

Glycogen storage disorder 1b (GSD 1b) is due to recessive mutations in the *SLC37A4* gene expressing glucose-6-phosphate translocase. In addition to hypoglycaemia, GSD 1b is complicated by hyperlipidaemia, hyperuricaemia, growth retardation, hepatosplenomegaly, renal dysfunction and neutropaenia with other hematologic abnormalities (Burda and Hochuli 2015; Chou et al. 2015). Here we report the third case associating GSD 1b and Giant Cell Tumour (GCT) of the mandible while the patient was on Granulocyte Colony Stimulating Factor (G-CSF).

Case Report

Our patient was born following a normal pregnancy at term weighing 3.3 kg. He had transient hypoglycaemia in the

newborn period and was discharged home on day 14 of life. He represented at age 5 months with a diarrhoeal illness and hypoglycaemia. Hepatomegaly was noted at that time. Following a number of further admissions with hypoglycaemia during intercurrent illness, a liver biopsy was performed which reportedly demonstrated glycogen storage disease (although the details of this result are not available to us). Persistent neutropenia was apparent in the first year of life. Genetic sequencing demonstrated an apparently homozygous variant reported as pathogenic in the *SLC37A4* gene (c.1179G>A; p.Trp393*). Metabolic control was not optimal during the first years of life, with multiple hospital admissions and documented hypoglycaemia. Disease complications have included episodes of hypoglycaemia leading to intellectual disability, multiple episodes of sepsis, neutropenia, haemolytic anaemia, splenectomy and multiple hepatic adenomas. G-CSF was commenced at 5 years of age. His current dose of G-CSF is 300 mcg (5 mcg/kg) four times weekly, with Australian guidelines (Australian Medicines Handbook) suggesting 5 mcg/kg daily in cases of idiopathic or cyclic neutropenia.

He was diagnosed with GCT of the mandible at age 12 years. Interferon therapy for post excision management of his tumour was continued for 3 years post resection. He re-presented with increased gum bleeding 7 years later. A CT and biopsy of the site confirmed recurrence and tumour excision surgery was performed. Histology of the lesion revealed large giant cells consistent with giant cell tumour (Figs. 1 and 2). He has been placed on denosumab therapy for postoperative control of the giant cell tumour.

Discussion

GSD 1b and GCT of the mandible have previously been described in two other patients (Mortellaro et al. 2005; Amaral et al. 2009). Both were receiving G-CSF at the time of tumour occurrence. To our knowledge, this is the third case of a patient with GSD 1b and a giant cell tumour on G-CSF, suggesting a causative association.

Giant cell granulomas of the jaw are benign, locally aggressive tumours of the jaw of unknown aetiology but their occurrence has been observed in Neurofibromatosis type 1, Noonan syndrome and cherubism (O'Connell et al. 2015). These lesions arise from the supporting connective tissue of the marrow and are characterised histologically by ovoid stromal or spindle shaped cells interspersed with multinuclear cells and tend to recur locally despite surgery (Amanatullah et al. 2014; O'Connell et al. 2015).

Although the origins of giant cell tumours are unclear, it has been suggested that they may be derived from osteoclast progenitors (Liu et al. 2003). It has been hypothesized that long term use of G-CSF promotes osteoclastogenesis resulting in giant cell tumours (Amaral et al. 2009). G-CSF activates extracellular membrane receptors such as *c-fms.* These receptors then activate a signalling pathway that differentiates progenitor myeloid cells into osteoclasts (Kitaura et al. 2005).

It is interesting to note that the other two cases of GSD 1b who developed giant cell tumours were also on G-CSF (Mortellaro et al. 2005; Amaral et al. 2009). While generally accepted to be safe, a potential for carcinogenicity

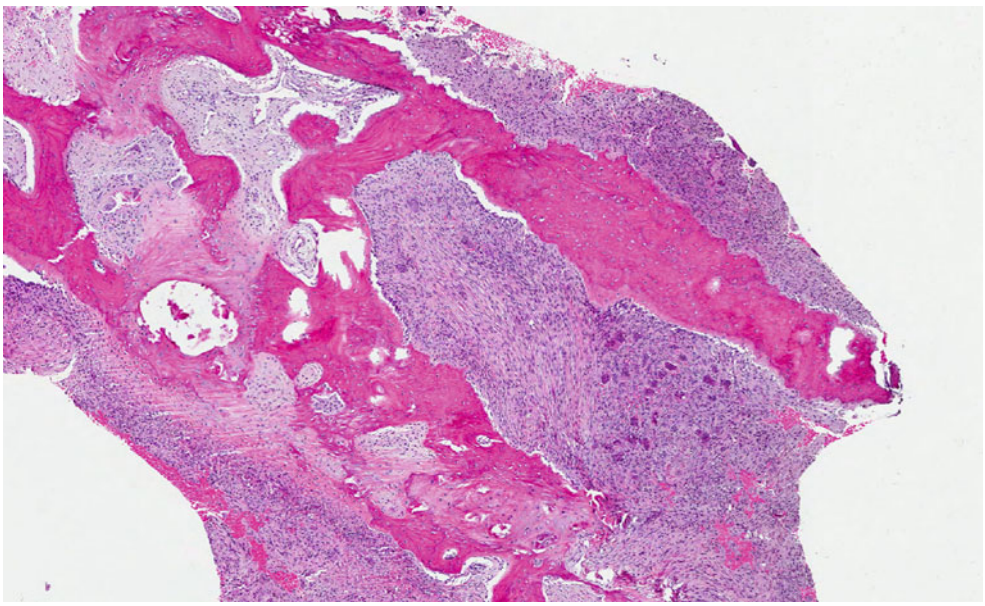

Fig. 1 Low power magnification (4× objective) of giant cell tumour of the mandible showing a giant cell lesion

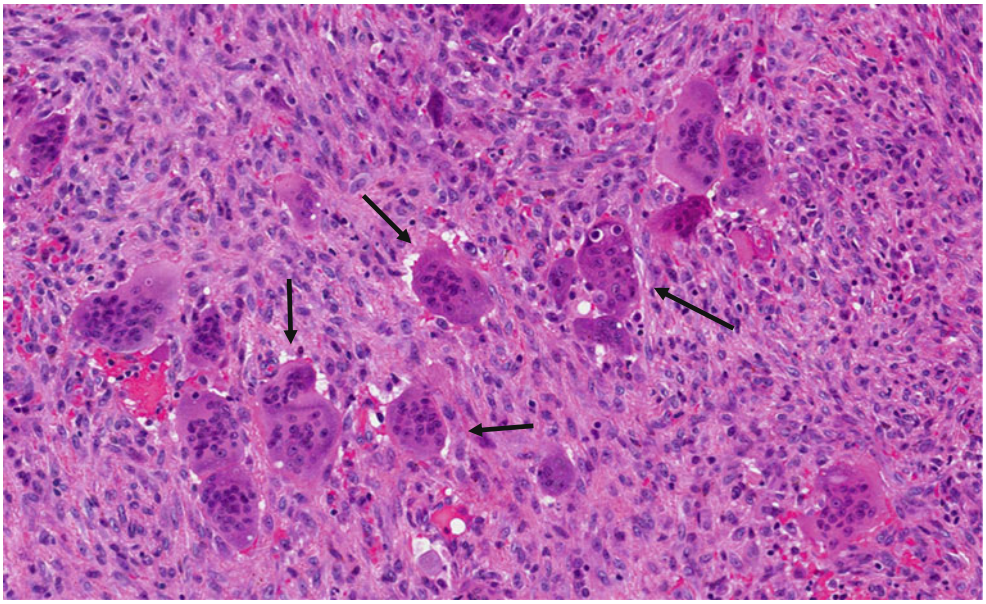

Fig. 2 Histological features of the giant cell tumour of the mandible at high power magnification (40× objective) showing large multinuclear cells in the stroma of the mandible with prominent inclusions (arrows)

due to the presence of G-CSF receptors in tumour cell lines exists (Schipperus et al. 1990). There have been reports of three patients with GSD 1b developing acute myelogenous leukaemia, two on G-CSF and one not on G-CSF (Simmons et al. 1984; Pinsk et al. 2002; Schroeder et al. 2008). In fact, previous consensus guidelines for GSD 1 management included annual bone marrow examination with cytologic studies in patients on G-CSF, although this is no longer included in the current consensus guidelines (Visser et al. 2002; Kishnani et al. 2014). The role of GSD1b and resultant aberrant glycogen in GCT tumourigenesis remains to be defined.

We also consider the possibility that the periodontitis and resulting chronic inflammation, as well as the aberrant glycogen seen in GSD1b may represent an additive effect together with G-CSF that results in abnormal cellular differentiation and growth. Oral manifestations of GSD 1b (periodontitis, recurrent oral ulceration, bleeding diatheses and dental caries) are thought to be related to neutropaenia and/or neutrophil dysfunction; similar oral manifestations are seen in other neutropaenic states (Barrett et al. 1990). This case of GCT in a patient with GSD1b on G-CSF highlights a possible association, and indicates that vigilance for this disease complication is warranted.

Conclusion

We describe the third reported case of GCT of the mandible recurring in a patient with GSD1b whilst the patient was on G-CSF therapy. Histology and imaging supported the diagnosis of GCT of the mandible. It remains to be established whether there is a cause and effect relationship between G-CSF therapy and the development of GCT in GSD type 1b.

Conflict of Interest

Raajiv Prasad, Jane Estrella, John Christodoulou, Geoffrey McKellar and Michel C. Tchan have no disclosures related to this manuscript.

Informed Consent

Informed consent was obtained from the patient and his parents for being included in this study.

Contributions of the Individual Authors

Raajiv Prasad and Jane Estrella have contributed equally to the writing of this manuscript. All authors have contributed to the planning, conduct and reporting of the work described in this chapter and all authors have approved the manuscript.

References

Amanatullah DF, Clark TR, Lopez MJ, Borys D, Tamurian RM (2014) Giant cell tumor of bone. Orthopedics 37:112–120

Amaral FR, Carvalho VM, Fraga MG, Amaral TM, Gomes CC, Gomez RS (2009) Oral giant cell granuloma in a patient with glycogen storage disease. Open Dent J 3:144–146

Barrett AP, Buckley DJ, Katelaris CH (1990) Oral complications in type 1B glycogen storage disease. Oral Surg Oral Med Oral Pathol 69:174–176

Burda P, Hochuli M (2015) Hepatic glycogen storage disorders: what have we learned in recent years? Curr Opin Clin Nutr Metab Care 18:415–421

Chou JY, Jun HS, Mansfield BC (2015) Type I glycogen storage diseases: disorders of the glucose-6-phosphatase/glucose-6-phosphate transporter complexes. J Inherit Metab Dis 38:511–519

Kishnani PS, Austin SL, Abdenur JE et al (2014) Diagnosis and management of glycogen storage disease type I: a practice guideline of the American College of Medical Genetics and Genomics. Genet Med 16:e1

Kitaura H, Zhou P, Kim HJ, Novack DV, Ross FP, Teitelbaum SL (2005) M-CSF mediates TNF-induced inflammatory osteolysis. J Clin Invest 115:3418–3427

Liu B, Yu SF, Li TJ (2003) Multinucleated giant cells in various forms of giant cell containing lesions of the jaws express features of osteoclasts. J Oral Pathol Med 32:367–375

Mortellaro C, Garagiola U, Carbone V, Cerutti F, Marci V, Bonda PL (2005) Unusual oral manifestations and evolution in glycogen storage disease type Ib. J Craniofac Surg 16:45–52

O'Connell JE, Bowe C, Murphy C, Toner M, Kearns GJ (2015) Aggressive giant cell lesion of the jaws: a review of management options and report of a mandibular lesion treated with denosumab. Oral Surg Oral Med Oral Pathol Oral Radiol 120: e191–e198

Pinsk M, Burzynski J, Yhap M, Fraser RB, Cummings B, Ste-Marie M (2002) Acute myelogenous leukemia and glycogen storage disease 1b. J Pediatr Hematol Oncol 24:756–758

Schipperus MR, Sonneveld P, Lindemans J et al (1990) The combined effects of Il-3, GM-CSF and G-CSF on the in vitro growth of myelodysplastic myeloid progenitor cells. Leuk Res 14:1019–1025

Schroeder T, Hildebrandt B, Mayatepek E, Germing U, Haas R (2008) A patient with glycogen storage disease type Ib presenting with acute myeloid leukemia (AML) bearing monosomy 7 and translocation t(3;8)(q26;q24) after 14 years of treatment with granulocyte colony-stimulating factor (G-CSF): a case report. J Med Case Rep 2:319

Simmons PS, Smithson WA, Gronert GA, Haymond MW (1984) Acute myelogenous leukemia and malignant hyperthermia in a patient with type 1b glycogen storage disease. J Pediatr 105:428–431

Visser G, Rake JP, Labrune P et al (2002) Consensus guidelines for management of glycogen storage disease type 1b – European Study on Glycogen Storage Disease Type 1. Eur J Pediatr 161 (Suppl 1):S120–S123

JIMD Reports
DOI 10.1007/8904_2017_70

RESEARCH REPORT

Cardiopulmonary Exercise Testing Reflects Improved Exercise Capacity in Response to Treatment in Morquio A Patients: Results of a 52-Week Pilot Study of Two Different Doses of Elosulfase Alfa

Kenneth I. Berger • Barbara K. Burton • Gregory D. Lewis • Mark Tarnopolsky • Paul R. Harmatz • John J. Mitchell • Nicole Muschol • Simon A. Jones • V. Reid Sutton • Gregory M. Pastores • Heather Lau • Rebecca Sparkes • Adam J. Shaywitz

Received: 17 February 2017 / Revised: 30 June 2017 / Accepted: 24 July 2017 / Published online: 21 November 2017

Abstract *Objective*: To assess impact of a 52-week elosulfase alfa enzyme replacement therapy (ERT) on exercise capacity in Morquio A patients and analyze cardiorespiratory and metabolic function during exercise to uncover exercise limitations beyond skeletal abnormalities.

Methods: Morquio A patients aged ≥7 years, able to walk >200 m in the 6-minute walk test (6MWT), received elosulfase alfa 2.0 mg/kg/week ($N = 15$) or 4.0 mg/kg/week ($N = 10$) for 52 weeks in the randomized, double-blind MOR-008 study (ClinicalTrials.gov NCT01609062) and its extension. Exercise capacity was assessed by 6MWT, 3-minute stair climb test (3MSCT), and cardiopulmonary exercise test (CPET; $N = 15$ dosage groups combined).

Results: Changes over 52 weeks in 6MWT and 3MSCT were minimal. Baseline CPET results showed impaired weight-adjusted peak oxygen uptake (VO_2), partly attributable to inability to increase tidal volume during exercise. CPET measures of exercise function showed significant improvement at 25 and/or 52 weeks in exercise duration, peak workload, O_2 pulse, and peak tidal volume (% increases in duration, 16.9 ($P = 0.0045$) and 9.4 ($P = 0.0807$); peak

Communicated by: Roberto Giugliani, MD, PhD

Electronic supplementary material: The online version of this article (https://doi.org/10.1007/8904_2017_70) contains supplementary material, which is available to authorized users.

K. I. Berger (✉) · G. M. Pastores · H. Lau
New York University School of Medicine, New York, NY, USA
e-mail: Kenneth.Berger@nyumc.org

K. I. Berger
André Cournand Pulmonary Physiology Laboratory, Bellevue Hospital, New York, NY, USA

B. K. Burton
Ann & Robert H. Lurie Children's Hospital of Chicago, Northwestern University Feinberg School of Medicine, Chicago, IL, USA

G. D. Lewis
Massachusetts General Hospital, Boston, MA, USA

M. Tarnopolsky
McMaster University Medical Centre, Hamilton, ON, Canada

P. R. Harmatz
UCSF Benioff Children's Hospital Oakland, Oakland, CA, USA

J. J. Mitchell
Montreal Children's Hospital, Montreal, QC, Canada

N. Muschol
University Medical Center Hamburg-Eppendorf, Hamburg, Germany

S. A. Jones
Willink Unit, St Mary's Hospital CMFT, MAHSC, University of Manchester, Manchester, UK

V. R. Sutton
Baylor College of Medicine, Texas Children's Hospital, Houston, TX, USA

G. M. Pastores
University College Dublin, Mater Misericordiae University Hospital, Dublin, Ireland

R. Sparkes
Alberta Children's Hospital, Calgary, AB, Canada

A. J. Shaywitz
BioMarin Pharmaceutical Inc., Novato, CA, USA

workload, 26.5 ($P = 0.0026$) and 21.2 ($P = 0.0132$); O_2 pulse, 10.7 ($P = 0.0187$) and 2.3 ($P = 0.643$); peak tidal volume, 11.7 ($P = 0.1117$) and 29.1 ($P = 0.0142$)). In addition, decreased VO_2/work ratio was noted (% decrease −7.6 [−11.9, 1.3] and −9.2 [−25.7, 5.1]), indicating performance of work at reduced oxygen cost.

Conclusions: CPET uncovers limitation in exercise capacity in Morquio A related to reduced lung function. ERT improves exercise capacity and efficiency of oxygen utilization, not attributable to changes in cardiac or pulmonary function. Further study of the long-term impact of ERT on exercise capacity and the clinical relevance of the observed changes is warranted.

Introduction

Morquio A syndrome (mucopolysaccharidosis IVA; OMIM 253000) is a rare autosomal recessive disease (1 per 71,000 to 1 per 500,000 live births) caused by a deficiency of the enzyme *N*-acetylgalactosamine-6-sulfatase (GALNS; EC 3.1.6.4); it is characterized by systemic accumulation of keratan sulfate (KS) and chondroitin-6-sulfate and disruption of cellular processes (Muenzer 2011; Yasuda et al. 2013; Leadley et al. 2014). The disease is genotypically and phenotypically very heterogeneous. Characteristic features include bone and joint abnormalities, short stature, obstructive airway/restrictive pulmonary disease, cardiac disease characterized by valve abnormalities and reduced stroke volume, spinal cord compression and/or atlantoaxial instability, hearing loss, impaired vision, and hepatomegaly (Montaño et al. 2007; Harmatz et al. 2013; Hendriksz et al. 2013, 2015).

Elosulfase alfa 2.0 mg/kg/week has been approved as enzyme replacement therapy (ERT) for Morquio A (Sanford and Lo 2014). In the pivotal phase 3 study ($N = 176$), treatment with 2.0 mg/kg/week was associated with a significant impact on endurance in the 6-minute walk test (6MWT) and an acceptable safety profile (Hendriksz et al. 2014). In parallel, a phase 2, randomized, double-blind, pilot study (MOR-008, ClinicalTrials.gov identifier NCT01609062) assessed the safety and efficacy of elosulfase alfa 2.0 and 4.0 mg/kg/week in 25 Morquio A patients. The primary outcome was safety over 27 weeks. Endurance in the 6MWT and 3-minute stair climb test (3MSCT) and exercise capacity in a cardiopulmonary exercise test (CPET) were secondary efficacy measures assessed at 24 and 25 weeks, respectively. Baseline CPET data showed reduced exercise capacity relative to the general population (Ten Harkel et al. 2011; Burton et al. 2015). At 25 weeks, a positive change in exercise capacity (increase in exercise duration, peak workload, and O_2 pulse) and a decrease in oxygen uptake relative to work (VO_2/watt) were observed (Burton et al. 2015). 6MWT and 3MSCT outcomes remained essentially unchanged during the primary treatment phase.

The present study evaluates the effect of ERT for 52 weeks on exercise capacity, as assessed by CPET and measures of endurance. In addition, given the multisystem involvement characteristic of Morquio A disease, detailed analysis of cardiorespiratory function was performed from the CPET data to uncover limitations to exercise beyond skeletal abnormalities.

Methods

Study Design

MOR-008 is a multinational, multicenter, phase 2, two-arm, randomized, double-blind, pilot study. Inclusion and exclusion criteria and study design of the primary treatment phase have been described previously (Burton et al. 2015). Briefly, after a 3-week screening period, 25 patients aged ≥7 years able to walk >200 m in the 6MWT and to perform an exercise test were randomized in a double-blind fashion to elosulfase alfa 2.0 mg/kg/week ($N = 15$) or 4.0 mg/kg/week ($N = 10$) for 27 weeks. Randomization was stratified by cohort: CPET ($N = 15$) and no CPET ($N = 10$). The primary endpoint was safety and tolerability of elosulfase alfa over 27 weeks. Secondary endpoints were effect on endurance, exercise capacity, respiratory function, muscle strength, cardiac function, pain, and urinary KS level. Patients who completed the primary treatment phase were enrolled in the extension, during which all patients continued on the same dose of elosulfase alfa up to 52 weeks. Each participant, or his/her legally authorized representative, provided written informed consent before entering the study.

Evaluation of Endurance and Exercise Capacity

Endurance was measured by the 6MWT (American Thoracic Society 2002) and the 3MSCT at screening, week 12, week 24 (primary treatment phase), and week 52 (extension) as previously described (Burton et al. 2015). Each test was performed twice at each time point within a 7-day window, with only one test allowed per day.

Exercise capacity during CPET was assessed in the first 15 patients enrolled in the study by cycle ergometry using an incremental workload protocol at baseline, week 25, and week 52. The workload was increased every minute to determine each patient's peak exercise capacity. Expired O_2 and CO_2 concentrations were analyzed using a metabolic cart; heart rate was monitored by continuous 3- or 12-lead

ECG, and O_2 saturation was measured via pulse oximetry. Breath-by-breath calculations, including exhaled minute ventilation (V_E), O_2 uptake (VO_2), CO_2 production (VCO_2), respiratory exchange ratio (RER), and peak and rest tidal volume (volume of air displaced between normal inhalation and exhalation), were made from conventional equations. The O_2 pulse was derived as the oxygen uptake per heart beat (VO_2/HR). VO_2 at the ventilatory threshold (VT; the level of oxygen consumption above which aerobic energy production is supplemented by anaerobic mechanisms) was calculated by the V-slope method (Albouaini et al. 2007).

Statistical Methods

As the sample size of the study was not determined by statistical power considerations, the primary analysis plan was to perform descriptive statistics at baseline, 24 weeks (endurance) or 25 weeks (CPET; primary treatment phase), and 52 weeks (extension). Correlations between peak VO_2, determined at each patient's maximal workload, and 6MWT and 3MSCT results were estimated using the Pearson correlation coefficient (r). Post hoc, paired t-test analysis was performed on the CPET variables to evaluate for significant changes at week 25 and week 52 compared with baseline. In addition, linear regression analysis was performed to determine if the change in peak workload from baseline to either week 25 or 52 was related to an improvement in an individual patient's ability to increase tidal volume during exercise. Results are presented for the modified intent-to-treat (MITT) population consisting of all patients who were randomized to study treatment, received at least one dose of study drug, and had at least one posttreatment observation.

Results

Patient Characteristics

All 25 patients (median age 12 years; range 8–21 years) completed the primary treatment phase and were enrolled in and completed 52 weeks of the extension study. One patient stopped ERT at 24 weeks (after having missed four previous infusions) when she moved further away from the study site but remained on the study. Another patient had a last infusion at 39 weeks. Demographics and baseline characteristics for all patients have been presented in a previous publication (Burton et al. 2015). Table 1 shows baseline characteristics for the 15 patients included in the CPET analysis. Baseline characteristics were reasonably well balanced between treatment groups. 6MWT and 3MSCT results were better than in the phase 3 study (Table 2) (Hendriksz et al. 2014). Lung function was impaired, as evidenced by a low median forced vital capacity (FVC; 1.17 L) and forced expiratory volume in 1 s (FEV_1; 0.93 L).

Endurance Outcomes

There were no meaningful changes from baseline in walk distance in the 6MWT in either dose group at 12 or 24 weeks (Table 2) (Burton et al. 2015). An improvement was seen after 52 weeks in the 4.0 mg/kg/week treatment

Table 1 Demographics and baseline characteristics of patients included in the cardiopulmonary exercise test (CPET) analysis (modified intent-to-treat population)

	Elosulfase alfa 2 mg/kg/week $N = 10$	Elosulfase alfa 4 mg/kg/week $N = 5$	Total $N = 15$
Age at enrolment (years) Median (range)	11 (8, 21)	12 (8, 14)	12 (8, 21)
Sex, N (%) Female	7 (70)	3 (60)	10 (66)
Height (cm) Median (range)	102.0 (85, 167)	108.0 (96, 147)	106.5 (85, 167)
Weight (kg) Median (range)	26.5 (12, 54)	22.0 (17, 49)	26.4 (12, 54)
6MWT (m) Median (range)	327 (273, 466)	338 (281, 453)	331 (273, 466)
3MSCT (stairs/min) Median (range)	61 (28, 84)	55 (30, 87)	58 (28, 87)
FVC (L) Median (range)	0.96 (0.68, 4.56)	1.24 (0.90, 2.77)	1.17 (0.68, 4.56)
FEV_1 (L) Median (range)	0.76 (0.57, 3.94)	1.12 (0.84, 2.20)	0.93 (0.57, 3.94)

3MSCT 3-minute stair climb test, *6MWT* 6-minute walk test, *FEV_1* forced expiratory volume in 1 s, *FVC* forced vital capacity

Table 2 Endurance outcomes at baseline and after follow-up at 24 and 52 weeks (modified intent-to-treat population)

			Week 24		Week 52	
	N	Baseline Mean (SD)	Mean (SD)	Median change (IQR)	Mean (SD)	Median change (IQR)
6MWT (m)	25[a]	372.2 (80.6)	364.5 (86.4)	1.4 (−29.3, 6.9)	395.6 (96.3)	9.9 (−15.8, 36.5)
3MSCT (stairs/min)	25[b]	65.0 (21.7)	68.6 (24.4)	4.8 (−3.6, 11.3)	66.3 (24.5)	0.4 (−8.2, 5.5)

IQR interquartile range, *3MSCT* 3-minute stair climb test, *6MWT* 6-minute walk test
[a] $N = 24$ at week 52
[b] $N = 24$ at week 24

group ($N = 10$); mean and median increases from baseline were 31.8 m (95% CI −7.2, 70.8) and 22.1 m, respectively (Supportive online material 1). Mean and median changes from baseline in the 2.0 mg/kg/week group were 9.0 m (95% CI −18.9, 37.0) and 1.9 m, respectively.

3MSCT results improved from baseline at both 24 and 52 weeks in the 4.0 mg/kg/week treatment group only (Supportive online material 1). The small sample size does not allow any conclusions regarding a dose-response effect of elosulfase alfa on endurance.

CPET Outcomes

Baseline and 25-week data that have been presented previously showed impaired weight-adjusted peak VO_2 rates: mean baseline 30.7 (SD 7.5) mL/kg/min vs. ≈40 mL/kg/min in healthy individuals (Table 3) (Ten Harkel et al. 2011; Burton et al. 2015). Similarly, peak heart rate during CPET averaged 164 beats/min, which is below age-matched reference values of 199–212 beats/min (for age range 8–21 years) (Table 3). Although peak exercise capacity was reduced, the peak RER (VCO_2/VO_2) at baseline was >1 indicating that patients exercised to workload that was beyond VT, compatible with adequate patient effort during the study (Table 3).

Further exploration of baseline data showed a resting respiratory rate (mean 24.5 breaths/min) that was relatively high for children and above the upper limit of normal for adults (Charbek 2015). Although the peak respiratory rate (mean 47.4 breaths/min) remained below the upper limit of normal of 60 breaths/min (ATS and ACCP 2003), there was evidence of an abnormal ventilatory response to exercise. Specifically, a minimal <2-fold increase in tidal volume was noted in most patients (vs. ≈2–3 times increase in healthy individuals, Santuz et al. 1997) (Supportive online material 2). The tidal volume response to exercise was particularly low in patients with a low FVC and low FEV_1 but comparable with healthy individuals in those with higher FVC and FEV_1 (Supportive online material 3). There was no evidence of dynamic cardiac impairment based on appropriate increase in stroke volume as assessed by O_2 pulse during exercise.

CPET data at 25 and 52 weeks showed a positive change in exercise capacity (Table 3, Fig. 1a–e). Exercise duration, peak workload, VO_2 at VT, peak tidal volume, and Δ tidal volume all increased with treatment. A small increase from baseline in O_2 pulse was seen after 25 weeks, but not sustained at 52 weeks. Work efficiency improved as defined by a decrease in the required O_2 uptake per unit of work (VO_2/watt) (not significant at week 52). There were numerical differences between the 2.0 mg/kg dose and the 4.0 mg/kg dose at week 25 and week 52 (Fig. 1a–e), but the small sample size did not allow statistical comparison between doses. Peak RER remained >1 after 25 and 52 weeks of treatment with values that were similar to baseline. Peak heart rate and respiratory rates remained stable.

The main reasons for discontinuing CPET were generalized fatigue or leg fatigue ($N = 13$ at baseline). Other reasons were shortness of breath or labored breathing ($N = 2$) and pain ($N = 1$). These reasons did not change markedly over time.

Linear regression analysis demonstrated that patients who were able to increase their tidal volume during exercise more at week 25 compared with baseline demonstrated the greatest improvement in peak exercise workload ($r^2 = 0.37$, $P = 0.02$). This relationship was less obvious at week 52 ($r^2 = 0.1622$, $P = 0.1622$) (Supportive online material 4).

Correlations Between Endurance Measures and Peak VO_2 (Supportive online material 5)

Correlation analysis showed strong positive relationships between peak VO_2 and endurance measures at baseline (6MWT, $r = 0.61$, and 3MSCT, $r = 0.55$). Changes from baseline to week 25 or 52 in peak VO_2 were not correlated with changes in 6MWT over the same period ($r = -0.10$ and $r = 0.05$, respectively); there was a moderately positive correlation between changes in peak VO_2 and 3MSCT at 25

Table 3 Cardiopulmonary exercise test (CPET) outcomes at baseline and after follow-up at 25 and 52 weeks (two dose groups combined; modified intent-to-treat population)

		Baseline	Week 25			Week 52		
	N	Mean (SD)	Mean (SD)	Median % change (IQR)	*P*-value	Mean (SD)	Median % change (IQR)	*P*-value
Exercise duration (min)	15	7.7 (2.3)	8.6 (2.5)	16.9 (−0.5, 23.1)	0.0045	8.4 (2.4)	9.4 (−5.7, 20.2)	0.0807
Peak VO_2 (mL/min)	15	807.1 (412.7)	890.1 (469.67)	5.3 (−6.3, 31.7)	0.0665	856.7 (486.9)	9.8 (−21.3, 25.9)	0.3597
Peak VO_2 (mL/kg/min)	15	30.7 (7.5)	32.5 (10.3)	3.1 (−14.2, 20.5)	0.3449	29.4 (8.8)	−0.8 (−27.8, 16.9)	0.4588
O_2 pulse (mL/beat)	15[a]	4.9 (2.2)	5.3 (2.5)	10.7 (1.3, 19.8)	0.0187	5.2 (2.4)	2.3 (−21.2, 26.8)	0.6343
Peak workload (watts)	15	40.9 (25.9)	50.3 (29.9)	26.5 (5.1, 42.4)	0.0026	48.7 (31.0)	21.2 (0.0, 47.5)	0.0132
VO_2/work ratio (mL/watt)	14	13.3 (3.2)	12.2 (3.2)	−7.6 (−11.9, 1.3)	0.0173	11.6 (4.1)	−9.2 (−25.7, 5.1)	0.2476
Peak RER	15	1.1 (0.1)	1.1 (0.2)	4.0 (−3.9, 10.8)	0.2899	1.0 (0.2)	0.0 (−8.1, 7.5)	0.4915
VO_2 at VT (mL/min)	15[b]	492.8 (217.0)	533.0 (250.4)	9.2 (−0.9, 19.5)	0.0650	592.3 (306.7)	18.3 (4.9, 30.7)	0.0472
Peak heart rate (beats/min)	15	164.3 (16.3)	167.3 (21.0)	4.0 (−9.6, 11.0)	0.6174	164.4 (19.6)	−0.7 (−3.5, 6.8)	0.9815
Rest RR (breaths/min)	15[c]	24.5 (5.8)	23.6 (8.0)	−6.3 (−18.2, 0.0)	0.7171	23.3 (6.6)	−6.1 (−27.6, 22.7)	0.2361
Peak RR (breaths/min)	15[c]	47.4 (10.9)	47.8 (13.5)	6.1 (−15.6, 16.7)	0.5501	45.6 (10.3)	−2.3 (−12.9, 1.8)	0.1000
Rest tidal volume (mL)	15[d]	324.3 (119.8)	331.6 (148.4)	−2.8 (−6.5, 7.9)	0.9493	383.2 (177.3)	23.9 (0.9, 38.2)	0.0879
Peak tidal volume (mL)	15[d]	578.9 (400.5)	663.0 (429.1)	11.7 (−0.0, 26.4)	0.1117	762.4 (523.6)	29.1 (3.3, 46.2)	0.0142
Δ tidal volume (mL)	15[d]	254.6 (300.5)	331.4 (297.2)	56.2 (17.1, 98.1)	0.1385	379.2 (379.6)	38.3 (−6.4, 237.1)	0.0457

Δ tidal volume (calculated as peak minus rest)
IQR interquartile range, *RER* respiratory exchange ratio, *RR* respiratory rate, *VT* ventilatory threshold, *VO_2* oxygen uptake
[a] $N = 14$ at week 52
[b] $N = 13$ at week 52
[c] $N = 14$ at week 25 and 13 at week 52
[d] $N = 14$ at week 25

and 52 weeks ($r = 0.35$ and $r = 0.38$, respectively). Positive correlations were not observed between the changes in VO_2 at VT with either 6MWT or 3MSCT at any time point.

Discussion

MOR-008 is the first study to use an incremental workload CPET in addition to volitional endurance tests (6MWT and 3MSCT) to evaluate exercise capacity in Morquio A patients. This study provided new insights into the pathophysiology and symptomatology of patients with Morquio A and the impact of ERT.

MOR-008 was specifically designed to recruit a patient population healthy enough to perform CPET and endurance tests. Therefore, the patients had better endurance results than those from the phase 3 study, i.e., a median of 331 m in the 6MWT versus approximately 220 m in the phase 3 study and a median of 58 stairs/min in the 3MSCT versus approximately 30 stairs/min in the phase 3 study (Hendriksz et al. 2014). Nevertheless, all patients showed reduced maximal exercise capacity, and the majority had an abnormal ventilatory response to exercise compared with healthy individuals (Ten Harkel et al. 2011). Baseline mean peak VO_2 and peak heart rate during CPET were considerably below age-/weight-matched reference values (ATS and ACCP 2003). Baseline tidal volume response was limited, related to the patients' reduced lung function and height. Resting respiratory rate was correspondingly elevated.

Maximal exercise capacity numerically increased after 25 weeks of elosulfase alfa treatment and remained relatively stable thereafter up to week 52 (Table 3). The greatest increases were seen in the tidal volume at peak workload and in the VO_2 at VT, indicating that patients were able to breathe more efficiently and to exercise to a higher workload before reaching their VT. Of note, the VO_2 at VT is not dependent on patient effort indicating that the

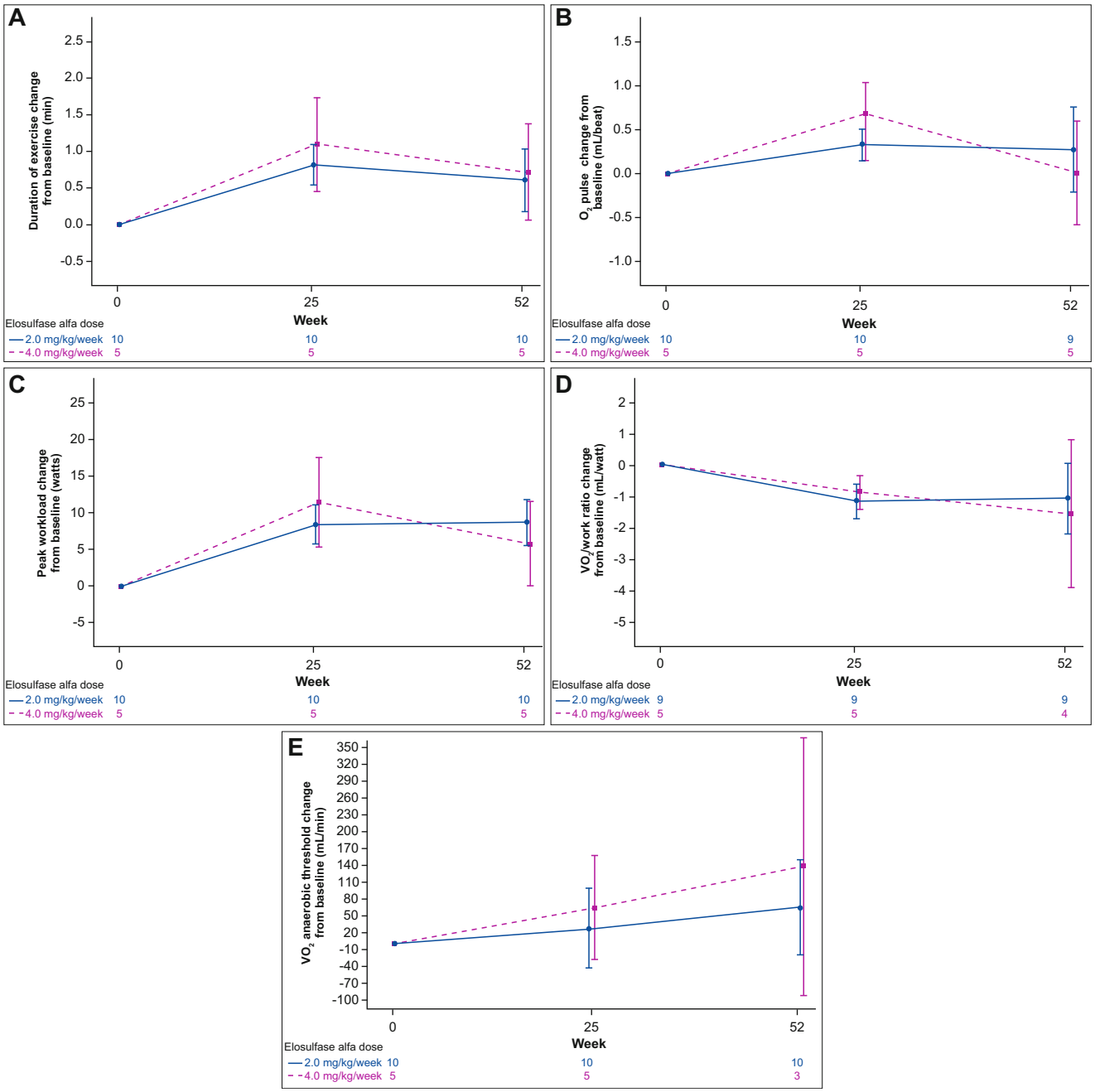

Fig. 1 Mean (standard error) change in cardiopulmonary exercise test (CPET) outcomes from baseline to week 52 with elosulfase alfa 2 mg/kg and 4 mg/kg per week (modified intent-to-treat population). *VO_2* oxygen uptake

changes seen in the CPET variables reflected physiological improvement. The VO_2 at VT continued to increase beyond 25 weeks (week 25, +9%; week 52, +18%) indicating progressive improvement in exercise capacity throughout the study period. Analysis of the remaining CPET parameters provided additional objective support that the increase in exercise capacity is not attributable to volitional factors. At baseline, mean peak RER was >1 indicating that patients exercised to a workload beyond VT, in accordance with adequate patient effort at study entry. While this does not preclude small test-to-test differences in volitional effort between subjects, the peak RER remained unchanged on subsequent CPET evaluations at weeks 25 and 52, indicating that patient performance did not change during the study. Moreover, patients showed minimal differences in peak heart rate and respiratory rate between

baseline and week 52 (which remained below age-adjusted norms), indicating that exercise was terminated at similar cardiorespiratory stress levels at each study visit.

These results illustrate how CPET provides an assessment of exercise capacity that is more comprehensive than the 6MWT and 3MSCT, which are submaximal and volitional tests that may depend on self-motivational factors (ATS and ACCP 2003; Guazzi et al. 2009; Crescimanno et al. 2015). The 6MWT and 3MSCT do not require special equipment or training to implement, but only provide indirect assessments of endurance and functionality (Fleming and Powers 2012) with no information on the factors that limit exertion. Although more complicated, CPET provides an integrated assessment of exercise responses from the cardiovascular, pulmonary, and skeletal muscle systems, thereby allowing evaluation of both submaximal and peak exercise responses (ATS and ACCP 2003; Albouaini et al. 2007). The fundamental differences between these tests might (partly) explain the apparent lack of correlation between CPET and endurance outcomes. While positive correlations between peak VO_2 and endurance measures were seen at baseline, changes in both measures over 25 or 52 weeks were not (6MWT) or only moderately (3MSCT) correlated. Changes in VO_2 at VT were also not positively correlated with endurance outcomes.

Despite the improvements observed in CPET measures of exercise capacity and work efficiency, improvements in endurance measures were small. These findings suggest that patients continued to self-regulate their performance to a similar degree on the volitional tests despite improvement in maximal exercise capacity. Alternatively, the relatively good endurance of the study population at baseline left little room for further improvement in the 6MWT or 3MSCT, particularly given the orthopedic abnormalities in these patients (50% with knee deformity, 40% with joint pain, and 27% with hip dysplasia at baseline) (Burton et al. 2015). Because of this ceiling effect, the 6MWT and 3MSCT test may be less suitable to assess treatment effects in patients with relatively good baseline endurance.

It is unlikely that a cardiac effect contributes to the effect of elosulfase alfa on exercise capacity, as no impact was seen on ejection fraction over 52 weeks (data on file, BioMarin). This was in accord with expectations based on data from the phase 3 study after 120 weeks of treatment (data on file, BioMarin). In the absence of a change in cardiac function, the increase in VO_2 at VT is compatible with improvements in either peripheral O_2 extraction or mitochondrial function. The rapid increases seen in work efficiency and VO_2 at VT are consistent with reports of improved sense of well-being and decreased fatigue in patients on elosulfase alfa in the phase 3 study, even before changes in height and lung function are seen (data on file, BioMarin). Overall, these findings suggest that ERT improves aerobic efficiency as evidenced by performance of work at reduced metabolic demand during CPET. Patients receiving ERT seem to better extract and/or utilize O_2 when exercising, despite their inability to increase tidal volume or further maximize heart or respiratory rate, which were already at maximal capacity prior to ERT. The effect of growth on exercise capacity was not assessed.

Limitations of the study design that should be considered when interpreting these results include the small sample size, which does not allow for statistical comparison between treatment groups, the lack of a control arm, and a possible training effect of some CPET variables (e.g., exercise duration) with repeated testing.

Conclusions

Overall, use of CPET in the evaluation of exercise capacity in patients with Morquio A uncovered a limitation in exercise performance related to reduced lung function (i.e., restrictive respiratory disease). In addition, the 52-week CPET outcomes of the MOR-008 pilot study provide evidence for a positive effect of elosulfase alfa on exercise capacity and efficiency of oxygen utilization that was not attributable to changes in either cardiac or respiratory function. As orthopedic challenges may limit the impact of treatment on endurance test results in these patients, analysis of data obtained during CPET may be a valuable addition to the 6MWT and 3MSCT to monitor treatment effects on cardiorespiratory capacity. Further study of the impact of ERT on exercise capacity in larger patient groups and with longer follow-up is warranted to establish the clinical relevance of the observed changes and the usefulness of CPET in the evaluation of Morquio A patients in clinical practice.

Acknowledgments The authors are grateful to Ismar Healthcare NV for their assistance in the writing of the manuscript, which was funded by BioMarin Pharmaceutical Inc. Fred Genter is acknowledged for his work as a statistician for the study.

Take-Home Message

Morquio A patients have a limitation in exercise performance, which is related to reduced lung function; elosulfase alfa enzyme replacement therapy for 52 weeks has a positive effect on exercise capacity and efficiency of oxygen utilization, not attributable to changes in either cardiac or pulmonary function.

Compliance with Ethics Guidelines

Conflict of Interest

Kenneth I. Berger has worked as consultant and study investigator for BioMarin Pharmaceutical Inc. and has received an honorarium.

Barbara K. Burton has worked as consultant and study investigator for BioMarin Pharmaceutical Inc. and has received an honorarium.

Gregory D. Lewis has worked as consultant and study investigator for BioMarin Pharmaceutical Inc. and has received an honorarium.

Mark Tarnopolsky has worked as consultant and study investigator for BioMarin Pharmaceutical Inc. and has received an honorarium.

Paul R. Harmatz has worked as consultant and study investigator for BioMarin Pharmaceutical Inc. and has received an honorarium.

John J. Mitchell has worked as consultant and study investigator for BioMarin Pharmaceutical Inc. and has received an honorarium.

Nicole Muschol has worked as consultant and study investigator for BioMarin Pharmaceutical Inc. and has received an honorarium.

Simon A. Jones has worked as consultant and study investigator for BioMarin Pharmaceutical Inc. and has received an honorarium.

Vernon R. Sutton has worked as consultant and study investigator for BioMarin Pharmaceutical Inc. and has received an honorarium.

Gregory M. Pastores has worked as consultant and study investigator for BioMarin Pharmaceutical Inc. and has received an honorarium.

Heather Lau has worked as consultant and study investigator for BioMarin Pharmaceutical Inc. and has received an honorarium.

Rebecca Sparkes has worked as consultant and study investigator for BioMarin Pharmaceutical Inc. and has received an honorarium.

Adam J. Shaywitz is an employee of BioMarin Pharmaceutical Inc.

This study was sponsored by BioMarin Pharmaceutical Inc. and supported, in part, by the National Center for Advancing Translational Sciences, National Institutes of Health (NIH), through UCSF-CTSI Grant Number UL1 TR000004 (Dr. Harmatz). Its contents are solely the responsibility of the authors and do not necessarily represent the official views of the NIH. Support in the process of manuscript development was also funded by BioMarin Pharmaceutical Inc.

Informed Consent

All procedures followed were in accordance with the ethical standards of the responsible committee on human experimentation (institutional and national) and with the Helsinki Declaration of 1975, as revised in 2000. Informed consent was obtained from all patients for being included in the study.

Animal Rights

This article does not contain any studies with human or animal subjects performed by any of the authors.

Details of the Contributions of Individual Authors

Barbara K. Burton, Kenneth I. Berger, Gregory D. Lewis, Mark Tarnopolsky, Paul R. Harmatz, John J. Mitchell, Nicole Muschol, Simon A. Jones, Vernon R. Sutton, Gregory M. Pastores, Heather Lau, and Rebecca Sparkes were all members of the steering committee, contributed to the planning of the study, and were involved in the clinical examinations and collection of patient data and in the preparation and critical review of the manuscript.

Adam J. Shaywitz assisted with conduction of the study, data analyses, and development of the manuscript.

References

Albouaini K, Egred M, Alahmar A, Wright DJ (2007) Cardiopulmonary exercise testing and its application. Postgrad Med J 83:675–682

American Thoracic Society (2002) ATS statement: guidelines for the six-minute walk test. Am J Respir Crit Care Med 166:111–117

ATS and ACCP (2003) ATS/ACCP statement on cardiopulmonary exercise testing. Am J Respir Crit Care Med 167:211–277

Burton BK, Berger KI, Lewis GD et al (2015) Safety and physiological effects of two different doses of elosulfase alfa in patients with morquio a syndrome: a randomized, double-blind, pilot study. Am J Med Genet A 167A:2272–2281

Charbek E (2015) Normal vital signs. Medscape. http://emedicine.medscape.com/article/2172054-overview

Crescimanno G, Modica R, Lo Mauro R, Musumeci O, Toscano A, Marrone O (2015) Role of the cardio-pulmonary exercise test and six-minute walking test in the evaluation of exercise performance in patients with late-onset Pompe disease. Neuromuscul Disord 25:542–547

Fleming TR, Powers JH (2012) Biomarkers and surrogate endpoints in clinical trials. Stat Med 31:2973–2984

Guazzi M, Dickstein K, Vicenzi M, Arena R (2009) Six-minute walk test and cardiopulmonary exercise testing in patients with chronic heart failure: a comparative analysis on clinical and prognostic insights. Circ Heart Fail 2:549–555

Harmatz P, Mengel KE, Giugliani R et al (2013) The Morquio A Clinical Assessment Program: baseline results illustrating progressive, multisystemic clinical impairments in Morquio A subjects. Mol Genet Metab 109:54–61

Hendriksz CJ, Al-Jawad M, Berger KI et al (2013) Clinical overview and treatment options for non-skeletal manifestations of mucopolysaccharidosis type IVA. J Inherit Metab Dis 36:309–322

Hendriksz CJ, Burton B, Fleming TR et al (2014) Efficacy and safety of enzyme replacement therapy with BMN 110 (elosulfase alfa) for Morquio A syndrome (mucopolysaccharidosis IVA): a phase 3 randomised placebo-controlled study. J Inherit Metab Dis 37:979–990

Hendriksz CJ, Berger KI, Giugliani R et al (2015) International guidelines for the management and treatment of Morquio A syndrome. Am J Med Genet A 167A:11–25

Leadley RM, Lang S, Misso K et al (2014) A systematic review of the prevalence of Morquio A syndrome: challenges for study reporting in rare diseases. Orphanet J Rare Dis 9:173

Montaño AM, Tomatsu S, Gottesman GS, Smith M, Orii T (2007) International Morquio A Registry: clinical manifestation and natural course of Morquio A disease. J Inherit Metab Dis 30:165–174

Muenzer J (2011) Overview of the mucopolysaccharidoses. Rheumatology (Oxford) 50(Suppl 5):v4–v12

Sanford M, Lo JH (2014) Elosulfase alfa: first global approval. Drugs 74:713–718

Santuz P, Baraldi E, Filippone M, Zacchello F (1997) Exercise performance in children with asthma: is it different from that of healthy controls? Eur Respir J 10:1254–1260

Ten Harkel ADJ, Takken T, Van Osch-Gevers M, Helbing WA (2011) Normal values for cardiopulmonary exercise testing in children. Eur J Cardiovasc Prev Rehabil 18:48–54

Yasuda E, Fushimi K, Suzuki Y et al (2013) Pathogenesis of Morquio A syndrome: an autopsied case reveals systemic storage disorder. Mol Genet Metab 109:301–311

JIMD Reports
DOI 10.1007/8904_2017_71

RESEARCH REPORT

EPG5-Related Vici Syndrome: A Primary Defect of Autophagic Regulation with an Emerging Phenotype Overlapping with Mitochondrial Disorders

Shanti Balasubramaniam · Lisa G. Riley · Anand Vasudevan · Mark J. Cowley · Velimir Gayevskiy · Carolyn M. Sue · Caitlin Edwards · Edward Edkins · Reimar Junckerstorff · C. Kiraly-Borri · P. Rowe · J. Christodoulou

Received: 06 June 2017 / Revised: 24 October 2017 / Accepted: 25 October 2017 / Published online: 21 November 2017

Abstract Vici syndrome is a rare, under-recognised, relentlessly progressive congenital multisystem disorder characterised by five principal features of callosal agenesis, cataracts, cardiomyopathy, combined immunodeficiency and oculocutaneous hypopigmentation. In addition, three equally consistent features (profound developmental delay, progressive failure to thrive and acquired microcephaly) are highly supportive of the diagnosis. Since its recognition as a distinct entity in 1988, an extended phenotype with sensorineural hearing loss, skeletal myopathy and variable involvement of virtually any organ system, including the lungs, thyroid, liver and kidneys, have been described.

Autosomal recessive mutations in *EPG5* encoding ectopic P-granules autophagy protein 5 (*EPG5*), a key

Communicated by: Saskia Brigitte Wortmann, M.D., Ph.D.

Lisa G. Riley and Anand Vasudevan contributed equally to this work.

S. Balasubramaniam
Department of Rheumatology and Metabolic Medicine, Princess Margaret Hospital, Perth, WA, Australia

S. Balasubramaniam (✉) · J. Christodoulou
Western Sydney Genetics Program, The Children's Hospital at Westmead, Sydney, NSW, Australia
e-mail: saras329@hotmail.com

S. Balasubramaniam · J. Christodoulou
Discipline of Genetic Medicine, Sydney Medical School, University of Sydney, Sydney, NSW, Australia

S. Balasubramaniam · L. G. Riley · J. Christodoulou
Discipline of Child & Adolescent Health, Sydney Medical School, University of Sydney, Sydney, NSW, Australia

L. G. Riley · J. Christodoulou
Genetic Metabolic Disorders Research Unit, The Children's Hospital at Westmead, KRI, Sydney, NSW, Australia

A. Vasudevan · C. Kiraly-Borri
Genetic Services of Western Australia, King Edward Memorial Hospital, Perth, WA, Australia

M. J. Cowley · V. Gayevskiy · C. M. Sue
Kinghorn Centre for Clinical Genomics, Garvan Institute of Medical Research, Sydney, NSW, Australia

C. M. Sue
Department of Neurogenetics, Kolling Institute of Medical Research, University of Sydney, Royal North Shore Hospital, Sydney, NSW, Australia

C. Edwards · E. Edkins
PathWest Laboratory Medicine WA, Section of Diagnostic Genomics, QEII Medical Centre, Nedlands, WA, Australia

R. Junckerstorff
PathWest Laboratory Medicine WA, Section of Neuropathology, Royal Perth Hospital, Perth, WA, Australia

R. Junckerstorff
School of Pathology and Laboratory Medicine, University of Western Australia, Perth, WA, Australia

P. Rowe
Department of Neurology, Princess Margaret Hospital, Perth, WA, Australia

P. Rowe
State Child Development Centre, West Perth, WA, Australia

J. Christodoulou
Neurodevelopmental Genomics Research Group, Murdoch Children's Research Institute, Melbourne, VIC, Australia

J. Christodoulou
Department of Paediatrics, Melbourne Medical School, University of Melbourne, Melbourne, VIC, Australia

autophagy regulator implicated in the formation of autolysosomes, were identified as the genetic cause of Vici syndrome. The eight key features outlined above are highly predictive of *EPG5* involvement, with pathogenic *EPG5* mutations identified in >90% of cases where six or more of these features are present. The manifestation of all eight features has a specificity of 97% and sensitivity of 89% for *EPG5*-related Vici syndrome. Nevertheless, substantial clinical overlap exists with other multisystem disorders, in particular congenital disorders of glycosylation and mitochondrial disorders. Clinical and pathological findings suggest Vici syndrome as a paradigm of congenital disorders of autophagy, a novel group of inherited neurometabolic conditions linking neurodevelopment and neurodegeneration due to primary autophagy defects.

Here we describe the diagnostic odyssey in a 4-year-old boy whose clinical presentation with multisystem manifestations including skeletal myopathy mimicked a mitochondrial disorder. A genetic diagnosis of Vici syndrome was made through whole genome sequencing which identified compound heterozygous variants in *EPG5*. We also review the myopathic presentation and morphological characterisation of previously reported cases.

Introduction

Vici syndrome [OMIM242840] is a severe, progressive, neurodevelopmental disorder caused by recessively inherited mutations in the key autophagy *EPG5* (ectopic P-granules autophagy protein 5) gene (Cullup et al. 2013). This multisystem disorder is classically characterised by the five cardinal features of callosal agenesis, cataracts, cardiomyopathy, combined immunodeficiency and oculocutaneous hypopigmentation (McClelland et al. 2010). Since its original description in 1988 (Vici et al. 1988), the phenotypic spectrum has continued to evolve with an increasing number of patients described and approximately 50 genetically confirmed cases reported to date (Vici et al. 1988; Al-Owain et al. 2010; Chiyonobu et al. 2002; Cullup et al. 2013; del Campo et al. 1999; Finocchi et al. 2012; McClelland et al. 2010; Miyata et al. 2007; Ozkale et al. 2012; Rogers et al. 2011; Said et al. 2012; Ehmke et al. 2014; Byrne et al. 2016a). These five manifestations in addition to three features recently described to occur almost universally in affected patients, namely, profound developmental delay, progressive failure to thrive and acquired microcephaly, are highly supportive of the diagnosis (Byrne et al. 2016a). The manifestation of all eight of these features has a specificity of 97% and a sensitivity of 89% for the presence of *EPG5* mutations (Byrne et al. 2016b).

Additional variable multisystem involvement, not infrequently observed in individual patients, include sensorineural hearing loss (McClelland et al. 2010), unilateral lung hypoplasia (Al-Owain et al. 2010), skeletal myopathy (Said et al. 2012), mild dysmorphism with coarse facial features, full lips and macroglossia resembling those observed in lysosomal storage disorders (Cullup et al. 2013; Byrne et al. 2016a), congenital midline defects such as cleft lip or palate, thymic aplasia and/or hypospadias (Vici et al. 1988), hydronephrosis, renal dysfunction and renal tubular acidosis (Miyata et al. 2007; Byrne et al. 2016a), thyroid agenesis and dysfunction (Cullup et al. 2013) and idiopathic thrombocytopenic purpura (ITP) (Huenerberg et al. 2016).

The identification of *EPG5* encoding a key autophagy regulator (ectopic P-granules autophagy protein 5) as the genetic cause of Vici syndrome (Cullup et al. 2013) has implicated an intriguing link between the autophagy pathway with neurodevelopmental and neurodegenerative features in this paradigm of a human multisystem disorder (Byrne et al. 2016b). Autophagy is an evolutionarily highly conserved intracellular degradative process that delivers cytoplasmic materials to the lysosome for degradation, playing a fundamental role in maintaining cellular homeostasis (Jiang and Mizushima 2014) and defence against infections (Schmid and Munz 2007). Autophagy has also emerged as a key regulator of cardiac and skeletal muscle homeostasis and functional remodelling (Sandri 2010; Portbury et al. 2011). An associated skeletal muscle myopathy as part of the syndrome has been described in detail by McClelland and colleagues in 2010 (McClelland et al. 2010) and subsequently confirmed in other reports (Al-Owain et al. 2010; Finocchi et al. 2012; Said et al. 2012; Byrne et al. 2016b).

We present the diagnostic odyssey in a patient with a multisystem disorder (profound psychomotor retardation, epilepsy, agenesis of corpus callosum, soft dysmorphism, visual impairment, liver dysfunction and microvesicular steatosis) and a predominant neuromuscular phenotype with skeletal muscle myopathy that was suggestive of a mitochondrial respiratory chain disorder.

Materials and Methods

Clinical Summary

The male patient was born to a non-consanguineous couple of English-Australian and Filipino background at 37 weeks of pregnancy with a birth weight of 2.32 kg (3rd–10th percentiles) and head circumference of 32.5 cm (3rd percentile). The antenatal history was unremarkable apart from two episodes of urinary tract infections at 12 and 18 weeks. He was discharged home a few days after birth, however re-presented at 3 weeks with feeding difficulties

when he was weaned off breast-feeding to bottle feeds. He subsequently displayed poor weight gain and had occasional episodes of choking on feeds despite various attempts to address the issue including changing formulas, teats and feeding bottles. He was referred to the Princess Margaret Hospital at 4 months because of failure to thrive. He was unable to fix or follow and had marked central hypotonia with diminished deep tendon reflexes. Ophthalmology assessment by video evoked potentials and electroretinogram identified impairment of the visual pathways bilaterally. Newborn hearing screen and formal audiometry with transient evoked otoacoustic emissions and tympanogram at 5 months were all normal. He developed tonic and myoclonic seizures at 4 months which were refractory to treatment with levetiracetam, oxcarbazepine and clonazepam. Griffith's Mental Development Scale examination performed at 5 months demonstrated global developmental delay, and he showed no evidence of functional vision. He scored the following subquotients: locomotor 15 days, personal and social 12 days, hearing and language 27 days, and eye and hand coordination unscorable and performance 1¾ months. His mother had two older children from a previous relationship, one of whom had a history of unilateral hearing loss.

Significant feeding intolerance and gastroesophageal reflux improved with elemental feeds and anti-reflux medication. He was initially fed through a nasogastric tube and was subsequently changed to gastrostomy feeds. He experienced frequent respiratory infections which were partly caused by his inability to control salivary secretions. He had progressive microcephaly with head circumference at 14 months at 43.5 cm (<3rd percentile), myopathic facies with a tented upper lip and bilateral partial ptosis. Facial dysmorphism included plagiocephaly, a flat nasal bridge, arched eyebrows, high arched plate and mild retrognathia (Fig. 1a, b). His ears were cupped, and the helices were overfolded over the vertical aspect. He had tapered fingers and mild bilateral fifth finger clinodactyly. Skin hypopigmentation was not overtly evident in the first 2–3 years of life; however by 4 years of age, a few macules were observed over his face and back of neck (Fig. 1a, b).

His brain MRI showed complete agenesis of the corpus callosum, colpocephaly with a high riding 3rd ventricle and disproportionate prominence of the occipital horns of the lateral ventricles, periventricular leukomalacia and delayed myelination as evidenced by little internal capsule myelination (Fig. 2a, b). He had decreased muscle tone and deep tendon reflexes. He was commenced on oral coenzyme Q 10, vitamin C, riboflavin, thiamine and carnitine. Liver histopathology and electron microscopy examination at 6 months showed prominent microvesicular steatosis within hepatocytes with fine cytoplasmic vacuolation and PAS-positive, diastase-sensitive glycogen demonstrated within the hepatocytes, in amounts compatible with the patient's age. Muscle biopsy from the right vastus lateralis muscle showed features consistent with a myopathic process with increased variability in fibre size, marked type 1 fibre predominance and small type 2 fibres. Staining for utrophin was positive in the muscle fibres. Dystrophin, sarcoglycans, alpha- and beta-dystroglycan, dysferlin, merosin, emerin,

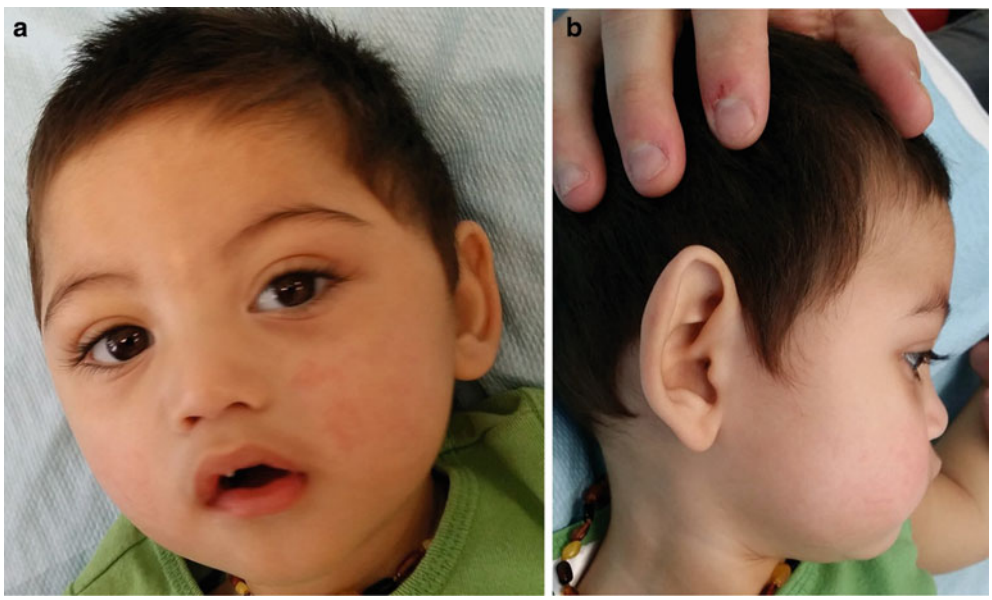

Fig. 1 Photographs showing facial dysmorphism. (**a**) Frontal view: flat nasal bridge, arched eyebrows, high arched plate and hypopigmented macule over glabella. (**b**) Right lateral view: plagiocephaly, a flat nasal bridge, mild retrognathia, cupped ears with overfolded helices over the vertical aspect and hypopigmented macule over posterolateral aspect of his neck

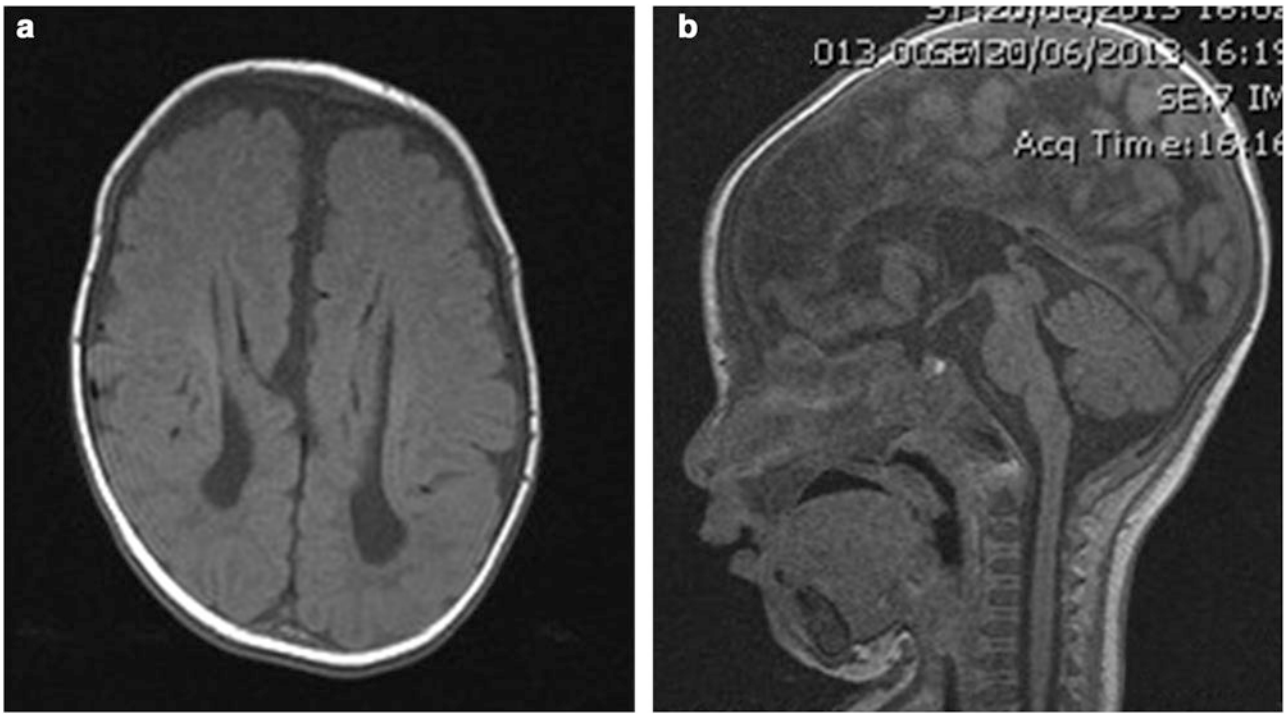

Fig. 2 MRI of the brain at 4 months of age. (**a**) Axial view: complete agenesis of the corpus callosum, colpocephaly with a high riding 3rd ventricle and disproportionate prominence of the occipital horns of the lateral ventricles, periventricular leukomalacia and delayed internal capsule myelination. (**b**) Sagittal view: complete agenesis of the corpus callosum and high riding 3rd ventricle

collagen VI and caveolin-3 immunohistology were normal. Muscle enzyme histochemistry for NADH- tetrazolium reductase (NADH-TR), succinate dehydrogenase and cytochrome oxidase was normal. Acid phosphatase stain showed patchy sarcoplasmic positivity in several fibres, and the spectrin stain displayed occasional vacuoles in few fibres. There was granular sarcoplasmic positivity for p62 in many fibres. Immunohistochemistry for LC3 was not performed as this stain was not available in our laboratory. Electron microscopy showed increased variability in fibre size with a few atrophic fibres showing redundant basal lamina. Increased intermyofibrillar lipid was observed in many fibres, some of which were associated with mild to moderately pleomorphic mitochondria. Several fibres showed aggregates of autophagic vacuoles (Fig. 3). A mitochondrial disorder was considered a possible differential diagnosis. Liver and muscle respiratory chain enzymology (RCE) were normal (Table 1). A summary of muscle morphology in our patient and in other previously reported cases is summarised in Table 2.

Laboratory investigations performed showed elevated creatine kinase 1,020 U/L (ref range 25–220), blood lactate 7.3 mmol/L (ref range < 2.1), pyruvate 0.15 mmol/L (ref range < 0.12), lactate/pyruvate ratio 48 (ref range 14–28), liver enzymes (ALT 134 U/L (ref < 60), ALT 74 U/L (ref < 35)) and plasma alanine 582 umol/L (ref range 143–439). Alphafetoprotein, CSF lactate 1.3 mmol/L (ref range 0.7–1.8) and pyruvate 0.08 mmol/L (ref range 0.03–0.10), ammonia, plasma acylcarnitine profile, urine amino and organic acid screens, serum transferrin, apolipoprotein C III isoforms, serum uric acid, plasma very-long-chain fatty acids, plasma phytanic acids, white blood cell lysosomal enzymes, serum 7-dehydrocholesterol, urine succinylpurines, purines, pyrimidines, polyols and oligosaccharides, CSF lactate, pyruvate, glucose and glycine and fibroblast pyruvate dehydrogenase enzymology were all normal. Immune workup including immunoglobulin levels, white cell counts and lymphocyte subsets were normal, suggesting normal humoral and cellular immune functions. Echocardiography performed at 4 years of age was normal. Genetic studies including chromosomal microarray, mitochondrial DNA sequencing in muscle and fibroblasts, *POLG* gene mutation analysis, targeted exome sequencing using an absent speech multigene panel which investigates overlapping conditions presenting with global developmental delay predominantly affecting the speech (*ANKRD11*,

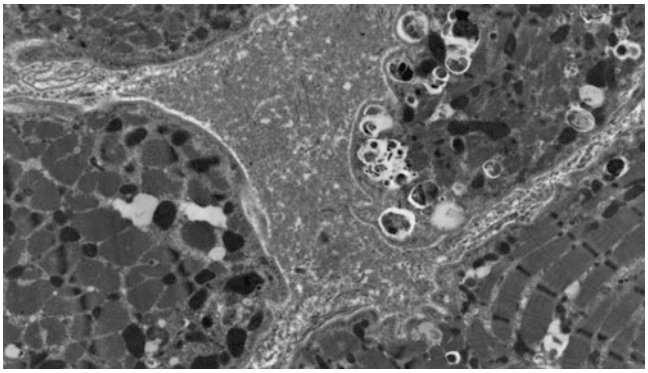

Fig. 3 Muscle electron microscopy. Aggregates of autophagic vacuoles in a muscle fibre

Table 1 Respiratory chain enzyme activities for patient 1

	Enzyme activity		CS ratio (%)	
Assay	Muscle	Liver	Muscle	Liver
Complex I (nmol/min/mg)	**84** (*19–72*)	**26** (*7.8–11.2*)	200	202
Complex II (nmol/min/mg)	**112** (26–63)	**93** (*54–73*)	249	109
Complex II + III (nmol/min/mg)	46 (30–76)		100	
Complex III (min/mg)	46.1 (12.8–50.9)	**15.5** (5.2–10.3)	158	146
Complex IV (min/mg)	8.06 (3.3–9.1)	0.56 (*0.45–0.87*)	122	**59**
Citrate synthase (nmol/min/mg)	**227** (85–179)	**38** (*26–31*)	176	–

Expressed relative to protein and as % residual activity relative to citrate synthase (CS)
Values outside the normal range are shown in bold. Reference ranges are shown in brackets

ARX, *ATRX*, *CDKL5*, *CNTNAP2*, *DYRK1A*, *EEF1A2*, *EHMT1*, *FOLR1*, *FOXG1*, *FRAXA*, *FRAXE*, *GRIN2A*, *HERC2*, *L1CAM*, *MBD5*, *MECP2*, *MEF2C*, *NRXN1*, *OPHN1*, *PCDH19*, *PNKP*, *SETBP1*, *SLC9A6*, *TCF4*, *UBE3A* and *ZEB2*) and whole exome sequencing results were non-contributory.

At 4 years, he remains profoundly delayed, hypotonic, non-ambulatory with only partial head control and non-verbal. He has significant failure to thrive, progressive microcephaly and refractory seizures. His electroencephalogram (EEG) at 4 years of age has remained abnormal with frequent epileptiform discharges, electroclinical seizures, asynchronous background with high amplitude slow waves and superimposed slightly faster frequencies at times. His electroencephalogram (EEG) at 4 years of age has remained abnormal with frequent epileptiform discharges, which continue to be maximal in the parietal regions. Sharp waves are often asynchronous, whilst the background at times is also asynchronous with high amplitude slow waves and superimposed slightly faster frequencies at times which may occur over either hemisphere. Epileptiform activity was seen throughout the recording. Brief relative decrements are seen of less than 1-s duration. Electroclinical seizures were also noted, and the video recording of the first demonstrated a brisk extensor-type movement of the upper limbs. This was associated with a reduction in the background amplitude and an admixture of frequencies. Compared to the interictal background, there was an increase in the amount of faster frequencies. A second event of slightly longer duration was associated with video showing movement with shaking of the head followed by extension of the upper limb and then movement of the head from side to side. The EEG correlate is of decrement with an increase in faster beta activity of 2–3 s duration followed by a posteriorly dominant rhythm of around 8 Hz with greater amplitude in the right hemisphere with an admixture of faster frequencies lasting for a further 3–4 s. Some nonspecific movement for 1 s was followed by a further brief relative decrement before the recording returns to the interictal state. The asynchronous EEG recorded on several occasions over the first 4 years of life is in keeping with absence of the corpus callosum. Repeat ophthalmology

Table 2 Summary of muscle morphology in our patient and in other previously reported cases

	Our patient	del Campo et al. (1999) – Case 4	Chiyonobu et al. (2002)		Miyata et al. (2007)		McClelland et al. (2010)	Al-Owain et al. (2010)	Rogers et al. (2011)		Finocchi et al. (2012)	Said et al. (2012)	Ozkale et al. (2012)	Ehmke et al. (2014)	Byrne et al. (2016a, b)	Hedberg-Oldfors et al. (2017)
			Sibling 1	Sibling 2	Sibling 1	Sibling 2			Sibling 1	Sibling 2						
Global delay	+	+	+	+	+	+	+	+	+	+	+	+	+	+	+	+
Hypotonia	+	+	+	+	+	+	+	+	+	+	+	+	+	+	+	+
Elevated CK	+	NA	+	+	+	+	CK normal	NA	NA	NA	+	+	+	+	+	+
Summary of muscle pathology	+	+	ND	ND	ND	ND	+	+	–	ND	+	+	ND	ND	16/17 patients	+
Increased fibre size variability																
Type 1 fibre predominance	+	NA					NA	+	–		+	+			5/17 patients	NA
Internalised/central nuclei	+	–					+	+	–		+	+			12/17 patients	+
Vacuoles	+	+					–	+	–		–	–			12/17 patients	+
Increased glycogen content	+	–					+	+	–		–	+			7/17 patients	+
Mitochondrial pathology	+	+					+	+	–		+	+			9/17 patients	+
Increased number of autophagosomes	–	–					–	–	–		–	–			1/17 patients	+
Exocytosis	+	–					+	–	–		–	–			1/17 patients	–
Autophagic vacuoles with sarcolemmal features	+														2/17 patients	–
p62-positive inclusions	+	ND					ND	ND	ND		ND	ND			2 patients	+
High expression of foetal and embryonic MyHC	–	ND					ND	ND	ND		ND	ND			ND	+
Respiratory chain enzyme studies	N	N					N	ND	ND		ND	N			3/8 patients: reduced complexes I, III and IV 2 patients, reduced complex IV 1 patient	ATPase activity – 259 nmol/min/mg protein ($N > 415$)

N normal, *ND* not done, *NA* not available

assessment at 4.5 years revealed impaired vision with absence of defensive blink and failure to react to visual stimuli, which was attributed to a cortical cause. His right optic disc was noted to be pale. No cataracts or ocular albinism were observed.

Respiratory Chain Enzyme Activities

Respiratory chain enzyme activities were assayed in patient skeletal muscle and liver as previously described (Frazier and Thorburn 2012).

Whole Genome Sequencing

Whole genome sequencing was performed at the Kinghorn Centre for Clinical Genomics (Garvan Institute, Sydney) on genomic DNA extracted from blood collected from the patient and his parents as previously described (Riley et al. 2017).

cDNA Synthesis Studies

RNA was obtained from white blood cell that had been cultured for 3–5 days with RMPI 1640, foetal calf serum, heparin, and glutamine together with phytohaemagglutinin (PHA). At the end of the culture period, cycloheximide was added, for 4–6 h before harvesting to inhibit nonsense-mediated decay. RNA was extracted using a QIAGEN RNeasy kit and kept at −80°C until cDNA was synthesised.

cDNA was made from 300 ng total RNA with poly dT and SuperScript III. PCR reactions were carried out with specific exonic primers designed to exclude known SNVs.

Results

Whole genome sequencing was undertaken on the patient and his parents to provide a genetic diagnosis. We identified compound heterozygous variants in *EPG5* Chr18(GRCh37): g.43456196C>T, c.4327C>T, p.Gln1443* and g.43487925G>A, c.6049+5G>A. Neither variant was present in ExAC. *EPG5* encodes ectopic P-granules autophagy protein 5 homologue (*C. elegans*), a large (2,579 amino acids) coiled coil domain containing protein that functions in autophagy. Variants in *EPG5* have been associated with Vici syndrome. The c.4327C>T variant in exon 24 introduces a premature stop codon, p.Gln1443*. The mRNA produced is most likely targeted for nonsense-mediated decay as the variant occurs in exon 24 of 44 of *EPG5* (Popp and Maquat 2016). The c.6049+5G>A variant is predicted to affect splicing, reducing the strength of the donor site by ~25% (14–52% across five prediction programmes, Alamut Visual). No candidates were identified within genes in the MitoCarta2.0 database (Calvo et al. 2015) or the mitochondrial genome. cDNA studies (Fig. 4) have confirmed that the c.6049+5G>A variant results in an out of frame deletion (exon 35 spliced out) that is expected to result in a truncated protein or nonsense-mediated RNA decay (Fig. 4).

Discussion

The *EPG5* gene, on chromosome 18q12.3, encodes the key autophagy regulator ectopic P-granules autophagy protein 5 (*EPG5*), a protein of 2,579 amino acids, and is predominantly expressed in the CNS, skeletal and cardiac muscle, thymus, immune cells, lungs and kidneys (Halama et al. 2007), tissues which are all involved in Vici syndrome. *EPG5* was initially identified amongst a group of genes found to be mutated in breast cancer tissue (Sjoblom et al. 2006) before Cullup and colleagues elucidated its causative role in Vici syndrome (Cullup et al. 2013).

Autophagy is an evolutionarily conserved lysosomal pathway that degrades intracellular constituents. It begins with the initial formation of isolation membranes or phagophores which subsequently envelop the portion of cytoplasm to be removed, forming autophagosomes that subsequently fuse with lysosomes resulting in autolysosomes. The *EPG5* protein has been implicated in the late step of autophagy in human cells involving autophagosome-lysosome fusion (Cullup et al. 2013) and, ultimately, impaired cargo delivery to the lysosome (Byrne et al. 2016b).

The ubiquitous expression of *EPG5* during embryonic development and physiologically enhanced autophagy in neurons and muscle likely explains the prominent central nervous system and neuromuscular involvement in Vici syndrome (Byrne et al. 2016a). The prominent feature of agenesis of the corpus callosum, often associated with colpocephaly and other brain malformations including neuronal migration and myelination defects, cerebellar vermis dysplasia, pontine hypoplasia and abnormalities of the septum pellucidum in patients with Vici syndrome, suggests that aberrant autophagy during foetal development adversely affects CNS development (Cullup et al. 2013). This suggestion is supported by the demonstration of increased neuronal proliferation and severe neural tube defects in mice with null mutations in *AMBRA1*, a positive autophagy regulator with predominant expression in neural tissues (Fimia et al. 2007; Cullup et al. 2013). Interestingly, the progressive loss of skills and profound acquired microcephaly in children surviving beyond infancy suggest a neurodegenerative component in addition to the prominent neurodevelopmental defects (Ebrahimi-Fakhari et al. 2016). Supporting this idea is the neurodegenerative phenotype in *Epg5*-deficient mice, with selective neuro-

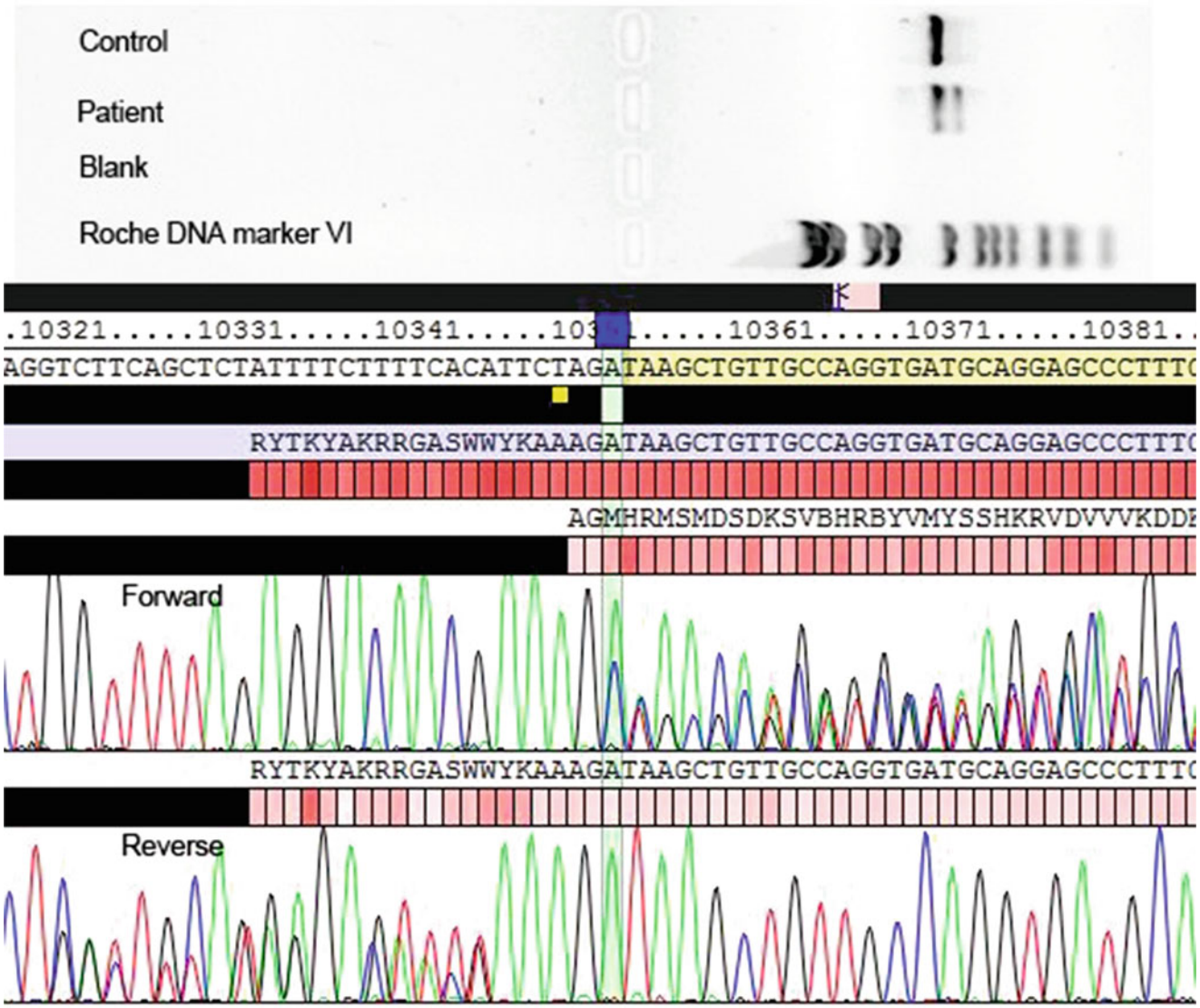

Fig. 4 cDNA sequencing studies. Exon 35 is missing in both forward and reverse directions, confirming that the c.6049+5G>A variant results in an out of frame deletion that is expected to result in a truncated protein or nonsense-mediated RNA decay

degeneration of cortical and spinal cord motor neurons resembling amyotrophic lateral sclerosis (Zhao et al. 2013) and the neurodegenerative phenotype in *Epg5*-deficient *Drosophila melanogaster* (Byrne et al. 2016b). These dual effects of defective autophagy on cellular development and maintenance (Byrne et al. 2016b) place *EPG5*-related Vici syndrome within a novel subclass of inborn errors of metabolism termed 'congenital disorders of autophagy', wherein dysregulated autophagy results in early-onset neurodevelopmental and neurodegenerative disorders (Ebrahimi-Fakhari et al. 2016).

Skeletal muscle myopathy, an important, less documented feature of Vici syndrome, had previously been suggested by the presence of profound hypotonia, generalised weakness, paucity of movements and variable elevations of creatine kinase in early case reports (Chiyonobu et al. 2002; Miyata et al. 2007) and morphological abnormalities in muscle biopsy in one reported patient that were suggestive of a mitochondrial cytopathy but with normal respiratory chain enzyme analysis (del Campo et al. 1999). Histopathologically, the associated myopathic features were subsequently documented in detail in an infant with a neuromuscular phenotype, characterised by increased variability in fibre size with type 1 fibre hypotrophy and normally sized type 2 fibres (potentially fulfilling the criteria for fibre type disproportion), prominent centralised nuclei in atrophic fibres, increased glycogen storage and variable vacuoles on light microscopy. Electron microscopy revealed redundant basal lamina and some small areas of debris between duplicated basal lamina

around several small fibres suggesting exocytosis, enlarged mitochondria with abnormal cristae and areas of membrane glycogen which may relate to degenerating mitochondria. Additional findings of increased Gomori trichrome and abnormal oxidative stains in some small fibres, increased lipid content and the suggestive electron microscopy also raised the possibility of a mitochondrial cytopathy; however, this was not supported by CSF and plasma lactate levels which were normal, as were respiratory chain enzyme activities (McClelland et al. 2010). In a separate study, skeletal myopathy was confirmed in 17 patients on pre-mortem muscle biopsy which was corroborated by evidence of myopathy on EMG/nerve conduction studies in six patients (Byrne et al. 2016a).

Morphologically, considerable overlap exists with primary neuromuscular disorders that have been linked to defects in the autophagic pathway, in particular centronuclear myopathies (Jungbluth and Gautel 2014) and vacuolar myopathies including Pompe disease, Danon disease (Malicdan and Nishino 2012) and X-linked myopathy with excessive autophagy (XMEA) (Ramachandran et al. 2013), glycogen storage disorders and mitochondrial myopathies (Byrne et al. 2016b). Whilst *EPG5*-related skeletal muscle myopathy has been defined as a primary vacuolar myopathy based on the presence of vacuoles visible on both light and electron microscopy, vacuoles can be absent or inconspicuous (Byrne et al. 2016a) as observed in our patient. Other prominent morphological features of myopathy in Vici syndrome include marked variability in fibre size with type 1 predominance and atrophy, increase in internal and centralised nuclei and increased glycogen storage on light microscopy (Byrne et al. 2016a). Ultrastructural examination by electron microscopy reveals altered mitochondrial morphology and variable degrees of subsarcolemmal accumulation of autophagic vacuoles, glycogen and mitochondria (Byrne et al. 2016a; Hedberg-Oldfors et al. 2017). Additional findings include reddish Gomori trichrome staining of atrophic fibres suggesting mitochondrial abnormalities and variably increased acid phosphatase staining (Byrne et al. 2016a). Immunofluorescence studies in skeletal muscle tissue showed upregulation of sarcomere-associated autophagy proteins (p62/SQSTM1), lysosome-associated membrane protein (LAMP2) (Byrne et al. 2016a; Hedberg-Oldfors et al. 2017) and NBR1 with numerous LC3-positive autophagosomes, potentially reflecting impaired autophagic flux (Cullup et al. 2013). The observation of variable respiratory chain enzyme abnormalities (Byrne et al. 2016a; Hedberg-Oldfors et al. 2017), in addition to abnormalities of mitochondrial internal structure and positioning reported in earlier studies (McClelland et al. 2010; Al-Owain et al. 2010; Finocchi et al. 2012), supports secondary mitochondrial dysfunction as a possible downstream effect of defective autophagy (Byrne et al. 2016a, b) and likely reflects the evolutionarily conserved role of the autophagy pathway in maintaining mitochondrial quality and function (Zhang et al. 2007). Defective autophagy has also been implicated in secondary mitochondrial dysfunction in various neuromuscular disorders (Katsetos et al. 2013).

In our patient, the compilation of histopathological features, including patchy sarcoplasmic positivity on acid phosphatase staining, electron microscopic findings of aggregates of sarcoplasmic autophagic vacuoles in several fibres and the increase in autophagy marker protein p62 in many fibres, is consistent with perturbed autophagy. Characterisation of autophagy in Vici syndrome revealed a wide spectrum of abnormalities, making it a paradigm for a human multisystem disorder associated with defective autophagy (Cullup et al. 2013; Ebrahimi-Fakhari et al. 2016). To further delineate if the increased p62/SQSTM1 and NBR1 levels are reflective of enhanced upstream induction or downstream clearance in autophagic flux, patient-derived and healthy control fibroblasts were treated with autophagy inducer rapamycin and inhibitor bafilomycin which suppresses the autolysosomal H+ ATPase required for acidification and subsequent degradation of lysosomal contents. The results precluded defects in the early steps in autophagy, including autophagosome formation and processing of LC3-I to LC3-II. Autophagosomal clearance was however impaired as demonstrated by decreased colocalisation of LC3 and NBR1 with LAMP1, indicative of reduced fusion of autophagosomes with lysosomes. This was further corroborated by accumulation of lysine-63-polyubiquitinated proteins, which are usually destined for autolysosomal degradation (Cullup et al. 2013). Deranged transcriptional regulation was observed with altered phosphorylation in the AKT-mTOR protein kinase pathway, a major pathway controlling the expression of autophagy proteins (Cullup et al. 2013). In retrospect, these histopathological features are consistent with previous studies suggestive of defective autophagy (Al-Owain et al. 2010; McClelland et al. 2010; Cullup et al. 2013), as demonstrated by the prominence of autophagic vacuoles, storage of abnormal material, secondary mitochondrial abnormalities in skeletal muscle and multisystem defects in the heart, immune system, skin pigmentation and central nervous system, implicating autophagy in a wide range of cellular processes (Cullup et al. 2013).

Our patient had histopathological and electron microscopic findings in muscle consistent with a myopathic process, with associated mitochondrial pleomorphism and aggregates of autophagosomes, making mitochondrial cytopathy a likely differential. In conjunction with his multisystemic clinical presentation with a predominant neuromuscular phenotype, biochemical parameters of lactic acidemia, elevated plasma alanine and raised lactate/pyruvate ratio, he was classified as being in the "probable" category of a mitochondrial respiratory chain defect based

on the modified Nijmegen criteria (http://mitochondrialdiseases.org/fmm/docs/CLINICAL%20CRITERIA.pdf) after exclusion of other differential diagnoses. In retrospect, several features of Vici syndrome were manifested in the patient; however due to the absence of a few cardinal findings including cardiomyopathy, cataracts and combined immunodeficiency, Vici syndrome had not been considered as a potential differential. This case highlights the utility of next-generation sequencing technologies including whole genome sequencing in providing a genetic diagnosis for complex rare diseases, particularly when the clinical phenotype does not conform in entirety to our current knowledge of a specific disorder. The emergence of rapid and more widely available next-generation DNA sequencing technology has not only led to the identification of novel diseases but will potentially contribute to the expansion of the phenotypic spectrum of known rare genetic disorders.

In conclusion, *EPG5*-related Vici syndrome is a paradigm of an emerging class of neurometabolic disorders termed 'congenital disorders of autophagy' as it highlights the consequences of dysfunctional autophagy and indicates an intriguing link between neurodevelopment and neurodegeneration. Substantial overlap exists with other multisystem disorders including mitochondrial disease, congenital disorders of glycosylation and lysosomal and glycogen storage disorders (Byrne et al. 2016b). Further characterisation of the phenotypic spectrum of Vici syndrome will enhance genetic diagnosis of the disorder which is imperative in facilitating genetic counselling and prenatal diagnosis. Similarly, exploring the associated secondary mitochondrial dysfunction observed in Vici syndrome could further facilitate our insights into the role of autophagy in maintaining mitochondrial quality and function (Ebrahimi-Fakhari et al. 2016).

Acknowledgements This research was supported by a New South Wales Office of Health and Medical Research Council Sydney Genomics Collaborative grant (CS and JC). We also gratefully acknowledge donations to JC by the Crane and Perkins families as well as the participation of the research subjects.

Key Messages

- A male patient presented with clinical features resembling a mitochondrial disorder including profound developmental delay, visual impairment, epilepsy and skeletal myopathy
- Two novel *EPG5* variants identified on WGS
- Muscle morphological studies showed increased variability of fibre size, rare internalised nuclei, mitochondrial abnormalities and aggregates of autophagosomes
- Considerable overlap exists between *EPG5*-related Vici syndrome and mitochondrial disorders

Details of the Contributions of Individual Authors

SB drafted the manuscript and was involved in the clinical management and diagnostic workup of the patient with AV, CK-B and PR. LR, MC, VG, CS, CE, EE and JC performed/supervised/interpreted molecular workup. All authors have read/critically revised the manuscript.

Compliance with Ethical Standards

Conflict of Interest

SB, LR, AV, MC, VG, TR, CS, RJ, CK and PR declare they have no conflict of interest. JC is a communicating editor of the Journal of Inherited Metabolic Disease.

Ethics

All procedures followed in this study were in accordance with the ethical standards of the responsible committee on human experimentation (institutional and national) and with the Helsinki Declaration of 1964, and its later amendments, and this project was approved by the Sydney Children's Hospitals Network Human Research Ethics Committee (reference number 10/CHW/113). Informed consent was obtained for all participants included in the study.

References

Al-Owain M, Al-Hashem A, Al-Muhaizea M et al (2010) Vici syndrome associated with unilateral lung hypoplasia and myopathy. Am J Med Genet A 152A(7):1849–1853

Byrne S, Jansen L, U-King-Im JM et al (2016a) EPG-related Vici syndrome: a paradigm of neurodevelopmental disorders with defective autophagy. Brain 139(3):765–781

Byrne S, Vici CD, Smith L et al (2016b) Vici syndrome: a review. Orphanet J Rare Dis 11:21

Calvo S, Clauser K, Mootha V (2015) MitoCarta2.0: an updated inventory of mammalian proteins. Nucleic Acids Res 44: D1251–D1257

Chiyonobu T, Yoshihara T, Fukushima Y (2002) Sister and brother with Vici syndrome: agenesis of the corpus callosum, albinism, and recurrent infections. Am J Med Genet 109(1):61–66

Cullup T, Kho AL, Dionisi-Vici C et al (2013) Recessive mutations in EPG5 cause Vici syndrome, a multisystem disorder with defective autophagy. Nat Genet 45(1):83–87

del Campo M, Hall BD, Aeby A et al (1999) Albinism and agenesis of the corpus callosum with profound developmental delay: Vici syndrome, evidence for autosomal recessive inheritance. Am J Med Genet 85(5):479–485

Ebrahimi-Fakhari D, Saffari A, Wahlster L et al (2016) Congenital disorders of autophagy: an emerging novel class of inborn errors of neuro-metabolism. Brain 139(Pt 2):317–337

Ehmke N, Parvaneh N, Krawitz P et al (2014) First description of a patient with Vici syndrome due to a mutation affecting the penultimate exon of EPG5 and review of the literature. Am J Med Genet A 164A(12):3170–3175

Fimia GM, Stoykova A, Romagnoli A et al (2007) Ambra1 regulates autophagy and development of the nervous system. Nature 447:1121–1125

Finocchi A, Angelino G, Cantarutti N et al (2012) Immunodeficiency in Vici syndrome: a heterogeneous phenotype. Am J Med Genet A 158A(2):434–439

Frazier A, Thorburn D (2012) Biochemical analyses of the electron transport chain complexes by spectrophotometry. Methods Mol Biol 837:49–62

Halama N, Grauling-Halama SA, Beder A et al (2007) Comparative integromics on the breast cancer associated gene KIAA1632: clues to a cancer antigen domain. Int J Oncol 31:205–210

Hedberg-Oldfors C, Darin N, Oldfors A (2017) Muscle pathology in Vici syndrome – a case study with a novel mutation in EPG5 and a summary of the literature. Neuromuscul Disord 27(8):771–776

Huenerberg K, Hudspeth M, Bergmann S et al (2016) Two cases of Vici syndrome associated with Idiopathic Thrombocytopenic Purpura (ITP) with a review of the literature. Am J Med Genet A 170A(5):1343–1346

Jiang P, Mizushima N (2014) Autophagy and human diseases. Cell Res 24:69–79

Jungbluth H, Gautel M (2014) Pathogenic mechanisms in centronuclear myopathies. Front Aging Neurosci 6:339

Katsetos CD, Koutzaki S, Melvin JJ (2013) Mitochondrial dysfunction in neuromuscular disorders. Semin Pediatr Neurol 20:202–215

Malicdan MC, Nishino I (2012) Autophagy in lysosomal myopathies. Brain Pathol 22:82–88

McClelland V, Cullup T, Bodi I et al (2010) Vici syndrome associated with sensorineural hearing loss and evidence of neuromuscular involvement on muscle biopsy. Am J Med Genet A 152A (3):741–747

Miyata R, Hayashi M, Sato H et al (2007) Sibling cases of Vici syndrome: sleep abnormalities and complications of renal tubular acidosis. Am J Med Genet A 143(2):189–194

Ozkale M, Erol I, Gumus A, Ozkale Y, Alehan F (2012) Vici syndrome associated with sensorineural hearing loss and laryngomalacia. Pediatr Neurol 47(5):375–378

Popp MW, Maquat LE (2016) Leveraging rules of nonsense-mediated mRNA decay for genome engineering and personalized medicine. Cell 165(6):1319–1322

Portbury AL, Willis MS, Patterson C (2011) Tearin' up my heart: proteolysis in the cardiac sarcomere. J Biol Chem 286: 9929–9934

Ramachandran N, Munteanu I, Wang P et al (2013) VMA21 deficiency prevents vacuolar ATPase assembly and causes autophagic vacuolar myopathy. Acta Neuropathol 125:439–457

Riley LG, Cowley MJ, Gayevskiy V et al (2017) A SLC39A8 variant causes manganese deficiency, and glycosylation and mitochondrial disorders. J Inherit Metab Dis 40(2):261–269

Rogers CR, Aufmuth B, Monesson S (2011) Vici syndrome: a rare autosomal recessive syndrome with brain anomalies, cardiomyopathy, and severe intellectual disability. Case Rep Genet 2011:1. https://doi.org/10.1155/2011/421582

Said E, Soler D, Sewry C (2012) Vici syndrome-a rapidly progressive neurodegenerative disorder with hypopigmentation, immunodeficiency and myopathic changes on muscle biopsy. Am J Med Genet A 158A(2):440–444

Sandri M (2010) Autophagy in skeletal muscle. FEBS Lett 584:1411–1416

Schmid D, Munz C (2007) Innate and adaptive immunity through autophagy. Immunity 27:11–21

Sjoblom T, Jones S, Wood LD et al (2006) The consensus coding sequences of human breast and colorectal cancers. Science 314:268–274

Vici CD, Sabetta G, Gambarara M et al (1988) Agenesis of the corpus callosum, combined immunodeficiency, bilateral cataract, and hypopigmentation in two brothers. Am J Med Genet 29(1):1–8

Zhang Y, Qi H, Taylor R et al (2007) The role of autophagy in mitochondria maintenance: characterization of mitochondrial functions in autophagy-deficient S. cerevisiae strains. Autophagy 3:337–346

Zhao H, Zhao YG, Wang X, Xu L et al (2013) Mice deficient in Epg5 exhibit selective neuronal vulnerability to degeneration. J Cell Biol 200:731–741

JIMD Reports
DOI 10.1007/8904_2017_73

RESEARCH REPORT

Compound Heterozygous Inheritance of Mutations in *Coenzyme Q8A* Results in Autosomal Recessive Cerebellar Ataxia and Coenzyme Q_{10} Deficiency in a Female Sib-Pair

Jessie C. Jacobsen · Whitney Whitford · Brendan Swan · Juliet Taylor · Donald R. Love · Rosamund Hill · Sarah Molyneux · Peter M. George · Richard Mackay · Stephen P. Robertson · Russell G. Snell · Klaus Lehnert

Received: 24 September 2017 / Revised: 29 October 2017 / Accepted: 02 November 2017 / Published online: 21 November 2017

Abstract Autosomal recessive ataxias are characterised by a fundamental loss in coordination of gait with associated atrophy of the cerebellum. There is significant clinical and genetic heterogeneity amongst inherited ataxias; however, an early molecular diagnosis is essential with low-risk treatments available for some of these conditions. We describe two female siblings who presented early in life with unsteady gait and cerebellar atrophy. Whole exome sequencing revealed compound heterozygous inheritance of two pathogenic mutations (p.Leu277Pro, c.1506+1G>A) in the coenzyme Q8A gene (*COQ8A*), a gene central to biosynthesis of coenzyme Q (CoQ). The paternally derived p.Leu277Pro mutation is predicted to disrupt a conserved motif in the substrate-binding pocket of the protein, resulting in inhibition of CoQ_{10} production. The maternal c.1506+1G>A mutation destroys a canonical splice donor site in exon 12 affecting transcript processing and subsequent protein translation. Mutations in this gene can result in primary coenzyme Q_{10} deficiency type 4, which is characterized by childhood onset of cerebellar ataxia and exercise intolerance, both of which were observed in this sib-pair. Muscle biopsies revealed unequivocally low levels of CoQ_{10}, and the siblings were subsequently established on a therapeutic dose of CoQ_{10} with distinct clinical evidence of improvement after 1 year of treatment. This case emphasises the importance of an early and accurate molecular diagnosis for suspected inherited ataxias, particularly given the availability of approved treatments for some subtypes.

Communicated by: Johan Lodewijk Karel Van Hove, MD, PhD

Electronic supplementary material: The online version of this article (https://doi.org/10.1007/8904_2017_73) contains supplementary material, which is available to authorized users.

J. C. Jacobsen · W. Whitford · B. Swan · R. G. Snell (✉) · K. Lehnert
Centre for Brain Research, School of Biological Sciences, The University of Auckland, Auckland, New Zealand
e-mail: r.snell@auckland.ac.nz

J. Taylor
Genetic Health Service New Zealand, Auckland City Hospital, Auckland, New Zealand

D. R. Love
Diagnostic Genetics, LabPLUS, Auckland City Hospital, Auckland, New Zealand

R. Hill
Department of Neurology, Auckland City Hospital, Auckland, New Zealand

S. P. Robertson
Dunedin School of Medicine, University of Otago, Dunedin, New Zealand

S. Molyneux · P. M. George · R. Mackay
Canterbury Health Laboratories, Christchurch, New Zealand

Introduction

Individuals with autosomal recessive cerebellar ataxia (ARCA) present with considerable clinical diversity but fundamentally have an inability to coordinate movement and balance due to cerebellar dysfunction. Individuals are typically diagnosed in childhood or as young adults (<30 years of age), with cerebellar atrophy visible by MRI (Montero et al. 2007). While categorisation of clinical entities has improved with the identification of the genetic basis for many of these conditions, there is still substantial

genetic heterogeneity, making diagnosis challenging and an efficient molecular diagnosis difficult. However, the importance of a precise genetic diagnosis (enabling discrimination between the many types of autosomal recessive ataxias) has been underlined by the realisation that a minority of these disorders can be effectively treated with pharmacotherapy, resulting in significant improvement in health.

The advent of next generation sequencing technologies has tremendously enhanced the efficiency of molecular diagnosis for complex and highly heterogeneous neurodevelopmental disorders such as the inherited ataxias, providing answers for families, facilitating family planning and occasionally presenting the prospect of treatment strategies. We have applied this approach to identify the genetic basis for an ARCA caused by a deficiency in CoQ_{10} synthesis, resulting in a treatment strategy for a family 9 years after symptom onset.

Cases

We describe a family with two girls who presented primarily with gait ataxia and cerebellar atrophy. There was no known consanguinity between the two Caucasian parents, and their family history was non-contributory. The proband (II.1) was born after an uncomplicated pregnancy and delivery at term. She sat, rolled and crawled at appropriate ages but only succeeded in walking, unsteadily, with a walker at 2 years and 6 months, and her gait remains unsteady at her current age of 11 years. She presented primarily with dysmetria (with no clonus); however there has been no discernable deterioration since her diagnosis. She is not dysmorphic, but does have reduced muscle bulk and tone. Her reflexes are normal, and she has no visual disturbance or nystagmus. MRI at 2 years and 2 months showed a small cerebellar vermis but normal height of the cerebellar hemispheres (Fig. 1a). A repeat MRI at 7 years and 9 months showed prominent cerebellar sulci, with a loss of height of the cerebellar hemispheres, and atrophy of the vermis (Fig. 1b). Both scans revealed a normal brainstem, including the pons.

The proband's sister (II.2) demonstrated a similar course, with truncal ataxia preventing walking until 3 years of age. At 2 years and 2 months, MRI revealed a small cerebellar vermis and increased spaces between the folia especially in the inferior cerebellum (Fig. 1c). The height of the cerebellar hemispheres was normal, and the brainstem and pons appeared normal. The proband also has a younger brother (III.3) who shows no clinical abnormalities at 3 years of age.

The metabolic workup for both girls has been extensive with no abnormalities in plasma cholesterol, plasma albumin, transferrin isoelectric focussing, plasma and urinary amino acids, urinary organic acids, cerebrospinal fluid (CSF) neurotransmitters and CSF lactate. Comparative genomic hybridisation (Agilent ISCA (v2)) revealed no significant imbalance. Liver mitochondrial enzymology was considered normal, and muscle mitochondrial enzymology revealed complex II + III to be low (reflecting the enzymatic deficiency later proposed by genetics – full mitochondrial analysis can be found in Supplementary Table 1). Electron microscopy analysis of the same muscle tissue showed no evidence of giant abnormal mitochondria. Other fine structures were unremarkable. Initial genetic investigations by Sanger sequencing ruled out mutations in

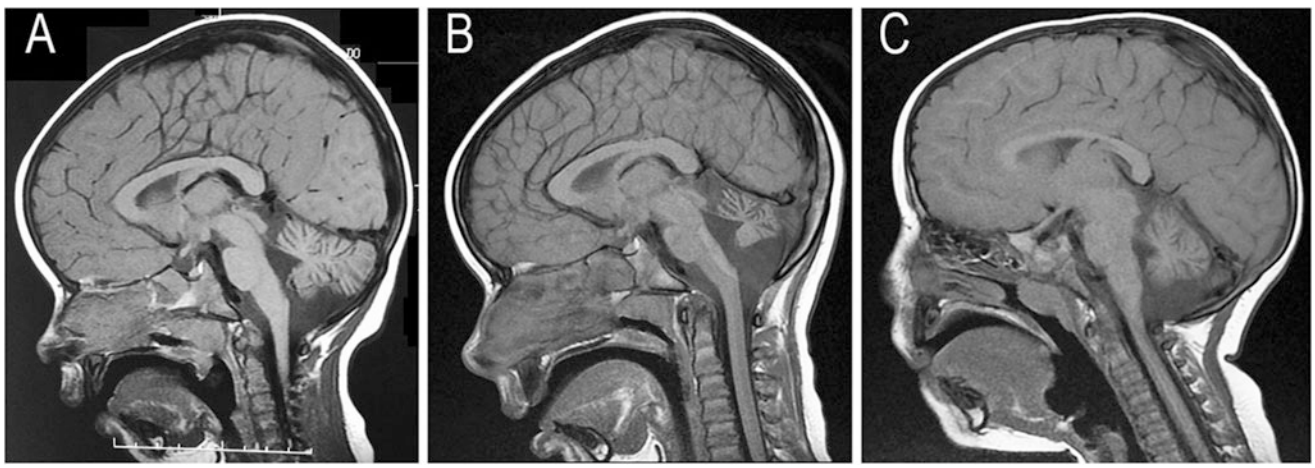

Fig. 1 T1-weighted midline sagittal MRI scans of the two siblings with *COQ8A* mutations. (**a**) Scan of the oldest sibling at 2 years and 2 months of age demonstrating a small cerebellar vermis; (**b**) follow-up scan of the older sibling at age 7 years and 9 months demonstrating progressive loss of volume of the cerebellar vermis and thinning of the folia consistent with an atrophic mechanism underlying her ataxic presentation; (**c**) scan of the younger sibling at age 2 years and 2 months demonstrating moderate volume loss in the cerebellar vermis and increased spaces between the folia

APTX, and no causative triplet repeat expansions were identified in *FRDA*, *ATXN1*, *ATXN2*, *ATXN3*, *CACNA1A*, *ATXN7*, *TBP*, and *ATN1*. We subsequently performed whole exome sequencing on both affected siblings (Supplementary Methods).

Variation filtering identified the presence of two single nucleotide variants (SNVs) in *COQ8A* (coenzyme Q8A, previous symbol *ADCK3* (AARF domain-containing kinase 3); NM_020247.4, OMIM 606980) in both affected children (Table 1). Sanger sequencing of parental DNA confirmed compound heterozygous inheritance of these variants. Mutations in *COQ8A* result in coenzyme Q_{10} deficiency, primary, 4 (COQ10D4, OMIM 612016), an autosomal recessive disorder characterized by childhood onset of cerebellar ataxia and exercise intolerance (Lagier-Tourenne et al. 2008), which is phenotypically concordant with this family's presentation.

The paternally derived SNV encodes a non-synonymous missense change from leucine to proline (c.830T>C, p.Leu277Pro) in exon 6. This amino acid is conserved in vertebrates from human to lamprey (UCSC (Kent et al. 2002), PhyloP (Pollard et al. 2010); Supplementary Figure 1) and is located in an N-terminal motif that is conserved across all members of the AARF domain-containing kinase family: the KxGK motif (positions 276–279) (Lagier-Tourenne et al. 2008). The variant has been previously observed in heterozygote state in a single European individual in the gnomAD dataset (AF = 4.48–06) (Lek et al. 2016). This variant is predicted to be damaging by mutation impact prediction algorithms (PolyPhen-2, SIFT Blink, SNPs&GO, PROVEAN, full details in Supplementary Table 2).

The maternally derived SNV alters the canonical splice donor site in exon 12 (c.1506+1G>A); this mutation has not been reported previously and is absent in public variant databases. BDGP splice site and ASSP programmes predict that this variant will destroy the splice donor site of exon 12, which is expected to affect removal of intron 12 from all reported protein-coding isoforms. The effect of the c.1506+1G>A splice site mutation was determined using RNA sequencing (Supplementary Methods) on blood obtained from both parents. No significant abundance differences were observed between the parents for any annotated *COQ8A* protein-coding transcript (200,000 vs. 190,926 FPKM, $p = 0.43$ for canonical transcript NM_020247.4). However, all mRNA molecules originating from the maternal c.1506+1G>A allele retained all or part of intron 12; conversely, intron 12 was correctly spliced in all mRNAs originating from the mother's wild-type allele and both paternal alleles. RNAseq fragments derived from the maternal wild-type allele were twice as abundant as those from the c.1506+1G>A allele (52 vs. 25 fragments). Mutation haplotypes and parental inheritance were validated by PCR followed by Sanger sequencing (Fig. 2).

Following the discovery of the *COQ8A* variants, muscle and plasma total CoQ_{10} were measured using high-performance liquid chromatography with electrochemical detection, similarly to Tang et al. (2001). The muscle CoQ_{10} was mildly reduced in II.1 (16.3 ± 3.4 nmol/g tissue, reference range 20–70 nmol/g wet tissue) when compared to biopsies from myopathy patients not suspected of CoQ_{10} deficiencies and previously published reference intervals (Lopez et al. 2006). Plasma CoQ_{10} was reported as low-normal (0.68 μmol/L, 0.52 μmol/L in II.1 and II.2, respectively; reference range 0.45–1.71 μmol/L), which is consistent with the literature on biosynthetic CoQ_{10} defects (Molyneux et al. 2005, 2008; Yubero et al. 2014).

The siblings underwent treatment with oral CoQ_{10} (20 mg/kg/day, (Blumkin et al. 2014)) and follow-up was performed at 12 months. Use of a validated clinical tool for the assessment of ataxia (Trouillas et al. 1997) was instituted to objectively measure the effect of treatment. The scale is scored 0–100 with a score of 0 signifying no ataxic symptoms and 100 indicating a maximal score. The proband's baseline score was 40/100, and after treatment for 12 months, the score had reduced to 29/100 (full ataxia assessment is detailed in Supplementary Table 3). The parents of the child also reported an improvement in energy and classroom performance, observations that were reinforced when teachers, blinded to the deliberate omission of daily doses of CoQ_{10}, volunteered their observations of discernible deterioration in function over the school day. The younger sibling also demonstrated an improvement in ataxia score from 49/100 to 43/100 over the same time frame as her sister.

Discussion

Autosomal recessive ataxias due to primary CoQ_{10} deficiency are a heterogeneous group of disorders caused by mutations in genes involved in the CoQ_{10} biosynthetic

Table 1 *COQ8A* variant annotations

Gene	Chr	HGVS DNA ref	HGVS protein ref	Variant type	Predicted effect	Genotype
COQ8A	1	NM_020247.4:c.830T>C	NM_020247.4:p.(Leu277Pro)	Missense	Aa change	Heterozygous
COQ8A	1	NG_012825.2:c.1506+1G>A	NG_012825.2:p.(=)	Splice donor	Destroys splice site	Heterozygous

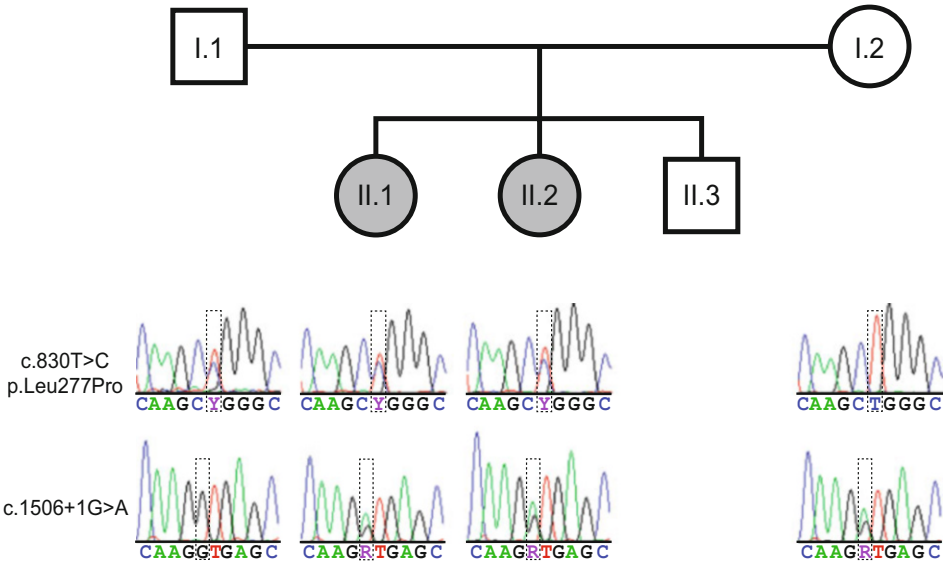

Fig. 2 Family pedigree and transmission of the c.830T>C and c.1506+1G>A mutations in the COQ8A gene. Sanger sequencing electropherograms for both loci are shown below the corresponding family member in the lower part of the figure

pathway (Desbats et al. 2015). Coenzyme Q_{10} acts as an electron carrier in the mitochondrial respiratory chain and serves as an antioxidant in the intracellular environment (Crane et al. 1993); hence there has been much clinical interest in its potential therapeutic benefits. Indeed, therapeutic doses of CoQ_{10} have been successful in ameliorating symptoms for some cases of primary CoQ_{10} deficiency ataxias (Mignot et al. 2013). We describe compound heterozygous mutations in *COQ8A*, a gene central to the CoQ_{10} biosynthetic pathway, in two female siblings who presented with gait ataxia and cerebellar atrophy. The older sibling had moderately decreased muscle CoQ_{10} and both underwent a trial of CoQ_{10}. Remarkably, both siblings showed improvement in their ataxia scores following 12 months of treatment, with functional improvements also evident in daily classroom performance.

Causative mutations in the *COQ8A* gene were first reported in childhood ataxia by Lagier-Tourenne in 2001 who proposed the term autosomal recessive cerebellar ataxia 2 (ARCA2) after observing cerebellar atrophy and exercise intolerance during childhood with an associated reduction of muscle CoQ_{10} (Lagier-Tourenne et al. 2008). *COQ8A* encodes an unorthodox protein kinase-like (uPKL) protein that localises to the mitochondrial matrix and is central to CoQ biosynthesis (Khadria et al. 2014; Stefely et al. 2016). The deletion of the yeast and *E. coli* homologues eliminates CoQ biosynthesis in these organisms (Poon et al. 2000; Do et al. 2001), and a mouse *COQ8A* knockout model exhibits an ataxic phenotype and pathological signatures that align with the human condition (including degeneration of cerebellar Purkinje cells and abnormal skeletal mitochondria morphology) (Stefely et al. 2016). The structure of the protein was originally described by Stefely et al. as an UbiB protein with an atypical protein kinase-like fold containing particular features inhibitory to protein kinase activity (Stefely et al. 2015). More recently, they provide evidence that the protein encoded by *COQ8A* functions similar to yeast Coq8p and further argue that it is in fact an uPKL with noncanonical activities which support CoQ biosynthesis (amongst other functions) (Stefely et al. 2016).

Atypical kinase COQ8A, mitochondrial, features a long N-terminal extension, which folds into α-helices to form a KxGQ motif which appears to play a central role in CoQ biosynthesis, as mutating the region results in autophosphorylation and inhibition of CoQ production in vivo (Stefely et al. 2015, 2016). The p.Leu277Pro mutation identified in this New Zealand family is located in one of the predicted alpha helical domains (GQα2), which contribute to the KxGQ motif. The well-described tendency of proline to distort and destabilise alpha helices in aqueous environments (Khan and Vihinen 2007) suggests that the mutation affects protein stability, as demonstrated for other known pathogenic mutations in the GQα2 helix (Stefely et al. 2015).

The second mutation, c.1506+1G>A, destroys the splice donor site in exon 12 resulting in retention of intron 12 leading to premature termination of COQ8A protein synthesis, ultimately resulting in reduced CoQ_{10} levels. Primary cell lines from an ACRA2 patient harbouring similar mutations to the case described here (splice and missense) showed reduced protein and total CoQ_{10} levels and exhibited ultrastructural changes to the mitochondria (Cullen et al. 2016).

Some patients with primary CoQ_{10} synthesis defects respond to supplementation with high-dose oral CoQ_{10} (Desbats et al. 2015); however, patients with *COQ8A* mutations show a somewhat varied response, with many not responding well (Lamperti et al. 2003; Aure et al. 2004; Lagier-Tourenne et al. 2008; Mollet et al. 2008; Anheim et al. 2010; Gerards et al. 2010; Horvath et al. 2012; Terracciano et al. 2012; Mignot et al. 2013; Blumkin et al. 2014; Liu et al. 2014; Barca et al. 2016; Hikmat et al. 2016; Malgireddy et al. 2016), as summarised in Supplementary Table 4. There have, however, been three reported cases of improvement, two of which are later onset than the girls presented here. The latest, reported by Barca et al., showed improvement in speech and gait in a 48-year man (onset at 20 years of age) after 1 year of treatment with 400 mg/day CoQ_{10} (Barca et al. 2016). This individual harbours a homozygous deletion (c.1511_1512delCT) that leads to a premature truncation of the protein (p. Ala504fs). This mutation is located 5 bp from the splice site mutation described in our New Zealand sib-pair, both of which reside in the protein kinase domain. Another study by Liu et al. reported improvement in a Pakistani sib-pair (age of onset: 10 years of age), who harbour a homozygous frameshift mutation (c.1844_1845insG) in the C-terminus of mitochondrial atypical kinase COQ8A, which is predicted to extend the open reading frame by 81 amino acids (Liu et al. 2014). These siblings showed significant improvements in myoclonic movements, ataxic gait and dysarthric speech 3 months after treatment with CoQ_{10} at 200 mg twice a day. The third reported case of improvement describes partial improvement in motor skills balance and strength at 5 years of age with 20 mg/kg/day oral CoQ_{10} (Blumkin et al. 2014). When the drug was ceased at 6 years of age (pre-empted by the patient who had an accompanying psychiatric condition), their condition deteriorated. This individual and her sister (milder presentation) harbour compound heterozygous mutations in the protein kinase domain (p.P502R), near the site disrupted by the splice site mutation described here, and a previously observed deletion at c.1750_1752delACC. There are also some self-reported improvements from patients on oral CoQ_{10} (Mollet et al. 2008; Liu et al. 2014). The sib-pair described here provides further evidence of the therapeutic benefits of CoQ_{10} for this condition in some families.

This case outlines the clinical and genetic heterogeneity of autosomal recessive ataxias and highlights the importance of early and accurate diagnosis (in this instance using whole exome sequencing). This seems particularly prudent given the possible response to a low-risk treatment option that could be given prior to severe central nervous system damage.

Acknowledgements We would like to thank Kristine Boxen at the Auckland Science Analytical Services for Sanger sequencing services and the New Zealand eScience Infrastructure for high-performance computing support.

Take-Home Message

Compound heterozygous *COQ8A* mutations cause treatment-responsive CoQ_{10} deficiency ataxia.

Contributions of Individual Authors

JCJ, KL and RGS designed and conducted experiments and wrote the manuscript; WW and BS conducted experiments; JT, DRL and RH clinically confirmed research results; SPR clinically evaluated patients and conducted the trial of CoQ_{10} treatment; SM, PMG and RM performed muscle and plasma CoQ_{10} analysis.

Corresponding Author

Professor Russell Snell.

Competing Interest Statement

JCJ, WW, BS, JT, DRL, RH, SM, PMG, RM, SPR, RGS and KL declare they have no conflict of interest.

Details of Funding

JCJ is supported by a Rutherford Discovery Fellowship from the New Zealand Government and administered by the Royal Society of New Zealand; SPR is supported by Curekids NZ. The research was funded by the Neurological Foundation of New Zealand, the University of Auckland and the Minds for Minds Charitable Trust.

Details of Ethics Approval

The study was approved by the New Zealand Northern B Health and Disability Ethics Committee (ref 12/NTB/59), and parents provided written informed consent.

Patient Consent Statement

All procedures followed were in accordance with the ethical standards of the responsible committee on human experimentation (institutional and national) and with the Helsinki Declaration of 1975, as revised in 2000. Informed consent was obtained from all patients for being included in the study.

References

Anheim M, Fleury M, Monga B et al (2010) Epidemiological, clinical, paraclinical and molecular study of a cohort of 102 patients affected with autosomal recessive progressive cerebellar ataxia from Alsace, Eastern France: implications for clinical management. Neurogenetics 11:1–12

Aure K, Benoist JF, Ogier de Baulny H, Romero NB, Rigal O, Lombes A (2004) Progression despite replacement of a myopathic form of coenzyme Q10 defect. Neurology 63:727–729

Barca E, Musumeci O, Montagnese F et al (2016) Cerebellar ataxia and severe muscle CoQ10 deficiency in a patient with a novel mutation in ADCK3. Clin Genet 90:156–160

Blumkin L, Leshinsky-Silver E, Zerem A, Yosovich K, Lerman-Sagie T, Lev D (2014) Heterozygous mutations in the ADCK3 gene in siblings with cerebellar atrophy and extreme phenotypic variability. JIMD Rep 12:103–107

Crane FL, Sun IL, Sun EE (1993) The essential functions of coenzyme Q. Clin Investig 71:S55–S59

Cullen JK, Abdul Murad N, Yeo A et al (2016) AarF domain containing kinase 3 (ADCK3) mutant cells display signs of oxidative stress, defects in mitochondrial homeostasis and lysosomal accumulation. PLoS One 11:e0148213

Desbats M, Lunardi G, Doimo M, Trevisson E, Salviati L (2015) Genetic bases and clinical manifestations of coenzyme Q10 (CoQ10) deficiency. J Inherit Metab Dis 38:145–156

Do TQ, Hsu AY, Jonassen T, Lee PT, Clarke CF (2001) A defect in coenzyme Q biosynthesis is responsible for the respiratory deficiency in Saccharomyces cerevisiae abc1 mutants. J Biol Chem 276:18161–18168

Gerards M, van den Bosch B, Calis C et al (2010) Nonsense mutations in CABC1/ADCK3 cause progressive cerebellar ataxia and atrophy. Mitochondrion 10:510–515

Hikmat O, Tzoulis C, Knappskog PM et al (2016) ADCK3 mutations with epilepsy, stroke-like episodes and ataxia: a POLG mimic? Eur J Neurol 23:1188–1194

Horvath R, Czermin B, Gulati S et al (2012) Adult-onset cerebellar ataxia due to mutations in CABC1/ADCK3. J Neurol Neurosurg Psychiatry 83:174–178

Kent WJ, Sugnet CW, Furey TS et al (2002) The human genome browser at UCSC. Genome Res 12:996–1006

Khadria AS, Mueller BK, Stefely JA, Tan CH, Pagliarini DJ, Senes A (2014) A Gly-zipper motif mediates homodimerization of the transmembrane domain of the mitochondrial kinase ADCK3. J Am Chem Soc 136:14068–14077

Khan S, Vihinen M (2007) Spectrum of disease-causing mutations in protein secondary structures. BMC Struct Biol 7:56

Lagier-Tourenne C, Tazir M, López LC et al (2008) ADCK3, an ancestral kinase, is mutated in a form of recessive ataxia associated with coenzyme Q10 deficiency. Am J Hum Genet 82:661–672

Lamperti C, Naini A, Hirano M et al (2003) Cerebellar ataxia and coenzyme Q10 deficiency. Neurology 60:1206–1208

Lek M, Karczewski KJ, Minikel EV et al (2016) Analysis of protein-coding genetic variation in 60,706 humans. Nature 536:285–291

Liu Y-T, Hersheson J, Plagnol V et al (2014) Autosomal-recessive cerebellar ataxia caused by a novel ADCK3 mutation that elongates the protein: clinical, genetic and biochemical characterisation. J Neurol Neurosurg Psychiatry 85:493–498

Lopez LC, Schuelke M, Quinzii CM et al (2006) Leigh syndrome with nephropathy and CoQ10 deficiency due to decaprenyl diphosphate synthase subunit 2 (PDSS2) mutations. Am J Hum Genet 79:1125–1129

Malgireddy K, Thompson R, Torres-Russotto D (2016) A novel CABC1/ADCK3 mutation in adult-onset cerebellar ataxia. Parkinsonism Relat Disord 33:151–152

Mignot C, Apartis E, Durr A et al (2013) Phenotypic variability in ARCA2 and identification of a core ataxic phenotype with slow progression. Orphanet J Rare Dis 8:173

Mollet J, Delahodde A, Serre V et al (2008) CABC1 gene mutations cause ubiquinone deficiency with cerebellar ataxia and seizures. Am J Hum Genet 82:623–630

Molyneux SL, Florkowski CM, Lever M, George PM (2005) Biological variation of coenzyme Q_{10}. Clin Chem 51:455–457

Molyneux SL, Young JM, Florkowski CM, Lever M, George PM (2008) Coenzyme Q10: is there a clinical role and a case for measurement? Clin Biochem Rev 29:71–82

Montero R, Pineda M, Aracil A et al (2007) Clinical, biochemical and molecular aspects of cerebellar ataxia and coenzyme Q10 deficiency. Cerebellum 6:118–122

Pollard KS, Hubisz MJ, Rosenbloom KR, Siepel A (2010) Detection of nonneutral substitution rates on mammalian phylogenies. Genome Res 20:110–121

Poon WW, Davis DE, Ha HT, Jonassen T, Rather PN, Clarke CF (2000) Identification of Escherichia coli ubiB, a gene required for the first monooxygenase step in ubiquinone biosynthesis. J Bacteriol 182:5139–5146

Stefely JA, Reidenbach Andrew G, Ulbrich A et al (2015) Mitochondrial ADCK3 employs an atypical protein kinase-like fold to enable coenzyme Q biosynthesis. Mol Cell 57:83–94

Stefely JA, Licitra F, Laredj L et al (2016) Cerebellar ataxia and coenzyme Q deficiency through loss of unorthodox kinase activity. Mol Cell 63:608–620

Tang PH, Miles MV, DeGrauw A, Hershey A, Pesce A (2001) HPLC analysis of reduced and oxidized coenzyme Q_{10} in human plasma. Clin Chem 47:256–265

Terracciano A, Renaldo F, Zanni G et al (2012) The use of muscle biopsy in the diagnosis of undefined ataxia with cerebellar atrophy in children. Eur J Paediatr Neurol 16:248–256

Trouillas P, Takayanagi T, Hallett M et al (1997) International cooperative ataxia rating scale for pharmacological assessment of the cerebellar syndrome. The Ataxia Neuropharmacology Committee of the World Federation of Neurology. J Neurol Sci 145:205–211

Yubero D, Montero R, Artuch R, Land JM, Heales SJR, Hargreaves IP (2014) Biochemical diagnosis of coenzyme Q(10) deficiency. Mol Syndromol 5:147–155

JIMD Reports
DOI 10.1007/8904_2017_75

RESEARCH REPORT

The Validity of Bioelectrical Impedance Analysis to Measure Body Composition in Phenylketonuria

Maureen Evans · Kay Nguo · Avihu Boneh · Helen Truby

Received: 21 September 2017 / Revised: 07 November 2017 / Accepted: 09 November 2017 / Published online: 24 November 2017

Abstract *Aim*: To compare the measurement of total body water (TBW) and fat-free mass (FFM) using the criterion method of deuterium dilution space (^2H_2O) with bioelectrical impedance analysis (BIA) using a portable QuadScan 4000, Bodystat® in children and adolescents with phenylketonuria (PKU).
Methods: Sixteen patients with PKU, median age is 12.5 (range 5–20.6) years, were recruited into this cross-sectional study. TBW was measured by both deuterium dilution and BIA on the same occasion as per a standard protocol. FFM was estimated from predictive equations.
Results: There was no significant difference between TBW_{Deut} and TBW_{BIA} ($p = 0.344$) or FFM_{Deut} and FFM_{BIA} ($p = 0.111$). TBW_{Deut} and TBW_{BIA} were highly correlated ($r = 0.990$, $p < 0.0001$), as were FFM_{Deut} and FFM_{BIA} ($r = 0.984$, $p < 0.0001$). Bland-Altman plots demonstrated that there was no proportional bias between the criterion method, TBW_{Deut}, and the test method TBW_{BIA}, in estimating TBW ($\beta = -0.056$, adjusted $r^2 = 0.069$, $p = 0.169$) or FFM ($\beta = -0.089$, adjusted $r^2 = 0.142$, $p = 0.083$).
Conclusion: Our results suggest that when compared with the criterion method, the QuadScan 4000, Bodystat® can reliably be used to predict TBW and FFM in patients with PKU. We suggest that due to the portability and non-invasive approach, this method can reliably be used to monitor body composition in the outpatient clinic setting, to further improve the monitoring and assessment of nutritional status in PKU.

Communicated by: Francois Feillet, MD, PhD

M. Evans (✉) · A. Boneh
Department of Metabolic Medicine, Royal Children's Hospital, Melbourne, VIC, Australia
e-mail: maureen.evans@rch.org.au; avihu.boneh@rch.org.au

M. Evans
Department of Nutrition and Food Services, Royal Children's Hospital, Melbourne, VIC, Australia

M. Evans · K. Nguo · A. Boneh · H. Truby
Department of Nutrition, Dietetics and Food, Monash University, Melbourne, VIC, Australia
e-mail: kay.nguo@monash.edu; helen.truby@monash.edu

A. Boneh
Department of Paediatrics, University of Melbourne, Melbourne, VIC, Australia

Introduction

Phenylketonuria (PKU; MIM ID #261600) is a rare inborn error of protein metabolism. Lifelong goals of management are to maintain blood phenylalanine (Phe) levels within a recommended target range associated with optimal neurocognitive outcome and maintain normal growth and development (Singh et al. 2016; van Spronsen et al. 2017). This requires adherence to a diet low in natural protein and supplemented with phe-free L-amino-acid-based formula, to meet estimated protein and micronutrient requirements (van Spronsen et al. 2017). The dietary alterations involved may increase the risk of decreased liner growth (Dobbelaere et al. 2003; Aldámiz-Echevarría et al. 2014), increased prevalence of overweight (Scaglioni et al. 2004; Burrage et al. 2012) with changes in body composition such as higher percentage of body fat (Albersen et al. 2010).

The measurement of body composition is a valuable tool in the evaluation of the effects of modified diets, and in particular protein modified diets, on somatic development (Huemer et al. 2007). The value of body composition

measurement in patients with PKU, in addition to other anthropometric parameters, including BMI and waist circumference, is now acknowledged (Albersen et al. 2010; MacDonald et al. 2011). Of the four body compartments used to assess body composition, fat, water, mineral and protein (dry lean mass), water is the largest component (Wells and Fewtrell 2006). Measuring additional components of body composition beyond just body fat mass is becoming progressively more important in clinical practice with increasing recognition of their effect on health outcomes (Wells and Fewtrell 2006). Multicompartment models, such as dual-energy X-ray absorptiometry (DEXA), that measure body composition are most accurate with good acceptability of measurements but are expensive, require exposure to radioactivity, are used predominantly in specialist research and do not specifically measure total body water (Wells and Fewtrell 2006). Deuterium dilution is a criterion or reference method to measure total body water (TBW) (TBW_{Deut}), and subsequently fat-free mass (FFM) (FFM_{Deut}) can be derived by using well-validated predictive equations (International Atomic Energy Agency 2010). This method is highly technical in its application and as such is not practical as a routine bedside method of measuring body composition and remains a research tool.

Currently there is no agreed or validated method of measuring body composition in PKU, and several methods have been reported, including bioelectrical impedance analysis (BIA) (Dobbelaere et al. 2003; Rocha et al. 2013b), body air-displacement plethysmography using a Bod Pod™ (Albersen et al. 2010), anthropometric skinfold measurements (Allen et al. 1996) and total body electrical conductivity (TOBEC) (Huemer et al. 2007). More recently, it has been recommended that methods such as BIA could be used to monitor longitudinal changes in body compartments in PKU, due to the ease and speed in performing this assessment in the clinical setting (Rocha et al. 2016). However, to date the method of BIA has not been validated for use in children with PKU.

BIA is a rapid, non-invasive, safe and inexpensive method to estimate body composition via accurate estimation of total body water (Böhm and Heitmann 2013; Mulasi et al. 2015). BIA methodology measures impedance to the flow of electrical current through the water component of body cells and uses empirical linear regression models to measure TBW and predict FFM. It offers the advantage of relative simplicity in obtaining results repeatedly with an instrument that is both functionally robust and physically portable. However, there are limitations in its use, particularly in populations with abnormal hydration status and/or 'body geometry' (Mulasi et al. 2015), and it is important that this method be applied critically with consideration of factors that might lead to variable results (Jackson et al. 2013).

The purpose of this study was to compare the performance of a multi-frequency BIA machine (QuadScan 4000, Bodystat®) to measure TBW (TBW_{BIA}) and FFM (FFM_{BIA}), compared with the criterion method, deuterium dilution, in a group of patients with PKU.

Participants and Methods

This study was approved by the RCH Human Research Ethic Committee: HREC #32056D.

Sixteen patients with PKU (seven males, nine females) were recruited after signed consents were obtained from parents and/or participants. All participants had early and continuous treatment with a low-phe diet and phe-free amino acid formula. Patients over 4 years of age and who were continent of urine and who had no known co-morbidities that may affect hydration stats were considered eligible. In this cross-sectional study, all measurements (anthropometric, BIA and urine for deuterium dilution analysis) were collected on the same day for individual patients. Patients were well with no sign of illness or infection. Urine samples were collected, and measurements were taken and recorded by a single experienced practitioner (ME) using a standardised operating procedure. Data were collected between July 2016 and March 2017. Deuterium dilution analysis was performed by a trained technician (KN).

Anthropometry and BIA Measurements

Patients were instructed to eat and drink normally the day prior to measurement but fast from food and fluids from bedtime until the morning of the measurements. These occurred in the patient's home and close to usual waking time after they had voided their bladder. Height was measured to the nearest 0.1 cm using a stadiometer, and weight was measured to the nearest 0.1 kg using a digital weight measuring scale. Participants were in light clothing with no shoes. All anthropometric measurements were expressed as age- and gender-specific z-scores, using the epidemiological software package Epi Info (version 3.5.1), based on the Centres for Disease Control and Prevention (Atlanta, GA) 2002 reference database.

Body composition was then measured by BIA in patients lying in the supine position and with electrodes in the tetrapolar (wrist-ankle) arrangement using the multi-frequency BIA analyser QuadScan 4000, Bodystat® (Isle of White, United Kingdom LTD.) as per the manufacturer's instructions. This analyser measures impedance at 5-, 50-, 100-, and 200-kHz and uses the 50-kHz frequency to predict the value of TBW and FFM. An undisclosed

proprietary equation developed by the manufacturer calculated TBW. The BIA analyser measures FFM using predictive linear regression equations including the equation of Houtkooper for children (Houtkooper et al. 1992). Measurements were taken in duplicate over approximately 1 min. After the measurements, all impedance, water values and lean weight (FFM) values were recorded.

Criterion Method: Deuterium Isotopic Dilution

TBW was measured using the deuterium dilution technique according to the International Atomic Energy Agency standard procedures (International Atomic Energy Agency 2010). The baseline fasting spot urine sample was collected for determination of background isotope enrichment. Participants were then provided a dose of 1:10 dilution of deuterium oxide (99.8 atom % excess; Sercon Ltd., Crewe, UK) following the recommended doses for participants of different body weights. The bottle containing the dose was rinsed with 50 mL tap water to ensure no labelled water remained in the bottle. Patients were advised to drink, eat and move normally after samples had been collected but avoid exercise. A spot mid flow urine sample was collected at 5 h, and total urine output was measured from dosing with the isotope until the end of the 5-h equilibration period. Equilibration is the process whereby the deuterium oxide is evenly mixed throughout the body water resulting in all compartments of body water containing equal concentrations of deuterium. The spot urine samples were stored frozen at −20°C for batch analysis.

Analysis of deuterium enrichment was determined with an Isoprime Dual Inlet Isotope Ratio Mass Spectrometer (Isoprime, Manchester, UK) coupled in-line with a Multiprep-Gilson Autosampler. Hydrogen analyses were completed by an overnight equilibration with hydrogen gas at 40°C using Hokko coils. All samples were analysed in duplicate, and laboratory standards were calibrated using the international standards USGS45, USGS46, and GFLES-4. Results were reported in ‰ (delta per mil units) relative to Standard Mean Ocean Water (SMOW). TBW was calculated assuming that the deuterium oxide space is 4.1% higher than TBW due to exchange of hydrogen with non-aqueous hydrogen in the body. TBW was then converted to fat-free mass using Lohman's age- and sex-specific 'constants' for the hydration of fat-free mass (Lohman 1993).

Statistical Analysis

Shapiro-Wilk's test ($p > 0.05$) was used to explore data distribution. Normally distributed data were examined using Pearson correlation coefficient and Lin's concordance coefficient to evaluate the relationship between TBW and FFM determined by the two methods. Paired samples t-test was used to evaluate the difference between the mean values of TBW_{BIA} and TBW_{Deut} and between the mean values of FFM_{BIA} and FFM_{Deut}. The Bland-Altman method was used to compare two measurements of the same variable and thus used to evaluate agreement between the TBW_{BIA} and TBW_{Deut} and between the FFM_{BIA} and FFM_{Deut}. This method calculated the mean difference between the two methods of measurement (the 'bias') and 95% limits of agreement as the mean difference (1.96 SD). A Bland-Altman plot was then constructed to explore the difference scores of the two measurements against the mean for each subject. To test for proportional bias, a linear regression of difference between measurements on the mean of the measurements was completed. Statistical analyses were performed using SPSS for Windows software version 23 (IBM, Illinois, Chicago, IL). Significance was set at $p < 0.05$. Data are expressed as mean (SD) and median (range).

Results

Participants were 16 patients with PKU (7 males, 9 females). Median age is 12.5 years (range 5–20.6 years). Participants' anthropometric results are summarised in Table 1. Measurements of TBW and FFM taken from the duplicate BIA readings were identical in 14/16 participants and within 1% for 2/16 patients, and the mean of these values was used.

Total Body Water

Values are summarised in Table 1. A Shapiro-Wilk's test ($p > 0.05$) demonstrated that the TBW_{Deut} ($p = 0.098$) and TBW_{BIA} ($p = 0.198$) results were both normally distributed. When comparing the variance in TBW values between those obtained without correcting for urine output during the 5 h after deuterium dosing, i.e. 'uncorrected' and those values obtained after 'correction' for urine output, the difference observed was minimal (median of 1.5%; 0.3–6.6%). Given this small difference, uncorrected values were used in the subsequent analysis. Figure 1a depicts the relationship between TBW_{Deut} and TBW_{BIA} ($r = 0.990$, $p < 0.0001$). Lin's concordance coefficient confirmed the significance of the correlation; Rc = 0.987, 95% CI [0.967–0.995]. One-sample t-test of the difference between TBW_{Deut} and TBW_{BIA} was not significant ($p = 0.344$). Paired samples t-test showed no significant difference between the means of the TBW_{Deut} and the TBW_{BIA} measurements ($p = 0.344$) (Table 1). Variability between

Table 1 Participants' anthropometric characteristics and results summary

Measurement/analyses	Value	*P* value
Weight kg, z-score: median (range)	43.9 (19.6–74.5), 0.42 (−2.58–1.85)	
Height cm, z-score: median (range)	154 (114–171.2), 0.35 (−2.52–1.67)	
BMI, score, z-score: median (range)	18.0 (13.37–26.87), −0.13 (−2.13–1.79)	
Total body water (TBW) kg: mean (SD)	TBW_{Deut} mean 24.08 (±9.37) TBW_{BIA} mean 24.44 (±9.91)	$p = 0.344$
Fat-free mass (FFM) kg: mean (SD)	FFM_{Deut} mean 31.81 (±12.77) FFM_{BIA} mean 32.93 (±13.93)	$p = 0.111$
TBW correlation between methods	TBW_{Deut} and TBW_{BIA}	$p < 0.0001$
Lin's concordance coefficient	TBW_{Deut} and TBW_{BIA}	$Rc = 0.987$
FFM correlation between methods	FFM_{Deut} and FFM_{BIA}	$p < 0.0001$
Lin's concordance coefficient	FFM_{Deut} and FFM_{BIA}	$Rc = 0.969$
Bland-Altman analysis	TBW_{Deut} and TBW_{BIA} FFM_{Deut} and FFM_{BIA}	$p = 0.169$ $p = 0.083$
Shapiro-Wilk's analysis	TBW_{Deut} TBW_{BIA}	$p = 0.098$ $p = 0.198$

TBW_{Deut} and TBW_{BIA} measurements for individuals showed a median of 4.32% with range 0.45–9.1%.

Bland-Altman analysis and subsequent plot of the difference between the TBW measurement and the mean of the TBW measurements is depicted in Fig. 1b. Results indicate that there was no significant proportional bias between the criterion method, TBW_{Deut}, and the test method, TBW_{BIA}, to measure TBW ($\beta = -0.056$, adjusted $r^2 = 0.069$, $p = 0.169$).

Fat-Free Mass Determination

Correlation analysis showed that FFM calculated from BIA correlated significantly with FFM calculated from TBW_{Deut} using the equation FFM = TBW/Hydration coefficient ($r = 0.984$, $p < 0.0001$) (Fig. 2a). Lin's concordance coefficient confirmed the significance of the correlation; Rc = 0.969, 95% CI [0.924–0.988]. One-sample t-test of the difference between FFM_{Deut} and FFM_{BIA} was not significant ($p = 0.111$). Paired samples t-test showed no significant difference between the means of the FFM_{Deut} and the FFM_{BIA} measurements ($p = 0.111$) (see Table 1).

Bland-Altman analysis and plot is depicted in Fig. 2b. Results indicate no proportional bias between the deuterium dilution and BIA methods to measure FFM ($\beta = -0.089$, $r^2 = 0.142$, $p = 0.083$).

Discussion

Anthropometric assessment of height and weight and the subsequent calculation of BMI are valuable clinical tools that monitor growth against standards and allow screening for overweight. However, they are not sufficient on their own for the comprehensive assessment of nutritional status and body composition in health and disease (Battezzati et al. 2003). Longitudinal body composition monitoring in PKU in an outpatient setting may allow individualised nutritional management strategies based on lean body mass rather than the relatively blunt instrument of body weight (MacDonald et al. 2011). It also provides important information in relation to disorder-specific management strategies in the context of overall longer-term good health (Albersen et al. 2010) by enabling a better understanding of the course of an individual's anthropometric and body composition profiles (Rocha et al. 2013a).

The implementation of a reliable, quick and easy method to measure body composition in the outpatient clinic setting would be advantageous for clinicians managing individuals with PKU. Bioelectrical impedance machines are very useful due to their non-invasive nature, safety, ease of use, portability and relatively low cost compared to other clinically available methods of measuring body composition (Mulasi et al. 2015). However, the proprietary and confidential nature of each manufacturer's algorithm equations from which body compartments are derived make it essential that each machine is validated for use in a population of interest. In this study, we compared the performance of the QuadScan 4000, Bodystat® against a criterion method, deuterium dilution, to determine TBW in a group of 16 patients with PKU. As both TBW values determined by deuterium dilution and the impedance values determined by BIA can be used to calculate FFM (Cleary et al. 2008), we compared these methods for the estimation of FFM.

When comparing mean values of both methods, we found no significant difference between TBW_{Deut} and TBW_{BIA} and between FFM_{Deut} and FFM_{BIA}. We also show a significant correlation between TBW_{Deut} and TBW_{BIA} and between FFM_{Deut} and FFM_{BIA}. Bland-Altman analysis

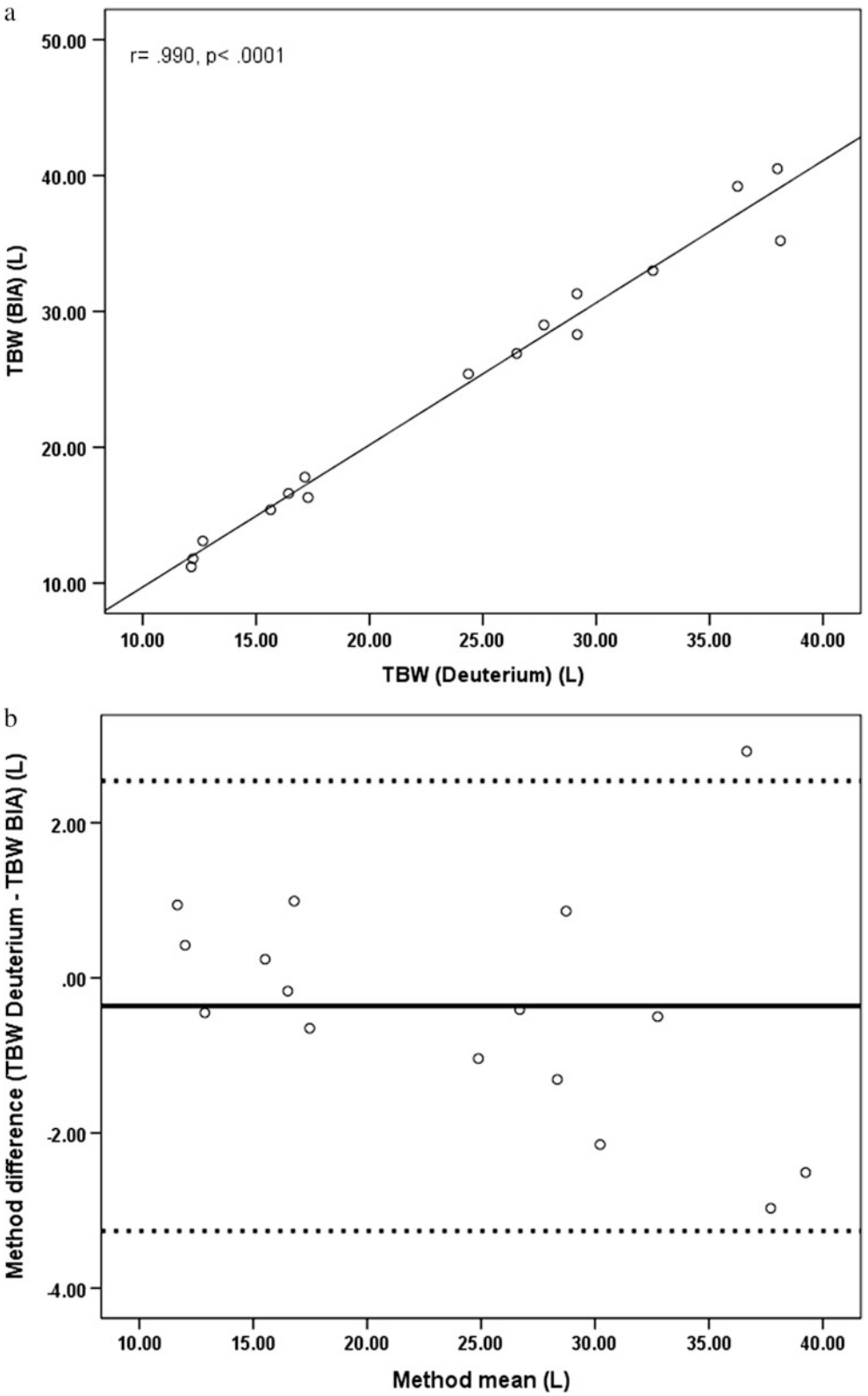

Fig. 1 (**a**) Correlation between TBW calculated from BIA versus TBW calculated from deuterium dilution. (**b**) The solid line indicates the mean; the dashed lines represent the upper (mean + (1.96 SD)) and lower (mean − (1.96 SD)) levels of the 95% CI. Each dot represents the method difference versus the method mean for individuals

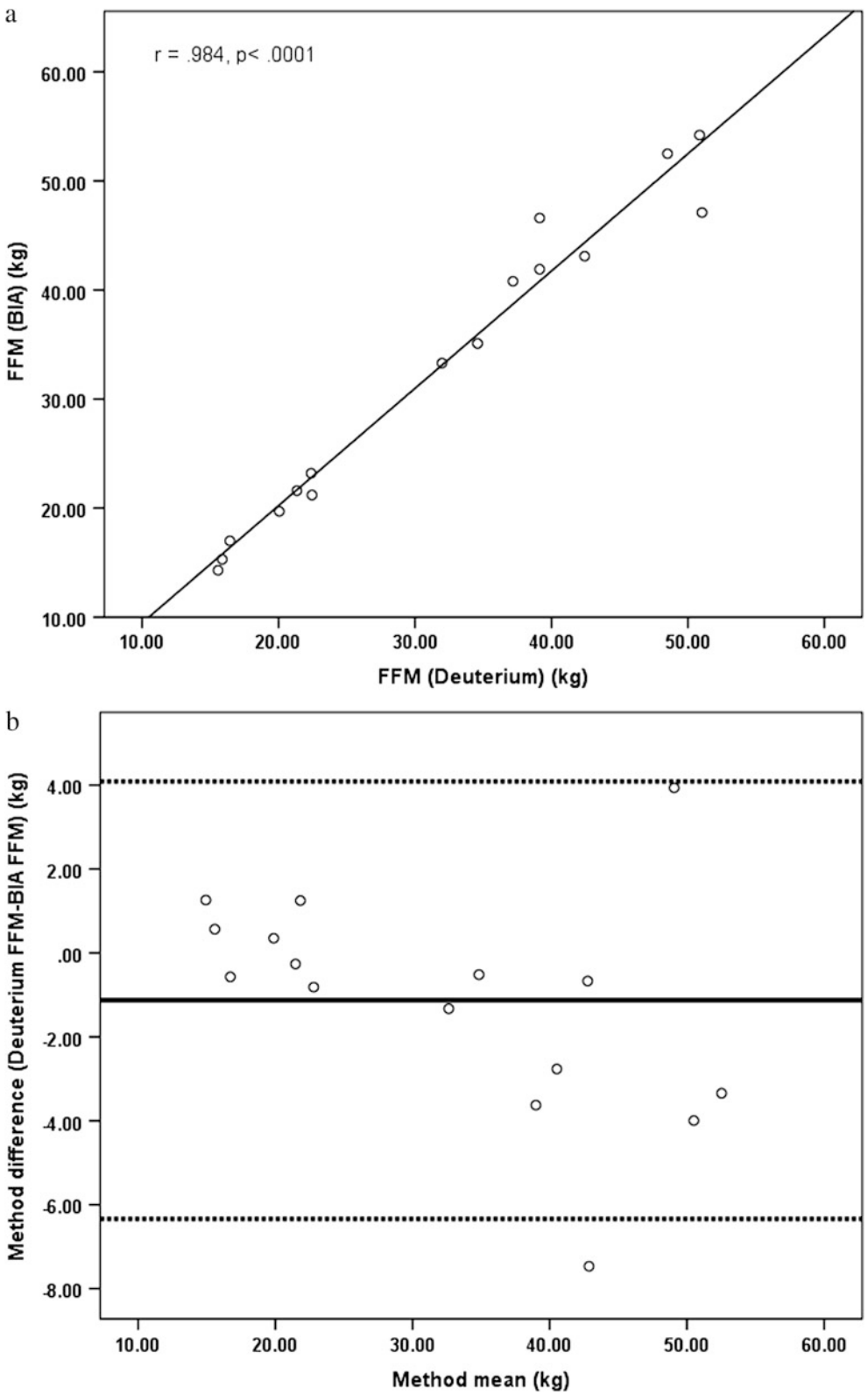

Fig. 2 (**a**) Correlation between FFM calculated from BIA versus FFM calculated from deuterium dilution. (**b**) The solid line indicates the mean; the dashed lines represent the upper (mean + (1.96 SD)) and lower (mean − (1.96 SD)) levels of the 95% CI. Each dot represents the method difference versus the method mean for individuals

confirmed that there was no significant proportional bias between the methods (Martin Bland and Altman 1986), although there slight bias for TBW_{Deut} to be greater than TBW_{BIA} and for FFM_{BIA} to be greater than FFM_{Deut}. Consequently, we conclude that deuterium dilution and BIA using the QuadScan 4000, Bodystat® can be used to measure TBW and estimate FFM in patients with PKU.

We observed individual differences in measurements between TBW_{BIA} and TBW_{Deut}, and three of four participants with the greatest difference were 13- and 14-year-old males who are entering puberty and therefore likely to be undergoing a rapid change in body composition with changes in hydration status and increased FFM deposition. It is possible that because deuterium dose is based on body weight alone, this measurement was not precise enough to account for the potential body composition and hydration status changes in these boys. A study that included individuals of a similar age and pubertal stage may better address this potential issue. However, as the outliers in the difference between the measurements were minimal, this demonstrated a strength in the methods tested.

Other studies have reported differences in TBW values obtained for individuals from deuterium dilution and from BIA. In a BIA validation study performed in pregnant women with or without HIV infection, a systematic predictive bias was seen in TBW using BIA at each time point during the pregnancy despite TBW_{Deut} and TBW_{BIA} being highly correlated (Kupka et al. 2011).

We also show a strong and statistically significant correlation between FFM results obtained using both methods. We suggest, therefore, that the proprietary regression equations within the QuadScan 4000, Bodystat® analyser, which have been developed for the healthy population, are valid in individuals with PKU. It is possible that no predictive bias was seen between the methods in our study because our participants with PKU are free living with normal physical development.

While it has been shown that BIA alone can be used as a surrogate to measure FFM in a paediatric population (Pietrobelli et al. 2003), predictive equations used in BIA analysis have also been validated in several population groups including healthy children (Cordain et al. 1988; Ellis et al. 1999), overweight and obese children (Cleary et al. 2008) and young female gymnasts (Eckerson et al. 1997). Population-specific BIA equations have also been developed when required, such as race-combined equations for large epidemiological studies (Sun et al. 2003). A study of healthy individuals aged 4–24 years showed that while $height^2$/impedance was a strong predictor of lean mass, some variability was observed in the younger years and older adolescent years, suggesting that no single BIA equation may be applied over all age groups (Montagnese et al. 2013).

This study is limited by the relatively small number of participants and their wide age range, which included adolescents likely to be experiencing pubertal body composition changes. Ongoing evaluation of BIA methodology to measure body composition could be done to ensure that predictive equations using raw impedance values to estimate FFM can be applied across all ages. With more data, it may be possible to develop PKU-specific equations if required in the future. Further study may also produce predictive equations for other metabolic disorders requiring dietary modification.

In summary, our results show no differences between the criterion deuterium dilution method and BIA in measuring TBW and predicting FFM in a group of children and adolescents with PKU. We suggest that BIA using QuadScan 4000, Bodystat® can be used to measure body composition in the outpatient clinic setting, to further improve the assessment of nutritional outcomes for patients with PKU.

Acknowledgments Analysis was undertaken at the Stable Isotope Geochemistry Laboratory, School of Earth and Environmental Sciences, and the University of Queensland, and we thank Kim Baublys and Wei Zhou for their assistance.

Synopsis

No predictive bias existed when measuring total body water or fat-free mass by deuterium dilution and bioelectrical impedance analysis (BIA) using the QuadScan 4000, Bodystat®; we therefore suggest that this instrument could be used as a method to monitor body composition in the outpatient clinic setting in patients with phenylketonuria.

Contributions of Individual Authors

All authors contribute to the submitted paper: contributing content development, drafting and revising the manuscript and providing final approval of the version to be submitted:

1. Maureen Evans has been responsible for conception and design of the project, data and sample collection, statistical analysis, researching and drafting of the manuscript through its various stages of development and completed the final version for submission.
2. Kay Nguo was responsible for the analysis and interpretation of the deuterium dilution samples and revising the manuscript critically for content and format.
3. Avihu Boneh was responsible for the interpretation of data and for revising the manuscript critically for content and format.

4. Helen Truby was responsible for supervising the project, conception and design and revising the manuscript critically for content and format.

Corresponding Author

Maureen Evans, Department of Metabolic Medicine, Royal Children's Hospital, Melbourne, Australia. Tel.: +61383416376. Email address: maureen.evans@rch.org.au.

Competing Interest Statement

No person was provided with an honorarium, grant, or other form of payment to conduct the study or produce the manuscript. Maureen Evans, Kay Nguo, Avihu Boneh and Helen Truby declare that they have no conflict of interest.

Details of Funding

This research did not receive any specific grant or sponsorship from funding agencies in the public, commercial or not-for-profit sectors.

Details of Ethics Approval

This study was approved by the RCH Human Research Ethics Committee: HREC #32056D.

Patient Consent Statement

This manuscript does not contain any personal information about patients. Informed consent was obtained for all study participants as a requirement of the RCH Human Research Ethics Committee process.

References

Albersen M, Bonthuis M, de Roos N et al (2010) Whole body composition analysis by the BodPod air-displacement plethysmography method in children with phenylketonuria shows a higher body fat percentage. J Inherit Metab Dis 33:283–288

Aldámiz-Echevarría L, Bueno MA, Couce ML et al (2014) Anthropometric characteristics and nutrition in a cohort of PAH-deficient patients. Clin Nutr 33:702–717

Allen JR, Baur LA, Waters DL et al (1996) Body protein in prepubertal children with phenylketonuria. Eur J Clin Nutr 50:178–186

Battezzati A, Bertoli S, Testolin C, Testolin G (2003) Body composition assessment: an indispensable tool for disease management. Acta Diabetol 40:S151–S153

Böhm A, Heitmann BL (2013) The use of bioelectrical impedance analysis for body composition in epidemiological studies. Eur J Clin Nutr 67:S79–S85

Burrage LC, McConnell J, Haesler R et al (2012) High prevalence of overweight and obesity in females with phenylketonuria. Mol Genet Metab 107:43–48

Cleary J, Daniells S, Okely AD, Batterham M, Nicholls J (2008) Predictive validity of four bioelectrical impedance equations in determining percent fat mass in overweight and obese children. J Am Diet Assoc 108:136–139

Cordain L, Whicker RE, Johnson JE (1988) Body composition determination in children using bioelectrical impedance. Growth Dev Aging 52:37–40

Dobbelaere D, Michaud L, Debrabander A et al (2003) Evaluation of nutritional status and pathophysiology of growth retardation in patients with phenylketonuria. J Inherit Metab Dis 26:1–11

Eckerson JM, Evetovich TK, Stout JR et al (1997) Validity of bioelectrical impedence equations for estimating fat-free weight in high school female gymnasts. Med Sci Sports Exerc 29:962–968

Ellis KJ, Shypailo RJ, Wong WW (1999) Measurement of body water by multifrequency bioelectrical impedance spectroscopy in a multiethnic pediatric population. [Erratum appears in Am J Clin Nutr 2000 Jun;71(6):1618]. Am J Clin Nutr 70:847–853

Houtkooper LB, Going SB, Lohman TG, Roche AF, Van Loan M (1992) Bioelectrical impedance estimation of fat-free body mass in children and youth: a cross-validation study. J Appl Physiol 72:366–373

Huemer M, Huemer C, Moslinger D, Huter D, Stockler-Ipsiroglu S (2007) Growth and body composition in children with classical phenylketonuria: results in 34 patients and review of the literature. J Inherit Metab Dis 30:694–699

International Atomic Energy Agency (2010) Introduction to body composition assessment using the deuterium dilution technique with analysis of urine samples by isoptope ratio mass spectrometry. International Atomic Energy Agency, Division of Human Health, Vienna

Jackson AA, Johnson M, Durkin K, Wootton S (2013) Body composition assessment in nutrition research: value of BIA technology. Eur J Clin Nutr 67:S71–S78

Kupka R, Manji K, Wroe E et al (2011) Comparison of isotope dilution with bioelectrical impedance analysis among HIV-infected and HIV-uninfected pregnant women in Tanzania. Int J Body Compos Res 9:1–10

Lohman T (1993) Advances in body composition assessment. Human Kinetics Publishers, Champaign

MacDonald A, Rocha JC, Rijn M, Feillet F (2011) Nutrition in phenylketonuria. Mol Genet Metab 104:S10–S18

Martin Bland J, Altman D (1986) Statistical methods for assessing agreement between two methods of clinical measurement. Lancet 327:307–310

Montagnese C, Williams JE, Haroun D, Siervo M, Fewtrell MS, Wells JCK (2013) Is a single bioelectrical impedance equation valid for children of wide ranges of age, pubertal status and nutritional status? Evidence from the 4-component model. Eur J Clin Nutr 67:S34–S39

Mulasi U, Kuchnia AJ, Cole AJ, Earthman CP (2015) Bioimpedance at the bedside. Nutr Clin Pract 30:180–193

Pietrobelli A, Andreoli A, Cervelli V, Carbonelli MG, Peroni DG, Lorenzo A (2003) Predicting fat-free mass in children using bioimpedance analysis. Acta Diabetol 40:s212–s215

Rocha JC, MacDonald A, Trefz F (2013a) Is overweight an issue in phenylketonuria? Mol Genet Metab 110:S18–S24

Rocha JC, Spronsen FJ, Almeida MF, Ramos E, Guimaraes JT, Borges N (2013b) Early dietary treated patients with phenylketonuria can achieve normal growth and body composition. Mol Genet Metab 110:S40–S43

Rocha JC, van Rijn M, van Dam E et al (2016) Weight management in phenylketonuria: what should be monitored. Ann Nutr Metab 68:60–65

Scaglioni S, Verduci E, Fiori L et al (2004) Body mass index rebound and overweight at 8 years of age in hyperphenylalaninaemic children. Acta Paediatr 93:1596–1600

Singh RH, Cunningham AC, Mofidi S et al (2016) Updated, web-based nutrition management guideline for PKU: an evidence and consensus based approach. Mol Genet Metab 118:72–83

Sun SS, Chumlea WC, Heymsfield SB et al (2003) Development of bioelectrical impedance analysis prediction equations for body composition with the use of a multicomponent model for use in epidemiologic surveys. Am J Clin Nutr 77:331–340

van Spronsen FJ, van Wegberg AMJ, Ahring K et al (2017) Key European guidelines for the diagnosis and management of patients with phenylketonuria. Lancet Diabetes Endocrinol. https://doi.org/10.1016/S2213-8587(16)30320-5

Wells JCK, Fewtrell MS (2006) Measuring body composition. Arch Dis Child 91:612–617

JIMD Reports
DOI 10.1007/8904_2017_77

RESEARCH REPORT

Effect of Storage Conditions on Stability of Ophthalmological Compounded Cysteamine Eye Drops

Ahmed Reda · Ann Van Schepdael · Erwin Adams · Prasanta Paul · David Devolder · Mohamed A. Elmonem · Koenraad Veys · Ingele Casteels · Lambertus van den Heuvel · Elena Levtchenko

Received: 11 October 2017 / Revised: 06 November 2017 / Accepted: 15 November 2017 / Published online: 07 December 2017

Abstract Cystinosis is a hereditary genetic disease that results in the accumulation of cystine crystals in the lysosomes, leading to many clinical manifestations. One of these manifestations is the formation of corneal cystine crystals, which can cause serious ocular complications. The only available drug to treat cystinosis is cysteamine, which breaks cystine and depletes its accumulation in the lysosomes. However, the oral form of cysteamine is not effective in treating corneal manifestations. Thus, ophthalmic solutions of cysteamine are applied. Because the commercial cysteamine eye drops are not available in most countries, hospital pharmacies are responsible for preparing "homemade" drops usually without a control of stability of cysteamine in different storage conditions. Hence, we aimed in this study to investigate the effect of different storage conditions on the stability of a cysteamine ophthalmic compounded solution. Cysteamine ophthalmic solution was prepared in the hospital pharmacy and sterilized using a candle filter. The preparations are then stored either in the freezer at −20°C or in the refrigerator at +4°C for up to 52 weeks. The amount of cysteamine hydrochloride in the preparation at different time points was determined using capillary electrophoresis (CE). Storage of the cysteamine ophthalmic preparations at +4° resulted in significant loss of free cysteamine at all time points, from 1 to 52 weeks of storage, when compared with storage in the freezer (−20°C). We demonstrate that cysteamine 0.5% compounded eye drops are easily oxidized within the first week after storage at +4°C, rendering the preparation less effective. Storage at −20°C is recommended to prevent this process.

Communicated by: Bruce A Barshop, MD, PhD

A. Reda (✉) · M. A. Elmonem · K. Veys · L. van den Heuvel · E. Levtchenko
Department of Development and Regeneration, Organ System Cluster, Group of Biomedical Sciences, KU Leuven, Leuven, Belgium
e-mail: ahmed.reda@kuleuven.be

A. Van Schepdael · E. Adams · P. Paul
Farmaceutische Analyse, KU Leuven, Leuven, Belgium

D. Devolder
Hospital Pharmacy, University Hospitals Leuven, Leuven, Belgium

M. A. Elmonem
Department of Clinical and Chemical Pathology, Faculty of Medicine, Cairo University, Cairo, Egypt

K. Veys · L. van den Heuvel · E. Levtchenko
Department of Pediatrics, University Hospitals Leuven, Leuven, Belgium

I. Casteels
Department of Ophthalmology, University Hospitals Leuven, Leuven, Belgium

L. van den Heuvel
Department of Pediatric Nephrology, Radboud UMC, Nijmegen, The Netherlands

Introduction

Cystinosis is a hereditary systemic disease, characterized by accumulation of the amino acid cystine, in a crystalline form, inside the lysosomes of the cells (Elmonem et al. 2016). The disease is caused by bi-allelic mutations in the *CTNS* gene, which encodes for cystinosin protein. Cystinosin is a cystine-proton co-transporter located in the lysosomal membrane (Nesterova and Gahl 2013). Cystinosis is a rare disorder, with a prevalence of 1:100,000 to 1:200,000 live births (Elmonem et al. 2016). However, a higher prevalence was found in some regions, such as French Brittany, with 1:26,000 live births (Bois et al. 1976),

and Canadian Quebec, with 1:62,000 live births (De Braekeleer 1991). The most frequent mutation is the 57-kb deletion, which constitutes 50% of the causing mutations in North Europe and North America (Shotelersuk et al. 1998; Levtchenko et al. 2014). However, this specific mutation is not present in other regions of the world (Soliman et al. 2014).

There are three different forms of cystinosis, depending on the clinical presentation: infantile, juvenile, and corneal non-nephropathic. The infantile nephropathic form, which represents 95% of the cystinosis cases, is the most severe form. This form shows a renal Fanconi syndrome at a very early age (6–12 months of age) with a progressive loss of kidney function, leading to end-stage renal disease (ESRD) before puberty, if left untreated (Schnaper et al. 1992; Brodin-Sartorius et al. 2012). Meanwhile, the juvenile form, which represents less than 5% of the cases, is a milder form that is diagnosed around adolescence with milder symptoms (Servais et al. 2008). Finally, the ocular non-nephropathic form is a rare form in adults, which is only characterized by ocular disease without systemic manifestations. Notably, the mutation type determines the severity of the disease. Severe mutations are causing infantile nephropathic cystinosis, while mild mutations are found in patients with juvenile and ocular non-nephropathic cystinosis (Gahl et al. 2002).

All three allelic forms of cystinosis demonstrate corneal cystine accumulation leading to photophobia (Anikster et al. 2000; Gahl et al. 2002) and blepharospasm (Kaiser-Kupfer et al. 1986). Using slit lamp examination, crystals are first detected at 16 months of age in the peripheral cornea. In vivo confocal microscopy and anterior segment optical coherence tomography have higher resolution in detecting cystine crystals in different corneal layers (Liang et al. 2015). When left untreated, corneal disease progresses causing filamentary keratitis, corneal ulcerations, band keratopathy, corneal neuropathy, corneal vascularization, posterior synechiae, and pupillary block with secondary glaucoma (Liang et al. 2015). Complete loss of transparency can result in corneal blindness. However, corneal transplantation is generally not considered as a valid treatment option because cystine crystals from inflammatory cells can invade the corneal graft resulting in poor vision (Katz et al. 1987). Moreover, cystinosis can lead to retinal blindness in 10–15% of the patients (Gahl et al. 2002).

Currently, the only available treatment for cystinosis is β-mercaptoethylamine or cysteamine (Thoene et al. 1976). It is an amino thiol found naturally as a constituent of the coenzyme A (Cavallini et al. 1968). However, it is undetectable in normal individuals' plasma samples. Cysteamine is easily oxidized to form a disulfide bond, which enables it to break each cystine molecule accumulated in the lysosome into two cysteine molecules; one is transported outside the lysosome as itself, and the other is transported as a cysteamine-cysteine disulfide, both of which use other transporters than cystinosin (Gahl et al. 1985). Oral cysteamine administration will deplete crystals in vascularized structures as the retina, but unfortunately not the corneal cystine crystals (Cantani et al. 1983). Hence, cystinosis patients should apply ophthalmic cysteamine preparations, in order to deplete the corneal crystals (Kaiser-Kupfer et al. 1987, 1990).

Since cysteamine is easily oxidized to cystamine, it was worthy to investigate whether the oxidized form (cystamine) is effective, as an ophthalmic preparation, in depleting the corneal crystals. Regrettably, it has been shown that cystamine is not as effective as cysteamine in depleting the cystine corneal crystals (Iwata et al. 1998).

The development of commercial cysteamine eye drops has been hindered by the difficulties to obtain a stable cysteamine solution. To the moment, two commercial formulations have reached market authorization: 0.44% aqueous cysteamine hydrochloride solution (Cystaran™, Sigma-Tau Pharmaceuticals) and 0.55% cysteamine gel (Cystadrops®, Orphan Europe). Unfortunately, these commercial drops are not available in most countries, and most cystinosis patients around the globe rely on cysteamine ocular solutions prepared by their hospital pharmacies. These "homemade" drops are cheaper and are frequently considered as a valid alternative by local health-care authorities. In this study, we examined the stability of cysteamine ocular solution prepared in the pharmacy of our university hospital upon different storage conditions.

Methods

Formulation

All chemicals were of analytical grade. Ammonium acetate was sourced from Fisher Scientific (Loughborough, UK). The simulated formulation matrix was prepared with ascorbic acid (Acros Organics, Geel, Belgium), benzalkonium chloride (Sigma-Aldrich, Steinheim, Germany), KH_2PO_4 (Merck, Darmstadt, Germany), methanol (Acros Organics), NaCl (Fisher Scientific), and $Na_2HPO_4{\cdot}12\ H_2O$ (Chem-Lab, Zedelgem, Belgium). All solutions and sample dilution were performed in Milli-Q (Millipore, Massachusetts, USA) water. The cysteamine hydrochloride powder was obtained from Acros Organics (Belgium) for standard preparation, and the sodium benzoate (as internal standard (IS)) was from Sigma-Aldrich. Sodium hydroxide was sourced from Fisher Scientific for the preparation of capillary rinsing solutions. The preparation was sterilized using a candle filter to assure sterility.

Cysteamine Measurement

A stock solution of the simulated formulation matrix was prepared by incorporating all the components at the specified concentration: NaCl (3 mg/mL), $Na_2HPO_4 \cdot 12\ H_2O$ (8.25 mg/mL), KH_2PO_4 (1.16 mg/mL), ascorbic acid (0.2 mg/mL), and benzalkonium chloride (0.1 mg/mL). Afterward, a standard solution of cysteamine hydrochloride at the corresponding concentration in the formulation (0.5% w/v) was prepared by accurately weighing and diluting it with the simulated matrix. Finally, both the sample and the standard (1 mL) were diluted (10×) with Milli-Q water along with the transfer (0.3 mL) of the solution of sodium benzoate (0.6 mg/mL) as IS. The background electrolyte (BGE) of the experiment was a mixture of 15 mM ammonium acetate (with pH adjusted to 8.85) and methanol (90:10 v/v).

Cysteamine concentrations were determined using capillary electrophoresis (CE). A P/ACE MDQ, Beckman Coulter CE (Fullerton, CA, USA), instrument was used for the electrophoresis. Karat 32® software was used for instrument operations and UV data acquisition (195 nm). A bare fused silica capillary was used for the assay (total length 40 cm, effective length 30 cm, id 50 μm). All the weighings and the pH adjustment of the BGE were performed by a Mettler Toledo (Greifensee, Switzerland) electric balance and a Metrohm 691 pH meter (Herisau, Switzerland).

The new capillary was activated by a sequence of rinsing with different solutions (10 min each) in the following order: water, methanol, water, 1 mM sodium hydroxide, water, 0.1 mM sodium hydroxide, water. A simple daily capillary rinsing with 0.1 mM sodium hydroxide followed by water was adopted for the capillary activation. For the proper equilibration of BGE components, a BGE rinsing followed by electrophoresis at the working voltage (28 kV) for 10 min each was performed before the actual analysis. Finally, the optimum electrophoresis involved 3 min of inter-injection BGE rinsing followed by a hydrodynamic sample injection at 0.5 psi for 5 s and 5 min of electrophoresis at 28 kV.

Statistical Analysis

The statistical analysis was done using Sigma Plot 12.0 software (Systat Software Inc., IL, USA). Student's t-test was performed on at least three replicates from each experimental condition, while means and standard deviations were used in the graph, as stated in the figure legend. The p value was considered significant if it was ≤ 0.05.

Results

Cysteamine ophthalmic solutions (0.5%) were sterilized using a candle filter. The preparations were stored either at +4°C or at −20°C. Samples from ophthalmic preparations at two different storage conditions were collected at different time points: 1, 2, 4, 12, 26, and 52 weeks. Cysteamine levels in the different samples were determined using the CE technique.

Statistical analysis showed that the percentage of cysteamine left of label claim was significantly less at +4°C compared to −20°C storage at all time-points (Fig. 1), with p value <0.001. The results also showed that the percentage of cysteamine left of the label claim decreased with time upon refrigerator storage from 61.6% (±2%) after 1 week of storage to 22.9% (±1.9%) after 52 weeks of storage. Meanwhile, the freezing conditions tended to keep the same level of cysteamine at the different time points, from 85.1% (±0.9%) after 1 week of storage to 85.7 (±2.5%) after 52 weeks of storage.

Discussion

Cystinosis patients have to use ophthalmic cysteamine preparation in order to eliminate cystine crystals accumulated in the cornea because systemically used cysteamine does not reach avascular structures (Elmonem et al. 2016). Because cysteamine eye drops (Liang et al. 2017) are not commercially available in Belgium, we tested the stability of pharmacy-made cysteamine preparation (0.5% solution) compounded in our institution.

We followed a validated protocol using a candle filter to assure sterile preparation and added 0.01% benzalkonium chloride to prevent bacterial contamination. Based on previously published data, eye drops were kept frozen before analysis (Iwata et al. 1998).

As the patient has to apply the preparation frequently every day, ophthalmic solution is usually stored in the freezer once purchased. Upon usage, the preparation is thawed in the refrigerator or even at room temperature (and kept there for 1 week or more) for patients' convenience as it is not feasible to unfreeze the whole solution (for multiple doses) every time before administration. At these conditions, cysteamine is easily oxidized to cystamine. It has been shown that cystamine is not effective in eliminating the cystine crystals from the cornea (Iwata et al. 1998).

We mimicked these storage conditions in our laboratory and evaluated the percentage of free cysteamine remaining after storage.

The results showed that, when stored at +4°C, a significant amount of cysteamine in the ophthalmic preparation is oxidized within 1 week. This might explain that the majority of our patients continue to complain of photophobia and other ocular complications of cystinosis despite their compliance with "homemade" eye drops.

In contrast, novel aqueous 0.44% cysteamine hydrochloride solution Cystaran™ (Sigma-Tau Pharmaceuticals) can

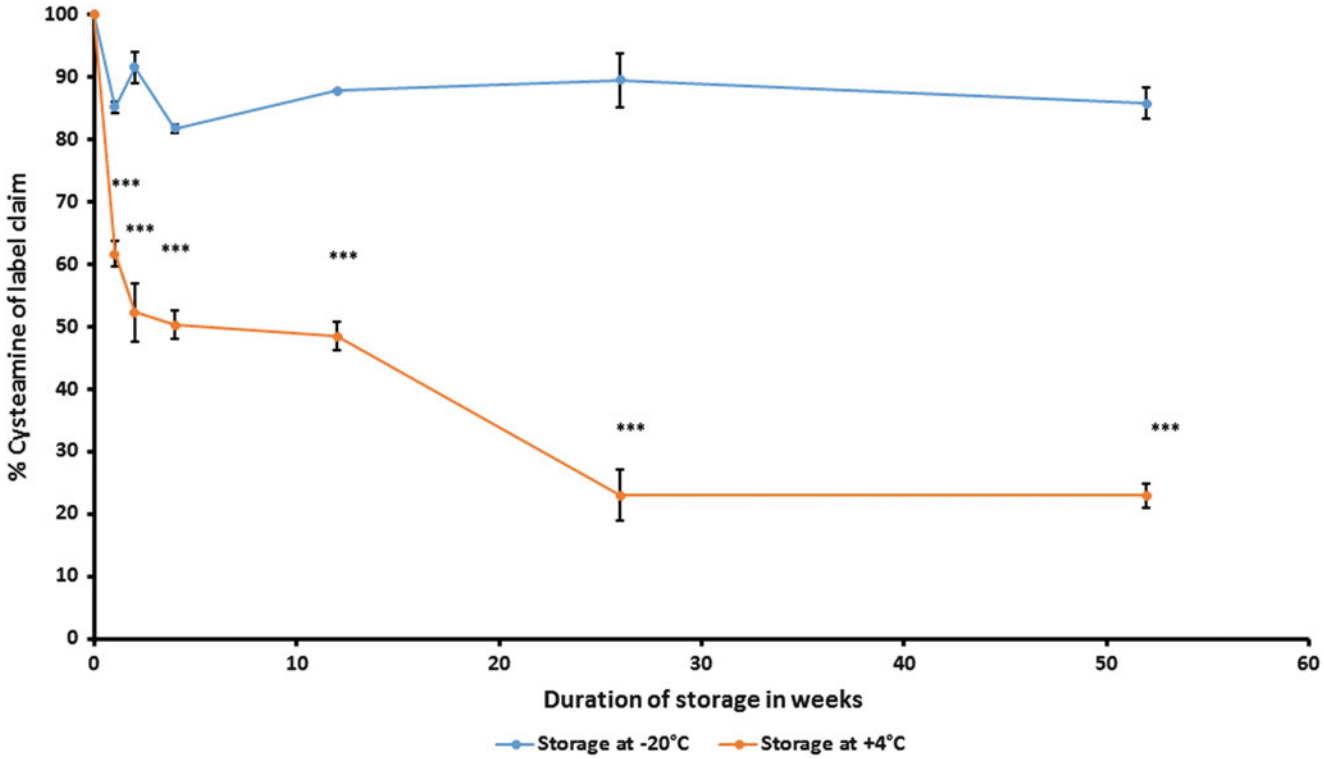

Fig. 1 Percentage of cysteamine left of label claim after 1, 2, 4, 12, 26, and 52 weeks of storage using different storage conditions; freezer (−20°C, in blue) or refrigerator (+4°C, in orange). The points represent the average values of three samples with the error bars representing the standard deviations (SD). For statistical analysis, student's t-test was applied between the two different conditions at the different time points ($p < 0.001$)

be kept at 4°C for at least 1 week and showed efficiency in reducing the corneal cystine score (CCCS) overtime. However, it has to be applied every waking hour complicating therapy compliance (Gahl et al. 2000). Another novel viscous preparation Cystadrops® (Orphan Europe) containing carmellose sodium as a viscous agent prolongs the precorneal residence time and can be stored at room temperature, protected from light, up to 7 days after opening. This gel-like solution showed excellent efficiency when applied four times daily when assessed using slit lamp examination, optical coherence tomography, and highly sensitive in vivo confocal microscopy (Liang et al. 2017). Moreover, clinical evaluation showed a significant reduction of photophobia in patients using Cystadrops® compared to standard cysteamine hydrochloride (0.1%) preparation.

Conclusion

In conclusion, we have demonstrated that cysteamine hydrochloride (0.5%) formulated ophthalmic preparation is easily oxidized within the first week after storage at +4°C, rendering the preparation less effective. Hence, storage at −20°C is recommended to preserve the efficiency of this preparation. Thus, in ideal setting, the preparation should be aliquoted, and each aliquot (for a single dose) should be thawed before each application.

Acknowledgment A.R. and E.L. are supported by the Irish cystinosis foundation. M.A.E. is supported by ERA-Net, E-Rare2-JTC2014: Novel therapies for cystinosis. E.L. is supported by the Research Foundation – Flanders (F.W.O. Vlaanderen), grant 1801110N, and the Cystinosis Research Network (CRN).

Synopsis

Cystinosis patients may get less effective ophthalmological treatment than what is expected.

Details of the Contributions of Individual Authors

Ahmed Reda, Lambertus van den Heuvel, and Elena Levtchenko contributed in planning. Ahmed Reda, Ann Van Schepdael, Erwin Adams, Prasanta Paul, David Devolder, and Ingele Casteels contributed in conducting. Ahmed Reda, Mohamed A. Elmonem, Koenraad Veys, Lambertus van den Heuvel, and Elena Levtchenko contributed in reporting.

Name of One Author Who Serves as Guarantor

Prof. Elena Levtchenko.

A Competing Interest Statement

Ahmed Reda, Ann Van Schepdael, Erwin Adams, Prasanta Paul, David Devolder, Mohamed A. Elmonem, Koenraad Veys, Ingele Casteels, and Lambertus van den Heuvel declare that they have no conflict of interest.

Elena Levtchenko has a consultancy agreement with Horizon Pharma and Orphan Europe and a financial grant support from Horizon Pharma.

Details of Funding

Ahmed Reda and Elena Levtchenko are supported by the Irish cystinosis foundation. Mohamed A. Elmonem is supported by ERA-Net, E-Rare2-JTC2014: Novel therapies for cystinosis. Elena Levtchenko is supported by the Research Foundation – Flanders (F.W.O. Vlaanderen), grant 1801110N, and the Cystinosis Research Network (CRN).

Details of Ethics Approval and Patient Consent

This article does not contain any studies with human or animal subjects performed by any of the authors.

References

Anikster Y, Lucero C, Guo J et al (2000) Ocular nonnephropathic cystinosis: clinical, biochemical, and molecular correlations. Pediatr Res 47:17–23

Bois E, Feingold J, Frenay P, Briard ML (1976) Infantile cystinosis in France: genetics, incidence, geographic distribution. J Med Genet 13:434–438

Brodin-Sartorius A, Tete MJ, Niaudet P et al (2012) Cysteamine therapy delays the progression of nephropathic cystinosis in late adolescents and adults. Kidney Int 81:179–189

Cantani A, Giardini O, Ciarnella Cantani A (1983) Nephropathic cystinosis: ineffectiveness of cysteamine therapy for ocular changes. Am J Ophthalmol 95:713–714

Cavallini D, Dupre S, Graziani MT, Tinti MG (1968) Identification of pantethinase in horse kidney extract. FEBS Lett 1:119–121

De Braekeleer M (1991) Hereditary disorders in Saguenay-Lac-St-Jean (Quebec, Canada). Hum Hered 41:141–146

Elmonem MA, Veys KR, Soliman NA, van Dyck M, van den Heuvel LP, Levtchenko E (2016) Cystinosis: a review. Orphanet J Rare Dis 11:47

Gahl WA, Tietze F, Butler JD, Schulman JD (1985) Cysteamine depletes cystinotic leucocyte granular fractions of cystine by the mechanism of disulphide interchange. Biochem J 228:545–550

Gahl WA, Kuehl EM, Iwata F, Lindblad A, Kaiser-Kupfer MI (2000) Corneal crystals in nephropathic cystinosis: natural history and treatment with cysteamine eyedrops. Mol Genet Metab 71:100–120

Gahl WA, Thoene JG, Schneider JA (2002) Cystinosis. N Engl J Med 347:111–121

Iwata F, Kuehl EM, Reed GF, McCain LM, Gahl WA, Kaiser-Kupfer MI (1998) A randomized clinical trial of topical cysteamine disulfide (cystamine) versus free thiol (cysteamine) in the treatment of corneal cystine crystals in cystinosis. Mol Genet Metab 64:237–242

Kaiser-Kupfer MI, Caruso RC, Minkler DS, Gahl WA (1986) Long-term ocular manifestations in nephropathic cystinosis. Arch Ophthalmol 104:706–711

Kaiser-Kupfer MI, Fujikawa L, Kuwabara T, Jain S, Gahl WA (1987) Removal of corneal crystals by topical cysteamine in nephropathic cystinosis. N Engl J Med 316:775–779

Kaiser-Kupfer MI, Gazzo MA, Datiles MB, Caruso RC, Kuehl EM, Gahl WA (1990) A randomized placebo-controlled trial of cysteamine eye drops in nephropathic cystinosis. Arch Ophthalmol 108:689–693

Katz B, Melles RB, Schneider JA (1987) Recurrent crystal deposition after keratoplasty in nephropathic cystinosis. Am J Ophthalmol 104:190–191

Levtchenko E, van den Heuvel L, Emma F, Antignac C (2014) Clinical utility gene card for: cystinosis. Eur J Hum Genet 22. https://doi.org/10.1038/ejhg.2013.204

Liang H, Baudouin C, Tahiri Joutei Hassani R, Brignole-Baudouin F, Labbe A (2015) Photophobia and corneal crystal density in nephropathic cystinosis: an in vivo confocal microscopy and anterior-segment optical coherence tomography study. Invest Ophthalmol Vis Sci 56:3218–3225

Liang H, Labbe A, Le Mouhaer J, Plisson C, Baudouin C (2017) A new viscous cysteamine eye drops treatment for ophthalmic cystinosis: an open-label randomized comparative phase III pivotal study. Invest Ophthalmol Vis Sci 58:2275–2283

Nesterova G, Gahl WA (2013) Cystinosis: the evolution of a treatable disease. Pediatr Nephrol 28:51–59

Schnaper HW, Cottel J, Merrill S et al (1992) Early occurrence of end-stage renal disease in a patient with infantile nephropathic cystinosis. J Pediatr 120:575–578

Servais A, Moriniere V, Grunfeld JP et al (2008) Late-onset nephropathic cystinosis: clinical presentation, outcome, and genotyping. Clin J Am Soc Nephrol 3:27–35

Shotelersuk V, Larson D, Anikster Y et al (1998) CTNS mutations in an American-based population of cystinosis patients. Am J Hum Genet 63:1352–1362

Soliman NA, Elmonem MA, van den Heuvel L et al (2014) Mutational Spectrum of the CTNS gene in Egyptian patients with nephropathic cystinosis. JIMD Rep 14:87–97

Thoene JG, Oshima RG, Crawhall JC, Olson DL, Schneider JA (1976) Cystinosis. Intracellular cystine depletion by aminothiols in vitro and in vivo. J Clin Invest 58:180–189

JIMD Reports
DOI 10.1007/8904_2017_79

RESEARCH REPORT

Leber Hereditary Optic Neuropathy and Longitudinally Extensive Transverse Myelitis

C. Bursle · K. Riney · J. Stringer · D. Moore · G. Gole · L. S. Kearns · D. A. Mackey · D. Coman

Received: 02 August 2017 / Revised: 02 November 2017 / Accepted: 27 November 2017 / Published online: 17 December 2017

Abstract Leber Hereditary Optic Neuropathy is an inherited optic neuropathy caused by mitochondrial DNA point mutations leading to sudden, painless loss of vision. We report a case of an 8-year-old boy presenting with a radiological phenotype of longitudinally extensive transverse myelitis on a background of severe visual impairment secondary to Leber Hereditary Optic Neuropathy (LHON). He was found to have dual mitochondrial DNA mutations at 14484 (*MTND6* gene) and 4160 (*MTND1* gene) in a family with a severe form of LHON characterised by not only an unusually high penetrance of optic neuropathy, but also severe extra-ocular neurological complications. The m.14484T>C mutation is a common LHON mutation, but the m.4160T>C mutation is to our knowledge not reported outside this family and appears to drive the neurological manifestations. To our knowledge there have been no previous reports of spinal cord lesions in children with LHON.

Communicated by: Manuel Schiff

C. Bursle · K. Riney · J. Stringer · D. Coman (✉)
Neurosciences Unit, The Lady Cilento Children's Hospital, Brisbane, QLD, Australia
e-mail: david.coman@health.qld.gov.au; david.coman@hotmail.com

D. Coman
UnitingCare Clinical School, The Wesley Hospital, Brisbane, QLD, Australia

C. Bursle · K. Riney · D. Coman
School of Medicine, The University of Queensland, Brisbane, QLD, Australia

D. Moore · D. Coman
Department of Paediatrics, The Wesley Hospital, Brisbane, QLD, Australia

G. Gole
Department of Ophthalmology, The Lady Cilento Children's Hospital, Brisbane, QLD, Australia

L. S. Kearns
Centre for Eye Research Australia, Royal Victorian Eye and Ear Hospital, East Melbourne, VIC, Australia

L. S. Kearns
Ophthalmology, Department of Surgery, University of Melbourne, Parkville, VIC, Australia

D. A. Mackey
Lions Eye Institute, Centre for Ophthalmology and Visual Science, University of Western Australia, Perth, WA, Australia

D. A. Mackey
School of Medicine, Menzies Institute for Medical Research, University of Tasmania, Hobart, TAS, Australia

Introduction

Leber Hereditary Optic Neuropathy (LHON) (OMIM #535000) is a mitochondrial disorder in which the primary manifestation is visual loss due to the degeneration of retinal ganglion cells. LHON is one of the most common inherited optic neuropathies, with a prevalence in Europe of between 1 in 30,000 and 1 in 50,000 (Man et al. 2003; Spruijt et al. 2006; Puomila et al. 2007). LHON is caused by point mutations in mitochondrial DNA (mtDNA) genes encoding subunits of complex 1 of the respiratory chain, particularly those encoding the ND1 (OMIM 516000), ND4 (OMIM 516004) and ND6 (OMIM 516006) subunits (Mackey et al. 1996; Valentino et al. 2004). 90% of LHON cases harbour one of three point mutations in mtDNA, m.3460G>A (*MTND1* gene, OMIM 516000), m.11778G>A (*MTND4* gene OMIM 516004) and m.14484T>C (*MTND6* gene OMIM 516006) (Newman 2005). Penetrance is incomplete, and as 80–90% of affected individuals carry homoplasmic mutations, heteroplasmy alone is not responsible for the decreased pene-

trance in LHON (Man et al. 2003; Harding and Sweeney 1995). Our patient belongs to a large Queensland family (Qld1, OMIM 535000) reported to have a severe LHON phenotype characterised by high penetrance of visual loss (with visual loss developing in approximately 100% of male and at least 60% of female family members in the maternal line) and a high incidence of neurological phenotypes (Wallace 1970; Mackey and Buttery 1992; Mackey 1994).

LHON was originally considered an isolated ophthalmic disorder, caused by selective degeneration of the retinal ganglion cells (Carelli et al. 2004; Man et al. 2009). However, extra-ocular neurological manifestations have been reported, including movement disorders, peripheral neuropathy, brainstem and basal ganglia involvement and multiple sclerosis-like syndromes. These have been termed "LHON plus syndromes", some of which have been linked to mtDNA point mutations other than the three common mutations seen in LHON, but which also affect mitochondrial respiratory chain complex 1 activity and present with optic neuropathy in the majority of affected carriers (Wallace 1970; Jun et al. 1994; Paulus et al. 1993).

Longitudinally extensive transverse myelitis (LETM) is a magnetic resonance imaging diagnosis defined as intramedullary hyperintense T2-weighted signal abnormality spanning three or more vertebral segments (Wingerchuk et al. 2006). The differential diagnosis of LETM is broad, including compressive, infective, demyelinating/inflammatory, vascular and neoplastic causes (Mirbagheri et al. 2016), although use of this terminology commonly implies a demyelinating/inflammatory aetiology. We now report a paediatric patient from the LHON Qld1 family with extensive myelopathy resembling LETM.

Case Report

A molecular diagnosis of LHON was confirmed in our patient at 6 years of age, with testing performed in the context of visual deterioration and a family history. Visual acuity was measured at 4/60 using a Snellen chart bilaterally and he required the use of a cane to aid mobility.

Mitochondrial DNA polymerase chain reaction restriction fragment length polymorphism (PCR RFLP) analysis was performed. The following mutations were detected: MT-ND1:p.L285P (c.854 T>C) (m.4160T>C) homoplasmic and MT-ND6:p.M64V (c.190 A>G) (m.14484T>C) homoplasmic. These mutations, a primary mutation in ND6 (m.14484T>C) and a secondary mutation (m.4160T>C), are those described in the Qld 1 pedigree (Wallace 1970; Mackey 1994). The known pedigree omitting paternal descendants is shown in Fig. 1. Our patient's maternal grandmother's death at age 58 was said to be secondary to Leigh syndrome. The patient has one sister aged 11 who currently has normal vision and is in good general health.

At 8 years of age, the boy presented with an 8-day history of abnormal gait of gradual onset, in the context of 3 weeks of lower limb and back pain. He had episodic profuse diaphoresis, beginning 7 days prior to the abnormal gait and initially associated with 24 h of fever that did not persist. He had a single episode of faecal incontinence at the time of his fever. He was also noted to have a bilateral manual tremor.

At presentation there was asymmetrical proximal lower limb weakness, more prominent on right, resulting in abnormal gait and difficulty rising from the ground and climbing onto a bed. He had normal tone, but absent right lower limb deep tendon reflexes, and an equivocal plantar

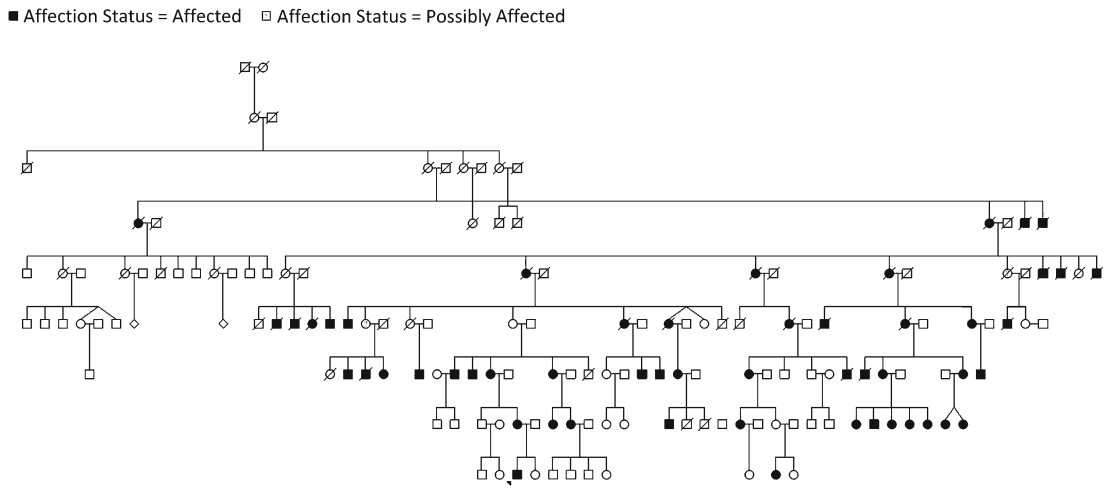

Fig. 1 Qld1 known pedigree omitting paternal descendants

response on that side. The patient reported decreased sensation to the left lower limb in a non-dermatomal distribution, and also on the plantar surface of the right foot. Power was only reduced to 4+/5 and he was able to walk with relatively mild gait abnormality, acknowledging that his sensory disturbance and his pre-existing visual impairment may have affected his gait. The patient had evidence of dysautonomia; initial blood pressure was 139/98 mmHg and there was ongoing intermittent hypertension for the first 7 days of the admission. Paroxysmal, sharply demarcated left hemifacial diaphoresis was seen corresponding to the hypertension, although there was no fever or tachycardia. The right visual acuity was 6/360 and the left visual acuity was 6/270.

Magnetic resonance imaging (MRI) revealed extensive but symmetrical increased signal intensity on T2 weighted imaging throughout the spinal cord extending from the conus to the medulla suggestive of myelopathy. There was swelling of the cord at the C4/5 level and at the conus, with no associated enhancement. Diffusion weighted imaging was not performed on the spinal cord, although through the medulla showed symmetrical prominent increased signal within two central rounded areas of the ventral cord. The remainder of the brain was normal, although spectroscopy was not performed. The optic nerves were noted to be small in calibre. These radiographic features were considered to be mitochondrial in aetiology, based on the history of LHON, but with an inflammatory component.

Full blood count, inflammatory markers and complement studies (C3/C4) were normal, aside from a very mild increase in the erythrocyte sedimentation rate (ESR) (10 mm/h). There was a speckled antinuclear antibody (ANA) titre of 40. A mild elevation in aspartate transaminase (AST) and alanine transferase (ALT) was noted and the lactate was normal. Anti-MOG (myelin oligodendrocyte glycoprotein) and anti-NMO (neuromyelitis optica) antibodies were negative. A lumbar puncture was not performed due to the noted cord swelling.

The patient received intravenous immunoglobulin 2 g/kg over 2 days and pulse methylprednisolone 30 mg/kg/day for 5 days, followed by oral prednisolone at 2 mg/kg/day for 2 weeks, weaned off over a further 3 weeks. He was commenced on idebenone at 300 mg three times daily. The autonomic manifestations of sweating and hypertension resolved over a week, and the patient underwent inpatient rehabilitation. By the time he was discharged 11 days after admission, he had only subtle residual asymmetric lower limb weakness but was ambulant.

At follow up 3 months after admission, he had essentially returned to his baseline prior to his illness, but with mild clumsiness in the right leg seen on running, and decreased deep tendon reflexes on that side. There had been a full resolution of sensory and autonomic symptoms. Repeat MRI demonstrated residual symmetric increased signal intensity on T2 weighted imaging still present extending throughout the spinal cord.

Discussion

While LHON was originally considered an isolated ophthalmic disorder, coexisting neurological disorders and other features such as kyphosis and cardiac conduction abnormalities are relatively common, and many of these additional findings are unsurprising given the underlying complex 1 respiratory chain defect (Nikoskelainen et al. 1995; Paulus et al. 1993). In one Finnish study of 46 patients with LHON vision loss from 24 families, 59% were found to have neurological abnormalities in addition to LHON. “LHON plus” neurological manifestations include tremor, dystonia, migraine, seizures, progressive encephalopathy with basal ganglia involvement, peripheral neuropathy, myoclonus and cerebellar ataxia (Nikoskelainen et al. 1995; Murakami et al. 1996; Funalot et al. 2002).

Our patient belongs to a large Queensland family (Qld1) reported to have a severe LHON phenotype. Significant neurological complications have been described in this LHON Qld1 family, including dysarthria, ataxia, spastic paraplegia, and a severe acute infantile or childhood encephalopathy in at least nine family members with a fatal outcome in at least three. There was no definite evidence of a demyelinating process, including at autopsy in two of these cases (Wallace 1970). Modern imaging was not available at the time of Wallace’s report; however, none of the described cases appears readily attributable to an isolated spinal cord process. The combination of m.14484T>C and m.4160T>C mutations is to our knowledge not reported outside this family. The m.4160T>C mutation is not described elsewhere, aside from a single entry in the Genbank database, in an unaffected individual. A third mutation m.4136A>G, in the ND1 gene, has been reported in a branch of the Qld 1 family, and appeared to be homoplasmic in the family members tested. It has been proposed to be an intragenic suppressor mutation, ameliorating the biochemical and clinical manifestations in this branch of the family (Howell et al. 1991). Several family members outside this small branch tested negative, but none of our patient’s antecedents appears to have been tested (Howell et al. 1991).

Our patient’s episode of extensive spinal cord pathology could represent a separate coincidental issue, however; the coexistence of two relatively rare disorders seems particularly unlikely, given that numerous cases of apparent demyelination have been reported in LHON (Pfeffer et al. 2013; Shiraishi et al. 2014; Harding et al. 1992; Parry-Jones et al. 2008; Perez et al. 2009). This syndrome, known as LHON-multiple sclerosis (LHON-MS), is essentially clini-

cally and radiologically indistinguishable from multiple sclerosis, but with less ocular pain and a poorer visual prognosis (Pfeffer et al. 2013; Matthews et al. 2015). The pathophysiology of multiple sclerosis is also incompletely understood, and has been postulated to involve a complex I defect, with biochemical evidence of complex I deficiency having being noted in muscle in MS patients as well as in animal models (Sadeghian et al. 2016; Kumleh et al. 2006). LHON-MS has not been reported in childhood, and while spinal cord changes have been noted on MRI in these patients, they rarely occur without concurrent white matter lesions in the brain (Pfeffer et al. 2013; Matthews et al. 2015; La Russa et al. 2011). Our patient had extensive spinal cord changes suggestive of demyelination but negative anti-AQP4 antibodies, and did not meet the diagnostic criteria for neuromyelitis optica, which is an inflammatory demyelinating disorder which causes optic neuritis and myelitis (Crout et al. 2016). Table 1 summarises 15 cases of LHON and spinal cord MRI changes, of which m.14484T>C mutations account for 6, or 40%, including our patient with dual mutations.

The pathology underpinning the spinal cord and brain pathology in patients with LHON and features resembling MS and LETM remains unclear. Only three cases of LHON with spinal cord involvement have been reported with post-mortem pathological data. A case of posterior column spinal cord degeneration was reported in a 39-year-old woman with subacute bilateral visual failure 5 years previously and m.3460G>A homoplasmy. The picture was of a subacute metabolic axonopathy with additional features of a Leigh-like syndrome on brain MRI, with no evidence of demyelination or remyelination at autopsy after her unexpected death 2 months later (Jaros et al. 2007). Neuropathology was also performed in a case of atypical MS-like disease in a patient with homoplasmic m.14484T>C mutations and spinal cord (cervical gracile fasciculus) as well as cerebral white matter changes (Kovács et al. 2005). Post-mortem studies demonstrated axonal damage, active demyelination, cystic necrosis, inactive demyelinated areas and vacuolated white matter (Kovács et al. 2005). This suggests metabolic injury including demyelination in the pathology of at least some patients with this pattern of disease. A third pathological study was performed in the pre-molecular era on a 58-year-old LHON patient who was otherwise neurologically normal aside from bilateral impaired position sense in the toes. Demyelination and gliosis were noted in the optic tracts and also the gracilis columns of the cervical spine. A slight degree of myelin sheath destruction was described in the peripheral nerves of the lower extremities. The spinal and peripheral changes were postulated to be related to severe malnutrition secondary to the cardiac failure which resulted in his death; however, impaired position sense in the patient's brother increased the uncertainty about whether it was LHON-related (Kwittken and Barest 1958). It has been postulated that tissue injury in LHON patients may provoke an immune response in susceptible individuals, for example by liberation of mitochondrial proteins (autoantigens) (Palace 2009). It is, however, by no means certain that there is an inflammatory or autoimmune component to the demyelination seen in this disorder, as white matter pathology including demyelination is seen in other disorders involving complex I deficiency (Filosto et al. 2007).

Longitudinally extensive transverse myelitis is a radiological descriptor encompassing a broad variety of differential diagnoses which may be narrowed down by specific imaging features, history, clinical findings and other investigations. Metabolic myelopathy is an important differential diagnosis. Mitochondrial disorders including LHON should be considered as part of the broad differential in adults and children presenting with LTEM, even when appearances are typical of demyelination. To the best of our knowledge there are no reported cases of demyelinating disease or spinal cord lesions in children with LHON mutations, with the youngest reported patient with LHON-MS being 18 years at onset of non-visual manifestations (Pfeffer et al. 2013).

In summary, we present a unique case of extensive subacute myelopathy in a child with early onset visual loss due to LHON in a family reported to have a high rate of neurological manifestations. Neurological complications have not been reported for several decades in this family, although our patient's grandmother is said to have died from complications of Leigh syndrome. Such cases challenge and extend current knowledge of this disorder, as well as highlighting the need to consider mitochondrial disorders as a cause of myelitis or myelopathy.

Acknowledgement CERA receives Operational Infrastructure Support from the Victorian Government.

Synopsis

Extensive myelopathy in a child with LHON; an unusual extraocular manifestation.

Authors' Contributions

Carolyn Bursle is a metabolic fellow who was involved in patient care and drove manuscript development.

Kate Riney is a neurologist who was involved in patient care and manuscript development.

Table 1 Reported LHON cases with spinal cord involvement

	LHON genotype	Age at presentation of spinal cord pathology (after visual onset)	Clinical features (i.e. NMO)	Reported spinal imaging features	CSF oligoclonal bands	Anti-NMO antibodies	Treatment	Additional diagnosis if made, outcome	Reference
Case 1	m.11778G→A	20 (3 years)	Two episodes bilateral lower limb paralysis and hypoesthesia, brisk DTRs	T2 hyperintensity T1–T6 level No gadolinium enhancement	Neg	Positive	Steroids	NMO, partial recovery, ambulant	Shiraishi et al. (2014)
Case 2	m.3460G→A	25 (7 years)	Lower limb sensory changes, weakness, urinary dysfunction	Lesions T8–9, T11, gadolinium enhancement	NA	NA	NA	NMO, incomplete recovery	Ghezzi et al. (2004)
Case 3	4216 and 4917	31 (7 years)	Three episodes lower limb weakness, urinary dysfunction, C4 sensory level	T2 hyperintense lesion C4–T4, with expansion, later atrophy	Neg	NA	Steroids	Relapsing NMO, good recovery, walking independently	Celebisoy et al. (2006)
Case 4	m.14484T→C	65 (−1 year)	Lower limb pain, weakness, gait imbalance, axonal polyneuropathy	T2 hyperintensity posterior columns entire C spine, no enhancement	Neg	Negative	Not reported	NMO, deficits stable for 1 year, followed by optic neuropathy	McClelland et al. (2011)
Case 5	m.3460G→A	39 (5 years)	Pyramidal pattern lower limb weakness, nystagmus, absent ankle jerks	T2 hyperintensity dorsal columns	Neg	NA	Not reported	Unexpected death – Leigh-like subacute degeneration at autopsy brain and spinal cord	Jaros et al. (2007)
Case 6	m.14484T→C	38 (13 years)	Left leg weakness, paraethesiae, ataxia, urinary retention	NA, brain only	Neg	NA	Steroids – improvement noted	Secondary progressive MS? Death due to bronchopneumonia. Pathology: active demyelination in cerebral white matter lesions, axonal degeneration in cervical gracile fascicle and dorsal roots of spine	Kovács et al. (2005) and Horváth et al. (2000)
Case 7	m.14484T→C	35 (approx. 10 years)	Lower limb weakness, hypoesthesia	Diffuse T2 hyperintensity T6–T11, gadolinium enhancement	Pos	NA	Steroids	RRMS, moderate improvement, recurrence after 4 months	La Russa et al. (2011)

(continued)

Table 1 (continued)

	LHON genotype	Age at presentation of spinal cord pathology (after visual onset)	Clinical features (i.e. NMO)	Reported spinal imaging features	CSF oligoclonal bands	Anti-NMO antibodies	Treatment	Additional diagnosis if made, outcome	Reference
Case 8	m.14484T→C	28 (concurrent)	Sensory changes thorax and hand	T2 hyperintensity upper C spine odontoid level	Neg	NA	Steroids	MS, incomplete recovery	Bhatti and Newman (1999)
Case 9	m.14484T→C	33 (6 months)	Three episodes limb weakness, sensory changes, urinary frequency and urgency, brisk DTRs	T2 hyperintensity T10	Pos	NA	Steroids	MS, partial recovery	Parry-Jones et al. (2008)
Case 10	m.11778G>A	42 (8 years)	Lower limb weakness, brisk DTRs, extensor plantars	Multiple T2 hyperintensities throughout the cervical and upper thoracic cord	NA	NA	NA	NA	Tran et al. (2001)
Case 10	m.11778G>A	27 (−3 years)	Sensory episodes, Lhermitte symptom	Cervical spine lesions	NA	NA	NA	RRMS	Pfeffer et al. (2013)
Case 11	m.11778G>A	27 (no visual involvement)	Episodes sensory loss, ataxia, weakness, LL spasticity	Cervical spine lesions	NA	NA	NA	RRMS-secondary progressive course after 4 years	Pfeffer et al. (2013)
Case 12	m.3460G→A	27 (2 years)	Recurrent sensory episodes, one episode transverse myelitis	Cervical spine lesions	Neg	NA	NA	RRMS	Pfeffer et al. (2013)
Case 13	m.3460G→A	20 (6 months)	Two episodes weakness, sensory loss, Lhermitte symptom	Cervical spine lesions	NA	NA	NA	RRMS	Pfeffer et al. (2013)
Current case	m.14484T→C, m.4160T>C	8 (2 years)	Lower limb weakness, sensory symptoms, dysautonomia	T2 hyperintensity whole spine, some swelling, no enhancement	NA	Neg	Steroids, idebenone	Near complete recovery	

NMO neuromyelitis optica, *OCB* oligoclonal bands, *RRMS* relapsing remitting multiple sclerosis, *NA* not available, *DTR* deep tendon reflexes

Josephine Stringer is a neurology fellow who was involved in patient care and manuscript development.

David Moore is a paediatrician involved in patient care and manuscript development.

Glen Gole is a paediatric ophthalmologist involved in patient care and manuscript development.

Lisa Kearns is an orthoptist and genetic counsellor who was involved in the curation of the genetic information for LHON families and was involved in manuscript development.

David Mackey is a genetic ophthalmologist with long-standing research involvement with the family and was involved in manuscript development.

David Coman is a metabolic physician involved in patient care and was instrumental in the manuscript design and development.

Corresponding Author

David Coman.

Conflict of Interest

The authors have no conflicts of interest to disclose.

Funding Source

N/A.

Ethics Approval

N/A.

Patient Consent

The patients' parents consent to publication of this case report.

References

Bhatti MT, Newman NJ (1999) A multiple sclerosis-like illness in a man harboring the mtDNA 14484 mutation. J Neuroophthalmol 19(1):28–33

Carelli V, Ross-Cisneros F, Sadun A (2004) Mitochondrial dysfunction as a cause of optic neuropathies. Prog Retin Eye Res 23:53–89

Celebisoy N, Akyurekli O, Copur A (2006) Devic's neuromyelitis optica: a case with mitochondrial DNA mutations. Eur Neurol 55 (2):93–95

Crout T, Parks L, Majithia V (2016) Neuromyelitis optica (Devic's syndrome): and appraisal. Curr Rheumatol Rep 18:54

Filosto M, Tomelleri G, Tonin P et al (2007) Neuropathology of mitochondrial diseases. Biosci Rep 27(1–3):23–30

Funalot B, Reynier P, Vighetto A et al (2002) Leigh-like encephalopathy complicating Leber's hereditary optic neuropathy. Ann Neurol 52(3):374–377

Ghezzi A, Baldini S, Zaffaroni M et al (2004) Devic's neuromyelitis optica and mitochondrial DNA mutation: a case report. Neurol Sci 25:S380–S382

Harding A, Sweeney M (1995) Pedigree analysis in Leber hereditary optic neuropathy families with a pathogenic mtDNA mutation. Am J Hum Genet 57:77–86

Harding AE, Sweeney MG, Miller DH et al (1992) Occurrence of a multiple sclerosis-like illness in women who have a Leber hereditary optic neuropathy mt-DNA mutation. Brain 115:979–989

Horváth R, Abicht A, Shoubridge E et al (2000) Leber's hereditary optic neuropathy presenting as multiple sclerosis-like disease of the CNS. J Neurol 247:65–67

Howell N, Kubacka I, Xu M, McCullough DA (1991) Leber Hereditary Optic Neuropathy involvemnet of mitochondrial MDI gene and evidence for an intragenic suppressor mutation. Am J Hum Genet 48:935–942

Jaros E, Mahad DJ, Hudson G et al (2007) Primary spinal cord neurodegeneration in Leber hereditary optic neuropathy. Neurology 69(2):214–216

Jun AS, Brown MD, Wallace DC (1994) A mitochondrial DNA mutation at nucleotide pair 14459 of the NADH dehydrogenase subunit 6 gene associated with maternally inherited Leber hereditary optic neuropathy and dystonia. Proc Natl Acad Sci U S A 91(13):6206–6210

Kovács GG, Höftberger R, Majtényi K et al (2005) Neuropathology of white matter disease in Leber's hereditary optic neuropathy. Brain 128(Pt 1):35–41

Kumleh HH, Riazi GH, Houshmand M et al (2006) Complex I deficiency in Persian multiple sclerosis patients. J Neurol Sci 243 (1–2):65–69

Kwittken J, Barest H (1958) The neuropathology of hereditary optic atrophy (Leber's disease); the first complete anatomic study. Am J Pathol 34(1):185–207

La Russa A, Cittadella R, Andreoli V et al (2011) Leber's hereditary optic neuropathy associated with a multiple-sclerosis-like picture in a man. Mult Scler 17(6):763–766

Mackey DA (1994) Three subgroups of patients from the United Kingdom with Leber hereditary optic neuropathy. Eye 8:431–436

Mackey DA, Buttery RG (1992) Leber hereditary optic neuropathy in Australia. Aust N Z J Ophthalmol 20:177–184

Mackey DA, Oostra RJ, Rosenberg T et al (1996) Primary pathogenic mtDNA mutations in multigeneration pedigrees with Leber hereditary optic neuropathy. Am J Hum Genet 59:481–485

Man PYW, Griffiths P, Brown D (2003) The epidemiology of Leber hereditary optic neuropathy in the North East of England. Am J Hum Genet 72:333–339

Man PYW, Griffiths PG, Hudson G, Chinnery PF (2009) Inherited mitochondrial optic neuropathies. J Med Genet 46:145–158

Matthews L, Enzinger C, Fazekas F et al (2015) MRI in Leber's hereditary optic neuropathy: the relationship to multiple sclerosis. J Neurol Neurosurg Psychiatry 86:537–542

McClelland CM, Van Stavern GP, Tselis AC (2011) Leber hereditary optic neuropathy mimicking neuromyelitis optica. J Neuroophthalmol 31:265–268

Mirbagheri S, Eckart Sorte D, Zamora CA, Mossa-Basha M, Newsome SD, Izbudak I (2016) Evaluation and management of

longitudinally extensive transverse myelitis: a guide for radiologists. Clin Radiol 71:960–971

Murakami T, Mita S, Tokunaga M et al (1996) Hereditary cerebellar ataxia with Leber's hereditary optic neuropathy mitochondrial DNA 11778 mutation. J Neurol Sci 142:111–113

Newman NJ (2005) Hereditary optic neuropathies: from the mitochondria to the optic nerve. Am J Ophthalmol 140:517–523

Nikoskelainen E, Marttila R, Houponen K et al (1995) Leber's "plus": neurological abnormalities in patients with Leber's hereditary optic neuropathy. J Neurol Neurosurg Psychiatry 59:160–164

Palace J (2009) Multiple sclerosis associated with Leber's hereditary optic neuropathy. J Neurol Sci 286:24–27

Parry-Jones AR, Mitchell JD, Gunarwardena WJ, Shaunak S (2008) Leber's hereditary optic neuropathy associated with multiple sclerosis: Harding's syndrome. Pract Neurol 8:118–121

Paulus W, Straube A, Bauer W, Harding AE (1993) Central nervous system involvement in Leber's optic neuropathy. J Neurol 240:251–253

Perez F, Anne O, Debruxelles S et al (2009) Leber's optic neuropathy associated with disseminated white matter disease: a case report and review. Clin Neurol Neurosurg 111:83–86

Pfeffer G, Burke A, Yu-Wai-Man P et al (2013) Clinical features of MS associated with Leber hereditary optic neuropathy mtDNA mutations. Neurology 81:2073–2081

Puomila A, Hämäläinen P, Kivioja S et al (2007) Epidemiology and penetrance of Leber hereditary optic neuropathy in Finland. Eur J Hum Genet 15:1079–1089

Sadeghian M, Mastrolia V, Rezaei Haddad A et al (2016) Mitochondrial dysfunction is an important cause of neurological deficits in an inflammatory model of multiple sclerosis. Sci Rep 14:333249

Shiraishi W, Hayashi S, Kamada T et al (2014) A case of neuromyelitis optica harboring both anti-aquaporin-4 antibodies and a pathogenic mitochondrial DNA mutation for Leber's hereditary optic neuropathy. Mult Scler J 20(2):258–260

Spruijt L, Kolbach DN, de Coo RF et al (2006) Influence of mutation type on clinical expression of Leber hereditary optic neuropathy. Am J Ophthalmol 141:676–682

Tran M, Bhargava R, MacDonald IM (2001) Leber hereditary optic neuropathy, progressive visual loss, and multiple-sclerosis-like symptoms. Am J Ophthalmol 132(4):591–593

Valentino ML, Barboni P, Ghelli A et al (2004) The ND1 gene of complex I is a mutational hot spot for Leber's hereditary optic neuropathy. Ann Neurol 56(5):631–641

Wallace DC (1970) A new manifestation of Leber's disease and a new explanation for the agency responsible for its unusual pattern of inheritance. Brain 93:121–132

Wingerchuk DM, Lennon VA, Pittock SJ et al (2006) Revised diagnostic criteria for neuromyelitis optica. Neurology 66(10):1485–1489

JIMD Reports
DOI 10.1007/8904_2017_78

RESEARCH REPORT

Mitochondrial Disease in Children: The Nephrologist's Perspective

Paula Pérez-Albert · Carmen de Lucas Collantes · Miguel Ángel Fernández-García · Teresa de Rojas · Cristina Aparicio López · Luis Gutiérrez-Solana

Received: 09 August 2017 / Revised: 20 November 2017 / Accepted: 22 November 2017 / Published online: 17 December 2017

Abstract Mitochondrial diseases (MD) are a heterogeneous group of clinical syndromes characterized by the involvement of different organ systems. They constitute the most prevalent hereditary metabolic disease group.
Objective: To review the importance of the kidney in MD from the nephrologist's perspective within the setting of a pediatric tertiary reference center.
Study design: Retrospective study of children (<18 years) with MD followed between 2000 and 2016 at a tertiary Spanish center.
Results: 52 patients were included. The mean age at the time of the study was 10 years (SD ± 5.1). The mean follow-up time was 6.1 years (SD ± 4.7). The median age at diagnosis was 2.5 years (0.3–13.5).

The median number of affected systems was two (range 1–6). The nervous system was the most affected system, with 51 patients (~98%) presenting with neurological involvement. 20 patients (~40%) presented with endocrinological manifestations, 18 (~35%) with vision problems, 16 (~30%) with gastrointestinal symptoms, 5 (~10%) patients developed hearing impairment, and 6 (~10%) cardiac disease.

We detected renal involvement in 13 patients (25%). Eight patients had tubular disease, most frequently hypercalciuria with hypouricemia and five patients had glomerular involvement, with proteinuria and/or decreased glomerular filtration rate as the most frequent symptoms. Only 21 patients (~40%) had been seen by a pediatric nephrologist.
Conclusions: Renal disease was a common occurrence in patients with mitochondrial disease, present in our study in 25% of patients. A regular screening of renal function parameters and the involvement of a nephrologist as part of the multidisciplinary approach to mitochondrial disease appears warranted.

Communicated by: Johan Lodewijk Karel Van Hove, MD, PhD

P. Pérez-Albert (✉)
Department of Pediatrics, Children's University Hospital Niño Jesús, Madrid, Spain
e-mail: paulaperezalbert@gmail.com

C. de Lucas Collantes · C. Aparicio López
Department of Pediatric Nephrology, Children's University Hospital Niño Jesús, Madrid, Spain

M. Á. Fernández-García · L. Gutiérrez-Solana
Department of Paediatric Neurology, Children's University Hospital Niño Jesús, Madrid, Spain

T. de Rojas
Medical and Translational Research Department, European Organisation for Research and Treatment of Cancer (EORTC), Brussels, Belgium

Introduction

Mitochondrial diseases (MD) are a complex and heterogeneous group of clinical syndromes characterized by secondary multi-organ involvement caused by mitochondrial dysfunction. Enzymatic deficiency in the mitochondrial respiratory chain usually leads to multisystem alterations, predominantly affecting organs with higher energy requirements, such as the brain, skeletal muscle, heart, liver, and kidneys (Darin et al. 2001; Scaglia et al. 2004; Verity et al. 2010). With an estimated incidence of 1 per 5,000 live newborns (Rahman 2012) or 1 in 4,300 adults (Gorman et al. 2015), MD constitute the most prevalent group of hereditary metabolic diseases in children.

No effective curative treatment has been found for MD, thus preventive or supportive measures and early diagnosis of associated complications are the only way to improve the quality of life of these patients (Pfeffer et al. 2012).

This comes at a high medical and socioeconomic cost (McCormack et al. 2017).

Few case series have been published (Martín-Hernández et al. 2005; Broomfield et al. 2015; Hikmat et al. 2017), making it difficult to know the real prevalence of individual organ involvement in patients with MD. The aim of our study was to analyze the extent of organs affected in a pediatric MD population, with particular interest in renal involvement.

Patients and Methods

Study Design

We performed a single-center retrospective study of children (0–18 years old) diagnosed with MD and followed-up at the Children's Hospital Niño Jesús of Madrid, Spain, between 2000 and 2016. Approval from the institutional Ethics Committee was obtained.

Inclusion and Exclusion Criteria

Patients were included if they were aged 0–18 years at the time of diagnosis and if they met at least one of the following criteria: (1) proven deficiency in one or more complexes of the mitochondrial respiratory chain found in muscle biopsy; (2) presence of at least one mutation, deletion or duplication in DNA sequences of mitochondrial or nuclear DNA responsible for the correct functioning of oxidative phosphorylation; (3) clinical compliance with MD defining criteria, including patients with "definite" or "probable" diagnosis according to the most widely accepted criteria (Bernier et al. 2002; Morava et al. 2006). Patients with incomplete records or "possible" rather than definite diagnosis of MD were excluded.

Data Collection

Clinical data were obtained from hospital records. The following disease-related clinical variables were recorded and/or investigated: sex, age at diagnosis, type of first symptom, clinical features (including neurological, cardiovascular, ophthalmological, hearing, endocrine, gastrointestinal, and renal involvement), enzyme assay reports for the mitochondrial respiratory chain complex (MRCC), genetic findings, and syndromic diagnosis. The estimated glomerular filtration rate (GFR) was calculated using the "original" Schwartz formula [GFR (mL/min/1.73 m^2) = K (age-dependent) × height (cm)/Creatinine (mg/dL)] in cases in which the patients' data were old enough; otherwise the modify Schwartz [GFR (mL/min/1.73 m^2) = K (0.413) × height (cm)/Creatinine (mg/dL)] was used (last 4 years). Normal ranges for creatinine, GFR, phosphate, calcium, uric acid, and calcium/creatinine ratios were adjusted for the patient's age are provided. Proteinuria was defined by urinary protein/creatinine (mg/mg) ratio measured in the first morning urine void, and was abnormal when the value was above 0.5 in patients under 2 years old and above 0.2 in patients aged 2 years and above.

Statistical Analysis

Data are summarized as means (Standard Deviation, SD) or as medians (range) when the values do not meet the criteria of a normal distribution. The Kolmogorov-Smirnov test was used to test the normality of distribution of the data. We evaluated differences between means using either the Student's t-test, or the Mann-Whitney U test when the variable data were not normally distributed. Chi square test and Fisher exact test were used to determine the association between qualitative variables. All analyses were performed using SPSS, version 22 (IBM® SPSS® Statistics). P-values <0.05 were considered as statistically significant.

Results

We reviewed 92 patients who had at some point received a provisional diagnosis of MD. In 40 of these patients, the diagnosis was not confirmed; these cases were excluded from our study. The remaining 52 patients met the inclusion criteria. Of the 52, 31 (~60%) were male and 21 (~40%) were female. The mean age at the time of study was 10 years (0.8–18). The mean follow-up time was 6.1 years (0.2–16.4). Nine (9/52; ~18%) patients had died from the time of diagnosis to the time our study commenced, with a mean age of death of 6.3 years (SD ± 4.7). The mean standard deviation of the weight percentile for age and sex was −1.1 (−3.6–1.7) and the mean standard deviation of the height percentile for age and sex was −2.1 (−8.1–1.2).

Initial and Definitive Diagnoses

The median age at diagnosis was 2.5 years (0.3–13.5). The mean age at diagnosis was lower in patients with renal involvement than in patients without renal involvement (2.98 vs 4.09) but this difference was not statistically significant ($p = 0.079$).

Only one (1/52; ~2%) patient had renal symptoms (hematuria) as a first manifestation of disease (Table 1). Neurological symptoms were the most frequent initial symptoms in 36/52 (~70%) patients.

Muscle biopsy was performed in 51 (51/52; ~98%) MD patients. A dysfunction of MRCC was found in 38 (38/52; ~73%) patients (Table 2). Half of these cases (19/38) had isolated complex I deficiency.

Table 1 Initial and multisystem involvement

	First symptom (%) $n = 52$	All patients (%) $n = 52$	Renal damage patients (%) $n = 13$
Neurologic symptoms	*36 (69.2)*	*51 (98.1)*	*13 (100)*
Epilepsy	8 (15.4)	4 (7.7)	0
Motor delay	1 (1.9)	2 (3.8)	0
Psychomotor delay + epilepsy	0	10 (19.2)	2 (15.4)
Encephalomyopathy	0	24 (46.2)	9 (69.2)
– Seizures (first year of life)	10 (19.2)	0	0
– Psychomotor delay or hypotony	17 (32.7)	0	0
Language disorder	0	5 (9.6)	1 (7.7)
Others[a]	0	6 (11.5)	1 (7.7)
Hearing loss	*0*	*5 (9.6)*	*2 (15.4)*
Ophthalmologic symptoms	*2 (3.8)*	*18 (34.6)*	*5 (38.5)*
Ptosis	2 (3.8)	4 (7.7)	2 (15.4)
Squint	0	2 (3.8)	1 (7.7)
Ophthalmoparesis + pigmentary retinitis	0	4 (7.7)	1 (7.7)
Ophthalmoparesis	0	2 (3.8)	0
Visual deficit	0	2 (3.8)	1 (7.7)
Optic atrophy	0	2 (3.8)	0
Myopia magna	0	1 (1.9)	0
Cataracts	0	1 (1.9)	0
Gastrointestinal symptoms	*3 (5.8)*	*16 (30.8)*	*6 (46.2)*
Failure to thrive	1 (1.9)	6 (11.5)	4 (30.8)
Gastroesophageal reflux	0	2 (3.8)	0
Pancreatitis	1 (1.9)	3 (5.8)	1 (7.7)
Liver disease	1 (1.9)	3 (5.8)	1 (7.7)
Vomiting	0	2 (3.8)	0
Endocrinological symptoms	*1 (1.9)*	*20 (38.5)*	*7 (53.8)*
Short stature	0	15 (28.8)	5 (38.5)
Diabetes mellitus	1 (1.9)	2 (3.8)	0
Early puberty	0	2 (3.8)	1 (7.7)
Hypocalcemia	0	1 (1.9)	1 (7.7)
Cardiac symptoms	*1 (1.9)*	*6 (11.5)*	*1 (7.7)*
Rhythm abnormalities	0	3 (5.8)	0
Cardiomyopathy	0	3 (5.8)	1 (7.7)
Sepsis episodes	*3 (5.8)*	N/A	N/A
Renal affectation	*1 (1.9)*	*13 (25)*	*13 (100)*
Unknown	*5 (9.6)*	N/A	N/A

N/A not applicable

[a] Migraine; Ataxia; Leukodystrophy and hemiplegic migraine; Spinocerebellar syndrome; Oculomotor apraxia and myopathy

Nearly one-third of all MD patients (16/52; ~30%) received a syndromic diagnosis. The most frequent diagnoses were Leigh syndrome (10/52; ~20%) and Kearns-Sayre syndrome (4/52; ~8%). One patient was diagnosed with MELAS syndrome and another one with Alpers-Huttenlocher syndrome. The diagnosis was accompanied by identification of molecular genetic alterations in 9 (9/52; ~17%) patients, with mitochondrial DNA depletion in 7 (7/52; ~14%) patients, and FOXRED1 gene mutation in 2 (2/52; ~4%) patients. In 26 (26/52; 50%) patients, the clinical diagnosis was confirmed only by the deficit of one or more MRCC. One patient was diagnosed on the basis of clinical

Table 2 Mitochondrial chain deficits in muscle biopsy ($n = 52$)

	Frequency (%)
Complex I	19 (36.5)
Complex II	1 (1.9)
Complex III	2 (3.8)
Complex IV	8 (15.4)
Deficit of all complexes	1 (1.9)
Other combinations	7 (13.5)
Normal	13 (25)
Not performed	1 (1.9)

manifestations and metabolic and analytical data compatible with MD according to the Bernier and Morava criteria (Bernier et al. 2002; Morava et al. 2006).

Multisystem Involvement

Multisystem involvement is shown in Table 1. Thirteen patients (25%) had renal symptoms directly attributed to the MD.

The median number of affected organs or systems was 2 (SD ± 1.3; 1–6). Patients with kidney disease appeared more likely to have multiple organs affected (three or more) when compared to patients without kidney disease [~54% (7/13) vs ~33% (13/39), respectively]. However, this difference was not statistically significant ($p = 0.18$). No correlations between number of organs affected and age of initial symptom, types of organs involved, each concrete syndrome, MRCC, or the molecular/genetic alteration were found.

Renal Impairment

Of the 52 patients, 13 (25%) (6 males and 7 females) had renal involvement. Eight (8/13; ~62%) patients had tubular alterations and 5 (5/13; ~38%) patients had glomerular involvement; this difference was not statistically significant ($p = 0.4$). The mean age of renal damage was 10.2 years (0.8–17.2), and the mean age at diagnosis was 2.98 years (0.8–8.8) with a mean follow-up time of 6.7 years (0.2–16.4).

Patients with tubular alterations (8/13) are shown in Table 3. One had Kearns-Sayre syndrome and one had Alpers-Huttenlocher syndrome. The most frequent renal dysfunction was hypercalciuria with hyperuricosuria and hypouricemia. Two patients had nephrocalcinosis and one had renal calculi without associated hypercalciuria.

One patient (#6) presented at 3 years of age with repeated pancreatitis and sepsis-like episodes, later developing ptosis. He was seen by a nephrologist from the age of 5 because of acidosis, hypokalemia, and nephrocalcinosis. He was eventually diagnosed with Fanconi syndrome after a study revealing hypercalciuria, generalized hyperaminoaciduria, phosphaturia, proteinuria, and glycosuria leading to chronic renal disease. At 8 years of age, after developing clumsiness and learning difficulties and finding a deletion of mitochondrial DNA, he was finally diagnosed with MD with a Kearns-Sayre phenotype.

Patients with glomerular involvement (5/13) are shown in Table 4. The most common symptoms were proteinuria and decreased GFR with two patients going into chronic renal failure. Two patients had Leigh syndrome, one of them with renal failure. Mean plasma creatinine (Cr) was 0.4 mg/dL (SD ± 0.7; Max. 2) with GFR of 87.6 mL/min/1.73 m^2 (SD ± 44; Min. 25); mean plasma urea was 36 mg/dL (SD ± 80.1; Max. 205) and mean plasma urate was 5.8 mg/dL (SD ± 2.4; Max. 9.7).

Patient #9, a 7-year-old male, with chronic stage G4 kidney disease (KDIGO guidelines 2012), presented with hypotonia from birth with progression to hypotonic-ataxic cerebral palsy, and later with associated hearing loss and visual impairment. MD was suspected in the first year of life, when a muscle biopsy showed a deficiency in complex IV of the mitochondrial respiratory chain. The GFR measured at that time (1-year old) was 50 mL/min/1.73 m^2, with a creatinine of 0.7 mg/dL and urea of 125 mg/dL.

Only one patient (#13) presented with renal symptoms, with an episode of macroscopic hematuria with C4 hypocomplementemia at age 4. This episode was triggered by an infection, but due to the persistence of microhematuria over the following years with no changes in the low C4 levels, the later was considered an isolated low C4 not related to the renal involvement. At age 6, he developed complex partial epilepsy that was difficult to manage and he was diagnosed with MD due to a deficit in complex II with alterations in complexes III, II + III, and I + III. Renal function remained stable, so a biopsy was not performed. Although a definitive diagnosis of his kidney disease has not been reached, there is no other known explanation for his renal symptoms.

Out of the 12 (12/51; 23%) patients who received therapies with known renal side effects, 2 (2/12) had renal involvement prior to commencing those treatments and five (5/12; ~42%) had probable drug-related renal toxicity; only one of them appeared to be in addition to preexisting tubular damage.

Three out of six patients treated with topiramate experienced acidosis. One of them also presented with hypercalciuria. None of the three patients treated with oxcarbamacepin developed side effects. Both patients who received zonisamide developed secondary hypercalciuria; one of them developed transient arterial hypertension after adrenocorticotropic hormone. The other patient treated

Table 3 Patients with tubular damage

	Sex	Age at last follow-up/death (years)	Mitochondrial disease diagnosis	Age at first symptom (years)	First symptom	Age at diagnosis (years)	Multisystem involvement	Age at diagnosis of renal impairment (years)	Renal involvement
1	F	17.2	DMRCC Complex IV + II limit Mitochondrial DNA depletion	0.3	Psychomotor delay Nystagmus	0.8	Encephalomyopathy Nystagmus	17	Hypercalciuria Ca/Cr ratio: 0.43 mg/mg ($N < 0.21$) Proteinuria 0.36 mg/mg ($N < 0.2$) Hypouricemia 1.1 mg/dL (2.8–6) Alkalosis pH 7.48 HCO_3 32.8 mmol/L
2	F	2 (dead)	POLG mutation Alpers-Huttenlocher syndrome	2	Epileptic status	2	Encephalomyopathy Short stature Liver disease	2	Hypercalciuria Ca/Cr ratio: 1.37 mg/mg ($N < 0.21$) Proteinuria 0.53 mg/mg ($N < 0.2$) Hypouricemia 0.9 mg/dL (2–5.1)
3	F	13.8	DMRCC I + II	0.3	Psychomotor delay	4.5	Encephalomyopathy Epilepsy Dysphagia Diabetes mellitus	12	Hypercalciuria Ca/Cr ratio: 0.31 mg/mg ($N < 0.21$) Hypouricemia 0.7 mg/dL (2.8–6)
4	M	11.4	Mitochondrial DNA depletion	0.9	Hypotonia Dystonia	2.5	Encephalomyopathy	11.4	Hypercalciuria Ca/Cr ratio: 0.3 mg/mg ($N < 0.21$) Hypouricemia 1.1 mg/dL (2.8–6)
5	F	15.8	DMRCC IV	0.3	Epileptic seizure	1.7	Encephalomyopathy Epilepsy Early puberty	10	Hypercalciuria Ca/Cr ratio: 0.4 mg/mg ($N < 0.21$) Hypouricemia 1.7 mg/dL (2.8–6) Intermittent proteinuria 0.49 mg/mg ($N < 0.21$) Nephrocalcinosis
6	M	10.1	Mitochondrial DNA depletion Kearns-Sayre syndrome	2.6	Pancreatitis Sepsis-like episode	8.8	Motor clumsiness Hearing loss Ptosis and pigmentary retinitis Pancreatitis Short stature	5.7	Fanconi syndrome

(continued)

Table 3 (continued)

	Sex	Age at last follow-up/death (years)	Mitochondrial disease diagnosis	Age at first symptom (years)	First symptom	Age at diagnosis (years)	Multisystem involvement	Age at diagnosis of renal impairment (years)	Renal involvement
7	F	1 (dead)	DMRCC all	0.1	Epileptic seizure	1	Neutropenia Early onset myoclonic encephalopathy	0.2	Cystinuria (not generalized aminoaciduria)
8	M	15	DMRCC I	0.3	Cardiogenic shock Intrauterine growth restriction	Unknown	Encephalomyopathy Epilepsy Cardiogenic shock Hypocalcemia and hyperphosphatemia	1.2	Nephrolitiasis Hyperuricemia 9.6 mg/dL (2.8–7.2) Metabolic alkalosis pH 7.37 HCO_3 30.8 mmol/L

F female, *M* male, *DMRCC* deficit in the mitochondrial respiratory chain complex, *N* normal range, *Ca/Cr* calcium/creatinine urinary ratio

Table 4 Patients with glomerular damage

	Sex	Age at last follow-up (years)	Mitochondrial disease diagnosis	Age at first symptom (years)	First symptom	Age at diagnosis (years)	Multisystem involvement	Age at diagnosis of renal impairment (years)	Renal involvement	GFR (mL/min/1.73 m^2)	Uric (mg/dL)
9	M	7.7	DMRCC IV	0.5	Hypotony	1	Encephalomyopathy Malnutrition Hearing loss Strabismus	1	CKD	27 ($N > 90$)	9.7 (2–5.1)
10	F	1	DMRCC I + IV Leigh syndrome	0.6	Psychomotor regression	1	Encephalomyopathy	0.8	CKD	57 ($N > 78$)	4.9 (2–5.1)
11	M	8.1	Leigh syndrome	1	Psychomotor delay	2.2	Ataxia Ptosis	8.1	Hyperuricemia	121 ($N > 90$)	5.9 (2–5.1)
12	F	15.6	DMRCC III + IV	1	Psychomotor delay	3.3	Encephalomyopathy Cerebellar atrophy Short stature	15	Low proteinuria Microhematuria	300 ($N > 90$)	5.2 (2.8–6)
13	M	6.7	DMRCC I, II + III	4	Hematuria	6.7	Epilepsy Autism spectrum disorder	4	Hematuria	123 ($N > 90$)	3.3 (2–5.1)

F female, *M* male, *DMRCC* deficit mitochondrial respiratory chain complex, *CKD* chronic kidney disease, *N* normal range

with adrenocorticotropic hormone, with previous tubular damage, developed hypertension as well but no direct nephrotoxicity.

Only 21/52 (~40%) of MD patients in this study were seen by a pediatric nephrologist, mostly in older years.

Discussion

Mitochondria are organelles present in most cells of the organism. They generate energy through ATP production, in a process of aerobic oxidation that takes place in the mitochondrial respiratory chain, which is composed of five enzyme complexes (I, II, III, IV, and V) (Zeviani and Di Donato 2004; DiMauro and Hirano 2005). Dysfunction of the mitochondrial respiratory chain can be caused by genetic mutations in either nuclear or mitochondrial DNA (Moslemi and Darin 2007). Many mutations in mitochondrial DNA have been reported and are collected in online databases (http://www.mitomap.org) (Emma and Salviati 2017).

Due to the ubiquity of the mitochondria, multiple organs are usually involved in MD. In our study, only 14/52 (~27%) patients had a single affected organ/system; the rest had multiple organs affected, with 10/52 (~20%) patients having more than three symptomatic organs. It is therefore necessary to raise awareness to the need of multidisciplinary management and follow-up. The complexity of this disease can only be effectively managed as a joint effort by different medical specialists.

In this regard, multidisciplinary needs can lead to unorganized care, and underestimating comorbidities is a dangerous possibility. In our study, we found that only 40% (21/52) of the patients had ever been seen by a pediatric nephrologist despite 25% of MD patients suffering from renal involvement and several drugs used for MD treatment being nephrotoxic. It is nevertheless encouraging that in recent years increased proportion of patients are being referred to a nephrologist and/or have undergone a complete kidney function screening.

The simplistic unilateral approach to MD that occurs at times in the clinics is also reflected in the literature, with a strong focus on the neurologist perspective (Emma and Salviati 2017). However, although neurological involvement is frequently the guiding symptom, it is remarkable that 21% (11/52) of our patients presented with other affected organs. This heterogeneity is scarcely reflected in the literature, with few published multidisciplinary series (Broomfield et al. 2015; Hikmat et al. 2017) and even fewer series with a focus on renal damage (Lee et al. 2001; Emma et al. 2011; Rahman and Hall 2013; O'Toole 2014).

The kidney is a highly energetic organ, and thus rich in mitochondria, and is particularly susceptible to being affected in MD. A wide range of alterations have been described, from glomerular to tubular and tubulointerstitial damage, and even corticosteroid-resistant nephrotic syndrome in patients with coenzyme Q10 gene mutations (Lee et al. 2001; Emma et al. 2011; Rahman and Hall 2013; O'Toole 2014).

The prevalence of renal involvement in our sample was 25% (13/52). This is notably lower than the 50% (21/42) previously reported in a Spanish cohort (Martín-Hernández et al. 2005), and the 85% (17/20) reported by Broomfield et al. (Broomfield et al. 2015); however, it is higher than the series presented by Hikmat et al., with 11% (3/27) reported renal involvement (Hikmat et al. 2017). This variability could be explained by the heterogeneity of MD, the ascertainment, and the inclusion criteria of these different studies.

Nevertheless, our study has some limitations that may underestimate the prevalence of renal damage. The most important limitation consists of potentially missing data due to the retrospective nature of the analysis. Also, the lack of a pediatric nephrologist assessment in 60% (31/52) of the patients could have resulted in an incomplete renal evaluation, particularly in those patients in which no Ca/Cr and Protein/Cr ratios in urine were performed (48%; 25/52).

Beyond the study limitations, the low detected rate of renal damage may also reflect a lack of awareness of the importance of the kidney in MD. This adds to the fact that renal damage is most frequently asymptomatic in these patients (Martín-Hernández et al. 2005). Our study should raise awareness about the need for renal investigations and adequate renal specialist involvement in the management of children with MD, since it is well known that presymptomatic detection of renal damage and early intervention improve outcome. Exhaustive renal function testing is already recommended for all patients and should be a common practice (Broomfield et al. 2015).

We identified tubular damage in 8/52 patients (~15%). The most prevalent findings in our study include hypercalciuria and hypouricemia secondary to involvement of a single transporter. Only one patient with Kearns-Sayre syndrome presented with renal Fanconi syndrome, the most severe form of tubular involvement, which has been reported in previous studies (Emma et al. 2011; Klootwijk et al. 2014; O'Toole 2014).

Other forms of renal damage include chronic tubulointerstitial nephritis, cystic renal diseases, or glomerular proteinuria, which often progresses gradually and triggers terminal renal failure (Emma et al. 2012; Rahman and Hall 2013; O'Toole 2014). We found glomerular involvement in 5/52 (~10%) patients, out of whom two patients (2/5; 40%) had chronic renal disease. These findings underscore the importance of including MD in the differential diagnosis of patients with renal tubulopathy and/or renal failure

(Rötig et al. 1995; Rahman and Hall 2013; Broomfield et al. 2015).

Our study has important limitations due to its retrospective and mono-centric nature. However, some of its strengths include the diagnosis of specific syndromes in almost one-third of the patients (31%; 16/52), the molecular/genetic confirmation in 17% (9/52) of the patients, and the fact that the center is the most important pediatric reference center in our country. This study adds to the still scarce but much needed literature focusing on kidney damage in MD.

Conclusion

Our data confirm the wide clinical spectrum and multi-organ involvement in MD highlighting the need for a multidisciplinary team. The kidney should be seen as a key disease-susceptible organ, making it essential to monitor renal function in children with MD. Raising awareness and intensive kidney screening strategies performed not only by the nephrologist but also by other concerned specialists will lead to early treatment and improved renal outcome.

In light of our study, we recommend an annual renal evaluation including blood test with electrolytes, blood gases, uric and GFR, and first-morning urine with Ca/Cr and Protein/Cr ratios. A biannual ultrasound for nephrocalcinosis screening is also recommended.

Additional Information Tables: Laboratory Reference Parameters for Children

Table 5 Estimated glomerular filtration rate (GFR) (mean ± SD) (Santos and García Nieto 2006)

Age	GFR (mL/min/1.73 m^2)
1–2 months	64.6 ± 5.8
3–4 months	85.8 ± 4.8
5–8 months	87.7 ± 11.9
9–12 months	86.9 ± 8.4
1–6 years	130.0 ± 4.9
7–10 years	135.8 ± 4.3
>11 years	136.1 ± 6.3

Table 6 Plasma creatinine levels (Hospital's laboratory reference values n.d.)

Age	Range (mg/dL)	
0–21 days	0.32	1.06
21 days–1 year	0.24	0.42
1–2 years	0.16	0.42
2–5 years	0.19	0.51
5–10 years	0.33	0.73
10–18 years	0.4	1.0

Table 7 Plasma uric levels (Hospital's laboratory reference values n.d.)

	Age (years)	Range (mg/dL)	
Female	<1	2.1	6.5
	1–10	2.0	5.1
	10–14	2.8	6.0
	>14	2.8	6.0
Male	<1	2.1	6.5
	1–10	2.0	5.1
	10–13	2.8	6.0
	>13	2.8	7.2

Table 8 Plasma phosphate levels (Hospital's laboratory reference values n.d.)

Age (years)	Range (mg/dL)	
<1	4.8	7.5
1–2	4.5	6.7
2–6	4.5	6.5
6–15	2.7	5.3
>15	2.5	4.5

Table 9 Urinary Ca/Cr ratios (Santos and García Nieto 2006)

Age	Ca/Cr (mg/mg) hypercalciuria
0–6 months	0.8
7–12 months	0.6
<2 years	0.47
>2 years	0.21

Original Scwartz formula: GFR (mL/min/1.73 m^2) = K (age-dependent) × height (cm)/Creatinine (mg/dL). $K = 0.33$ (preterm infants 0–1 year); 0.45 (full-term infants 0–1 years); 0.55 (1–12 years); 0.70 (male >12 years) and 0.55 (female >12 years).

Synopsis

Renal involvement in mitochondrial diseases can affect the different segments of the nephron, leading to a broad spectrum of symptoms; thus, a close follow-up of the renal function is recommended in these children.

Authors Contributions

PP and CdL designed the study; PP, CdL, and MAF conducted the study and wrote the manuscript; TdR contributed to the analysis and reporting of the results; CdL, TdR, CA, and LGS supervised the study and critically reviewed the manuscript. All authors read and approved the final manuscript.

Corresponding Author

Paula Pérez-Albert.

Conflict of Interest

Paula Pérez-Albert, Carmen de Lucas Collantes, Miguel Ángel Fernández-García, Teresa de Rojas, Cristina Aparicio López, and Luis Gutiérrez-Solana declare that they have no conflict of interest.

Funding

The authors confirm independence from the sponsors; the content of the chapter has not been influenced by the sponsors.

Ethics Approval

This study has been carried out in accordance with the ethical standards approved by the ethical committee of the Niño Jesús Hospital, which is in accordance with the national committee on human experimentation and the Helsinki Declaration of 1975 and the revised version of 2015. For this retrospective study, formal consent was not required by the ethics committee.

References

Bernier FP, Boneh A, Dennett X, Chow CW, Cleary MA, Thorburn DR (2002) Diagnostic criteria for respiratory chain disorders in adults and children. Neurology 59:1406–1411

Broomfield A, Sweeney MG, Woodward CE et al (2015) Paediatric single mitochondrial DNA deletion disorders: an overlapping spectrum of disease. J Inherit Metab Dis 38:445–457

Darin N, Oldfors A, Moslemi AR, Holme E, Tulinius M (2001) The incidence of mitochondrial encephalomyopathies in childhood: clinical features and morphological, biochemical, and DNA abnormalities. Ann Neurol 49:377–383

DiMauro S, Hirano M (2005) Mitochondrial encephalomyopathies: an update. Neuromuscul Disord 15:276–286

Emma F, Salviati L (2017) Mitochondrial cytopathies and the kidney. Nephrol Ther 13(Suppl 1):S23–S28

Emma F, Montini G, Salviati L, Dionisi-Vici C (2011) Renal mitochondrial cytopathies. Int J Nephrol 2011:609213

Emma F, Bertini E, Salviati L, Montini G (2012) Renal involvement in mitochondrial cytopathies. Pediatr Nephrol 27:539–550

Gorman AM, Schaefer YN et al (2015) Prevalence of nuclear and mitochondrial DNA mutations related to adult mitochondrial disease. Ann Neurol 77(5):753–759

Hikmat O, Tzoulis C, Chong WK et al (2017) The clinical spectrum and natural history of early-onset diseases due to DNA polymerase gamma mutations. Genet Med. https://doi.org/10.1038/gim.2017.35

Hospital's laboratory reference values. The local laboratory performed a study in healthy children with the laboratory techniques used in the Hospital

Klootwijk ED, Reichold M, Helip-Wooley A et al (2014) Mistargeting of peroxisomal EHHADH and inherited renal Fanconi's syndrome. N Engl J Med 370(2):129–138

Lee YS, Kim Yap H, Barshop BA, Lee YS, Rajalingam S, Loke KY (2001) Mitochondrial tubulopathy: the many faces of mitochondrial disorders. Pediatr Nephrol 16:710–712

Martín-Hernández E, García-Silva MT, Vara J et al (2005) Renal pathology in children with mitochondrial diseases. Pediatr Nephrol 20:1299–1305

McCormack S, Xiao R, Kilbaugh T et al (2017) Hospitalizations for mitochondrial disease across the lifespan in the U.S. Mol Genet Metab 121(2):119–126

Morava E, Van den Heuvel L, Hol F et al (2006) Mitochondrial disease criteria: diagnostic applications in children. Neurology 67:1823–1826

Moslemi AR, Darin N (2007) Molecular genetics and clinical aspects of mitochondrial disorders in childhood. Mitochondrion 7(4):241–252

O'Toole JF (2014) Renal manifestations of genetic mitochondrial disease. Int J Nephrol Renovasc Dis 7:57–67

Pfeffer G, Majamaa K, Turnbull DM, Chinnery PF (2012) Treatment for mitochondrial disorders. Cochrane Database Syst Rev 4: CD004426

Rahman S (2012) Mitochondrial disease and epilepsy. Dev Med Child Neurol 54:397–406

Rahman S, Hall AM (2013) Mitochondrial disease: and important cause of end-stage renal failure. Pediatr Nephrol 28:357–361

Rötig A, Lehnert A, Rustin P et al (1995) Kidney involvement in mitochondrial disorders. Adv Nephrol Necker Hosp 24:367–378

Santos F, García Nieto V (2006) Basal renal function. In: Paediatric nephrology, 2nd edn. Grupo Aula Médica, Madrid, p 39

Scaglia F, Towbin JA, Craigen WJ et al (2004) Clinical spectrum, morbidity, and mortality in 113 pediatric patients with mitochondrial disease. Pediatrics 114:925–931

Verity CM, Winstone AM, Stellitano L, Krishnakumar D, Will R, McFarland R (2010) The clinical presentation of mitochondrial diseases in children with progressive intellectual and neurological deterioration: a national, prospective, population-based study. Dev Med Child Neurol 52:434–440

Zeviani M, Di Donato S (2004) Mitochondrial disorders. Brain 127:2153–2172

JIMD Reports
DOI 10.1007/8904_2017_85

RESEARCH REPORT

Characterization of Phenyalanine Hydroxylase Gene Mutations in Chilean PKU Patients

V. Hamilton • L. Santa María • K. Fuenzalida • P. Morales • L. R. Desviat • M. Ugarte • B. Pérez • J. F. Cabello • V. Cornejo

Received: 11 July 2017 / Revised: 1 December 2017 / Accepted: 7 December 2017 / Published online: 30 December 2017

Abstract Phenylketonuria (PKU, OMIM 261600) is an autosomal recessive disease, caused by mutations in the Phenylalanine Hydroxylase (*PAH*) gene situated in chromosome 12q22-q24.2. This gene has 13 exons. To date, 991 mutations have been described. The genotype is one of the main factors that determine the phenotype of this disease. *Objective:* Characterize PKU genotype and phenotype seen in Chilean PKU patients. *Methods:* We studied the *PAH* gene by restriction fragment length polymorphism (RFLP) and/or sequencing techniques to identify pathogenic mutations in 71 PKU subjects. We classified the phenotype according to Guldberg predicted value. *Results:* We identified 26 different mutations in 134 of the 142 alleles studied (94.4%), 88.7% of the subjects had biallelic pathogenic mutations while 11.3% had only one pathogenic mutation identified. Compound heterozygous represented 85.9% of the cases. Exon 7 included the majority of mutations (26.9%) and 50% of mutations were missense. The most frequent mutations were c.1066-11G > A, c.442-?_509+?del and p.Val388Met. The majority of subjects (52.3%) had the classic phenotype. *Conclusions:* The most frequent mutations in our Chilean PKU population were p.Val388Met, c.442?_509+?del and c.1066-11G > A. It is possible to predict phenotype by detecting the genotype, and use this information to determine disease prognosis and adjust patient's medical and nutritional management accordingly.

Highlights

- A strong correlation between genotype and phenotype in PKU has been described.
- For the first time in Chile, we analyzed a large number of mutations in the PAH, in order to characterize genotype and phenotype.
- In our PKU population the three most frequent mutations were p.Val388Met (17.2%), c.442-?_509+?del (14.9%), and IVS10-11G > A (12.7%).
- Because of the shared history of Spanish colonization, these results could be extrapolated to the rest of Latin America, assisting other countries in a strategy to direct the study to common mutations.
- There was a correlation between predicted phenotype and observed phenotype, except in subjects with p.Val388Met mutation.
- The complete categorization of patients is essential for our center to identify the most vulnerable patients (classic PKU) and create strategies to prevent any difficulties in long-term nutritional treatment.

Introduction

Phenylketonuria (PKU) is an autosomal recessive disease, caused by a total or partial deficit in the phenylalanine hydroxylase activity, which converts phenylalanine (Phe) to tyrosine (Tyr) (Mitchell 2011). This enzyme deficiency causes Phe accumulation (hyperphenylalaninemia) damaging the nervous system, leading to intellectual impairment,

Communicated by: Nenad Blau, PhD

V. Hamilton (✉) · L. Santa María · K. Fuenzalida · P. Morales · J. F. Cabello · V. Cornejo
Instituto de Nutrición y Tecnología de los Alimentos, Dr. Fernando Monckeberg Barros, Universidad de Chile, Santiago, Chile
e-mail: vhamilton@inta.uchile.cl

L. R. Desviat · M. Ugarte · B. Pérez
Centro de Diagnóstico de Enfermedades Moleculares (CEDEM), CIBERER Universidad Autónoma de Madrid, Madrid, Spain

unless treated opportunely (Greene and Longo 2014). Newborn screening (NBS) for PKU in Chile started in 1992, establishing an incidence of 1:18,916 newborns (Cornejo et al. 2010). The Chilean cohort of PKU cases is one of the largest cohorts followed in a single Metabolic Center.

The PAH gene is located on chromosome 12q22-q24.2, is 90 kb in size with 13 exons and 12 introns (Scriver 2007). PKU is a heterogeneous inborn error of metabolism and to date, 991 mutations have been reported in databases (www.pahdb.mcgill.ca and http://www.biopku.org/pah/home.asp) (Wettstein et al. 2015). Almost 60% are missense mutations, mostly located on catalytic domain (Waters 2003; Blau 2016).

Researchers, especially Guldberg, have demonstrated a strong correlation between the genotype and phenotype in PKU (Guldberg et al. 1998; Pey et al. 2003). In addition, genotype can be used to predict the response to sapropterin dihydrochloride, BH4 the synthetic cofactor of the enzyme, necessary to activate PAH activity (Werner et al. 2011).

The NBS program in Chile does not include molecular testing to confirm the diagnosis, like screening programs in other countries (Gizewska et al. 2016). In Chile, PKU patients are diagnosed using Phe level in the newborn period, confirmed with tandem mass spectrometry (MS/MS) and Phe/Tyr ratio at 17.5 ± 8.7 days of age. For the first time in Chile, we characterized the genotype and phenotype of a large cohort of patients. We planned to use this information to personalize treatment for each patient.

Subjects and Methods

A total of 71 Chilean PKU patients that comply with the follow-up program from our Metabolic Center at INTA, University of Chile, were included in this study from a total of 288 patients diagnosed in the NBS program since 1992. The subjects for this study were between 3 months and 32 years of age. The sample was 59.2% male and 40.8% female. Every patient signed the informed consent approved by our institution ethics committee. The samples of 32 PKU patients were analyzed for mutations in Chile and the rest were studied in the Center of Diagnosis of Metabolic Diseases, Madrid, Spain as part of a previous study (Trujillano et al. 2014).

Genetic Analysis

Genomic DNA was isolated from the leukocytes of blood samples using Wizard→ Genomic DNA purification kit (Promega), following supplier instructions. All 13 exons with their flanking intronic sequences were amplified by PCR (primers sequence provided upon request). PCR conditions were 95°C for 5 min and 36 cycles of 95°C for 25 s to denature DNA, 25 s at 55°C for annealing and 40 s at 72°C to elongate, and the last cycle for elongation lasted 7 min. For PCR, FastStart Taq DNA Polymerase from Roche® was used, which is highly specific on rich GC sequences, adjusting the supplier protocol.

Data from the previous study in Spain determined the most common mutations. Thus, for an early and fast screening for these mutations (for exon 11: p.Val388Met, intron 10: c.1066-11G > A and exon 7: p.Arg261Gln) we used a Restriction Fragment Length Polymorphism (RFLP) protocol (Desviat et al. 1995), that use BsaAI (p.Val388-Met), DdeI (c.1066-11G > A), and HinfI (p. Arg261Gln) restriction enzymes, respectively. These mutations were also confirmed by sequencing.

All PCR products were sequenced by Macrogen, Korea. The obtained sequences were compared with the wild type sequence of the human PAH (NM_0002777.1).

Multiplex ligation-dependent probe amplification (MLPA) was performed to detect large genomic deletions in patients without identified mutations on one or both alleles, by the commercially available SALSA MLPA kit P055-D1 PAH (MRC-Holland®).

Mutation nomenclature followed the guidelines and recommendations of the Human Genome Variation Society (http://varnomen.hgvs.org/).

Genotype–Phenotype Correlation

To predict phenotype we assigned all mutations an arbitrary value (AV) by Guldberg [Classic PKU = 1, Moderate PKU = 2, Mild PKU = 4 and Mild Hyperphenylalaninemia (MHP) = 8] obtained from BIOPKU database. Guldberg phenotype classification is the same as the one published in Phenylketonuria Scientific Review Conference (Camp et al. 2014). This classification separates mild PKU into two different phenotypes: moderate PKU (900–1,200 μmol/L) and mild PKU (600–900 μmol/L). We used this classification so we could have four different phenotypes to compare them with Guldberg AV.

Phenotypes resulting from a combination of the two mutant alleles were expressed as the sum of the two AVs (Guldberg et al. 1998). These phenotypes were classified according to the predicted residual enzymatic activity based on in vitro expression studies according to PAH database (http://www.pahdb.mcgill.ca). We correlated the predicted phenotype with the observed phenotype for patients with complete mutation analysis. Additionally, we searched the BIOPKU database for the BH4 response for each patient.

Statistical Analysis

To correlate the predicted phenotype with the observed phenotype, the Fisher exact test was used. Significance

level was set at $p < 0.05$. Statistical analysis was performed using STATA 13.

Results

We identified 26 different mutations in 134 of the 142 alleles studied (94.4%), completing the analysis in 88.7% of the subjects. Biallelic mutations were detected in 63 cases and only one mutation was identified in 8 (11.3%). Twenty-eight alleles were identified by RFLP as a first screening. The rest of the mutations were identified by sequencing analysis. Most of the subjects were compound heterozygous (85.9%). The exon containing more mutations was exon 7 (26.7%) (p.Arg243Gln, p.Leu249Phefs*92, p.Arg252Trp, p.Arg261Gln, p.Pro275Arg, p.Thr278Asn, p.Glu280Lys or p.Pro281Leu), followed by 7.7% on exon 5 (c.442-?_509+?del and p.Arg158Gln), 7.7% on exon 11 (p.Val388Met and p.Glu390Gly), and 7.7% on intron 10 (c.1066-11G > A and c.1066-3C > T).

The mutational spectrum included 50% missense, 34.6% splicing, 11.5% deletions, and 3.8% nonsense mutations. Twenty-one mutations were located on the catalytic domain, two on regulatory domain and three on the oligomerization domain (Table 1).

Table 2 shows the subjects with biallelic mutations and their phenotype, based on Guldberg prediction, which showed that 52.4% of our subjects had classic PKU, 28.6% had mild PKU, 4.8% had an undefined phenotype due to no phenotype information on mutation p.Pro275Leu, and the rest had MHP and Mild/MHP PKU.

Overall there was a correlation between predicted phenotype and observed phenotype ($p < 0.007$), however in the subjects with the p.Val388Met mutation we observed discordance between phenotypes ($p = 0.569$) (see Table 3).

Discussion

Genotype characterization allowed us to predict the phenotype in our Chilean patients, which could guide medical and nutritional management. Knowing the exact phenotype could help estimate Phe tolerance and metabolic control throughout life, individualizing treatment (Singh et al. 2016).

With the available data of the mutational spectrum in countries like Brazil, Mexico, and Chile (with this study), it can be concluded that p.Val388Met is one of the most common mutations (21.2%, 8.3%, and 17.3%, respectively). This concordance in mutations could relate to the common origins of these populations traced to the Iberian Peninsula (Santos et al. 2008; Vela-Amieva et al. 2015). The Spanish colonization of our region may allow for extrapolation of results to the rest of Latin America and guide the search to the specific mutations, which may lower costs for neighboring countries.

It has been shown that the allele which confers a residual enzymatic activity is pseudo-dominant, meaning that this mutation grants the final phenotype (Zschocke 2008; Guldberg et al. 1998). In our patients, this theory is not supported as the p.Val388Met mutation correlated with the observed phenotype in only 26.3% of the population (Table 3). The p.Val388Met mutation affects protein folding and the active tetramer formation (Aldamiz-Echevarria et al. 2016; Gamez et al. 2000) and retains 28% of enzyme activity leading to a mild to moderate phenotype. Most of our group had a more severe phenotype, especially when combined with a null variant (p.Thr278Asn, p.Glu280Lys, p.Arg252Trp, p.Leu249Phefs*92, c.442-?_509+?del, c.441 + 5G > A, c.1066-11G > A and c.1066-3C > T). The destabilizing mutations could be responsible for the phenotype–genotype inconsistencies. Reports indicate that when p.Val388Met is associated with a null mutation, the enzyme activity reduces by 12–15%, causing a classic phenotype (Leandro et al. 2000), which can be explained by the existence of a negative interallelic complementation on proteins expressed from two different pathogenic variants (Leandro et al. 2006; Vela-Amieva et al. 2015).

Other reason for why there is not always a correlation is that single gene disorders are not simple "traits," but rather complex "traits," because of modifier genes and epigenetic factors, such as a function of the blood–brain barrier, intestinal absorption of Phe, and Phe hepatic uptake among others that affect phenotype (Scriver and Waters 1999; Aldamiz-Echevarria et al. 2016).

Genotype can also be used to predict the response to sapropterin dihydrochloride (BH4), the synthetic cofactor of the enzyme and necessary to activate PAH activity. BH4 has been used in Europe and North America for more than 10 years, as monotherapy or together with a Phe-restricted diet, depending on drug response per patient (Blau et al. 2011; Werner et al. 2011). Recent reports have revealed that 60–80% of patients with mild PKU and hyperphenylalaninemia (HPA) would benefit from using this drug for treatment (Blau et al. 2011; Wettstein et al. 2015). Mutation analysis in Chilean PKU patients showed that 20% of our analyzed sample could use BH4 as part of their treatment. This information is important for choosing patients for future clinical studies with this drug in our country.

A phenylalanine-restricted diet is the most effective treatment for PKU demonstrated to date. With the diet, it is possible to avoid intellectual disability caused by neurotox-

Table 1 *PAH* gene mutations from PKU patients in Chile

Systematic name (DNA)	Trivial name (protein)	Location	Mutation type	Domain	Alleles number	Alleles frequency
c.1162G > A	p.Val388Met	Exon 11	Missense	Catalytic	23	17.2
c.442-?_509+?del	Ex5del	Exon 5	Deletion	Catalytic	20	14.9
c.1066-11G > A	IVS10-11G > A	Intron 10	Splicing	Catalytic	17	12.7
c.782G > A	p.Arg261Gln	Exon 7	Missense	Catalytic	10	7.5
c.913-7A > G	IVS8-7A > G	Intron 8	Splicing	Catalytic	8	6.0
c.1066-3C > T	IVS10-3C > T	Intron 10	Splicing	Catalytic	7	5.2
c.838G > A	p.Glu280Lys	Exon 7	Missense	Catalytic	7	5.2
c.754C > T	p.Arg252Trp	Exon 7	Missense	Catalytic	6	4.5
c.441 + 5G > A	IVS4 + 5G > T	Intron 4	Splicing	Catalytic	4	3.0
c.824C > G	p.Pro275Arg	Exon 7	Missense	Catalytic	4	3.0
c.842C > T	p.Pro281Leu	Exon 8	Missense	Catalytic	4	3.0
c.728G > A	p.Arg243Gln	Exon 7	Missense	Catalytic	4	3.0
c.1169A > G	p.Glu390Gly	Exon 11	Missense	Catalytic	3	2.2
c.707-7A > T	IVS6-7A > T	Intron 6	Splicing	Catalytic	2	1.5
c.833C > A	p.Thr278Asn	Exon 7	Missense	Catalytic	2	1.5
c.842 + 1G > A	IVS7 + 1G > A	Intron 7	Splicing	Catalytic	2	1.5
c.1045 T > C	p.Ser349Pro	Exon 10	Missense	Catalytic	2	1.5
c.745del	p.Leu249Phefs*92	Exon 3	Deletion	Catalytic	1	0.7
c.331C > T	p.R111*	Exon 3	Nonsense	Regulatory	1	0.7
c.527G > T	p.Arg176Leu	Exon 6	Missense	Catalytic	1	0.7
c.1241A > G	p.Tyr414Cys	Exon 12	Missense	Oligomerization	1	0.7
c.473G > A	p.Arg158Gln	Exon 5	Missense	Catalytic	1	0.7
c.168 + 5G > A	IVS2 + 5G > A	Intron 2	Splicing	Regulatory	1	0.7
c.1315 + 1G > A	IVS12 + 1G > A	Intron 12	Splicing	Oligomerization	1	0.7
c.1199 + 5G > A	IVS11 + 5G > A	Intron 11	Splicing	Oligomerization	1	0.7
c.1200-?_1315+?Del	p.Asn401_Ser439del	Exon 4	Deletion	Catalytic	1	0.7

icity of phenylalanine (Singh et al. 2016). In Chile, the diet is the only treatment available. Identifying patient phenotype allows for early categorization of disease severity and identification of the classic PKU patients, which are the most vulnerable. Many barriers have been described for treatment compliance, such as the Phe-free substitute's palatability and difficulties in food preparation, among others. These factors make optimal metabolic control difficult, especially in classic PKU patients because they tolerate less daily Phe intake and have higher Phe levels, therefore monitoring of these variables should be more meticulous. This study helps to complete all the information with respect to our PKU patients and allows for personalized treatment and follow-up.

Conclusions

Chilean genotype characterization allowed us to identify the predicted phenotype in our patients, which could guide medical and nutritional management.

We completed mutation analysis for the majority of pathogenic variant alleles in the PAH gene for our Chilean patients. The most common mutations in our patients were p.Val388Met, c.442-?_509+?del and c.1066-11G > A. Because of the shared history of Spanish colonization these results may be extrapolated to the rest of Latin America, assisting other countries to direct study to the most common mutations lowering costs and time.

There was a correlation between predicted phenotype and observed phenotype in our PKU patients. However cases with the p.Val388Met mutation have a more severe phenotype than expected – an important consideration for treatment.

The complete categorization of patient's phenotype is essential for our center to identify the most vulnerable patients (classic PKU) and create strategies to prevent any difficulties in long-term nutritional treatment.

Table 2 Genotype and phenotype of PKU patients in Chile

Mutations	# of patients	AV1	AV2	SUM AV	Predicted phenotype	BH4
p. Val388Met/p. Val388Met	4	4	4	8	Mild/MHP	Yes
IVS10-11G > A/Ex5del	3	1	1	2	Classic	Undefined
Ex5del/Ex5del	3	1	1	2	Classic	Undefined
IVS10-11G > A/IVS10-11G > A	2	1	1	2	Classic	No
IVS10-11G > A/IVS8-7A > G	2	1	1	2	Classic	Undefined
IVS10-11G > A/p.Val388Met	2	1	4	5	Mild	No
IVS10-3C > T/p. Val388Met	2	1	4	5	Mild	Undefined
IVS4 + 5G > T/p.Val388Met	2	1	4	5	Mild	No
IVS8-7A > G/Ex5del	2	1	1	2	Classic	Undefined
IVS8-7A > G/p.Ser349Pro	2	1	1	2	Classic	Undefined
p. Val388Met/p.Glu280Lys	3	4	1	5	Mild	No
p. Arg243Gln/p. Glu280Lys	2	1	1	2	Classic	Undefined
p.Arg252Trp/Ex5del	2	1	1	2	Classic	Undefined
p. Arg261Gln/p.Val388Met	2	4	4	8	Mild/MHP	Yes
IVS10-11G > A/IVS10-3C > T	1	1	1	2	Classic	Undefined
IVS10-11G > A/p. Pro275Arg	1	1	U	U	U	Undefined
IVS10-11G > A/p.Arg158Gln	1	1	1	2	Classic	No
IVS10-3C > T/IVS4 + 5G > T	1	1	1	2	Classic	Undefined
IVS10-3C > T/IVS7 + 1G > A	1	1	1	2	Classic	Undefined
IVS4 + 5G > T/IVS10-11G > A	1	1	1	2	Classic	No
IVS6-7A > T/IVS6-7A > T	1	1	1	2	Classic	Undefined
IVS8-7A > G/IVS10-11G > A	1	1	1	2	Classic	No
IVS8-7A > G/IVS7 + 1G > A	1	1	1	2	Classic	Undefined
p. Glu280Lys/IVS12 + 1G > A	1	1	1	2	Classic	No
p.Glu280Lys/p.Asn401_Ser439del	1	1	1	2	Classic	Undefined
p.Glu390Gly/IVS2 + 5G > A	1	4	1	5	Mild	Yes
Ex5del/IVS11 + 5G > A	1	1	1	2	Classic	Undefined
p.Leu249Phefs*92/p. Val388Met	1	1	4	5	Mild	Undefined
p.Pro275Arg/Ex5del	1	U	1	U	U	Undefined
p. Pro275Arg/p.Pro275Arg	1	U	U	U	U	Undefined
p.Pro281Leu/Ex5del	1	U	1	U	U	Undefined
p.Arg111*/p.Thr278Asn	1	1	1	2	Classic	Undefined
p.Arg176Leu/p.Pro281Lue	1	8	1	9	MHP	Yes
p.R252W/IVS10-3C > T	1	1	1	2	Classic	Undefined
p.Arg252Trp/p.Pro281Leu	1	1	1	2	Classic	No
p. Arg252Trp/p. Val388Met	1	1	4	5	Mild	No
p. Arg261Gln/p.Glu390Gly	1	4	8	12	MHP	Yes
p.Arg261Gln/Ex5del	1	4	1	5	Mild	Undefined
p. Arg261Gln/p.Pro281Leu	1	4	1	5	Mild	No
p. Arg261Gln/p.Arg243Gln	1	4	1	5	Mild	Yes
p.Arg261Gln/p.Arg261Gln	1	4	4	8	Mild/MHP	Yes
p.Thr278Asn/p. Val388Met	1	1	4	5	Mild	Undefined
p.Val388Met/Ex5del	1	4	1	5	Mild	Undefined
p.Tyr414Cys/Ex5del	1	4	1	5	Mild	Undefined
Total	63					

AV1 arbitrary value by Guldberg to mutation in allele 1. *AV2* arbitrary value by Guldberg to mutation in allele 2. *SUM AV* sum of both AV to predict phenotype. *BH4* BH4 response searched in BIOPKU database for each genotype. *MHP* mild hyperphenylalaninemia. *U* undefined

Table 3 Genotype and phenotype correlation in patients with the p. Val388Met mutation

Mutations	Expected phenotype	Observed phenotype
p. Val388Met/p. Val388Met	Mild/moderate	Mild
p. Val388Met/p. Val388Met	Mild/moderate	Mild
p. Val388Met/p. Val388Met	Mild/moderate	Classic
p. Val388Met/p. Val388Met	Mild/moderate	Mild
p.Thr278Asn/p. Val388Met	Mild	MHP
p.Glu280Lys/p. Val388Met	Mild	Classic
p.Glu280Lys/p. Val388Met	Mild	Classic
p.Glu280Lys/p. Val388Met	Mild	Moderate
p.Arg252Trp/p. Val388Met	Mild	Classic
p.Leu249Phefs*92/p. Val388Met	Mild	Classic
p.Arg261Gln/p. Val388Met	Mild/MHP	Mild
p.Arg261Gln/p. Val388Met	Mild/MHP	Classic
IVS4 + 5G > T/p. Val388Met	Mild	Classic
IVS4 + 5G > T/p. Val388Met	Mild	Classic
IVS10-11G > A/p. Val388Met	Mild	Classic
IVS10-11G > A/p. Val388Met	Mild	Classic
IVS10-3C > T/p. Val388Met	Mild	Classic
IVS10-3C > T/p. Val388Met	Mild	Classic
Ex5del/p. Val388Met	Mild	Classic

MHP mild hyperphenylalaninemia

Compliance with Ethics Guidelines

Conflict of Interest

Valerie Hamilton, Lorena Santa María, Karen Fuenzalida, Paulina Morales, Verónica Cornejo, Belén Pérez, Magdalena Ugarte, and Lourdes Desviat declare that they have no conflict of interest.

Informed Consent

All procedures followed were in accordance with the ethical standards of the responsible committee on human experimentation (institutional and national) and with the Helsinki Declaration of 1975, as revised in 2000 (5). The IRB and the Institute of Nutrition and Food Technologies (INTA) approved a waiver of consent for registries and chart reviews.

Details of the contributions of individual authors:

Valerie Hamilton contributed to the study conception and design; acquisition, analysis and interpretation of the data, drafting of the manuscript and patient follow-up.

Karen Fuenzalida contributed to the study conception and analysis of the data.

Paulina Morales contributed to the study conception.

Lorena Santa María contributed to the study conception and design, acquisition, analysis and interpretation of the data, and revising the manuscript.

Juan Francisco Cabello contributed to revising the manuscript and patient follow-up.

Verónica Cornejo contributed to acquisition of the study and patient follow-up.

Belén Pérez contributed to the study conception, analysis of the data, and revising the manuscript.

Magdalena Ugarte contributed revising the manuscript.

Lourdes Desviat contributed revising the manuscript.

All authors gave approval of the final manuscript.

References

Aldamiz-Echevarria L, Llarena M, Bueno MA, Dalmau J, Vitoria I, Fernandez-Marmiesse A, Andrade F, Blasco J, Alcalde C, Gil D, Garcia MC, Gonzalez-Lamuno D, Ruiz M, Ruiz MA, Pena-Quintana L, Gonzalez D, Sanchez-Valverde F, Desviat LR, Perez B, Couce ML (2016) Molecular epidemiology, genotype-phenotype correlation and BH4 responsiveness in Spanish patients with phenylketonuria. J Hum Genet 61(8):731–744

Blau N (2016) Genetics of phenylketonuria: then and now. Hum Mutat 37(6):508–515

Blau N, Hennermann JB, Langenbeck U, Lichter-Konecki U (2011) Diagnosis, classification, and genetics of phenylketonuria and tetrahydrobiopterin (BH4) deficiencies. Mol Genet Metab 104 (Suppl):S2–S9

Camp KM, Parisi MA, Acosta PB, Berry GT, Bilder DA, Blau N, Bodamer OA, Brosco JP, Brown CS, Burlina AB, Burton BK, Chang CS, Coates PM, Cunningham AC, Dobrowolski SF, Ferguson JH, Franklin TD, Frazier DM, Grange DK, Greene CL, Groft SC, Harding CO, Howell RR, Huntington KL, Hyatt-Knorr HD, Jevaji IP, Levy HL, Lichter-Konecki U, Lindegren ML, Lloyd-Puryear MA, Matalon K, MacDonald A, McPheeters ML, Mitchell JJ, Mofidi S, Moseley KD, Mueller CM, Mulberg AE, Nerurkar LS, Ogata BN, Pariser AR, Prasad S, Pridjian G, Rasmussen SA, Reddy UM, Rohr FJ, Singh RH, Sirrs SM, Stremer SE, Tagle DA, Thompson SM, Urv TK, Utz JR, van Spronsen F, Vockley J, Waisbren SE, Weglicki LS, White DA, Whitley CB, Wilfond BS, Yannicelli S, Young JM (2014) Phenylketonuria scientific review conference: state of the science and future research needs. Mol Genet Metab 112(2):87–122

Cornejo V, Raimann E, Cabello JF, Valiente A, Becerra C, Opazo M, Colombo M (2010) Past, present and future of newborn screening in Chile. J Inherit Metab Dis 33(Suppl 3):S301–S306

Desviat LR, Perez B, De Lucca M, Cornejo V, Schmidt B, Ugarte M (1995) Evidence in Latin America of recurrence of V388M, a phenylketonuria mutation with high in vitro residual activity. Am J Hum Genet 57(2):337–342

Gamez A, Perez B, Ugarte M, Desviat LR (2000) Expression analysis of phenylketonuria mutations. Effect on folding and stability of the phenylalanine hydroxylase protein. J Biol Chem 275 (38):29737–29742

Gizewska M, MacDonald A, Belanger-Quintana A, Burlina A, Cleary M, Coskun T, Feillet F, Muntau AC, Trefz FK, van Spronsen FJ, Blau N (2016) Diagnostic and management practices for phenylketonuria in 19 countries of the South and Eastern European Region: survey results. Eur J Pediatr 175(2):261–272

Greene CL, Longo N (2014) National Institutes of Health (NIH) review of evidence in phenylalanine hydroxylase deficiency (phenylketonuria) and recommendations/guidelines for therapy

from the American College of Medical Genetics (ACMG) and Genetics Metabolic Dietitians International (GMDI). Mol Genet Metab 112(2):85–86

Guldberg P, Rey F, Zschocke J, Romano V, Francois B, Michiels L, Ullrich K, Hoffmann GF, Burgard P, Schmidt H, Meli C, Riva E, Dianzani I, Ponzone A, Rey J, Guttler F (1998) A European multicenter study of phenylalanine hydroxylase deficiency: classification of 105 mutations and a general system for genotype-based prediction of metabolic phenotype. Am J Hum Genet 63(1):71–79

Leandro P, Rivera I, Lechner MC, de Almeida IT, Konecki D (2000) The V388M mutation results in a kinetic variant form of phenylalanine hydroxylase. Mol Genet Metab 69(3):204–212

Leandro J, Nascimento C, de Almeida IT, Leandro P (2006) Co-expression of different subunits of human phenylalanine hydroxylase: evidence of negative interallelic complementation. Biochim Biophys Acta 1762(5):544–550

Mitchell JJ Jr (2011) The findings of the Dartmouth Atlas Project: a challenge to clinical and ethical excellence in end-of-life care. J Clin Ethics 22(3):267–276

Pey AL, Desviat LR, Gamez A, Ugarte M, Perez B (2003) Phenylketonuria: genotype-phenotype correlations based on expression analysis of structural and functional mutations in PAH. Hum Mutat 21(4):370–378

Santos LL, Castro-Magalhaes M, Fonseca CG, Starling AL, Januario JN, Aguiar MJ, Carvalho MR (2008) PKU in Minas Gerais State, Brazil: mutation analysis. Ann Hum Genet 72(Pt 6):774–779

Scriver CR (2007) The PAH gene, phenylketonuria, and a paradigm shift. Hum Mutat 28(9):831–845

Scriver CR, Waters PJ (1999) Monogenic traits are not simple: lessons from phenylketonuria. Trends Genet 15(7):267–272

Singh RH, Cunningham AC, Mofidi S, Douglas TD, Frazier DM, Hook DG, Jeffers L, McCune H, Moseley KD, Ogata B, Pendyal S, Skrabal J, Splett PL, Stembridge A, Wessel A, Rohr F (2016) Updated, web-based nutrition management guideline for PKU: an evidence and consensus based approach. Mol Genet Metab 118 (2):72–83

Trujillano D, Perez B, Gonzalez J, Tornador C, Navarrete R, Escaramis G, Ossowski S, Armengol L, Cornejo V, Desviat LR, Ugarte M, Estivill X (2014) Accurate molecular diagnosis of phenylketonuria and tetrahydrobiopterin-deficient hyperphenylalaninemias using high-throughput targeted sequencing. Eur J Hum Genet 22(4):528–534

Vela-Amieva M, Abreu-Gonzalez M, Gonzalez-del Angel A, Ibarra-Gonzalez I, Fernandez-Lainez C, Barrientos-Rios R, Monroy-Santoyo S, Guillen-Lopez S, Alcantara-Ortigoza MA (2015) Phenylalanine hydroxylase deficiency in Mexico: genotype-phenotype correlations, BH4 responsiveness and evidence of a founder effect. Clin Genet 88(1):62–67

Waters PJ (2003) How PAH gene mutations cause hyper-phenylalaninemia and why mechanism matters: insights from in vitro expression. Hum Mutat 21(4):357–369

Werner ER, Blau N, Thony B (2011) Tetrahydrobiopterin: biochemistry and pathophysiology. Biochem J 438(3):397–414

Wettstein S, Underhaug J, Perez B, Marsden BD, Yue WW, Martinez A, Blau N (2015) Linking genotypes database with locus-specific database and genotype-phenotype correlation in phenylketonuria. Eur J Hum Genet 23(3):302–309

Zschocke J (2008) Dominant versus recessive: molecular mechanisms in metabolic disease. J Inherit Metab Dis 31 (5):599–618

JIMD Reports
DOI 10.1007/8904_2017_83

RESEARCH REPORT

Long-Term Systematic Monitoring of Four Polish Transaldolase Deficient Patients

Patryk Lipiński · Joanna Pawłowska · Teresa Stradomska · Elżbieta Ciara · Irena Jankowska · Piotr Socha · Anna Tylki-Szymańska

Received: 05 August 2017 / Revised: 06 December 2017 / Accepted: 07 December 2017 / Published online: 03 January 2018

Abstract *Introduction*: Transaldolase deficiency (TALDO; OMIM 606003) is a rare inborn autosomal recessive error of the pentose phosphate pathway that, to date, has been diagnosed in 33 patients. Tżhere are few reports regarding the long-term follow-up of these patients.

The *aim* of our study is to present the disease progression in the form of a systematic long-term follow-up of four Polish patients with TALDO.

Methods and Results: We report four patients who manifested early onset TALDO. They were monitored with systematic clinical and laboratory examinations for 4–13 years. The dominant feature was an early liver injury, with subsequent renal tubulopathy. All patients presented with osteopenia and poor physical development. Our data shows that polyol concentrations seem to decrease with age.

Conclusions: In our patients, a progressive coagulopathy was the most sensitive parameter of liver dysfunction. Nodular fibrosis of the liver developed over the natural course of TALDO. This is the first report of long-term systematic clinical and biochemical monitoring of the disease progress in patients with TALDO.

Abbreviations

AFP	Alpha-fetoprotein
ALT	Alanine transaminase
APTT	Activated partial thromboplastin time
AST	Aspartate transaminase
CT	Computed tomography
GFR	Glomerular filtration rate
GSH	Reduced glutathione
HCC	Hepatocellular carcinoma
INR	International normalized ratio
IUGR	Intrauterine growth retardation
LTx	Liver transplantation
NAC	N-acetylcysteine
NADPH	Nicotinamide adenine dinucleotide phosphate
PELD	Pediatric end-stage liver disease
PLT	Platelet count
PPP	Pentose phosphate pathway
PT	Prothrombin time
TALDO	Transaldolase deficiency
TALDO1	Transaldolase gene name
US	Ultrasound

Introduction

Transaldolase deficiency (TALDO; OMIM 606003) was first described in 2001, and is a rare inborn autosomal recessive error of the pentose phosphate pathway; the initial reported patient had liver dysfunction from birth, subsequently developing liver cirrhosis at the age of 2 years (Verhoeven et al. 2001). Twenty-nine TALDO patients have

Communicated by: Bridget Wilcken

P. Lipiński · J. Pawłowska · I. Jankowska · P. Socha
Department of Gastroenterology, Hepatology, Feeding Disorders and Paediatrics, The Children's Memorial Health Institute, Warsaw, Poland

T. Stradomska
Department of Biochemistry, Radioimmunology and Experimental Medicine, The Children's Memorial Health Institute, Warsaw, Poland

E. Ciara
Department of Molecular Genetics, The Children's Memorial Health Institute, Warsaw, Poland

A. Tylki-Szymańska (✉)
Department of Paediatrics, Nutrition and Metabolic Diseases, The Children's Memorial Health Institute, Warsaw, Poland
e-mail: a.tylki@czd.pl; atylki@op.pl

previously been diagnosed in the neonatal or early infantile period (Verhoeven et al. 2001, 2005; Loeffen et al. 2012; Valayonnopoulos et al. 2006; Wamelink et al. 2007, 2008; Tylki-Szymanska et al. 2009, 2014; Eyaid et al. 2013; LeDuc et al. 2013; Jassim et al. 2014; Al-Shamsi et al. 2015; Banne et al. 2016; Rodan and Berry 2017).

There are few reports regarding the long-term follow-up of TALDO. The oldest reported patient was diagnosed at the age of 25 years. He had already presented in childhood (exact age not available) with hepatomegaly, thrombocytopenia, and normal transaminases (Al-Shamsi et al. 2015). The first reported patient died at the age of 17 years because of liver failure (Loeffen et al. 2012). The other patient was 9 years of age at the last follow-up, presenting with liver cirrhosis, tubulopathy, and chronic kidney failure (Loeffen et al. 2012). In addition, LeDuc et al. reported the diagnosis of an 8-year-old boy with an asymptomatic presentation, identified because of HCC found in his transaldolase-deficient brother (LeDuc et al. 2013).

The aim of our study is to present the disease progression of TALDO, in the form of long-term follow-up of four Polish patients. To the best of our knowledge, this is the first reported description of such long-term clinical and biochemical monitoring of the course of TALDO.

Patients and Methods

Patients' General Characteristics

The study population consists of four boys of Polish origin, from three families; two of them were born to consanguineous parents (I and II). All the studied patients exhibited early onset of the disease. The diagnosis was established in the infantile period and was confirmed by biochemical and molecular analyses. These data were previously reported (Tylki-Szymanska et al. 2009, 2014).

In all the patients, the disorder was manifested antenatally; intrauterine growth retardation was seen in *Patients I*, *II,* and *III* while the presence of fluid in the pericardium and abdominal cavity in *Patient IV* was described as *hydrops fetalis*. Pregnancies of *Patients I* and *II* were associated with excessive weight gain in the mother and an unusually enlarged placenta.

In all the patients during the neonatal period, hepatosplenomegaly with coagulopathy, hypoalbuminemia, elevated transaminases, and thrombocytopenia were noted. Facial features were confirmed by the clinical geneticist as normal. Additionally, psychomotor development was assessed as normal by achievement of motor milestones at the appropriate age. Patients had characteristically thin skin with a network of visible vessels and spider angiomas. *Patients II*, *III*, and *IV* also presented with cavernous hemangiomas.

Methods of Diagnosis

Liver dysfunction, alone or combined with renal abnormalities (nephrolithiasis in *Patients III* and *IV*) prompted measurement of urinary polyols. Urinary arabitol levels and D-/L-arabitol ratio was performed using a gas chromatography method (Stradomska and Mileniczuk 2002). All identified molecular variants were prioritized according to the population frequency and the predicted effect on the protein. Pathogenic consequences were defined according to the conservation of the affected amino acids and in silico predictions.[1]

Follow-Up: Clinical and Laboratory Data

Patients were followed up with clinical and laboratory examinations approximately every 6 months from diagnosis. *Patient IV* was lost to follow-up at the age of 4 years. Therefore, the follow-up time of studied patients ranges from 4 to 13 years. Individual patients' characteristics, clinical and laboratory data are summarized in Tables 1, 2, and 3.

Clinical and laboratory data were gathered through the retrospective analysis of the patients' medical records, as well as current investigations.

Patients' Individual Characteristics

Patient I

During the neonatal period, the patient presented with a tendency toward external bleeding, abnormal coagulation profile (including prolonged INR and APTT), anemia, and thrombocytopenia. Deficiencies in factors XI and XII were diagnosed.

At the age of 1.3 years, hepatosplenomegaly with moderately elevated transaminases, clotting disturbances, cholestasis, anemia, and thrombocytopenia were noted. Abdominal ultrasound (US) revealed nodular fibrosis of the liver.

At the age of 3.5 years, *Patient I* presented with poor physical, but normal intellectual, development. He exhibited

[1] In silico prediction of the potential protein functionality of identified molecular variants was performed with: PolyPhen-2 – Polymorphism Phenotyping v2 (http://genetics.bwh.harvard.edu/pph2/index.shtml); MutationAssessor (http://mutationassessor.org); LRT – Likelihood Ratio Test (http://www.genetics.wustl.edu/jflab/lrt_query.html); SIFT – Sorting Intolerant From Tolerant (http://sift.jcvi.org/www/SIFT_BLink_submit.html); MutationTaster (http://www.mutationtaster.org/); Alamut Visual (http://www.interactive-biosoftware.com/alamut-visual/); FATHMM – Functional Analysis through Hidden Markov Models FATHMM (https://omictools.com/functional-analysis-through-hidden-markov-models-tool); MetaSVM – MetaSVM score for non-synonymous variants; MetaLR – MetaLR score for non-synonymous variants.

Table 1 Individual TALDO deficient patients' characteristics, an early onset presentation and long-term follow-up

Patient	I	II (the younger brother of I)	III	IV
Gender	Male	Male	Male	Male
Genotype	Homozygote	Homozygote	Homozygote	Compound heterozygote
	c.575G>A, p.Arg192His	c.575G>A, p.Arg192His	c.462-174_981 +53del; p.?	c.575G>A, p.Arg192His/c.462-174_981+53del; p.?
Parents' consanguinity	+	+	–	–
Pregnancy	Uneventful; excessive weight gain in the mother	Uneventful; excessive weight gain in the mother	Oligohydramnios, intrauterine growth retardation	Intrauterine growth retardation, fluid in the pericardium and abdominal cavity
Delivery, weeks	38 Unusually enlarged placenta	37 Unusually enlarged placenta	41	37
Birth weight, g	2,380	2,700	2,150	2,410
Birth length, cm	48	50	48	51
Newborn and neonatal period				
Hepatosplenomegaly	+	+	+	+
Liver function problems	+	+	+	+
Bleeding diathesis	+	+	+	+
Anemia	+	+	+	+
Thrombocytopenia	+	+	+	+
Congenital heart defects	–	–	–	–
Renal problems	–	–	–	+[a]
Developmental delay	–	–	–	–
Dysmorphia	–	–	–	–
Skin changes	+[b]	+[c]	+[d]	+[e]
Other abnormalities	+[f]	+[g]	–	+[f]
Follow-up				
Age at last evaluation (years)	13.0	10.0	7.0	4.0
Liver stiffness in FibroScan measurements at last evaluation				
Probe M, kPa	14.3	20.9	8.9	n.a.
Probe S2, kPa	18.8	62.4	n.a.	n.a.
Number of liver decompensation episodes during follow-up	2	2	None	None
Listed for liver transplantation + age of listing (years)	Yes 11.0	Yes 8.0	No	No
Age of first renal problems (years)	5.5	4.5	2.0	0.5
Renal problems at last evaluation	Tubulopathy (proteinuria, hypercalciuria, renal acidosis)	Tubulopathy (proteinuria, hypercalciuria, renal acidosis)	Nephrolithiasis tubulopathy (proteinuria, renal acidosis)	Nephrolithiasis tubulopathy (proteinuria, hypercalciuria)

+ present, – absent, *n.a.* not analyzed

[a] Recurrent urinary tract infections, at the age of 4 months few small calculi in both kidneys were found

[b] Thin skin with a visible vascular network

[c] Thin and silky skin with few cavernous *hemangiomas*

[d] Thin skin with a network of visible vessels, spider angiomas, and multiple *hemangiomas*

[e] Skin changes in the form of visibly dilated vessels, spider angiomas, and cavernous *hemangiomas*

[f] Bilateral cryptorchidism

[g] Unilateral cryptorchidism

Table 2 Laboratory and biochemical data

	Laboratory references						
Age (years)	Hb 0–2 weeks, 14.9–23.7; 2 weeks–2 months, 13.4–9.8; 2–6 months, 9.4–13; 6 months–1 year, 11.1–14.1; 1–2 years, 11.3–14.1; 2–6 years, 11.5–13.5; 6–12 years, 11.5–15.5; 12–18 years, boys, 13–16 mg/dL	PLT 150–450 × 10^3/μL	AST <52 U/L	ALT <18 months, $N < 55$/60 U/L; 18 months–12 years, boys, $N < 40$ U/L; >12 years, boys, $N < 26$ U/L	INR 0.9–1.2	AFP <5.0 IU/mL	D-/L-arabitol enantiomer ratio <3.0 mmol/mol creatinine
Patient I							
1.3	11.2–12.0	47	141–258	68–146	1.49	2,100	n.a.
3.5	12.5	80	173–190	95–136	1.52–1.87	620	14.5
5.5	10.2–11.5	59	82	44	1.34	57.4	9.15
7.5	8.2–10.4	59–71	66–132	27–40	1.31–1.45	n.a.	n.a.
10.0	11.3	83	76	36	1.48	7.5	n.a.
11.0	10.4	75	109	62	1.48	5.4	8.2
12.5	11.1	99	91	66	1.51	5.1	n.a.
Patient II							
0.1	8.6	104	55–84	66–87	n.a.	45,450	n.a.
0.4	11.2	116	94	105	1.27	21,618	13.0
1.8	8.7	78	277	113	2.08	n.a.	n.a.
4.5	10.7–11.4	83	227	82	1.60	n.a.	n.a.
6.0	10.0	155	258	80	1.56	64.1	n.a.
8.0	12.4	127	115	58	1.53	44.3	7.8
9.5	13.5	126	139	65	1.51	31.6	n.a.
Patient III							
0.1	11.2–15.9	31–125	90	72	1.88	n.a.	8.50
0.7	11.3	117	71	39	1.85	n.a.	8.37
1.0	11.1	126	133	60	1.32	49.3	n.a.
2.0	11.6	101	58	38	1.23	44.8	n.a.
7.0	11.6	106	28	16	1.10	4.62	7.5
Patient IV							
0.1	11.1	35	84–97	24–30	1.92	n.a.	n.a.
0.3	11.5	66	72	33	1.49	n.a.	n.a.
1.0	12.0	64	168	50	1.81	278	n.a.
1.4	12.6	59	163	42	1.65	n.a.	13.2
2.0	11.6	85	192	45	1.69	150	11.7
4.0	11.2	63	213	55	1.50	102	n.a.

hepatosplenomegaly, undescended testes, and thin pale skin with a visible vascular network. Thrombocytopenia and moderately elevated transaminases were still observed. Abdominal US showed disseminated small nodular changes of the liver. A gastroscopy revealed first to second degree esophageal varices, according to the Paquet classification. Elevated excretion of polyols and seven-carbon sugars was detected in the urine (Tylki-Szymanska et al. 2009). Transaldolase activity was undetectable in fibroblasts. Thus, TALDO deficiency was suspected. Molecular analysis revealed a presumed homozygous known mutation c.575G>A in exon 5 of *TALDO1* (Tylki-Szymanska et al.

Table 3 Nephrological findings in studied patients

Patient	I			II			III		IV			
Age (years)	4.0	5.5	12.0	1.0	4.5	9.0	1.0	7.0	0.6	1.8	2.5	4.0
Proteinuria	–	+	Glomerulo-tubular	–	Glomerulo-tubular	Glomerulo-tubular	–	Glomerulo-tubular	–	–	+	–
Concentration	–	n.a.	alb: 880.5 (<20)	–	alb: 21,083.3 (<20)	alb: 198.7 (<20)	–	alb: 10,290.3 (<20)	–	–	n.a.	–
LMWP, mg/g creatinine (reference range)			α1-m: 86.6 (<20) α2-m: 17.0 (<100)		α1-m: 65.5 (<20) α2-m: 28.5 (<100)	α1-m: 65.5 (<20) α2-m: 28.5 (<100)		α1-m: 314.8 (<20) α2-m: 435.5 (<100)				
Proteinuria, g/L	–	0.9	0.13	–	1.06	0.94	–	1.25	–	–	n.a.	–
Renal acidosis	–	+	+	–	+	+	–	+	–	–	n.a.	–
Glucosuria	–	–	–	–	–	–	–	–	–	–	–	–
GFR, mL/min/1.73 m^2	105	45.3	75.0	110	110.1	116.8	154.9	159.2	78.1	181.9	205.5	180.5
Serum creatinine, μmol/L	38.9	41.5	69.8	29	34.5	36.2	17.7	27.4	26.52	22.9	18.0	17.0
Calcium-creatinine ratio, Mmol/mmol (reference range <1.10)	0.99	0.33	2.32	1.04	0.95	2.85	0.27	0.60	2.03	n.a.	4.8	n.a.
Renal ultrasound	Normal	Normal	Increased echogenicity of renal parenchyma, abrogated cortex-medulla differentiation, no renal calculi	Normal	Normal	Increased echogenicity of renal parenchyma, maintained cortex-medulla differentiation, no renal calculi	Normal	Renal calculus (9 × 7 mm) in the left kidney	Bilateral renomegaly (kidney length: 6.8 and 6.5 cm) with maintained cortex-medulla differentiation and several calculi in both kidneys	Bilateral renomegaly (kidney length: 8.4 and 8.2 cm), several calculi in both kidneys (the largest in the left kidney pelvis – 1.1 cm)	Bilateral renomegaly (kidney length: 8.5 and 8.3 cm), renal calculus (1.3 cm) in the left kidney	Bilateral renomegaly (kidney length 9.0 and 9.0 cm)

LMWP low-molecular-weight-proteinuria, *alb* albumin, *α1-m* alpha-1 microglobulin, *α2-m* alpha-2 macroglobulin, + present, – absent

2009). The mutation results in the missense substitution p.(Arg192His) of a highly conserved amino acid, but there are only small physicochemical differences between arginine and histidine and this substitution does not exhibit a shift in polarity of the amino acid (Tylki-Szymanska et al. 2009).

At the age of 5.5 years, he was admitted to the hospital because of severe liver decompensation with massively increasing ascites, and palpebral and scrotal edema. Thrombocytopenia, low albumin levels requiring supplementation, slightly elevated transaminases, coagulopathy (requiring vitamin K administration), and mild proteinuria were noted.

At the age of 7.5 years, esophageal variceal bleeding occurred. He manifested convulsions, hyperammonemia, and consciousness disturbances, finally progressing to coma. Spontaneous bacterial peritonitis developed. Thrombocytopenia, hypoalbuminemia (requiring repeated albumin supplementation), moderately elevated AST, coagulopathy (requiring vitamin K administration), and proteinuria (1.25 g/L) were observed during the 2-month hospitalization. He was discharged to the pediatric hospice for palliative treatment.

At the age of 10 years, gastroscopy revealed second degree esophageal varices, requiring endoscopic ligation. The laboratory data were consistent with those noted previously.

At the age of 11 years, he was admitted to the hospital for preliminary investigations for LTx. The PELD score was 7. Hypercalciuria (calcium-creatinine ratio: 1.32 mmol/mmol), renal phosphate loss (hypophosphatemia: 0.97 mmol/L), and proteinuria (0.43 g/L) were observed.

Currently, at the age of 12.5 years, *Patient I* is in quite good clinical condition. Laboratory data show moderately elevated transaminases and slowly progressing coagulopathy (still requiring vitamin K administration). Glomerulotubular proteinuria, hypercalciuria (calcium excretion 11.7 mg/kg/day), renal phosphate loss, hypophosphatemia (0.83 mmol/L), and metabolic acidosis are present. Renal US shows increased echogenicity of the parenchyma and abrogated cortex-medulla differentiation. Fibroscan measurements reveal moderately increased liver stiffness (Table 1). His psychomotor development is normal; however, he is presenting with osteopenia and poor physical outcomes, measuring in the <3rd percentile for both height-for-age and weight-for-age. He is qualified for hormonal studies because of cryptorchidism (results are pending).

Patient II

Since delivery, *Patient II* suffered bleeding diathesis (with the same coagulation profile as *Patient I* with deficiencies in factors XI and XII), severe anemia, thrombocytopenia, and slightly elevated transaminases. A thin, silky skin with cavernous hemangiomas and unilateral cryptorchidism were noted.

At the age of 5 months, hepatosplenomegaly was observed. Abdominal US revealed a homogeneous liver parenchyma. Anemia, moderately elevated transaminases, cholestasis, and bleeding diathesis were noted. Diagnostics of TALDO deficiency was commenced as a part of familial screening. Polyols and seven-carbon sugars were elevated (Tylki-Szymanska et al. 2009). Molecular analysis revealed the same genotype as in *Patient I* (Tylki-Szymanska et al. 2009).

At the age of 1.8 years, *Patient II* presented with anemia, progressive thrombocytopenia, coagulopathy (requiring vitamin K administration), moderately elevated transaminases, and cholestasis. Abdominal US revealed nodular fibrosis.

At the age of 4.5 years, he was admitted to the hospital due to severe liver decompensation, presenting with massively increasing ascites and scrotal edema. Thrombocytopenia, coagulopathy (requiring vitamin K administration), moderately elevated transaminases, cholestasis, and hypoalbuminemia (requiring albumin supplementation) were noted. Gastroscopy revealed first degree esophageal varices, according to the Paquet classification. Tubulopathy was noted for the first time (Table 3).

At the age of 6 years, *Patient II* was in good clinical condition, but had anemia, moderately elevated AST, and slightly elevated ALT, hypoalbuminemia (still requiring albumin supplementation) and coagulopathy (requiring vitamin K administration). A gastroscopy revealed first degree esophageal varices.

At the age of 8 years, he was admitted to the hospital for preliminary investigations for LTx. Progressive thrombocytopenia, moderately elevated AST, and slightly elevated ALT, coagulopathy (requiring vitamin K administration), and cholestasis were noted. The PELD score was 12. Abdominal US revealed a small liver with strongly heterogeneous parenchyma.

Currently, at the age of 9.5 years, *Patient II* is in a satisfactory clinical condition. Laboratory data show moderately elevated AST, slightly elevated ALT, and progressive coagulopathy (still requiring vitamin K administration). Glomerulo-tubular proteinuria, hypercalciuria (calcium excretion 13.3 mg/kg/day), renal phosphate loss (hypophosphatemia 0.97 mmol/L), and metabolic acidosis are present. Renal US shows increased echogenicity of the parenchyma and abrogated cortex-medulla differentiation. Fibroscan measurements reveal highly increased liver stiffness (Table 1). His psychomotor development is normal. He has osteopenia: 10–25th percentile, height-for-age; and <3rd percentile, weight-for-age.

Patient III

Clinical and laboratory examinations in the first days of life revealed progressive anemia, thrombocytopenia, and an abnormal coagulation profile (including prolonged INR and APTT). Like *Patients I* and *II*, deficiencies in factors XI and XII were diagnosed.

At the age of 1 month, *Patient III* was hospitalized because of hepatosplenomegaly and failure to thrive. Thin skin with a network of visible vessels, spider angiomas, and multiple hemangiomas were observed. Anemia, thrombocytopenia, slightly elevated transaminases, and bleeding diathesis were still noted. Sugars and polyols were measured, revealing elevated excretion in the urine (Tylki-Szymanska et al. 2014). A homozygous deletion c.462-174_981+53del in the *TALDO1* gene was identified. This deletion spans 1,317 bps and alters the acceptor splice site of exon 5 (Tylki-Szymanska et al. 2014).

At the age of 12 months, he presented with hepatosplenomegaly, moderately elevated AST and slightly elevated ALT, coagulopathy (as previously diagnosed, requiring vitamin K administration), and hypoalbuminemia (requiring albumin supplementation).

Patient III was diagnosed at the age of 2 years with nodular fibrosis of liver. Additionally, a small calculus in the left kidney was found. Laboratory data showed anemia and coagulopathy (requiring vitamin K administration).

Currently, at the age of 7 years, *Patient III* exhibits mild hepatosplenomegaly, and nephrolithiasis of the left kidney. On physical examination, hemangiomas and telangiectasias of the skin are present. Laboratory data show anemia and thrombocytopenia. Fibroscan measurements reveal mildly increased liver stiffness (Table 1). Nephrological studies show glomerulo-tubular proteinuria (Table 3). *Patient III*'s mental development is normal; he is presenting with osteopenia: 25th percentile, height-for-age; and 3rd percentile weight-for-age.

Patient IV

Clinical examination in the first days of life showed splenomegaly and bilateral cryptorchidism. Anemia, thrombocytopenia, coagulopathy (including abnormal INR), and mildly elevated AST were noted.

At the age of 4 months, *Patient IV* presented with hepatosplenomegaly, anemia and thrombocytopenia, moderately elevated AST, and bleeding diathesis. Abdominal CT showed small calculi in both kidneys.

Recurrent urinary tract infections were noted from birth. At the age of 7 months, hypercalciuria (calcium excretion 7.57 mg/kg/day) was noted. Renal US showed bilateral renomegaly with maintained cortex-medulla differentiation and several calculi in both kidneys.

At the age of 12 months, he presented with hepatosplenomegaly, anemia and thrombocytopenia, moderately elevated AST, and bleeding diathesis.

At the age of 15 months, urinary sugars and polyols were measured, and the profile suggested TALDO deficiency (Tylki-Szymanska et al. 2014). Molecular analysis revealed two mutations (c.575G>A, c.462-174_981+53del) in the *TALDO1* gene. Each parent was identified as a carrier of one of these mutations, confirming their biallelic distribution (compound heterozygosity) in the child (Tylki-Szymanska et al. 2014).

At the age of 2 years, thrombocytopenia, moderately elevated AST, and coagulopathy (requiring vitamin K administration) were present. Abdominal US revealed hepatosplenomegaly with heterogeneous liver parenchyma (nodular fibrosis), bilateral renomegaly, and several calculi in both kidneys.

At the age of 2.5 years, *Patient IV* sustained a head injury with severe subcutaneous bleeding requiring transfusion of large amounts of platelet concentrates and fresh frozen plasma. Urine analysis revealed proteinuria, extremely high hypercalciuria (calcium-creatinine ratio: 4.8 mmol/mmol).

At the age of 3 years, ureterorenoscopic lithotripsy was undertaken. The patient was lost to follow-up after the age of 4 years, at which time he presented with hepatosplenomegaly, bilateral renomegaly, thrombocytopenia, progressive coagulopathy (requiring vitamin K administration), and moderately elevated AST.

Discussion

Clinical Presentation and Systematic Monitoring

All our patients presented with early onset TALDO. *Patients I* and *II* suffered from severe liver dysfunction from birth, subsequently developing liver fibrosis and cirrhosis. The first renal manifestations, in the form of tubulopathy, were noted at the age of 4.5 and 5.5 years, respectively. In *Patients III* and *IV*, a milder hepatic phenotype (without liver decompensation episodes) was observed, probably due to the earlier (fetal) development of liver fibrosis. The first renal abnormalities were manifested earlier, at the age of 2 and 6 months, respectively, in the form of nephrolithiasis and tubulopathy.

Most of the patients described in the literature presented with severe symptoms in the neonatal period (Verhoeven et al. 2001, 2005; Loeffen et al. 2012; Valayonnopoulos et al. 2006; Wamelink et al. 2007, 2008; Tylki-Szymanska

et al. 2009, 2014; Eyaid et al. 2013; LeDuc et al. 2013; Jassim et al. 2014; Al-Shamsi et al. 2015; Banne et al. 2016; Rodan and Berry 2017). Reports from the literature and our observations suggest the existence of two main presentations of TALDO: an early onset presentation (prenatal or neonatal disease) which constitutes a severe form, in most of the cases rapidly fatal, and a late onset presentation (early or late infantile form) which comprises a slowly progressive form of the disease with favorable long-term outcome.

In both early and late onset presentations, liver dysfunction begins in early fetal life. In the early onset presentation, liver disease is manifested in the form of clotting disturbances, elevated transaminases, hypoalbuminemia, and skin changes in newborns. Progressive liver failure then leads to reduced lifespan. In patients with later onset of symptoms, liver dysfunction progresses more slowly, with liver fibrosis and cirrhosis developing.

The kidneys are affected in TALDO in the form of renal tubular dysfunction (Loeffen et al. 2012). The earliest laboratory findings in our patients were hypercalciuria and proteinuria. Clinical examinations revealed features of osteopenia, as a consequence of tubulopathy. In the most severe cases, a generalized proximal tubulopathy, renal Fanconi syndrome, may develop. Loeffen et al. (2012) reported that, among nine patients with TALDO, aging from 1 year to adolescence, seven had proteinuria, glucosuria, aminoaciduria, hypercalciuria, nephrocalcinosis, metabolic acidosis, complete renal Fanconi syndrome, and moderate chronic kidney disease. The earliest and most prevalent finding of kidney disease was low molecular weight proteinuria (Loeffen et al. 2012).

Renal phenotype is most commonly manifested later than liver dysfunction, although in our *Patients III* and *IV*, and other patients from the literature, renal abnormalities were also manifested in early infancy (Loeffen et al. 2012).

TALDO also presents with skin manifestations (Verhoeven et al. 2001, 2005; Loeffen et al. 2012; Valayonnopoulos et al. 2006; Wamelink et al. 2007, 2008; Tylki-Szymanska et al. 2009, 2014; Eyaid et al. 2013; LeDuc et al. 2013; Jassim et al. 2014; Al-Shamsi et al. 2015; Banne et al. 2016; Rodan and Berry 2017). Telangiectasias are related to significant damage of the liver. Hemangiomas observed in our *Patients II*, *III*, and *IV*, and other patients are probably secondary to disturbed placental formation and function (Verhoeven et al. 2001, 2005; Loeffen et al. 2012; Valayonnopoulos et al. 2006; Wamelink et al. 2007, 2008; Tylki-Szymanska et al. 2009, 2014; Eyaid et al. 2013; LeDuc et al. 2013; Jassim et al. 2014; Al-Shamsi et al. 2015; Banne et al. 2016; Rodan and Berry 2017). Nonetheless, cutis laxa or hypertrichosis described by other authors was not present in our patients.

The patients described in this report presented with normal facial features. As most (79%) of the children reported with TALDO were the offspring of consanguineous parents (including 12 patients from one Arabian tribe) (Verhoeven et al. 2001, 2005; Loeffen et al. 2012; Valayonnopoulos et al. 2006; Wamelink et al. 2007, 2008; Tylki-Szymanska et al. 2009, 2014; Eyaid et al. 2013; LeDuc et al. 2013; Jassim et al. 2014; Al-Shamsi et al. 2015; Banne et al. 2016; Rodan and Berry 2017), dysmorphic features should be described by a clinical geneticist/dysmorphologist and should be similar in related patients.

Pathogenesis and Biochemical Monitoring

The pathogenesis of liver and kidney diseases in TALDO is most probably a toxic impact of the accumulated sugars and polyols on the hepatocytes and kidney tubules (Loeffen et al. 2012). The formulation of the PPP without TALDO leads to the accumulation of sedoheptulose-7-phosphate, ribose-5-phosphate, ribulose-5-phosphate, xylulose-5-phosphate and C5-polyols: D-ribitol; D-arabitol; and D-xylitol (Perl et al. 2006; Perl 2007). The polyol concentrations are probably the highest in the neonatal period (LeDuc et al. 2013). Our data shows that polyol concentrations seem to decrease with age (Table 2).

To our knowledge this is the first description in the literature regarding such a long-term monitoring of biochemical studies in patients with TALDO.

Treatment

There is no effective treatment for TALDO. LTx at an early stage of the disease could perhaps be useful but some authors hypothesize that disease recurrence is a risk (LeDuc et al. 2013; Al-Shamsi et al. 2015). Only one child with TALDO has been reported to have undergone liver transplantation (at the age of 1 year) and was followed up; the patient was doing well at the age of 3 years with normal coagulation profile and slightly elevated transaminases (Al-Shamsi et al. 2015).

All our patients were treated symptomatically. *Patients I* and *II* were listed for LTx at the age of 11 and 8 years, respectively, but they are currently disqualified from such treatment due to their overall satisfactory condition.

Recently, Rodan et al. described a case of TALDO in an infant, who manifested with multisystem disease and was treated with NAC for 6 months (Rodan and Berry 2017). The authors concluded that this supplementation probably helps to normalize AFP levels and could result in decreased hepatocyte injury. The data from our patients show that AFP levels normalized with age.

Conclusions

TALDO manifested in our patients as an early onset disorder. The dominant feature was an early liver injury with subsequent renal abnormalities in the form of tubulopathy. Progressive coagulopathy is a sensitive parameter indicating liver dysfunction in TALDO.

Despite the severe phenotype, the patients remain in a relatively good clinical condition.

Acknowledgements We thank Colleen Elso, PhD, from Edanz Group (www.edanzediting.com/ac) for editing a draft of this manuscript.

References

Al-Shamsi AM, Ben-Salem S, Hertecant J, Al-Jasmi F (2015) Transaldolase deficiency caused by the homozygous p.R192C mutation of the TALDO1 gene in four Emirati patients with considerable phenotypic variability. Eur J Pediatr 174:661–668

Banne E, Meiner V, Shaag A, Katz-Brull R, Gamliel A, Korman S et al (2016) Transaldolase deficiency: a new case expands the phenotypic spectrum. JIMD Rep 26:31–36

Eyaid W, Al Harbi T, Anazi S, Wamelink MM, Jakobs C, Al Salammah M, Alkuraya FS (2013) Transaldolase deficiency: report of 12 new cases and further delineation of the phenotype. J Inherit Metab Dis 36:997–1004

Jassim N, Alghaihab M, Saleh SA, Alfadhel M, Wamelink MM, Eyaid W (2014) Pulmonary manifestations in a patient with transaldolase deficiency. JIMD Rep 12:47–50

LeDuc CA, Crouch EE, Wilson A, Lefkowitch J, Wamelink MMC, Jakobs C, Salomons GS, Sun X, Shen Y, Chung WK (2013) Novel association of early onset hepatocellular carcinoma with transaldolase deficiency. JIMD Rep. https://doi.org/10.1007/8904_2013_254

Loeffen YG, Biebuyck N, Wamelink MM, Jakobs C, Mulder MF, Tylki-Szymańska A, Bökenkamp A (2012) Nephrological abnormalities in patients with transaldolase deficiency. Nephrol Dial Transplant 27:3224–3227

Perl A (2007) The pathogenesis of transaldolase deficiency. IUBMB Life 59:365–373

Perl A, Qian Y, Chohan KR, Shirley CR, Amidon W, Banerjee S et al (2006) Transaldolase is essential for maintenance the mitochondrial transmembrane potential and fertility of spermatozoa. Proc Natl Acad Sci U S A 103:14813–14818

Rodan LH, Berry GT (2017) N-Acetylcysteine therapy in an infant with transaldolase deficiency is well tolerated and associated with normalization of alpha fetoprotein levels. JIMD Rep 31:73–77

Stradomska TJ, Mileniczuk Z (2002) Gas chromatographic determination of D-/L-arabinitol ratio in healthy Polish children. J Chromatogr B Analyt Technol Biomed Life Sci 773:175–181

Tylki-Szymanska A, Stradomska TJ, Wamelink MM, Salomons GS, Taybert J, Pawłowska J, Jakobs C (2009) Transaldolase deficiency in two new patients with a relative mild phenotype. Mol Genet Metab 97:15–17

Tylki-Szymanska A, Wamelink MM, Stradomska TJ, Salomons GS, Taybert J, Dąbrowska-Leonik N, Rurarz M (2014) Clinical and molecular characteristics of two transaldolase-deficient patients. Eur J Pediatr. https://doi.org/10.1007/s00431-014-2261-2

Valayonnopoulos V, Verhoeven NM, Mention K, Salomons GA, Sommelet D, Gonzales M, Touati G, de Lyonalay P, Jakobs C, Saudubray JM (2006) Transaldolase deficiency: a new cause of hydrops fetalis and neonatal multi-organ disease. Pediatrics 149:713–717

Verhoeven NM, Huck JH, Roos B, Struys EA, Salomons GS, Douwes AC, Jakobs C (2001) Transaldolase deficiency: liver cirrhosis associated with a new inborn error in the pentose phosphate pathway. Am J Hum Genet 68:1086–1092

Verhoeven NM, Wallot M, Huck JH, Dirsch O, Ballauf A, Neudorf U, Jakobs C (2005) A newborn with severe liver failure, cardiomyopathy and transaldolase deficiency. J Inherit Metab Dis 28:169–179

Wamelink MM, Smith DE, Jansen EE, Verhoeven NM, Struys EA, Jakobs C (2007) Detection of transaldolase deficiency by quantification of novel seven-carbon chain carbohydrate biomarkers in urine. J Inherit Metab Dis 30:735–742

Wamelink MM, Struys EA, Salomons GS, Fowler D, Jakobs C, Clayton PT (2008) Transaldolase deficiency in a two-year-old boy with cirrhosis. Mol Genet Metab 94:255–258

JIMD Reports
DOI 10.1007/8904_2017_87

RESEARCH REPORT

Coping Strategies, Stress, and Support Needs in Caregivers of Children with Mucopolysaccharidosis

Amy Schadewald · Ericka Kimball · Li Ou

Received: 18 September 2017 / Revised: 08 December 2017 / Accepted: 15 December 2017 / Published online: 04 January 2018

Abstract The mucopolysaccharidoses are a set of rare, inherited conditions that can have a catastrophic impact on those affected and their families. Because of the rarity of these disorders, little is known regarding the challenges faced by families of those affected and what coping mechanisms are commonly used. Coping is a way to manage demands that occur in one's environment or within oneself. Medical social workers historically have facilitated this process while providing support to patients who are responding to pressures of their diagnosis and the system.

A questionnaire of demographics and qualitative questions, along with the Pediatric Inventory for Parents (PIP) and Brief COPE, was sent by electronic survey to caregivers of children with MPS. The results of Brief COPE showed that problem-focused coping was more frequently used than emotion-focused ($p < 0.001$) or dysfunctional coping ($p < 0.0001$). Acceptance was the most frequently used coping strategy ($p < 0.05$). The results of PIP showed that emotionally distressing events were the most difficult ($p < 0.001$), while events related to medical care occurred at the highest frequency ($p < 0.001$). Psychosocial support provided by medical social workers significantly increased acceptance of caregivers ($p = 0.04$). Guidance on what to expect provided by any member of the care team increased denial ($p = 0.02$) and the difficulty of emotional distress ($p = 0.04$). This study identified commonly used coping strategies and measured stress among caregivers of children with MPS, as well as access to and use of psychosocial support services. Results highlight the urgency to improve the coverage and quality of psychosocial support and other support services.

Communicated by: Robert Steiner

A. Schadewald (✉)
University of Minnesota Health, Minneapolis, MN, USA
e-mail: aschade1@fairview.org

E. Kimball
Portland State University School of Social Work, Portland, OR, USA

L. Ou
Gene Therapy Center, Department of Pediatrics, University of Minnesota, Minneapolis, MN, USA

Introduction

The mucopolysaccharidoses (MPSs) are a group of rare, inherited metabolic disorders, which belong to a family of more than 40 identified lysosomal diseases (Schultz et al. 2011). Major symptoms of MPS diseases include cardiopulmonary disease, growth delay, skeletal dysplasias, organomegaly, and shortened life span. Patients with severe MPSs I, II, III, or VII exhibit progressive neurodegeneration and mental retardation. Current therapies for treatment include hematopoietic stem cell transplantation (HSCT) and enzyme replacement therapy (ERT). HSCT has a high rate of mortality (10–15%) and severe morbidity. ERT has negligible neurological improvements because the blood-brain barrier prevents intravenously infused enzyme from entering the brain.

The impact of parenting children with MPS can be "devastating" with major challenges being emotional distress, financial strains, and severe behavior difficulties (Nidiffer and Kelly 1983). A study conducted in the UK reported that families with children with MPS withdrew from social outings and restricted visitors to their homes, reducing the social support they could access (Bax and Colville 1995). Characteristics, such as child behavior difficulties or levels of social support, may contribute to parental distress. Grant et al. (2013) showed that caregivers

of children with MPS III were less future-oriented and goal-directed than caregivers of children with intellectual disabilities. Due to extreme heterogeneity in symptom presentation and lack of established phenotype-genotype correlation (Ou et al. 2017), it is difficult for professionals to predict disease progression (Valstar et al. 2008). Previous findings suggest that the unpredictability of MPS may contribute to increased stress levels.

Medical social workers have a long history of providing psychosocial support for physical and mental health concerns (Globerman and Bogo 2002). Regarding patient experience, Gibbons and Plath (2009) determined that medical social workers' relationship- and rapport-building skills and ability to provide empathy, practical assistance, and advocacy were essential to their role on the multidisciplinary team. Medical social workers utilize strong psychosocial assessment skills that incorporate systems and community knowledge to solve problems and provide emotional support. They practice holistically as they work with psychosocial issues that may be a barrier to achieving optimal health and help address the relationship between diagnosis and environment (Craig et al. 2015; Lazarus 1993). By gathering data to inform best practices in psychosocial intervention for caregivers, it would be expected that children have better outcomes in coping with their health-care needs. Medical social workers historically have facilitated development of coping skills while providing consistent support to patients who are responding to pressures of their diagnosis and the system (Craig et al. 2015; Lazarus 1993).

Objectives

Identify coping strategies used and measure stress among caregivers of children with MPS, and determine how these caregivers access and use psychosocial support services. Each type of MPS has differences in presentation; variation in stress and coping among syndromes was not measured in this study.

Methods and Materials

Methods

A mixed methods design was used. Two validated measures, the Brief COPE and the Pediatric Inventory for Parents (PIP), were adapted to measure coping strategies and stress among caregivers of children with MPS, respectively. Participants were asked a mix of open- and closed-ended questions about their experiences with the medical system and access to and use of psychosocial support services.

Participants

A survey link was sent through the National MPS Society to caregivers of children with MPS. Eligible participants were over the age of 18 years, and a primary caregiver of a child with an MPS disorder aged 18 years or younger.

Brief COPE

The Brief COPE (Carver 1997) is a self-report questionnaire with 14 subscales assessing coping techniques including self-distraction, active coping, denial, substance use, use of emotional support, use of instrumental support, behavioral disengagement, venting, positive reframing, planning, humor, acceptance, religion, and self-blame. Items are rated on a Likert scale (1 = I haven't been doing this at all to 4 = I've been doing this a lot). Reliability and validity of this measure have been documented within medical populations (Yusoff et al. 2010). Two subscales had poor internal consistency in the current study (α = 0.477 for behavior disengagement and 0.438 for self-distraction). Internal consistency for the remaining subscales ranged from 0.519 to 0.904.

The subscales were grouped into three composite scores: problem-focused coping (active coping, planning, use of instrumental support), emotion-focused coping (acceptance, positive reframing, humor, religion, use of emotional support), and dysfunctional coping strategies (behavior disengagement, denial, self-distraction, self-blame, substance use, venting). The internal consistency of each category was analyzed (α = 0.575 for problem-focused, 0.557 for emotional-focused, and 0.548 for dysfunctional coping strategies).

Pediatric Inventory for Parents

The PIP (Streisand et al. 2001) is a self-report measure of parenting stress related to caring for a child with an illness. There are four subscales with frequency and difficulty scores: communication, medical care, emotional distress, and role function. This measure was selected given the life-limiting nature and high level of physical health difficulties of MPS diseases. The reliability and validity of PIP were reported to be high (α range, 0.8–0.96) in a previous study (Grant et al. 2013). Since some participants skipped questions in this inventory, the total score of each subscale could not accurately reflect the data. Therefore, the average frequency and difficulty scores of each subscale were used for analysis. All subscales had good internal consistency (Cronbach's α 0.623–0.896).

Questionnaire

Participants were asked a mix of open- and closed-ended questions. A checklist was provided about services offered at time of diagnosis, including guidance on what to expect related to disease process by any provider on the care team (GE), education on behavioral changes that may occur related to the diagnosis and appropriate interventions (EDB), assistance with practical concerns such as insurance and finances (AIF), and opportunity to process emotions (EMS). Participants were cased about access to a licensed social worker and in what type of setting. Open-ended questions were included for deeper understanding of overall experience, stress, and support needs.

Data Analysis

Less than 5% of data was missing on any individual scale. For each scale, Little's MCAR test was not significant (all p values > 0.05) indicating that the data were missing completely at random. SPSS 20.0 was used to analyze data, p value <0.05 (two-tailed tests) to denote statistical significance. The assumption of normality was not met for a number of outcome variables; therefore nonparametric tests were used.

Results

Demographic Data

Eleven of 93 participants did not provide enough information for analysis and were excluded in further analyses. Twenty-one participants (25%) were aged 25–34, 42 (50%) were aged 35–44, and 16 (22.6%) were aged 45–64. Sixty-two participants (81.7%) were Caucasian, eight (9.8%) were Hispanic, four (4.8%) were African, and three (3.7%) were Asian. In terms of education background: 24 (29.3%) undergraduate degree, 12 (14.6%) graduate degree, 11 (13.4%) high school degree, and 8 (9.8%) associate degree. Sixty-seven (81.7%) were married, six divorced, six single, and three separated. Sixty-six participants (80.5%) had one child with MPS, while 16 had two children with MPS. Out of 100 children with MPS, 34 were female (age, 8.7 ± 4.8 years old) and 56 were male (age, 8.2 ± 4.5 years old). The participants were caregivers to children with various MPS disorders: 21 MPS I, 19 MPS II, 14 MPS IIIA, 9 MPS IIIB, 7 MPS IVA, and 9 MPS VI.

Support Services

Participants were asked about experiences at time of diagnosis and were provided with a checklist inquiring about services provided to them. Of 63 respondents, 38 (58%) were offered general guidance on what to expect (GE) related to disease process. Nineteen (29%) were offered education on behavioral changes that may occur related to the diagnosis and appropriate interventions (EDB), 18 (28%) were offered assistance with practical concerns such as insurance and finances (AIF), and 13 (20%) were offered opportunity to process emotions (EMS). Of those not offered these services, 53 (81.5%) participants would have been interested in EMS, 46 (70.8%) interested in EDB, 40 (61.5%) in AIF, and 35 (53.9%) in GE.

Of 75 respondents, 57 (76%) preferred that help be offered, while 18 (24%) preferred to ask for help. Fifty-nine of 72 respondents (77.6%) participated in online support networks (e.g., Facebook), 30 (39.4%) attended in-person patient/family meetings specific to MPS or lysosomal storage disease (LSD), 17 (22.4%) participated in counseling services, and 3 (3.9%) participated in in-person support groups.

Of 73 respondents, 9 (12.3%) had access to a medical social worker that works specifically with children with MPS. Out of these nine, five had regular contacts with this individual, indicating the rarity of social work professionals working specifically with children with MPS. Alternatively, 30 (41.7%) out of 72 participants had access to a social worker in other settings: 8 in primary care clinic, 14 from the child's school, and 4 who were private therapists or counselors.

Coping Strategies

The individual scales of Brief COPE were evaluated and illustrated in Fig. 1. Acceptance had the highest score (3.4 ± 0.84) and was significantly higher ($p < 0.05$) than other scales except active coping (3.0 ± 0.96) and planning (3.1 ± 0.92). Denial, substance use, and behavior disengagement have the lowest score: 1.4 ± 0.80, 1.2 ± 0.51, and 1.3 ± 0.65, respectively. The 14 scales were classified into three categories as previously described (Cooper et al. 2008). There was significant difference between these categories: problem-focused coping the highest (2.8 ± 0.56) and dysfunctional coping the lowest (1.7 ± 0.42) (Fig. 1). The correlation of individual scales was evaluated by Pearson's correlation (Table 1). Further, the correlation between the three categories was analyzed: emotional-focused coping was significantly correlated with problem-focused coping ($r = 0.508$, $p < 0.0001$).

To evaluate the relationship between psychosocial support and coping strategies, the individual scales of the Brief COPE and psychosocial support were analyzed by a general liner model. Five participants had regular contact with a social worker that specifically works with children with MPS; therefore we compared all participants that had

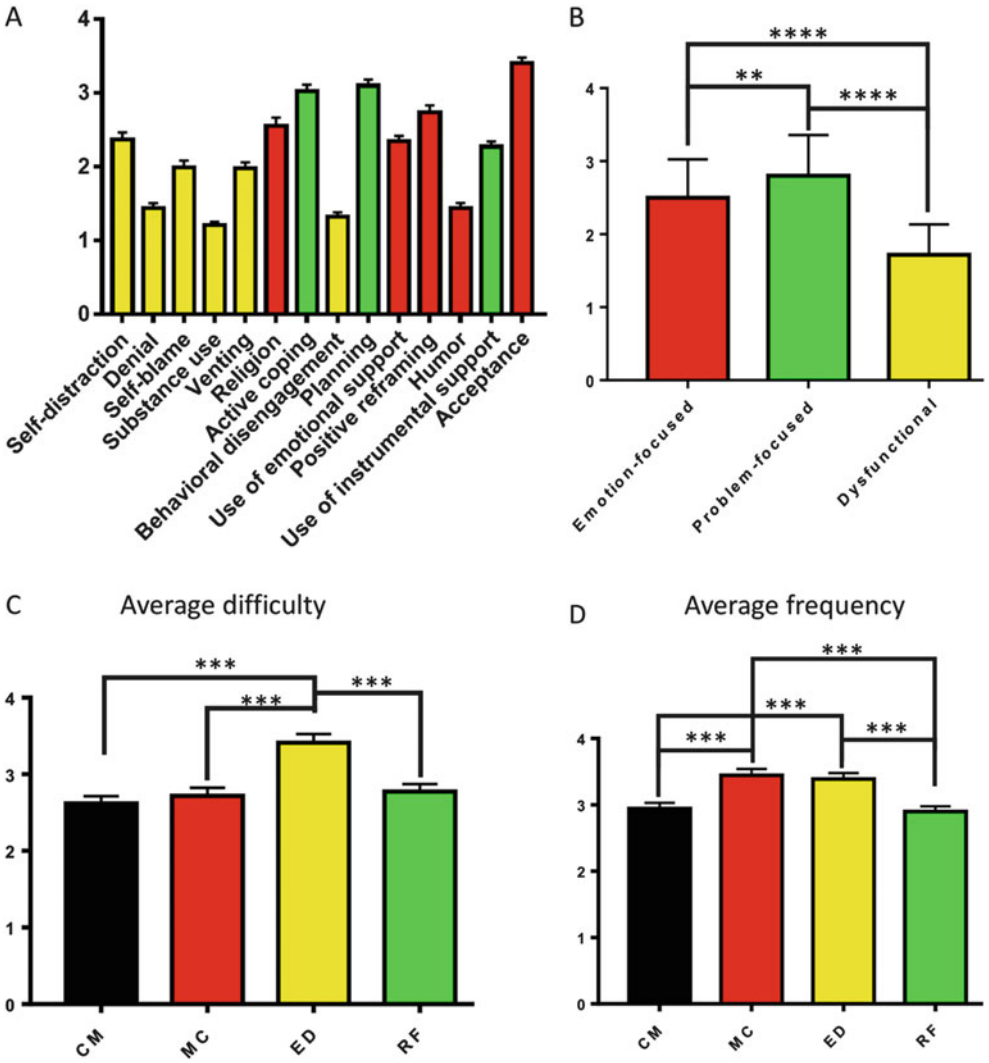

Fig. 1 Comparison of scales of Brief COPE and stress in caregivers of MPS children. (**a**) Average score of each individual scale. For simplicity consideration, the statistical significance was not marked. (**b**) Average score of each category. (**c**, **d**) Indicate stress difficulty and frequency, respectively. *CM* communication, *MC* medical care, *ED* emotional distress, *RF* role function. Data were represented as mean ± standard errors. $^{**}p < 0.01$, $^{***}p < 0.001$, $^{****}p < 0.0001$

access to social workers across settings with those who had no access to social workers. Multiple factors including age, marriage status, education level, number of children with MPS, and types of initial support received were included. Psychosocial support from a social worker significantly increased acceptance ($p = 0.043$) but had no significant impacts on other individual scales or categories. These results demonstrated that psychosocial support increased acceptance of caregivers but required refinement in improving other positive coping strategies.

Self-blame decreased as education levels of caregivers increased ($p = 0.014$), while positive reframing increased as number of children with MPS increased ($p = 0.008$). Denial decreased as age of caregivers increased ($p = 0.039$), and EDB significantly decreased denial ($p = 0.018$). Unexpectedly, GE increased denial ($p = 0.021$), indicating the necessity to improve this in the future.

Stress

To investigate the stressors of caregivers of children with MPS, the PIP was employed. There are four subscales with frequency and difficulty scores: communication (CM), medical care (MC), emotional distress (ED), and role function (RF). A total of 45 participants provided enough information for analysis. Emotional distress was related as significantly more difficult than any other category ($p < 0.0001$) (Fig. 1c). In terms of frequency, emotional distress and medical care were significantly higher than the other two categories ($p < 0.0001$) (Fig. 1d). These results

Table 1 Correlation between individual scales of Brief COPE

Correlations	Self-distraction	Behavior disengagement	Use of instrumental support	Planning	Denial	Self-blame	Substance use	Venting	Religion	Active coping	Use of emotional support	Positive reframing	Humor	Acceptance
Self-distraction							0.256*	0.297*					0.368**	
Behavior disengagement					0.256*	0.521**								
Use of instrumental support											0.707**			
Planning									0.292*	0.527**	0.408**	0.278*		
Denial						0.341**								−0.363**
Self-blame														
Substance use								0.424**					0.429**	
Venting														
Religion											0.265*	0.530**		
Active coping												0.458**		
Use of emotional support														
Positive reframing														0.354**
Humor														0.257*
Acceptance														

For simplicity consideration, the correlation between two factors was only shown once. *$p < 0.05$, **$p < 0.01$

showed that emotional distress was the major contributor to stress of caregivers. Pearson's correlation was performed among frequency and difficulty of all categories. As shown in Table 2, there were significant correlations in difficulty and frequency between each category.

To determine the relationship between psychosocial support and stress, the individual scales in the PIP and psychosocial support were analyzed by a general liner model. Multiple factors including age, marriage status, education level, number of children with MPS, and types of initial support received were included. Psychosocial support had no significant impact on stress levels in the individual scales or the aforementioned four categories. These results indicate a necessity to improve psychosocial support to decrease stress of caregivers. When offered education on behavioral changes and interventions, communication difficulty significantly decreased ($p = 0.041$). The difficulty of role function decreased as ages of caregivers increased ($p = 0.028$). The frequency of emotional distress decreased as education levels and ages of caregivers increased ($p = 0.009$ and 0.031, respectively). The difficulty of emotional distress decreased as education levels of caregivers increased ($p = 0.019$). However, when provided guidance on what to expect related to disease progression, emotional distress increased ($p = 0.044$), strongly suggesting the need to improve that discussion.

Correlation between coping strategies and stress was also evaluated. As shown in Table 3, emotional-focused coping was negatively correlated with the difficulty of medical care stress ($r = -0.31$, $p = 0.04$), while total coping scores were positively correlated with the frequency of role function stress ($r = 0.31$, $p = 0.04$). Individual scales of coping strategies showed that most dysfunctional coping strategies were correlated with stress.

Qualitative Questions

Qualitative questions were included for a deeper understanding of the unique needs and concerns of caregivers. Twenty-one percent of respondents rated online support groups and networking with other families as the most helpful service. Notably, 10.7% respondents received no support services. In terms of what services caregivers would like more of, 19 respondents (36.5%) mentioned emotional support services, and 28 respondents (53.8%) mentioned information on community resources. Finally, many respondents reported feelings of sadness, loneliness, and concerns about lack of support, information, and public awareness.

Discussion

Previous studies have identified unique challenges involved in parenting a child with MPS (Nidiffer and Kelly 1983; Bax and Colville 1995; Grant et al. 2013; Cooper et al. 2008; Ucar et al. 2010). This is the first study to measure stress, coping, and access to and use of social work support and other psychosocial services among caregivers of children with MPS.

Coping and Stress

Caregivers who used more problem-focused coping used more emotion-focused coping (and vice versa). In individual scales, positive correlations mainly existed between scales within the same category (e.g., self-distraction with substance use and venting, behavior disengagement with denial and self-blame, planning, and active coping). There was a negative correlation between denial and acceptance,

Table 2 Correlation between individual scales of PIP

Correlations	CM_F	MC_F	ED_F	RF_F	CM_D	MC_D	ED_D	RF_D
CM_F		0.554*	0.635*	0.611*	0.764*	0.550*	0.534*	0.453*
MC_F			0.642*	0.669*	0.450*	0.667*	0.575*	0.557*
ED_F				0.787*	0.731*	0.698*	0.867*	0.776*
RF_F					0.633*	0.628*	0.710*	0.849*
CM_D						0.786*	0.706*	0.668*
MC_D							0.699*	0.714*
ED_D								0.752*
RF_D								

For simplicity consideration, the correlation between two factors was only shown once
CM_F communication stress frequency, *CM_D* communication stress difficulty, *MC_F* medical care stress frequency, *MC_D* medical care stress difficulty, *ED_F* emotional distress frequency, *ED_D* emotional distress difficulty, *RF_F* role function stress frequency, *RF_D* role function difficulty
*$p < 0.01$

Table 3 Correlation between coping strategies and stress

	r value	*p* value	
Dysfunctional coping	0.6	<0.001	TSF
	0.65	<0.001	TSD
	0.47	0.001	CM_F
	0.63	<0.001	CM_D
	0.5	<0.001	MC_F
	0.62	<0.001	MC_D
	0.64	<0.001	ED_F
	0.57	<0.001	ED_D
	0.43	<0.001	RF_F
	0.48	<0.001	RF_D
Emotional-focused	−0.31	0.04	MC_D
Total coping	0.31	0.04	RF_F
Behavior disengagement	0.3	0.048	TSD
	0.33	0.026	CM_D
	0.31	0.041	ED_F
Self-distraction	0.3	0.041	MC_F
	0.3	0.047	MC_D
	0.3	0.048	RF_F
Venting	0.37	0.012	CM_D
	0.31	0.037	MC_D
Self-blame	0.62	<0.001	TSF
	0.56	<0.001	TSD
	0.5	<0.001	CM_F
	0.5	0.001	CM_D
	0.5	<0.001	MC_F
	0.44	0.003	MC_D
	0.65	<0.001	ED_F
	0.56	<0.001	ED_D
	0.47	0.001	RF_F
	0.48	0.001	RF_D
Denial	0.41	0.05	TSF
	0.48	0.001	TSF
	0.4	0.007	CM_F
	0.49	0.001	CM_D
	0.33	0.028	MC_F
	0.5	<0.001	MC_D
	0.43	0.003	ED_F
	0.38	0.01	ED_D
	0.03	0.032	RF_D

CM_F communication stress frequency, *CM_D* communication stress difficulty, *MC_F* medical care stress frequency, *MC_D* medical care stress difficulty, *ED_F* emotional distress frequency, *ED_D* emotional distress difficulty, *RF_F* role function stress frequency, *RF_D* role function difficulty, *TSF* total stress frequency, *TSD* total stress difficulty

which is unsurprising considering the incompatibility of these two strategies. Additionally, dysfunctional coping was positively correlated with total stress and each category of stress (Table 3). Several dysfunctional coping strategies including venting, self-distraction, self-blame, behavior disengagement, and denial were correlated with stress indicating that dysfunctional coping may significantly increase stress. Further, emotion-focused coping was negatively correlated with the frequency of medical care stress, suggesting a positive impact of emotion-focused coping. Interestingly, there was a significant correlation between total coping scores and the frequency of role function stress ($p = 0.04$), which may be contributed by dysfunctional coping.

Psychosocial Support

Psychosocial support provided by medical social workers had positive impacts on acceptance. This could be because increased emotional support may help individuals develop ways to cope with MPS. EDB (education on behavioral changes and appropriate interventions) decreased denial and the frequency of communication stress; this kind of conversation provides practical tools to help manage behaviors. This supports the need for early intervention that provides psychosocial services and concrete support to caregivers. Services around emotional support services and education on community resources were specifically identified areas of need by caregivers. Furthermore, specific guidance on disease progression to help minimize denial and emotional distress should be provided.

Guidance on what to expect in disease progression requires remarkable improvements because it increased denial and emotional distress. These discussions need to be tailored with individual caregiver coping styles or stress levels in mind. Considering the impact of EDB on decreasing communication stress, more resource and attention should be allocated to this type of service. EDB offers practical advice for problem-solving and intervention which may increase caregiver confidence.

Other Factors

This study evaluated the impacts of several other factors (e.g., education level, age) on coping and stress. Higher education decreased self-blame and emotional distress; while older caregivers had less denial, the difficulty of role function stress and the frequency of emotional distress decreased. These are important factors to consider in terms of service outreach and provision. Younger and less educated caregivers may need more concrete and ongoing support from a social worker, while older and those with higher education may need less intense guidance. Although previous studies showed the importance of marital support (Grant et al. 2013), in this study marital status had no

impact on coping and stress. Collectively, these factors should be considered in data analysis of future studies.

Implications for Clinical Practice

Considering severe stress and lack of support, it is suggested that clinicians screen for anxiety and depression in caregivers and refer to appropriate psychological services as deemed appropriate. Screening tools provide a starting point for clinical interventions. Because those who had access to social workers reported an increase in the use of acceptance as a coping skill, inclusion of comprehensive social work services to assess and treat psychosocial needs is an important consideration. Respondents preferred proactive assessment and intervention. Early interventions to increase emotional- or problem-focused coping and decrease dysfunctional coping could be offered.

Online support groups and connection with other parents were rated as most helpful by caregivers. Online support groups are a cost-effective consideration to help reduce feelings of isolation and connect caregivers from geographically diverse locations. Social workers can help establish or be actively involved in such groups.

Social workers need to be better trained in MPS, in providing individualized caregivers services and psychosocial supports. Additionally, program development to better support caregivers in a variety of areas including one-to-one and group counseling and increased availability of social workers to caregivers is needed.

Future Research

A weakness of this study is selection bias. Those who participated may have an unknown reason for selecting and completing the questionnaire. Also, a larger sample size would have permitted separate analysis by gender, age, or type or phase of the disorder. Specifically, because stress and coping may look different among MPS syndromes.

Researchers should be aware of the impact of such studies on psychological functioning of caregivers. Future studies should consider applying a combination of psychometrically strong tools and qualitative interviews in a sensitive manner that respects the role of parent as expert-by-experience.

Acknowledgments Dr. Li Ou is a fellow of the Lysosomal Disease Network (U54NS065768). The Lysosomal Disease Network is a part of the Rare Diseases Clinical Research Network (RDCRN), an initiative of the Office of Rare Diseases Research (ORDR) and NCATS. This consortium is funded through collaboration between NCATS, the National Institute of Neurological Disorders and Stroke (NINDS), and the National Institute of Diabetes and Digestive and Kidney Diseases (NIDDK). The authors would like to thank Jennifer Werner for building the questionnaire within Survey Monkey.

Synopsis

Unique patterns of stress and coping strategies of caregivers of children with MPS were identified, as well as gaps in psychosocial support services to help inform best practice for the future.

Details of Author Contributions

Amy Schadewald was involved in conception and design of this study, critically revising the article, and interpretation of the qualitative data. Ericka Kimball was involved in conception and design of this study and critically revising the article. Li Ou was involved in analysis and interpretation of the data, drafting, and critically revising the article. All authors are in agreement with submission of this draft to JIMD.

Corresponding Author

Amy Schadewald, MSW, LICSW, ACM.

Competing Interest Statement

Amy Schadewald, Ericka Kimball, and Li Ou have no competing interests to declare.

Details of Funding

The authors confirm independence from sponsors; the article has not been influenced by the sponsors.

Details of Ethics Approval

This study was approved by the University of Minnesota Institutional Review Board (IRB, study #1702S0831) and supported by the National MPS Society.

Patient Consent Statement

Patient data was not used for this study.

Institutional Committee for Care and Use of Laboratory Animals

This article does not contain any studies with animal subjects performed by any of the authors.

References

Bax MC, Colville GA (1995) Behaviour in mucopolysaccharide disorders. Arch Dis Child 73(1):77–81

Carver CS (1997) You want to measure coping but your protocol's too long: consider the brief COPE. Int J Behav Med 4(1):92–100

Cooper C, Katona C, Livingston G (2008) Validity and reliability of the brief COPE in carers of people with dementia: the LASER-AD study. J Nerv Ment Dis 196(11):838–843

Craig SL, Betancourt I, Muskat B (2015) Thinking big, supporting families and enabling coping: the value of social work in patient and family centered health care. Soc Work Health Care 54(5):422–443

Gibbons J, Plath D (2009) Single contacts with hospital social workers: the clients' experiences. Soc Work Health Care 48(8):721–735

Globerman J, Bogo M (2002) The impact of hospital restructuring on social work field education. Health Soc Work 27(1):7–16

Grant S, Cross E, Wraith JE et al (2013) Parental social support, coping strategies, resilience factors, stress, anxiety and depression levels in parents of children with MPS III (Sanfilippo syndrome) or children with intellectual disabilities (ID). J Inherit Metab Dis 36(2):281–291

Lazarus RS (1993) Coping theory and research: past, present and future. Psychosom Med 55:234–247

Nidiffer FD, Kelly TE (1983) Developmental and degenerative patterns associated with cognitive, behavioural and motor difficulties in the Sanfilippo syndrome: an epidemiological study. J Ment Defic Res 27(Pt 3):185–203

Ou L, Przybilla MJ, Whitley CB (2017) Phenotype prediction for mucopolysaccharidosis type I by in silico analysis. Orphanet J Rare Dis 12(1):125

Schultz ML, Tecedor L, Chang M, Davidson BL (2011) Clarifying lysosomal storage diseases. Trends Neurosci 34(8):401–410

Streisand R, Braniecki S, Tercyak KP, Kazak AE (2001) Childhood illness-related parenting stress: the pediatric inventory for parents. J Pediatr Psychol 26(3):155–162

Ucar SK, Ozbaran B, Demiral N, Yuncu Z, Erermis S, Coker M (2010) Clinical overview of children with mucopolysaccharidosis type III a and effect of Risperidone treatment on children and their mothers psychological status. Brain Dev 32(2):156–161

Valstar MJ, Ruijter GJG, van Diggelen OP, Poorthuis BJ, Wijburg F (2008) Sanfilippo syndrome: a mini-review. J Inherit Metab Dis 31(2):240–252

Yusoff N, Low WY, Yip CH (2010) Reliability and validity of the brief COPE scale (English version) among women with breast cancer undergoing treatment of adjuvant chemotherapy: a Malaysian study. Med J Malaysia 65(1):41–44. 32(2):156–161

JIMD Reports
DOI 10.1007/8904_2017_86

RESEARCH REPORT

Beneficial Effect of BH_4 Treatment in a 15-Year-Old Boy with Biallelic Mutations in *DNAJC12*

Monique G. M. de Sain-van der Velden · Willemijn F. E. Kuper · Marie-Anne Kuijper · Lenneke A. T. van Kats · Hubertus C. M. T. Prinsen · Astrid C. J. Balemans · Gepke Visser · Koen L. I. van Gassen · Peter M. van Hasselt

Received: 10 October 2017 / Revised: 30 November 2017 / Accepted: 12 December 2017 / Published online: 30 January 2018

Abstract *Background*: Biallelic mutations in *DNAJC12* were recently identified as a BH_4-responsive cause of hyperphenylalaninemia (HPA). Outcome was only favorable when treatment was initiated early in life. We report on a 15-year-old boy with HPA due to a homozygous deletion in *DNAJC12* in whom – despite his advanced age – treatment was initiated.

Case: A boy with developmental delay, an extrapyramidal movement disorder, and persistently elevated plasma phenylalanine levels was diagnosed with *DNAJC12* deficiency at the age of 15 years. Diagnosis was made upon exome reanalysis revealing a homozygous 6.9 kb deletion in *DNAJC12* which had not been detected by the standard exome analysis pipeline. Treatment with the BH_4 analog sapropterin dihydrochloride (10 mg/kg/day) was initiated and evoked a 50% reduction of the plasma phenylalanine levels. More strikingly, a marked improvement in daily functioning and improved exercise tolerance was noted. Additionally, gait analysis before and after treatment initiation revealed a partial normalization of his movement disorder.

Conclusion: Patients with hyperphenylalaninemia due to *DNAJC12* deficiency may benefit from treatment with a BH_4 analog – even when introduced at a later age.

Communicated by: Martina Huemer, M.D.

"Monique G. M. de Sain-van der Velden" and "Willemijn F. E. Kuper" contributed equally to this work.

M. G. M. de Sain-van der Velden · H. C. M. T. Prinsen · K. L. I. van Gassen
Department of Genetics, University Medical Center Utrecht, Utrecht University, Utrecht, The Netherlands
e-mail: M.G.deSain@umcutrecht.nl; B.Prinsen@umcutrecht.nl; K.L.I.vanGassen-2@umcutrecht.nl

W. F. E. Kuper · G. Visser · P. M. van Hasselt (✉)
Department of Metabolic Diseases, Wilhelmina Children's Hospital, University Medical Center Utrecht, Utrecht, The Netherlands
e-mail: w.f.e.kuper@umcutrecht.nl; G.Visser-4@umcutrecht.nl; p.vanhasselt@umcutrecht.nl

M.-A. Kuijper · L. A. T. van Kats · A. C. J. Balemans
Centre of Excellence for Rehabilitation Medicine Utrecht, Rehabilitation Centre De Hoogstraat, Utrecht, The Netherlands
e-mail: m.a.kuijper@dehoogstraat.nl; l.v.kats@dehoogstraat.nl; a.balemans@vumc.nl

A. C. J. Balemans
Department of Rehabilitation Medicine, Amsterdam Movement Sciences, VU University Medical Center, Amsterdam, The Netherlands

Introduction

Recently, biallelic mutations in *DNAJC12* (OMIM #606060) were identified as a cause of (moderate) hyperphenylalaninemia (HPA) clinically and biochemically mimicking the tetrahydrobiopterin (BH_4) metabolism disorders putatively due to an interacting function of *DNAJC12* with phenylalanine hydroxylase (PAH), tyrosine hydroxylase and tryptophan hydroxylase (Anikster et al. 2017; Blau 2016; Longo 2009; Kaufman et al. 1978; Ng et al. 2015). The currently described phenotypic spectrum of *DNAJC12* deficiency ranges from intellectual disability and severe neurological symptoms (Anikster et al. 2017) to a very mild neurological phenotype (van Spronsen et al. 2017) or early onset parkinsonism (Straniero et al. 2017). A favorable outcome could be achieved when treatment including a BH_4 analog was initiated early in life (Anikster et al. 2017). Here, we describe in a patient with HPA due to biallelic mutations in *DNAJC12* the beneficial effects of treatment with a BH_4 analog even when initiated later in life.

Case

The patient, a boy born to consanguineous Moroccan parents, was referred to our department because of development delay and a movement disorder at the age of 7 years. Development during the first years of his life was reportedly normal. Clinical features at presentation included an extrapyramidal movement disorder with continuous involuntary movements and dysarthria. In addition, he was reported to be socially withdrawn. Although newborn screening for phenylketonuria (PKU) had been negative, metabolic investigations performed at 7 years of age revealed an increased phenylalanine concentration in plasma (564 μmol/L, normal <98 μmol/L), urine (69 mmol/mol creatinine, normal <20 mmol/mol creatinine), and cerebrospinal fluid (CSF) (92 μmol/L, normal <16 μmol/L). Additional investigations in CSF showed a decreased 5-hydroxyindoleacetic acid concentration (13 nmol/L, normal: 50–300 nmol/L) with normal concentrations of homovanillic acid (119 nmol/L, normal: 100–800 nmol/L), neopterin (15 nmol/L, normal: 9–20 nmol/L), and biopterin (26 nmol/L, normal: 10–34 nmol/L). To unravel a BH_4 metabolism defect a combined phenylalanine-BH_4 loading test was performed. Three hours after oral phenylalanine loading (100 mg/kg body weight), synthetic BH_4 was administered orally (at a dose of 20 mg/kg body weight). Phenylalanine concentration decreased by 22 and 55%, 4 and 8 h after BH_4 administration, respectively. A similar pattern has been described in patients with dihydropteridine reductase (DHPR) deficiency but DHPR activity was normal and no mutations were found in the *QDPR* gene, nor in the other known genes associated with HPA (i.e., *PAH*, *GCH1*, *PTS* and *PCB1*) (Ponzone et al. 1993). Additional genetic investigations over the years, including SNP array analysis and diagnostic whole exome sequencing, did not lead to a diagnosis. Based on the recent identification of biallelic mutations in *DNAJC12* as a cause of a BH_4-like neurological disorder including moderate HPA, we reanalyzed the exome variant data of this patient and found no mutations. Visual inspection of the bam alignment file, however, showed a homozygous deletion of approximately 7 kb. This appeared to be the same deletion as the deletion described, also in patients of Moroccan descent (Anikster et al. 2017). Indeed, PCR and Sanger sequencing validation showed that it was identical. The nomenclature according to the human genome variation society (www.hgvs.org) is, however, NM_021800.2: c.298-953_503-2589del p.(?). The deletion is flanked by a homologous sequence, suggesting that the deletion occurred by homologous recombination. Such deletions will not be detected by standard exome variant calling pipelines.

This diagnosis prompted initiation of treatment with sapropterin dihydrochloride (KUVAN®), a synthetic BH_4 analog, at a dose of 10 mg/kg/day in the patient, now aged 15 years. Phenylalanine concentrations, which had been stable (556 ± 51 μmol/L) for years, dropped to 209–315 μmol/L within 2 weeks. More importantly, a clear clinical improvement was noticed. Before treatment, the patient was introverted and had exhibited debilitating fatigue, requiring afternoon naps. Strikingly, exercise provoked a severe exhaustion resulting in a decreased consciousness which was confirmed when performing an exercise test. Within days after initiation of treatment with the BH_4 analog, he became more energetic, no longer needing his afternoon naps, showing more initiative. In addition, contact with others clearly improved. Exercise testing conducted 4 weeks after treatment initiation confirmed an increased power (+33%) and an increased aerobic capacity (+15%) (Brehm et al. 2014; McGinley et al. 2009). In addition, there was a measurable improvement of the movement disorder, as underlined by gait analysis, showing a disappearance of a (pathological) early heel-rise in midstance and an improvement of knee flexion in loading response (see Fig. 1). The positive effects were still present at latest follow-up 8 months after treatment initiation including stable and slightly improved outcomes on gait and exercise analysis.

Discussion

We report on the beneficial effects of treatment with a BH_4 analog initiated later in life in a patient with HPA due to biallelic mutations in *DNAJC12*. Patient and parent reported improvements were quantified using gait and exercise analysis demonstrating both an improvement of the patients' movement disorder and an overall increase in strength and fitness.

Although, obviously, treatment initiated at this age cannot undo irreversible damage due to *DNAJC12*-associated metabolic processes, the effects in our patient suggest it can ameliorate the acute effects of a deficiency and may be able to prevent further damage. This observation nuances the statement by Anikster et al. that late treatment cannot resolve the resulted developmental delay (Anikster et al. 2017).

In contrast to previous patients, who received a mixture of treatments precluding conclusions regarding the added value of each of these treatments, our patient's treatment consisted solely of BH_4 supplementation. This suggests that BH_4 – rather than neurotransmitter supplementation – plays a central role in treatment outcome, possibly by making BH_4 associated reactions more favorable allowing more substrate to be converted into product. In addition, the positive short-term effect observed in our patient suggests that this treatment could also influence symptoms in milder forms of *DNAJC12*-associated HPA (van Spronsen et al. 2017; Straniero et al. 2017). Identification of additional

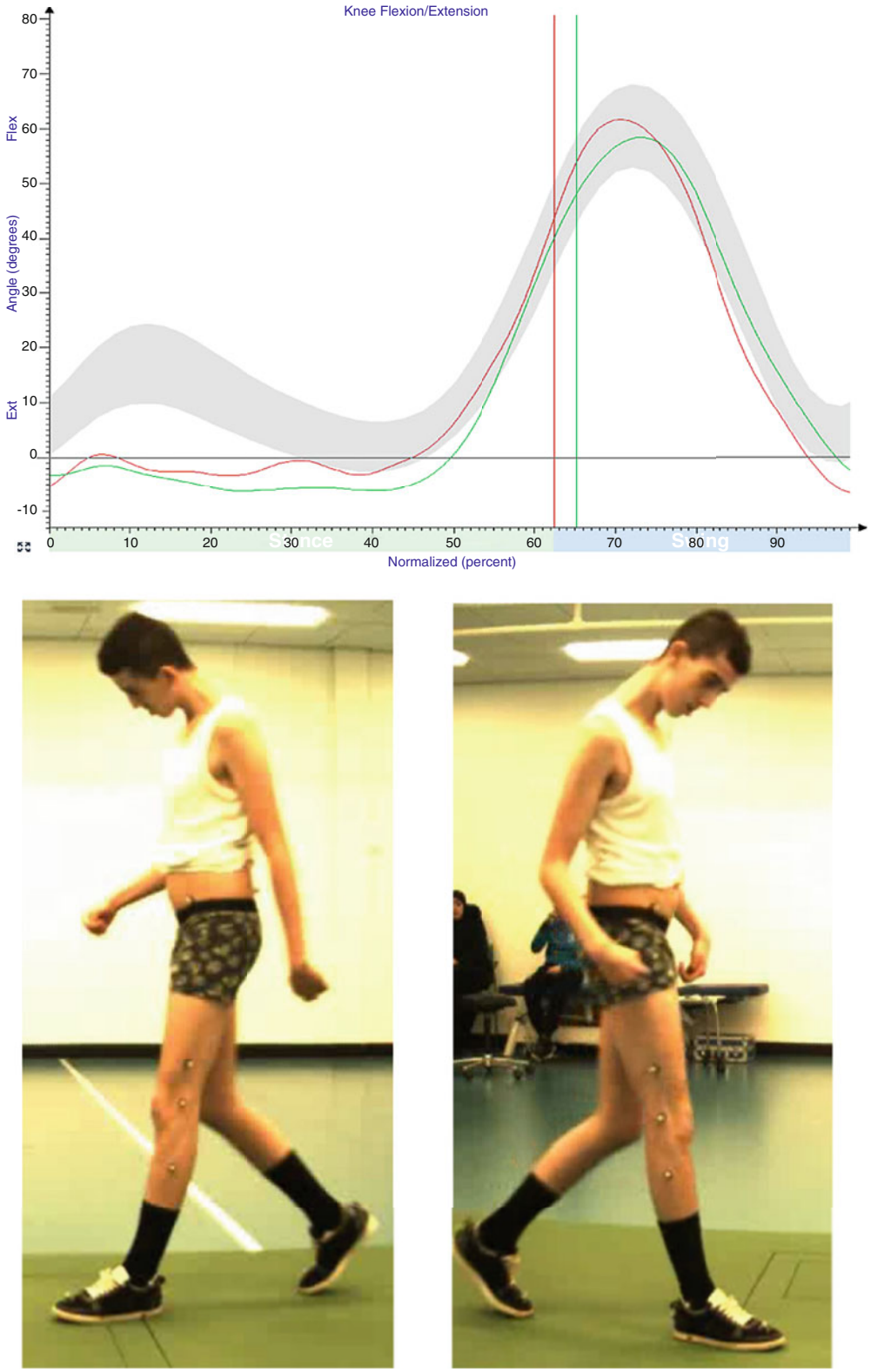

Fig. 1 Improved knee flexion in stance after treatment in a patient with hyperphenylalaninemia due to biallelic mutations in *DNAJC12*. Knee angle in the sagittal plane during gait prior to treatment (left) and 4 weeks after treatment initiation (right) demonstrating less hyperextension of the knee. Upper panels represent three-dimensional gait analysis. Red = left leg. Green = right leg. Gray = reference values. Representative photographs are provided in the lower panels. Instrumented gait analysis was performed with an 8-camera system (Vicon Motion Systems, Lake Forest, CA), all kinematic data was processed using Vicon Plug-in-gait Lowerbody Model

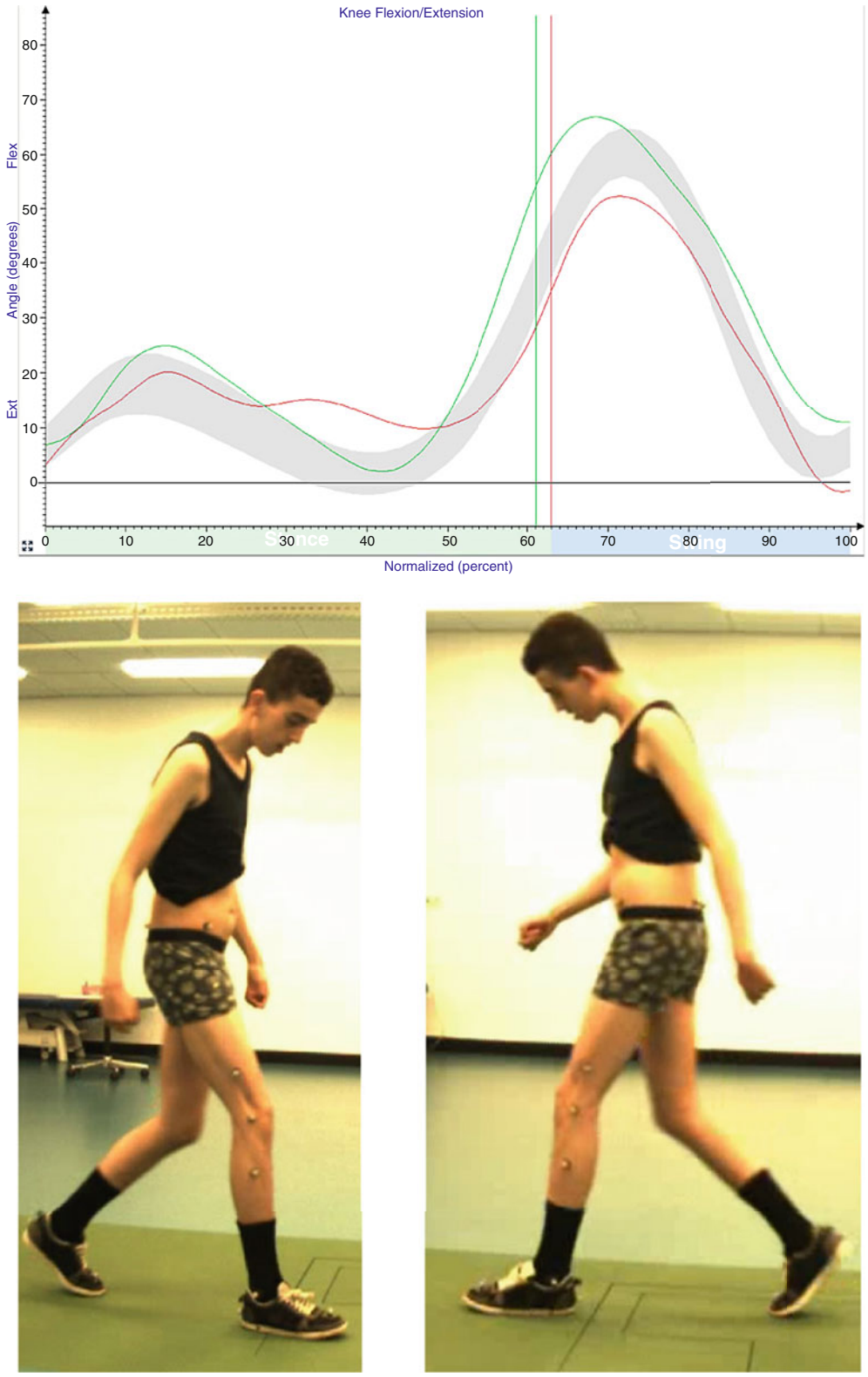

Fig. 1 (continued)

cases of HPA due to biallelic mutations in *DNAJC12* will be needed to elucidate the remaining therapeutic window in late identified cases.

It is noteworthy that our patient was not identified by population newborn screening, which was also reported in one of the six patients described by Anikster et al. (2017). Analysis for *DNAJC12* variants should be included in the differential diagnosis of HPA. The 6.9 kb microdeletion found in our case was initially also missed as the previously reported cases sharing this mutation (Anikster et al. 2017). Therefore, diagnostics for the *DNAJC12* gene should include a test that can detect this deletion, in particular in a patient of Moroccan descent. Current exome variant calling pipelines usually fail to recognize small microdeletions.

In summary, our report highlights the beneficial effect of treatment with a BH_4 analog in a patient with biallelic mutations in *DNAJC12* – even though treatment was only introduced later in life.

Synopsis

Treatment with a BH_4-analog only in a patient with *DNAJC12* deficiency diagnosed in puberty has a beneficial effect.

Compliance with Ethics Guidelines

Conflict of Interest

Monique G. M. de Sain-van der Velden, Willemijn F. E. Kuper, Marie-Anne Kuijper, Lenneke A. T. van Kats, Hubertus C. M. T. Prinsen, Astrid C. J. Balemans, Gepke Visser, Koen L. I. van Gassen, and Peter M. van Hasselt declare that they have no conflict of interest.

Informed Consent

Parents provided informed consent prior to article submission to use their child's history information, metabolic and genetic test results and photographs. Signed consent form for publication was obtained.

This article does not contain any studies with human or animal subjects performed by any of the authors.

Details of the Contributions of Individual Authors

Monique de Sain-van der Velden performed the metabolic investigations and drafted and revised the manuscript.

Willemijn Kuper supported Peter van Hasselt in the clinical care for the patient and drafted and revised the manuscript.

Marie-Anne Kuijper is the rehabilitation physician who provided clinical care for the patient in the rehabilitation center, contributed to the figure and revised the manuscript.

Koen van Gassen performed the genetic investigation that demonstrated the homozygous deletions in *DNAJC12* and revised the manuscript.

Lenneke van Kats performed the movement analyses contributing to the figure and revised the manuscript.

Astrid Balemans performed the movement analyses contributing to the figure and revised the manuscript.

Gepke Visser supported Peter van Hasselt in the clinical care for the patient and revised the manuscript.

Berthil Prinsen contributed in the metabolic investigations and revised the manuscript.

Peter van Hasselt is the pediatrician metabolic diseases who provided clinical care for the patient and revised the manuscript.

Corresponding Author

Peter M. van Hasselt.

References

Anikster Y, Haack TB, Vilboux T, Pode-Shakked B, Thony B, Shen N et al (2017) Biallelic mutations in DNAJC12 cause hyperphenylalaninemia, dystonia, and intellectual disability. Am J Hum Genet 100:257–266

Blau N (2016) Genetics of phenylketonuria: then and now. Hum Mutat 37:508–515

Brehm MA, Balemans ACJ, Becher JG, Dallmeijer AJ (2014) Reliability of a progressive maximal cycle ergometer test to assess peak oxygen uptake in children with mild to moderate cerebral palsy. Phys Ther 94(1):121–128

Kaufman S, Berlow S, Summer GK, Milstien S, Schulman JD, Orloff S et al (1978) Hyperphenylalaninemia due to a deficiency of biopterin. A variant form of phenylketonuria. N Engl J Med 299(13):673–679

Longo N (2009) Disorders of biopterin metabolism. J Inherit Metab Dis 32(3):333–342

McGinley JL, Baker R, Wolfe R, Morris ME (2009) The reliability of three-dimensional kinematic gait measurements: a systematic review. Gait Posture 29:360–369

Ng J, Papandreou A, Heales SJ, Kurian MA (2015) Monoamine neurotransmitter disorders – clinical advances and future perspectives. Nat Rev Neurol 11(10):567–584

Ponzone A, Guardamagna O, Spada M, Ferraris S, Ponzone R, Kierat L, Blau N (1993) Differential diagnosis of hyperphenylalaninaemia by a combined phenylalanine-tetrahydrobiopterin loading test. Eur J Pediatr 152:655–661

Straniero L, Guella I, Cilia R, Parkkinen L, Rimoldi V, Young A et al (2017) DNAJC12 and dopa-responsive nonprogressive parkinsonism. Ann Neurol 82(4):640–646. https://doi.org/10.1002/ana.25048

van Spronsen FJ, Himmelreich N, Rüfenacht V, Shen N, Vliet DV, Al-Owain M (2017) Heterogeneous clinical spectrum of DNAJC12-deficient hyperphenylalaninemia: from attention deficit to severe dystonia and intellectual disability. J Med Genet. https://doi.org/10.1136/jmedgenet-2017-104875

JIMD Reports
DOI 10.1007/8904_2018_88

RESEARCH REPORT

Secondary Hemophagocytic Syndrome Associated with COG6 Gene Defect: Report and Review

Nouf Althonaian · Abdulrahman Alsultan · Eva Morava · Majid Alfadhel

Received: 13 December 2017 / Revised: 16 January 2018 / Accepted: 18 January 2018 / Published online: 15 February 2018

Abstract Hemophagocytic lymphohistiocytosis (HLH) is a rare but potentially fatal disease that is characterized by proliferation and infiltration of hyperactivated macrophages and T-lymphocytes. Clinically, it is characterized by prolonged fever, hepatosplenomegaly, hypertriglyceridemia, hypofibrinogenemia, pancytopenia, and hemophagocytosis in the bone marrow, spleen, or lymph nodes. It can be classified as primary if it is due to a genetic defect, or secondary if it is due to a different etiology such as severe infection, immune deficiency syndrome, rheumatological disorder, malignancy, and inborn errors of metabolism such as galactosemia, multiple sulfatase deficiency, lysinuric protein intolerance, Gaucher disease, Niemann–Pick disease, Wolman disease, propionic acidemia, methylmalonic acidemia, biotinidase deficiency, cobalamin C defect, galactosialidosis, Pearson syndrome, and long-chain 3-hydroxyacyl-CoA dehydrogenase (LCHAD) deficiency. For the first time in the literature, we report on a 5-year-old girl diagnosed with a *Component of Oligomeric Golgi Complex 6* (*COG6*) gene defect complicated by HLH. Finally, we review the literature on inborn errors of metabolism associated with HLH and compare the previously reported patients of *COG6* gene defect with our patient.

Communicated by: Jaak Jaeken, Em. Professor of Paediatrics

N. Althonaian · M. Alfadhel
King Saud bin Abdulaziz University for Health Sciences, King Abdulaziz Medical City, Ministry of National Guard-Health Affairs (NGHA), Riyadh, Saudi Arabia

A. Alsultan
Department of Pediatrics, College of Medicine, King Saud University, Riyadh, Saudi Arabia

E. Morava
Department of Clinical Genomics, Mayo Clinic, Rochester, MN, USA

M. Alfadhel (✉)
Division of Genetics, Department of Pediatrics, King Abdullah Specialized Children Hospital, King Abdullah International Medical Research Centre, King Abdulaziz Medical City, Ministry of National Guard-Health Affairs (NGHA), Riyadh, Saudi Arabia
e-mail: dralfadhelm@gmail.com

Introduction

Hemophagocytic lymphohistiocytosis (HLH) is a rare but potentially fatal disease that is characterized by proliferation and infiltration of hyperactivated macrophages and T-lymphocytes (Verbsky and Grossman 2006). It is divided into primary and secondary HLH.

Primary HLH or familial erythrophagocytic lymphohistiocytosis (FEL) is an autosomal recessive disorder that affects infants and young children and is lethal in most patients (Janka 1983). Onset is classically within the first months or years of life. However, it can occur at any age (Janka 1983). Clinically, it is characterized by prolonged fever, hepatosplenomegaly, hypertriglyceridemia, and hypofibrinogenemia associated with pancytopenia. The following neurologic manifestations may occur early or may develop later: hypotonia, hypertonia, convulsions, cranial nerve palsies, ataxia, hemiplegia, quadriplegia, increased intracranial pressure, irritability, neck stiffness, blindness, and loss of consciousness. Lymphadenopathy and skin rash are additional less common findings. The mortality rate without treatment is high; HLH progression and infection account for the majority of deaths in untreated individuals (Zhang et al. 1993).

Primary HLH is caused by biallelic mutations in one of the following genes: *PRF1*, *UNC13D*, *STX11*, *STXBP2*,

RAB27A, *LYST*, *SH2D1A*, *BIRC4*, *IL2GR*, *IL7R*, *CD3e*, *RAG-1*, *ORA1*, *CD27*, and *ITK* (Sepulveda and de Saint Basile 2017; Tang and Xu 2011). The diagnostic criteria for HLH involve homozygous or compound heterozygous mutations in one of the aforementioned genes in addition to five out of the following eight clinical characteristics: fever, splenomegaly, cytopenia affecting at least two of three lineages in the peripheral blood, hypertriglyceridemia, hypofibrinogenemia, and hemophagocytosis in the bone marrow, spleen, and/or lymph nodes. Furthermore, the following characteristics are associated with the disease: low or absent natural killer (NK) cell activity, hyperferritinemia >500 μg/L, and high levels of soluble interleukin-2 receptor (sIL-2r) (Henter et al. 2007; Sepulveda and de Saint Basile 2017).

Secondary HLH may develop due to various etiologies, and it is difficult to differentiate from primary (familial) HLH by clinical or histologic characteristics alone. Molecular genetic testing is the best way to differentiate between primary and secondary HLH (Janka 1983). The causes of secondary HLH include the following: severe infection (usually viral), malignancy (such as lymphoma), rheumatologic disorders (such as juvenile idiopathic arthritis), and immune deficiency states (such as Griscelli syndrome type 2 and Chediak–Higashi syndrome) (Henter et al. 1993; Menasche et al. 2000; Dzoljic et al. 2015; An et al. 2017).

Inborn errors of metabolism (IEMs) have also been associated with secondary HLH (Table 1): galactosemia, multiple sulfatase deficiency, lysinuric protein intolerance, Gaucher disease, Niemann–Pick disease, Wolman disease, propionic acidemia, methylmalonic acidemia, biotinidase deficiency, cobalamin C defect, galactosialidosis, Pearson syndrome, and long-chain 3-hydroxyacyl-CoA dehydrogenase (LCHAD) deficiency (Olcay et al. 1998; Duval et al. 1999; Wu et al. 2005; Topaloglu et al. 2008; Sharpe et al. 2009; Karaman et al. 2010; Gokce et al. 2012; Kundak et al. 2012; Taurisano et al. 2014; Erdol et al. 2016).

To our knowledge, HLH with congenital disorders of glycosylation has not previously been reported. Herein, for the first time in the literature, we report on a 5-year-old girl diagnosed with a *Component of Oligomeric Golgi Complex 6* (*COG6*) gene defect (Shaheen syndrome, which is a type IIL congenital disorder of glycosylation).

Patient Report

We report on a 5-year-old girl, born preterm at 34 weeks of gestation after a complicated pregnancy with intrauterine growth restriction (IUGR). Her birth weight was 1,500 g (−4.0 SD), birth length was 50 cm (0.5 SD), and head circumference was 28 cm (−3.5 SD). She is the child of healthy consanguineous Saudi parents. She stayed in the neonatal intensive care unit for 6 days due to respiratory distress, and urinary tract infection, which was treated successfully with antibiotics.

The first concern noted was poor feeding and lethargy at the age of 2 months. However, no specific diagnosis was made at the time. At the age of 3 years, she presented at our center with a 2-day history of fever (up to 40°C, which was decreased by antipyretic treatment) and vomiting associated with decreased oral intake and activity. She had motor and speech disability. She required support to stand and spoke only two words (functioning at the level of a 10-month-old). Additionally, she had a history of hypohydrosis.

On examination, her height was 86 cm (−2.5 SD), weight was 10.5 kg (−2.1 SD), and head circumference was 45 cm (−2.2 SD). She had dysmorphic features, including microcephaly, broad palpebral fissures, retrognathia, wide mouth with thin lips, prominent nose, and bilateral epicanthal fold. She had strabismus, enamel hypoplasia with dental caries and dark discoloration of the teeth, and axial hypotonia. Multiple lymph nodes were bilaterally detected in the anterior cervical, supraclavicular, and inguinal region. They varied in size (the largest was 1 cm) and were mobile, not tender, and not attached to the skin. There was no erythema or skin changes. The clinical examination was otherwise normal.

Radiological investigations revealed generalized osteopenia by skeletal survey, and magnetic resonance imaging (MRI) of the brain showed brain atrophy, a thin corpus callosum, and a tiny subdural hemorrhage in the right occipital lobe. Abdominal ultrasound showed normal liver and spleen. Biochemical investigations revealed elevated serum transaminases (aspartate transaminase [AST] 779 (5–34) U/L, alanine transaminase [ALT] 113 (5–55) U/L), and a slightly increased gamma-glutamyltransferase (γ-GT) level. Lactic acid concentrations ranged between 2.2 and 4.5 mmol/L (normal: <2.2 mmol/L), and there was generalized hyperaminoaciduria. Serum transferrin isoelectric focusing (TIF) showed a type 2 pattern. Whole-exome sequencing revealed a previously reported homozygous pathogenic variant of the *COG6* gene, c.1167-24A>G (Shaheen et al. 2013). The following investigations showed normal results: acylcarnitine profile, plasma amino acids, urine organic acids, ammonia, total homocysteine, creatine kinase level, abdominal ultrasound, hearing tests, respiratory chain enzymology in skin fibroblasts and muscle, partial thromboplastin time, and activated partial thromboplastin time.

At the age of 4 years, the patient exhibited episodic epistaxis and gum bleeding, no bruises, persistent fever, and decreased activity. Lab results showed low hemoglobin at 80 (110–145) g/L, low platelets at 27 (150–450) × 10^9/L, low fibrinogen at 0.61 (1.5–4.1) g/L, high ferritin at 1,744.8 (4.6–204) μg/L, hypertriglyceridemia at 7.01 (≤0.84) mmol/L, prolonged coagulation profile (PT: 13.4

Table 1 Summary of published patients of inborn errors of metabolism (IEM) associated with HLH

No.	References	Number of cases	Inborn error of metabolism (IEM)	Country	Gender	Age of onset	Fulfilled diagnostic criteria for HLH	Treated according to HLH protocol	Prognosis
1	Ikeda et al. (1998)	1	Multiple sulfatase deficiency	Japan	M	10 months	Yes	No	Improved dramatically
2	Olcay et al. (1998)	1	Galactosialidosis	Turkey	M	7 months	Yes	No	Improved dramatically
3	Duval et al. (1999)	4	Lysinuric protein intolerance	France	4 M	3 months	Yes	Yes	NA
4	Wu et al. (2005)	1	Cobalamin C disease	USA	F	4 months	Yes	No	Improved dramatically
5	Topaloglu et al. (2008)	1	Pearson syndrome	France	M	7 months	Yes	No	Died
6	Sharpe et al. (2009)	1	Gaucher disease	Turkey	F	5.5 months	Yes	Yes	Died
7	Karaman et al. (2010)	1	Niemann–Pick disease	Turkey	F	3 months	Yes	No	Died
8	Gokce et al. (2012)	3	Propionic acidemia	Turkey	2 M, 1 F	Mean 4 years	Yes	Yes	One died Two improved dramatically
9	Kardas et al. (2012)	1	Biotinidase deficiency	Turkey	M	4 months	Yes	No	Improved dramatically
10	Taurisano et al. (2014)	1	Wolman disease	Italy	F	4 months	Yes	No	Died
11	Kundak et al. (2012)	1	Galactosemia	Turkey	F	12 days	Yes	Yes	Improved dramatically
12	Erdol et al. (2016)	1	LCHAD deficiency	Turkey	F	4 months	Yes	Yes	Died
13	This chapter	1	*COG6* gene defect	Saudi Arabia	F	4 years	Yes	Yes	Improved dramatically

M male, *F* female, *NA* not available

(9.38–12.3 s) seconds, INR: 1.23 (0.8–1.2) and PTT: 41 (24.8–34.9 s) seconds). Bone marrow biopsy showed hemophagocytosis in addition to low NK cells by flow cytometry. Spleen enlargement was detected by abdominal ultrasound. PCR-based tests for Epstein-Barr virus and cytomegalovirus in serum samples were negative. She had 7/8 HLH diagnostic criteria: fever, splenomegaly, cytopenia, hypertriglyceridemia, hemophagocytosis in bone marrow, low NK cells and high ferritin. Secondary HLH was confirmed after the negative result of sequencing the familial HLH gene panel covering the most common genes (Otrock et al. 2017); *PRF1*, *UNC13D*, *STX11*, and *STXBP2*, in addition to deletion/duplication analysis.

The patient was started on intravenous immunoglobulin, dexamethasone, and platelet transfusion (Zhang et al. 2013). Her lab results markedly improved in terms of liver function tests, and her hemoglobin, platelets, fibrinogen, ferritin, triglycerides, and coagulation results were almost normalized.

Currently, the patient is 5 years old with a global developmental disability, microcephaly, hypohydrosis, enamel hypoplasia, strabismus, splenomegaly, and hypotonia. Additionally, she has elevated transaminases, but otherwise normal lab results.

Discussion

The conserved oligomeric Golgi (COG) complex is a family of eight protein subunits that have a major role in regulating transport in the Golgi apparatus (Shaheen et al. 2013). Pathogenic variants of the *COG6* gene are a cause of Shaheen syndrome, an autosomal recessive disorder of glycosylation first described by Lubbehusen et al. (2010). Shaheen et al. reported on the largest cohort of patients with this disorder, consisting of 12 individuals from three consanguineous Saudi families. All these patients exhibited intellectual disability, global developmental disability, anhidrosis, palmoplantar keratosis, and progressive microcephaly (Shaheen et al. 2013). This is an autosomal recessive *N*- and *O*-linked glycosylation disorder (Sparks and Krasnewich 1993; Peanne et al. 2017; Foulquier et al. 2007).

CDG-COG6 is multisystem disorder, with at least 28 reported patients including detailed phenotypes in 17 (Table 2) (Lubbehusen et al. 2010; Huybrechts et al. 2012; Shaheen et al. 2013; Rymen et al. 2015; Alsubhi et al. 2017).

One of the distinctive features of *COG6* gene defect is hypohydrosis. This finding, in association with intellectual disability, could be a clue for diagnosis, to differentiate CDG-COG6 from other CDG.

Interestingly, the patient discussed in this case report had enamel hypoplasia with dental caries and black teeth discoloration, and this was reported in three other patients. Additionally, the present patient had intracranial bleeding in the form of subdural hemorrhage, similar to the first case reported in the literature (Lubbehusen et al. 2010). However, this bleeding ceased and had no consequences. Immunological manifestations include recurrent infections (41%). Rarely, patients have B-cell, T-cell, and neutrophil dysfunction, monocytosis, deficient polysaccharide antibody response, and combined immune deficiency (Rymen et al. 2015).

CDG-COG6 should be suspected in patients with a type 2 TIF pattern, which was found in 94% of the reported patients (but a normal pattern does not exclude it). Additional common laboratory findings include high transaminase levels (59%), pancytopenia (35%), prolonged coagulation profile (30%), high creatine kinase levels (24%), and high lactic acid levels (12%). Occasionally, patients have high lipase, high cholesterol, ferritin, and glucose, and low insulin growth factor-1 (IGF-1) (Alsubhi et al. 2017).

The mechanism underlying HLH associated with IEM remains unclear. However, it is hypothesized that increased metabolites decrease NK cell activity and increase cell activation and expansion. Furthermore, macrophage activation and tissue infiltration could be involved. This type of inflammatory response can cause extensive tissue damage and associated symptoms (Taurisano et al. 2014). Other potential pathomechanisms, similar to what is seen in lysosomal storage disorders like Gaucher disease, Niemann–Pick disease, and Wolman disease defects, affect the cellular secretory pathway due to the Golgi apparatus dysfunction and could lead to HLH based on a common pathomechanism.

Several COG-CDG show apparently an effect on the immune system, in the form of recurrent infections and unexplained high fever. These included COG4, COG6, COG7, and COG8 defects (Foulquier et al. 2007; Morava et al. 2007; Reynders et al. 2009; Huybrechts et al. 2012).

COG complex mutations are known to affect the morphology and function of Golgi apparatus, in addition to the cellular membrane trafficking (Ungar et al. 2002). Glycosylation involves a huge number of proteins carrying out variable functions, which may explain the multisystem involvement of the CDG including the perturbation of the immune system. Golgi apparatus is essential in regulating the immune system in variable mechanisms including the Major Histocompatibility Complex (MHC) proteins glycosylation (Ryan and Cobb 2012), Natural Killer (NK) cells cytotoxicity (Mace et al. 2014), and antibody glycosylation process. (Jennewein and Alter 2017) All these and other examples corroborate the role of the Golgi apparatus in general and the COG complex in maintaining immunological homeostasis mainly through the glycosylation process. However, as long as there is only one patient reported

Table 2 Most common clinical features of the previously reported patients of COG6 gene defect compared to the present patient

Characteristic	Previously reported cases	Present case	All cases
Number[a]	16	1	17
Gender	8 M, 8 F	F	8 M, 9 F
Country	8 (Saudi Arabia), 4 (Turkey), 4 (Morocco), 1 (Bulgaria)	Saudi Arabia	53% from Saudi Arabia
Consanguinity	11	Yes	71%
Clinical features			
Global developmental disability	17	Yes	100%
Dysmorphic features[b]	14	Yes	88%
Progressive microcephaly	14	Yes	88%
Failure to thrive	12	Yes	71%
Hypohydrosis	9	Yes	59%
Hypotonia	9	Yes	59%
Hepatosplenomegaly	7	Yes (only splenomegaly)	47%
Death	6	No	35%
Radiological findings (10/17)			
Thin corpus callosum	3	Yes	40%
Brain atrophy	3	Yes	40%
Laboratory findings			
Type 2 TIF pattern	15	Yes	94% (15/17, 1 patient not assessed and 1 normal)
Increased liver transaminase levels	9	Yes	59%
Pancytopenia	5	Yes	35%
Decreased coagulation factors	4	Yes	30%

M male, *F* female, *IUGR* intrauterine growth retardation, *TIF* transferrin isoelectric focusing

[a] 11 patients (4 males, 3 females, and 4 of unreported gender) reported by Shaheen et al. (2013) were excluded because of incomplete clinical profiles. The authors reported that all presented with similar clinical features to the index case

[b] Broad palpebral fissures, retrognathia, wide mouth with thin lips, prominent nose, slight epicanthus, short neck, asymmetric thorax, and post-axial polydactyly, anal anteposition

with this association, it is premature to speculate about a pathogenic link between COG6-CDG and HLH.

The diagnosis of HLH based on the reported criteria could be challenging particularly in vulnerable patients with metabolic diseases, which could affect variable body systems and present with signs and symptoms mimicking those of HLH (Otrock et al. 2017). Special precautions and a high index of suspicion should be considered as delaying the diagnosis and management could have serious consequences on the patient's outcome. In our patient, the management was started immediately once the criteria of HLH were fulfilled, while the diagnosis was confirmed only after the complete recovery of the patient by following her hematological and biochemical markers going back to the baseline, in addition to the negative familial HLH gene panel.

Conclusion

The present report is what we believe to be the first on a patient with COG6-CDG and HLH. Before concluding that this is not a fortuitous association, we have to wait for more patients with this combination. We recommend that clinicians consider HLH in any patient with a congenital glycosylation disorder presenting with prolonged fever, splenomegaly, hypertriglyceridemia, and hypofibrinogenemia associated with pancytopenia. A high index of suspicion and prompt management might improve the patients' outcome.

Acknowledgments We are grateful to the patient and her family reported in this article for their genuine support.

Take-Home Message

Hemophagocytosis could be the presenting clinical feature in several inborn errors, including lysosomal storage disorders associated with hepatosplenomegaly. In the present report, we describe the first Golgi secretory pathway-related patient with HLH and review the literature on reported GOG6-CDG patients with our patient.

General Rules

Author Contributions

NAT: write the first draft and prepare Tables 1 and 2, AAS: diagnose and manage the hematological manifestations and edit the manuscript, EM: review, edit the manuscript and contributed to the clinical diagnosis and management of the patients. MAF: supervise, coordinate the whole work associated with preparing, writing and submitting the manuscript and contributed to the clinical diagnosis and management of the patients.

The Name of the Corresponding Author

Majid Alfadhel.

Division of Genetics, Department of Pediatrics, King Saud bin Abdulaziz University for Health Sciences, King Abdulaziz Medical City, Riyadh, Saudi Arabia, PO Box 22490, Riyadh 11426. Tel +966 118 011 111; Fax: +966 118 053555. Email: dralfadhelm@gmail.com.

Funding Sources

No funding for this article from any institution or agency.

Competing Interests

None declared.

Informed Consent

Informed consent was obtained from parents of the patients included in the study. Proof that informed consent was obtained is available upon request.

Ethic Approval

The study was approved by the ethics committee at King Abdullah International Medical Research Centre (RC/16/113/R).

References

Alsubhi S, Alhashem A, Faqeih E et al (2017) Congenital disorders of glycosylation: the Saudi experience. Am J Med Genet A 173: 2614–2621

An Q, Jin MW, An XJ, Xu SM, Wang L (2017) Macrophage activation syndrome as a complication of juvenile rheumatoid arthritis. Eur Rev Med Pharmacol Sci 21:4322–4326

Duval M, Fenneteau O, Doireau V et al (1999) Intermittent hemophagocytic lymphohistiocytosis is a regular feature of lysinuric protein intolerance. J Pediatr 134:236–239

Dzoljic E, Stosic-Opincal T, Skender-Gazibara M et al (2015) Primary lymphoma of the brain in a young man whose brother died of hemophagocytic lymphohistiocytosis: case report. Srp Arh Celok Lek 143:63–67

Erdol S, Ture M, Baytan B, Yakut T, Saglam H (2016) An unusual case of LCHAD deficiency presenting with a clinical picture of hemophagocytic lymphohistiocytosis: secondary HLH or coincidence? J Pediatr Hematol Oncol 38:661–662

Foulquier F, Ungar D, Reynders E et al (2007) A new inborn error of glycosylation due to a Cog8 deficiency reveals a critical role for the Cog1–Cog8 interaction in COG complex formation. Hum Mol Genet 16:717–730

Gokce M, Unal O, Hismi B et al (2012) Secondary hemophagocytosis in 3 patients with organic acidemia involving propionate metabolism. Pediatr Hematol Oncol 29:92–98

Henter JI, Ehrnst A, Andersson J, Elinder G (1993) Familial hemophagocytic lymphohistiocytosis and viral infections. Acta Paediatr 82:369–372

Henter JI, Horne A, Arico M et al (2007) HLH-2004: diagnostic and therapeutic guidelines for hemophagocytic lymphohistiocytosis. Pediatr Blood Cancer 48:124–131

Huybrechts S, De Laet C, Bontems P et al (2012) Deficiency of subunit 6 of the conserved oligomeric Golgi complex (COG6-CDG): second patient, different phenotype. JIMD Rep 4:103–108

Ikeda H, Kato M, Matsunaga A, Shimizu Y, Katsuura M, Hayasaka K (1998) Multiple sulphatase deficiency and haemophagocytic syndrome. Eur J Pediatr 157(7):553–554

Janka GE (1983) Familial hemophagocytic lymphohistiocytosis. Eur J Pediatr 140:221–230

Jennewein MF, Alter G (2017) The immunoregulatory roles of antibody glycosylation. Trends Immunol 38:358–372

Karaman S, Urganci N, Kutluk G, Cetinkaya F (2010) Niemann–Pick disease associated with hemophagocytic syndrome. Turk J Haematol 27:303–307

Kardas F, Patiroglu T, Unal E, Chiang SC, Bryceson YT, Kendirci M (2012) Hemophagocytic syndrome in a 4-month-old infant with biotinidase deficiency. Pediatr Blood Cancer 59(1):191–193

Kundak AA, Zenciroglu A, Yarali N et al (2012) An unusual presentation of galactosemia: hemophagocytic lymphohistiocytosis. Turk J Haematol 29:401–404

Lubbehusen J, Thiel C, Rind N et al (2010) Fatal outcome due to deficiency of subunit 6 of the conserved oligomeric Golgi complex leading to a new type of congenital disorders of glycosylation. Hum Mol Genet 19:3623–3633

Mace EM, Dongre P, Hsu HT et al (2014) Cell biological steps and checkpoints in accessing NK cell cytotoxicity. Immunol Cell Biol 92:245–255

Menasche G, Pastural E, Feldmann J et al (2000) Mutations in RAB27A cause Griscelli syndrome associated with haemophagocytic syndrome. Nat Genet 25:173–176

Morava E, Zeevaert R, Korsch E et al (2007) A common mutation in the COG7 gene with a consistent phenotype including microcephaly, adducted thumbs, growth retardation, VSD and episodes of hyperthermia. Eur J Hum Genet 15:638–645

Olcay L, Gumruk F, Boduroglu K, Coskun T, Tuncbilek E (1998) Anaemia and thrombocytopenia due to haemophagocytosis in a 7-month-old boy with galactosialidosis. J Inherit Metab Dis 21: 679–680

Otrock ZK, Daver N, Kantarjian HM, Eby CS (2017) Diagnostic challenges of hemophagocytic lymphohistiocytosis. Clin Lymphoma Myeloma Leuk 17S:S105–S110

Peanne R, de Lonlay P, Foulquier F et al (2017) Congenital disorders of glycosylation (CDG): quo vadis? Eur J Med Genet. https://doi.org/10.1016/j.ejmg.2017

Reynders E, Foulquier F, Leao Teles E et al (2009) Golgi function and dysfunction in the first COG4-deficient CDG type II patient. Hum Mol Genet 18:3244–3256

Ryan SO, Cobb BA (2012) Roles for major histocompatibility complex glycosylation in immune function. Semin Immunopathol 34:425–441

Rymen D, Winter J, Van Hasselt PM et al (2015) Key features and clinical variability of COG6-CDG. Mol Genet Metab 116: 163–170

Sepulveda FE, de Saint Basile G (2017) Hemophagocytic syndrome: primary forms and predisposing conditions. Curr Opin Immunol 49:20–26

Shaheen R, Ansari S, Alshammari MJ et al (2013) A novel syndrome of hypohidrosis and intellectual disability is linked to COG6 deficiency. J Med Genet 50:431–436

Sharpe LR, Ancliff P, Amrolia P, Gilmour KC, Vellodi A (2009) Type II Gaucher disease manifesting as haemophagocytic lymphohistiocytosis. J Inherit Metab Dis 32(Suppl 1):S107–S110

Sparks SE, Krasnewich DM (1993) Congenital disorders of N-linked glycosylation and multiple pathway overview. In: Adam MP, Ardinger HH, Pagon RA et al (eds) GeneReviews®. University of Washington, Seattle, Seattle

Tang YM, Xu XJ (2011) Advances in hemophagocytic lymphohistiocytosis: pathogenesis, early diagnosis/differential diagnosis, and treatment. ScientificWorldJournal 11:697–708

Taurisano R, Maiorana A, De Benedetti F, Dionisi-Vici C, Boldrini R, Deodato F (2014) Wolman disease associated with hemophagocytic lymphohistiocytosis: attempts for an explanation. Eur J Pediatr 173:1391–1394

Topaloglu R, Lebre AS, Demirkaya E et al (2008) Two new cases with Pearson syndrome and review of Hacettepe experience. Turk J Pediatr 50:572–576

Ungar D, Oka T, Brittle EE et al (2002) Characterization of a mammalian Golgi-localized protein complex, COG, that is required for normal Golgi morphology and function. J Cell Biol 157: 405–415

Verbsky JW, Grossman WJ (2006) Hemophagocytic lymphohistiocytosis: diagnosis, pathophysiology, treatment, and future perspectives. Ann Med 38:20–31

Wu S, Gonzalez-Gomez I, Coates T, Yano S (2005) Cobalamin C disease presenting with hemophagocytic lymphohistiocytosis. Pediatr Hematol Oncol 22:717–721

Zhang K, Filipovich AH, Johnson J, Marsh RA, Villanueva J (1993) Hemophagocytic lymphohistiocytosis, familial. In: Adam MP, Ardinger HH, Pagon RA et al (eds) GeneReviews®. University of Washington, Seattle, Seattle

Zhang JR, Liang XL, Jin R, Lu G (2013) HLH-2004 protocol: diagnostic and therapeutic guidelines for childhood hemophagocytic lymphohistiocytosis. Zhongguo Dang Dai Er Ke Za Zhi 15:686–688

JIMD Reports
DOI 10.1007/8904_2018_89

RESEARCH REPORT

Mitochondrial Encephalopathy: First Portuguese Report of a VARS2 Causative Variant

Sandra Pereira · Mariana Adrião · Mafalda Sampaio · Margarida Ayres Basto · Esmeralda Rodrigues · Laura Vilarinho · Elisa Leão Teles · Isabel Alonso · Miguel Leão

Received: 17 September 2017 / Revised: 19 January 2018 / Accepted: 23 January 2018 / Published online: 25 February 2018

Abstract *Introduction:* Combined oxidative phosphorylation deficiency 20 (COXPD20) is a mitochondrial respiratory chain complex (RC) disorder, caused by disease-causing variants in the *VARS2* gene, which encodes a mitochondrial aminoacyl-tRNA synthetase. Here we describe a patient with fatal mitochondrial encephalopathy caused by a homozygous *VARS2* gene missense variant.

Case Report: We report the case of a girl, the first child of non-consanguineous and healthy parents, born from an uneventful term pregnancy, who presented, in the neonatal period, major hypotonia and microcephaly. At 4 months of age she showed poor eye contact, nystagmus, global psychomotor development delay and failure to thrive, without dysmorphic features. Focal seizures started at 24 months which evolved to a severe epileptic encephalopathy and finally to super refractory *status epilepticus,* leading to her death at 28 months of age. Etiologic investigation encompassing metabolic and genetic causes failed to disclose a diagnosis. Post-mortem exome sequencing allowed the identification of a pathogenic variant in *VARS2* gene in the homozygous state (c.1100C > T, p.Thr367Ile) in the patient, inherited from her heterozygous parents, leading to the diagnosis of COXPD2.

Conclusion: To the best of our knowledge, this is the fifth case described in the literature of a child with disease-causing variant in *VARS2*. With this report we expand the knowledge about the phenotype associated with this very rare mitochondrial defect, further emphasizing the use of exome sequencing as a very powerful diagnostic tool.

Communicated by: Daniela Karall

S. Pereira (✉) · M. Adrião · M. Sampaio · E. Rodrigues · E. L. Teles
Department of Pediatrics, Centro Hospitalar São João (CHSJ), Porto, Portugal
e-mail: sandravdpereira@gmail.com

M. Sampaio
Neuropediatric Unit, Department of Pediatrics, CHSJ, Porto, Portugal

M. A. Basto
Department of Neuroradiology, CHSJ, Porto, Portugal

E. Rodrigues · E. L. Teles
Metabolic Diseases Unit, Department of Pediatrics, CHSJ, Porto, Portugal

L. Vilarinho
Newborn Screening, Metabolism and Genetics Unit, Human Genetics Department, National Institute of Health Dr. Ricardo Jorge, Porto, Portugal

I. Alonso
UnIGENe and Centre for Predictive and Preventive Genetics (CGPP), Institute of Molecular and Cellular Biology (IBMC), University of Porto, Porto, Portugal

I. Alonso
Institute of Research and Innovation in Health, University of Porto, Porto, Portugal

M. Leão
Neurogenetics Unit, Department of Medical Genetics, SJHC, Porto, Portugal

M. Leão
Faculty of Medicine of the University of Porto (FMUP), Porto, Portugal

Introduction

Defects in the mitochondrial respiratory chain (RC) have emerged as the most common cause of childhood and adult neurometabolic disease, with an estimated prevalence of 1 per 5,000 live births (Taylor et al. 2014). RC is a multiheteromeric enzymatic structure that performs oxidative phosphorylation (OXPHOS), a fundamental reaction that supplies ~90% of the energy used by mammalian cells (Diodato et al. 2014; Baertling

et al. 2017). Signs and symptoms of the disorder may develop at any time throughout the patient's life, often occurring in association with neurological impairment and frequently resulting in chronic disability and premature death (Taylor et al. 2014).

The RC consists of five complexes, composed by ~85 structural proteins, 13 of which are encoded by mtDNA, whereas the others are encoded by nuclear genes. Aside from mitochondrial DNA-encoded ribosomal and transfer RNAs (rRNAs and tRNAs), the mitochondrial translation apparatus consists of more than 100 proteins, encoded by nuclear genes, translated by cytosolic ribosomes and imported into the mitochondria matrix. These include mitochondrial aminoacyl-tRNA-synthetases (mt-aaRSs), ribosomal structural and assembly proteins, tRNA modifying and methylating enzymes, and several initiation, elongation, and termination factors of mitochondrial translation (Taylor et al. 2014; Diodato et al. 2014; Baertling et al. 2017; Valente et al. 2007). An increasing number of mitochondrial translation disorders caused by causative variants in genes encoding mt-aaRSs, which catalyze the ligation of specific amino acids to their cognate tRNAs, have been discovered (Diodato et al. 2014).

Combined oxidative phosphorylation deficiency 20 (COXPD20 – OMIM #615917) is a disorder of the RC, caused by homozygous or compound heterozygous variants in the *VARS2* gene (OMIM #612802) located on chromosome 6p21 (https://www.omim.org/entry/615917). The *VARS2* gene encodes a mt-aaRS, which catalyzes the attachment of valine to tRNA(Val) for mitochondrial translation, designed as valyl tRNA-synthetase. Variants in this gene are associated with early-onset mitochondrial encephalopathies (Taylor et al. 2014; Online Mendelian Inheritance in Man 2017, https://www.omim.org/entry/615917).

Four patients with COXPD20 have been previously described. However, limited clinical information was provided, leaving the phenotype of *VARS2* deficiency largely uncharacterized (Taylor et al. 2014; Diodato et al. 2014; Baertling et al. 2017; Pronicka et al. 2016; Mikol and Polivka 2005).

Here we report the fifth case of COXPD20, identified by exome sequencing (ES), caused by a homozygous variant in *VARS2* in a patient with fatal mitochondrial encephalopathy. We present detailed clinical data to better characterize the phenotypic spectrum associated with this disease.

Case Report

We report the clinical description of a child, first daughter of Portuguese, non-consanguineous and healthy parents, who was born after an uneventful full-term pregnancy, by cesarean delivery due to pelvic presentation, with APGAR scores of 9 and 10, although small for the gestational age (weight: 2,755 g, 10th percentile, height 45.5 cm, 3th percentile and head circumference 32 cm, 5th percentile). Expanded newborn metabolic screening was normal. Since the neonatal period, she presented microcephaly, severe global hypotonia, progressive feedings difficulties, and failure to thrive. At 4 months, severe global psychomotor development delay was reported, with head lag, poor eye contact, and pendular nystagmus. Dysmorphic features were absent. At 6 months, a brain magnetic resonance imaging (MRI) showed global atrophy and a small glioepithelial cyst associated with left hippocampal molding. Renal and hepatic function tests, creatine kinase, lactate dehydrogenase, ammonia, total homocysteine, pH, and lactic acid were normal. Abdominal ultrasound was also normal. Otorhinolaryngology and cardiac evaluations (including echocardiogram) were unremarkable. Ophthalmologic evaluation revealed visual evoked potentials reduced amplitude with preserved latency, with no other ocular abnormalities. First metabolic evaluation disclosed lactate 5.35 mmol/L (normal 0.63–2.44), pyruvate 71 μmol/L (normal 54.1–119.9), L/P ratio 75 (normal 10–25), plasma aminoacid profile with a slight elevation of alanine (464 μmol/L; normal 236–400) and proline (330 μmol/L; normal 100–280) and a normal organic acids profile. Despite the normalization of lactate value, mitochondrial etiology was suspected. The glucose loading test didn't reveal hyperlactacidemia (fast lactate 2.56; fast pyruvate 115; fast L/P 22). After 2 g/kg glucose: lactate 1.98, pyruvate 122 and L/P ratio 16). Brain MRI was repeated at 12 months of age, revealing global atrophy and symmetrical diffuse T2 hyperintensity of the supra and infratentorial white matter (Fig. 1). Array comparative genomic hybridization (array-CGH) did not show copy-number changes. Deltoid muscle biopsy performed at 18 months revealed a histology with minimal and uncharacteristic changes, without ragged-red fibers. The biochemical study of respiratory chain complexes by spectrophotometry revealed an elevation of citrate synthase (CS) 215.6 nmol/min/mg NCP (non-collagenic proteins) (normal 85–180) with normal activity of complexes I–IV: 20.4 nmol/min/mg NCP/CS (normal 8.8–30.8), 13.4 nmol/min/mg NCP/CS (normal 12–35), 39.5 nmol/min/mg NCP/CS (normal 22.2–62.2), and 13.5 nmol/min/mg NCP/CS (normal 11.5–34.5), respectively; complex II + III 2.6 nmol/min/mg NCP/CS (normal 2.6–12).

At 24 months of age she had global psychomotor delay, with absent language, severe hypotonia without the ability to sit independently and spastic tetraparesis; pendular nystagmus was less evident. At this stage, focal seizures began, characterized by staring and tonic extension with clonic movements of the right superior limb, during sleep and while waking up, lasting less than 60 s. During video-electroencephalogram monitoring, a convulsive event was registered, as well as a left parietal focus with spike-waves extending to the middle line. Sodium valproate (20 mg/kg/day) was initiated, with partial control of

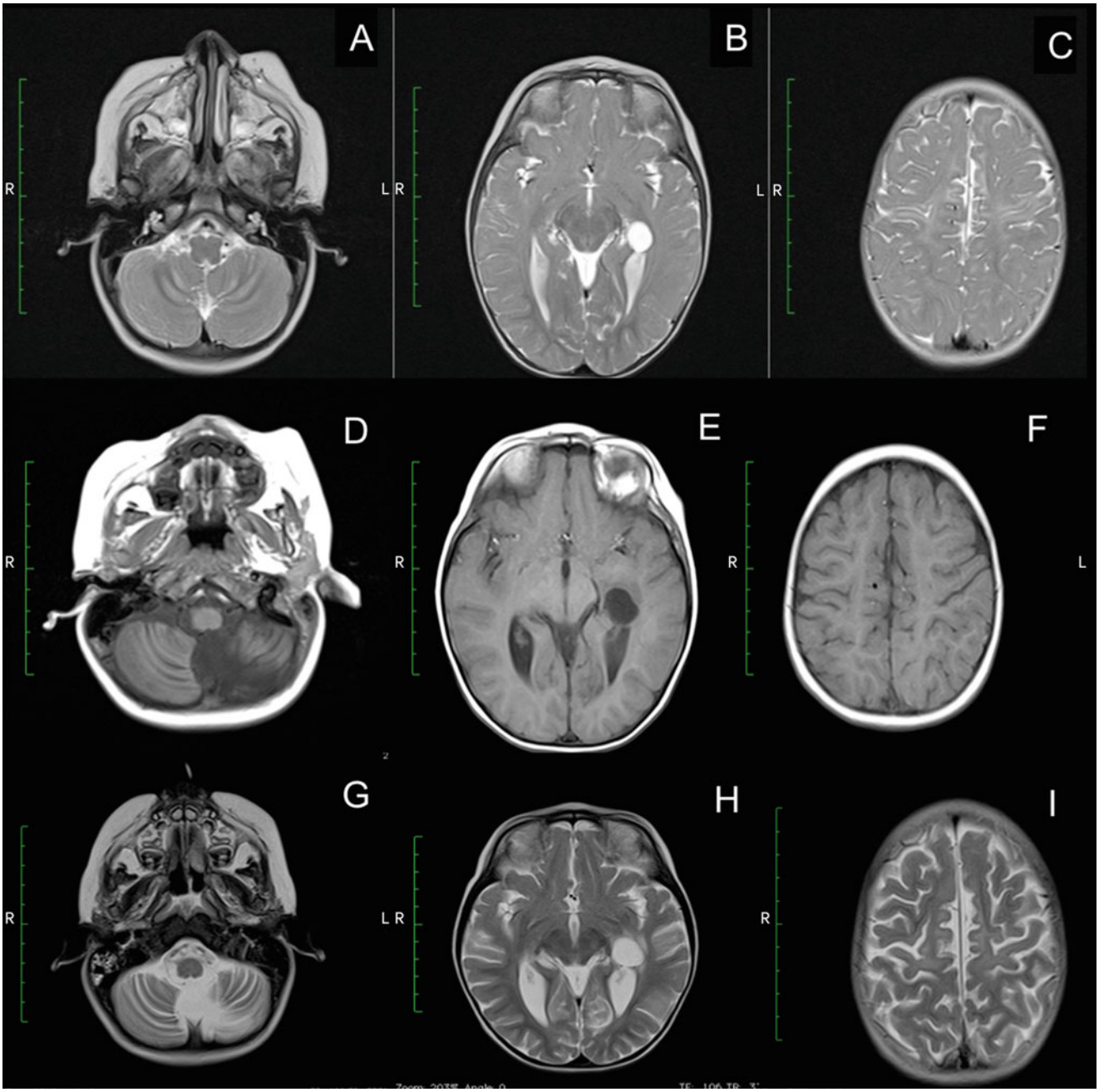

Fig. 1 (**a**–**c**) Axial T2 weighted images of the patient at age of 1 year. (**a**) Bilateral hypersignal of the cerebellar white matter. (**b**) Neuroglial cyst with left hippocampal molding. (**c**) Bilateral and symmetrical supratentorial white matter involvement. (**d**–**f**) Axial T1 weighted images of the patient at age of 24 months. (**d**) Loss of volume of cerebellum with enlargement of cerebellar folia and small size of left inferior cerebellar hemisphere. (**e**) Neuroglial cyst with left hippocampal molding. (**f**) More prominent decrease of supratentorial brain volume with loss of periventricular white matter. (**g**–**i**) Axial T2 weighted images of the patient at age of 26 months. (**g**, **h**) More severe and diffuse loss of brain volume than in the previous scan; sequelae lesions with volume loss of inferior left cerebellar hemisphere and left parieto-occipital cortical encephaloclastic lesion; (**i**) Bilateral and symmetrical supratentorial periventricular and subcortical white matter involvement

seizures (maximum dose of 40 mg/kg/day). Given the association of nystagmus, hypotonia, and epilepsy with fast rhythms in EEG, the hypothesis of infantile neuroaxonal dystrophy was considered and skin biopsy was performed, showing no axonal spheroids or any other abnormalities.

Due to the recurrence of seizures with right head deviation and right limb fencing posture, carbamazepine (maximum dose 20 mg/kg/day) and clobazam (2.5 mg per day) were sequentially added on. Despite these antiepileptic drugs, the clinical status evolved to an epileptic encephalopathy with

regression and admission to a pediatric department at the age of 26 months. EEG showed severe diffuse encephalopathy with slowing and focal left parietal epileptic activity with middle line involvement. At that time, metabolic reevaluation including LCR study was performed: plasma lactate 2.72 mmol/L, pyruvate 124 μmol/L and L/P ratio of 22; LCR lactate 1.45 mmol/L (normal 1.2–2.1), pyruvate 90 μmol/L (normal 59.2–89.2) and L/P 16 (normal 10–25). Plasma aminoacid profile showed a slight elevation of alanine 502 μmol/L (100–400), proline 544 μmol/L (118–230) and glycine 340 μmol/L (40–290). LCR aminoacids were normal, as urinary organic acids. Seizures progressed into *convulsive status epilepticus* (CSE) and led to admission in the Pediatric Intensive Care Unit (PICU). During hospitalization, multiple combinations of drugs were tried in order to try to control super refractory SE, namely midazolam, thiopental (maximum 10 mg/kg/h), methylprednisolone, ketamine, lidocaine (4 mg/kg/h), pyridoxine (22 mg/kg/day), propofol (maximum 8.9 mg/kg/h), lamotrigine (maximum 100 mg/day), topiramate, vigabatrin, levetiracetam, felbamate (50 mg 12/12 h), and lacosamide (4.5 mg 12/12 h). Ketogenic diet was tried but ketosis was never achieved. Brain MRI was repeated, revealing worsening of the previous global atrophy. Continuous EEG monitoring disclosed continuous polyspike or spike and wave discharges, with generalized distribution and right hemisphere lateralization, with periodic epileptiform discharges – a pattern of electrographic generalized status epilepticus. Mechanical ventilation was initiated followed by tracheostomy due to vocal cords' paresis. At this time a diagnostic panel for epileptic encephalopathies revealed two intronic variants in KCNB1 and RNASEH2C genes, both inherited from her asymptomatic father.

By 28 months she died in the PICU, due to cardio-respiratory arrest in the context of a severe epileptic encephalopathy. The anatomopathological report revealed an encephalon with severe neuronal loss and spongiosis.

Two years after the child's death, ES was performed using the SureSelect Human All Exon kit and a HiSeq sequencer (Illumina). For data analysis, a custom validated pipeline was applied using FastQC and QualiMap for quality control, BWA for alignment (GRCh37), GATK HaplotypeCaller for variant calling, and Ensembl VEP and GEMINI for annotation. Exome data was then filtered by focusing on variants that resulted in a change at the protein level and, if known in the databases, its minor allele frequency (MAF) had to be below 1%. All filtered variants were further analyzed using Alamut software (Interactive Biosoftware) for pathogenicity prediction, previous description in affected individuals using the Human Gene Mutation Database (HGMD) and frequency was confirmed at the Genome Aggregation Database (gnomAD). This pipeline allowed the identification of a homozygous c.1100C > T substitution at *VARS2* that replaces a highly conserved threonine by an isoleucine at codon 367 (p.Thr367Ile), that was subsequently confirmed, as well as both parents carrier status, by Sanger sequencing.

Discussion

Combined oxidative phosphorylation deficiency 20 (COXPD20) is a very rare mitochondrial respiratory chain complex (RC) disorder, caused by disease-causing variants in the *VARS2* gene. Variants in this gene have been recently identified as the cause of mitochondrial encephalopathy in four individuals. Our report widens the clinical phenotype related to *VARS2* deficiency. The presently described patient initially presented hypotonia, global psychomotor development delay, spastic tetraparesis and pendular nystagmus and later developed epileptic encephalopathy.

Mitochondrial diseases (MD) have emerged as a common cause of metabolic inherited diseases, but their diagnosis remains challenging due to clinical heterogeneity and constantly expanding number of causative genes (Taylor et al. 2014; Diodato et al. 2014; Valente et al. 2007). These disorders are characterized by morphological and/or functional mitochondrial abnormalities (Mikol and Polivka 2005) and the molecular mechanism potentially involves different gene products affecting mtDNA replication and expression, including *aaRS2* (Taylor et al. 2014). However, most mutations in *aaRS2* genes have been reported in single, or in just a few cases, which hampers the establishment of definitive genotype–phenotype correlations. In the study performed by Pronicka et al. (2016), most of the neonates with causative variants identified were born from the first pregnancy of healthy unrelated parents. Our patient, the first daughter of healthy parents, was carrying the c.1100C > T, p.Thr367Ile pathogenic variant, compatible with an autosomal recessive inheritance. In a study performed by Pronicka et al. (2016), 29 neonates with MD died before the establishment of a molecular diagnosis and half of the deaths occurred in the early neonatal period. In our case, the diagnosis was established 2 years after death and 4 years after the onset of the symptoms. Molecular confirmation of the clinical diagnosis allows adequate genetic counseling and the possibility of a prenatal diagnosis in future pregnancies.

Aside from our report, four additional patients with *VARS2* variants have been described (Tables 1 and 2). Taylor et al. (2014) reported a 10-year-old boy who presented in the first year of life with muscle weakness and hypotonia and later developed central nervous system disease, including progressive external ophthalmoplegia, ptosis, and ataxia, without family history of similar disease. Biochemical cells

Table 1 Characteristics of five patients with *VARS2* gene mutation according to RefSeq NM_001167734.1

NP	Sex	Country of origin	Family history	Age onset/ diagnosis	Muscle histology	Defect RC	HLact	Variants	Reference
1	M	British	N	<1 y/10 y	Mosaic for COX-positive fibers	cI, cIV	NR	c.[1135G > A]; [1877C > A] p.[Ala379Thr]; [Ala626Asp]	Taylor et al. (2014)
2	M	NR	NR	<1y/8 y	Normal	cI	NR	c.[1100C > T]; [1100C > T] p.[Thr367Ile]; [Thr367Ile]	Diodato et al. (2014)
3	M	Polish	Sibs	NN/10 y	NR	NR	NR	c.[1100C > T]; [1490G > A] p.[Thr367Ile]; [Arg497His]	Pronicka et al. (2016)
4	M	Greek	N	NN/	NR	NR	+	c.[601C > T]; [1100C > T] p.[Arg201Trp]; [Thr367Ile]	Baertling et al. (2017)
5	F	Portuguese	N	NN/4 y	Normal	N	+	c.[1100C > T]; [1100C > T] p.[Thr367Ile]; [Thr367Ile]	*Present case*

NP number of patient, *F* female, *M* male, *N* no, *NN* neonatal period, *NR* not reported, *RC* mitochondrial respiratory chain, *HLact* hyperlactacidemia

Table 2 Clinical presentations of five patients with *VARS2* gene mutation

	NP				
Clinical presentations	1	2	3	4	5
Microcephaly		+	NR	+	+
Failure to thrive				+	+
Hypotonia	+	+		+	+
Global developmental delay	+	+			+
Spastic tetraparesis					+
Dysmorphias		+			
Nystagmus					+
Ophthalmoplegia	+				
Exotropia				+	
Seizures		+		+	+
Ataxia	+				
Cardiomyopathy				+	

NP number of patient, *NR* not reported

studies showed a deficiency of mitochondrial respiratory complexes I and IV (Diodato et al. 2014). This patient was a compound heterozygous for *VARS2* variants c.1135G > A (p.Ala379Thr); c.1877C > A (p.Ala626Asp) (Taylor et al. 2014).

Diodato et al. (2014) reported a single patient with a homozygous missense variant c.1100C > T, (p.Thr367Ile) in *VARS2*. The patient was a boy with delayed psychomotor development, facial dysmorphism, and microcephaly that became apparent soon after birth. At 4 years of age, he developed seizures and myoclonic jerks. Brain MRI showed hyperintense lesions in the periventricular region, insulae, and right frontotemporal cortex. Muscle biopsy was histologically normal, but muscle homogenate showed isolated complex I deficiency (25% residual activity). Patient fibroblasts showed no enzymatic defects, but oxygen consumption was impaired, suggesting defective mitochondrial respiration (Diodato et al. 2014). Our case presents the same variant reported by Diodato et al. (2014) and has similar clinical manifestations; however, in our patient RC study was normal. Pronicka et al. (2016) described a neonate, born at a gestational age of 40 weeks with a birth weight of 3,420 g, who presented with stridor, lactic acidosis, and cardiomyopathy in the early neonatal period who was a compound heterozygous for the disease-causing variants: c.1100C > T (p.Thr367Ile), c.1490G > A (p.Arg497His) (Baertling et al. 2017; Pronicka et al. 2016).

Finally, Baertling et al. (2017) reported a case of a neonate presenting mitochondrial encephalopathy with severe lactic acidosis, hypertrophic cardiomyopathy, epi-

lepsy, and abnormalities on brain imaging including corpus callosum and cerebellum hypoplasia, as well as a massive lactate peak on MR-spectroscopy. As in the previous case, disease-causing variants in compound heterozygosity were documented, one of them a novel variant: c.601C > T p. Arg201Trp, c.1100C > T (p.Thr367Ile) (Baertling et al. 2017).

It was also noted the high prevalence of the causative variant c.1100C > T, p.(Thr367Ile) identified in 3 out of 4 of the previous reports (Table 1). Hypotonia was present in all patients and most of them also showed microcephaly, failure to thrive, global developmental delay, and seizures. Pendular nystagmus and spastic tetraparesis observed in our patient were not previously described (Table 2).

Interestingly, specific MRI patterns seem to be associated with some patients with aaRS2 variants (e.g., DARS2, EARS2, RARS2) (Diodato et al. 2014), although it is not possible to establish any pattern for *VARS2*. In the patient described by Diodato et al., MRI showed hyperintense lesions involving mainly the insulae and frontotemporal right cortex. In our case, MRI showed global atrophy and diffuse and symmetrical T2 hyperintensity of the supra and infratentorial white matter. Relevant histological modifications in muscle are ragged-red fibers with or without cytochrome C oxidase (COX) activity (Mikol and Polivka 2005). Diodato et al. (2014) reported a mosaic for COX-positive fibers in muscle biopsy, although our patient showed no abnormalities in muscle histology. The neuropathological finding in patients with mitochondrial encephalomyopathies is not specific and consists of spongiosis, neuronal loss, focal necrosis, capillary proliferation, and mineral deposits (Mikol and Polivka 2005). In our case, the anatomopathological report revealed an encephalon with severe lesions, with atrophy and spongiosis, that can be correlated with microcephaly as well as with a highly refractory epileptic encephalopathy.

It is important to notice that mutations in the *VARS2* gene should be considered in the differential diagnosis of mitochondrial encephalopathies. However, additional clinical reports are required to further define the phenotypic spectrum and the disease course associated with *VARS2* deficiency and to clarify whether MRI patterns and histology are specific or not. ES has led to an exponential increase in the identification of causative genes in MD (Pronicka et al. 2016; Wortmann et al. 2015).

In conclusion, variants in nuclear genes causing mitochondrial translation defects represent a new potentially broad field of MD. Causative variants in *VARS2* have been recently identified as the cause of mitochondrial encephalopathy in four individuals. Here we describe the fifth patient and expand the phenotypic spectrum of COXDP20. We also confirmed the relevance of ES as molecular diagnostic test for MD, mostly in single patients presenting with heterogeneous clinical syndromes but with biochemical markers suggesting a "mitochondrial signature."

Take-Home Message

Combined oxidative phosphorylation deficiency 20 (COXPD20) is a very rare mitochondrial respiratory chain complex disorder, caused by disease-causing variants in the *VARS2* gene. Our report extends the phenotypical spectrum of *VARS2*-related disorders and emphasizes Exome Sequencing ability to identify variants in nuclear gene in patients with suspected mitochondrial disease.

Contributions of Individual Authors

Sandra Pereira: analysis of clinical data and drafting the article.

Mariana Adrião: analysis of clinical data and drafting the article.

Margarida Ayres Basto: acquisition and interpretation of radiological data.

Mafalda Sampaio: analysis of clinical data and critical revision of the article.

Esmeralda Rodrigues: analysis of metabolic data and critical revision of the article.

Laura Vilarinho: acquisition, analysis, and interpretation of metabolic data and critical revision of the article.

Elisa Leão Teles: analysis of metabolic data and critical revision of the article.

Isabel Alonso: acquisition, analysis, and interpretation of genetic data and critical revision of the article.

Miguel Leão: final review and approval of the version to be published.

Conflict of Interest

Sandra Pereira, Mariana Adrião, Margarida Ayres, Mafalda Sampaio, Esmeralda Rodrigues, Laura Vilarinho, Elisa Leão Teles, Isabel Alonso, and Miguel Leão declare that they have no conflict of interest.

Details of Funding

The content of the article has not been influenced by the sponsors.

Details of Ethics Approval

Research in accordance with the Declaration of Helsinki and the International Medical Research.

A Patient Consent Statement

Written informed consent to publication was obtained.

This article does not contain any studies with human or animal subjects performed by any of the authors.

References

Baertling F, Alhaddad B, Seibt A et al (2017) Neonatal encephalocardiomyopathy caused by mutations in VARS2. Metab Brain Dis 32(1):267–270

Diodato D, Melchionda L, Haack TB et al (2014) VARS2 and TARS2 mutations in patients with mitochondrial encephalomyopathies. Hum Mutat 35(8):983–989

Mikol J, Polivka M (2005) Mitochondrial encephalomyopathies. Ann Pathol 25(4):282–291

Online Mendelian Inheritance in Man. Combined oxidative phosphorylation deficiency 20; coxpd20. June 2017. https://www.omim.org/entry/615917

Pronicka E, Piekutowska-Abramczuk D, Ciara E et al (2016) New perspective in diagnostics of mitochondrial disorders: two years' experience with whole-exome sequencing at a national paediatric centre. J Transl Med 14(1):174

Taylor RW, Pyle A, Griffin H et al (2014) Use of whole-exome sequencing to determine the genetic basis of multiple mitochondrial respiratory chain complex deficiencies. JAMA 312(1):68–77

Valente L, Tiranti V, Marsano RM et al (2007) Infantile encephalopathy and defective mitochondrial DNA translation in patients with mutations of mitochondrial elongation factors EFG1 and EFTu. Am J Hum Genet 80(1):44–58

Wortmann SB, Koolen DA, Smeitink JA, Van den Heuvel L, Rodenburg RJ (2015) Whole exome sequencing of suspected mitochondrial patients in clinical practice. J Inherit Metab Dis 38 (3):437–443